

## Durham E-Theses

---

### *Glycopolymers for targeted delivery applications*

Craig Fleming

#### How to cite:

---

Fleming, Craig (2006) Glycopolymers for targeted delivery applications. Doctoral thesis, Durham University.

#### Use policy

---

The full-text may be used and/or reproduced, and given to third parties in any format or medium, without prior permission or charge, for personal research or study, educational, or not-for-profit purposes provided that:

- a full bibliographic reference is made to the original source
- a <https://etheses.durham.ac.uk/id/eprint/2617/> is made to the metadata record in Durham E-Theses
- the full-text is not changed in any way

The full-text must not be sold in any format or medium without the formal permission of the copyright holders.

Please consult the [full Durham E-Theses policy](#) for further details.

# Glycopolymers for Targeted Delivery Applications

*Craig Fleming*

A thesis submitted to

University of Durham  
Department of Chemistry

in fulfilment of the requirements for the degree of

DOCTOR OF PHILOSOPHY

**The copyright of this thesis rests with the author or the university to which it was submitted. No quotation from it, or information derived from it may be published without the prior written consent of the author or university, and any information derived from it should be acknowledged.**

January 2006



29 NOV 2006

# **Statement of Copyright**

The copyright of this thesis rests with the author. No quotation from it should be published without his written consent and information derived from it should be acknowledged.

# **Declaration**

The work reported in this thesis was carried out in the Department of Chemistry at the University of Durham between September 2000 and July 2004. All the work was carried out by the author unless otherwise stated, and has not previously been submitted for a degree at this or any other university.

# Acknowledgements

I would like to everyone who has been involved in anyway during my research, without whom I would not have been able to fulfil the objectives of this project.

Without a doubt, I must first thank Dr Neil R. Cameron. His wisdom, encouragement, advice, support and most of all his patience were pivotal in aiding me during this exciting and novel work, and ultimately in completing this thesis. Truly I am grateful for all of his input.

I also wish to thank Dr Ben Davis (University of Oxford) who was an inspiration due to his infectious enthusiasm, and invaluable advice on various aspects of carbohydrate synthesis and their biological interactions.

My thanks must also go to JSR Farms and the DTI for providing the financial backing. In particular I would also like to thank the following employees of JSR Farms – Mr Paul Penny, Dr Ray Noble for sharing with me his knowledge and experience of biochemistry, and Dr André Maldjian for performing various analyses on the biological samples – his assistance was invaluable.

I would like to sincerely thank all of the support staff in the Department of Chemistry. There are too many to mention and I would not like to omit anyone, but all of their assistance was greatly appreciated.

Thanks must also go to all of the Cameron group members past and present who certainly made my experience and entertaining and enjoyable one.

Thanks to Dr. D Haddleton and Dr A Rullay (University of Warwick) for providing the dye used in the confocal experiments.

Dr Detlef Rath and his team at the Institut für Tierzucht und Tierverhalten, Mariensee, Germany for the use of their equipment and assistance with sex-sorting of semen.

My friends have been a tremendous source of support and encouragement, especially when times have been more difficult, you all know who you are – thank you! Thanks also to my brother for all his help and support. My parents deserve a special mention – their unwavering support for me throughout my studies and my life has been truly precious.

Last but not least I must thank Pam. She has been there for me throughout - first as my girlfriend, then my fiancée and now my wife. Without her love and support, I would not have succeeded.

*All animals are equal,  
but some animals are more equal than others*

*To my parents, Pam and 'bump'*

# Abstract

Currently, the area of polymeric drug delivery is one of intense international and interdisciplinary research. Many of the applications of materials derived from this research are focussed on therapeutic applications ultimately to be used in whole body systems. Herein, the research described focuses on a novel application of multicomponent glycopolymers.

The majority of pig breeding is conducted *via* artificial insemination. Whilst this offers many advantages, one of the major drawbacks is the adverse effect of oxidation on the spermatozoa during storage (which can be several days) prior to use. The supplementation of vitamin E is highly desirable, however due to its lypophilic character it cannot be added directly to the largely aqueous boar ejaculate mixture. Polymethacrylate derivatives were synthesised carrying carbohydrate residues, vitamin E residues and solubility enhancing amino residues. These vitamin E bearing glycopolymers were found to be soluble in aqueous media.

The interactions of these materials with boar spermatozoa were thoroughly investigated. It was demonstrated that supplementation with these glycopolymers significantly reduced cellular oxidation under induced oxidative conditions.

Analogous polymers were also synthesised containing a fluorescent dye. Confocal microscopy images were obtained of boar spermatozoa incubated with dye-labelled polymers with and without carbohydrate moieties in order to demonstrate that the internalisation of the polymers was enhanced by carbohydrate-lectin interactions.

*Craig Fleming, Durham, January 2006*

# **Abbreviations**

ADHD – Attention Deficit Hyperactivity Disorder  
AFM – Atomic Force Microscopy  
AI – Artificial Insemination  
AIBN – Azobisisobutyronitrile  
AROP – Anionic Ring Opening Polymerisation  
ASGPR – Asialoglycoprotein Receptor  
ATP – Adenosine Triphosphate  
BSA – Bovine Serum Albumin  
BTS – Beltsville Thawing Solution  
CAC – Critical Aggregation Concentration  
CASA – Computer Assisted Sperm Analyser  
CMLRP – Copper Mediated Living Radical Polymerisation  
CRD – Carbohydrate Recognition Domain  
CROP – Cationic Ring Opening Polymerisation  
DAPI – 4',6-Diamidino-2-phenylindole  
DCM – Dichloromethane  
DHA – Docosahexaenoic Acid  
DMAEA – Dimethylamino ethylacrylate  
DMAEMA – dimethylamino ethylmethacrylate  
DMF – Dimethyl formamide  
DMSO – Dimethyl Sulphoxide  
DNA – Deoxyribonucleic Acid  
DPA – Docosapentaenoic Acid  
EDCI – 1-ethyl-3-(3'-dimethylaminopropyl)carbodiimide  
EDTA – Ethylene Diamine Tetraacetic Acid  
EPA – Eicosapentaenoic Acid  
ESEM – Environmental Scanning Electron Microscopy  
GalNAc – N-acetylgalactosamine  
GBP – Galactose Binding Protein  
GDP-Fuc – Guanidine Diphosphate-Fucose  
GPC – Gel Permeation Chromatography

HEMA – 2-Hydroxyethyl Methacrylate  
HEPES – N-(2-hydroxyethyl)-piperazine-N'-2-ethanesulfonic acid  
HIV – Human Immunodeficiency Virus  
HOBt – N-Hydroxybenzotriazole  
HOPG – Highly Ordered Pyrolytic Graphite  
HPLC – High Performance Liquid Chromatography  
IR – Infrared  
LC-MS – Liquid Chromatography-Mass Spectrometry  
Man-6-P – Mannose-6-phosphate  
MDA – Malondialdehyde  
MMA – Methyl Methacrylate  
mRNA – messenger Ribonucleic Acid  
MWCO – Molecular Weight Cut-Off  
NASI – N-acryloxy Succinimide  
NCA – N-carboxyanhydride  
NMR – Nuclear Magnetic Resonance  
NMRP – Nitroxide Mediated Radical Polymerisation  
PD – Polydispersity  
PMMA – Poly(methyl Methacrylate)  
PNA – Peanut Agglutinin  
PUFA – Polyunsaturated Fatty Acid  
RAFT – Reversible Addition-Fragmentation Chain Transfer (polymerisation)  
RME – Receptor Mediated Endocytosis  
ROMP – Ring Opening Metathesis Polymerisation  
ROP – Ring Opening Polymerisation  
TBARS – Thiobarbituric Acid Reactive Substances  
TES – N-Tris(hydroxymethyl)methyl-2-aminoethanesulfonic Acid  
THF – Tetrahydrofuran  
TLC – Thin Layer Chromatography  
TRIS – Tris-hydroxymethylaminomethane  
UDP-Gal – Uridine Diphosphate-Galactose  
UV – Ultraviolet  
VEA – Vitamin E Acrylate (α-tocopheryl acrylate)  
VEMA – Vitamin E Methacrylate (α-tocopheryl methacrylate)

# Contents

<b>1</b>	<b>Introduction</b> .....	- 1 -
1.1	Cells.....	- 1 -
1.1.1	Cell Membranes.....	- 1 -
1.1.2	Mammalian Spermatozoa.....	- 2 -
1.1.3	Sperm Morphology.....	- 3 -
1.1.4	Sperm Cell Plasma Membrane.....	- 10 -
1.1.5	Boar Semen.....	- 11 -
1.1.6	Evaluation of Semen.....	- 13 -
1.1.7	Morphology.....	- 14 -
1.1.8	Semen Quality.....	- 14 -
1.1.9	Semen Collection in Boars.....	- 14 -
1.2	Pig Artificial Insemination (AI).....	- 15 -
1.2.1	Liquid storage.....	- 16 -
1.3	Carbohydrates.....	- 20 -
1.3.1	Glycobiology.....	- 21 -
1.3.2	The sugar code.....	- 22 -
1.4	Lectins.....	- 23 -
1.4.1	Classification of Animal Lectins.....	- 25 -
1.4.2	Lectin-Ligand Interactions.....	- 25 -
1.4.3	Sperm-Egg Binding.....	- 27 -
1.5	Lipids.....	- 28 -
1.6	Vitamin E.....	- 30 -
1.7	Drug Delivery.....	- 35 -
1.7.1	Polymeric Drug Delivery.....	- 39 -
1.7.2	Receptor Mediated Endocytosis.....	- 41 -
1.7.3	Glycopolymers.....	- 48 -

1.8	Summary.....	- 54 -
1.9	References .....	- 56 -
<b>2</b>	<b>Vitamin E polymer synthesis.....</b>	<b>- 62 -</b>
2.1	Introduction .....	- 62 -
2.2	Results and discussion.....	- 65 -
2.2.1	Glycomonomers.....	- 65 -
2.2.2	$\alpha$ -Tocopheryl monomers.....	- 67 -
2.2.3	Scale-up .....	- 68 -
2.2.4	Polymers .....	- 68 -
2.2.5	Concluding Comments .....	- 78 -
2.3	Experimental.....	- 80 -
2.3.1	Materials .....	- 80 -
2.3.2	Instrumentation.....	- 80 -
2.3.3	Synthesis of monomers and polymers.....	- 81 -
2.4	References .....	- 92 -
<b>3</b>	<b>Vitamin E polymer properties .....</b>	<b>- 94 -</b>
3.1	Introduction .....	- 94 -
3.2	Results and Discussion.....	- 95 -
3.2.1	Micellisation .....	- 98 -
3.3	Concluding remarks.....	- 106 -
3.4	Experimental.....	- 107 -
3.4.1	Atomic Force Microscopy (AFM).....	- 107 -
3.4.2	Light Scattering .....	- 109 -
3.4.3	ESEM.....	- 111 -
3.4.4	Solubilisation .....	- 111 -
3.5	References .....	- 112 -
<b>4</b>	<b>Biological experiments with multi-component polymers.....</b>	<b>- 113 -</b>
4.1	Introduction .....	- 113 -
4.2	Results and discussion.....	- 114 -

4.2.1	Motility and viability studies.....	- 114 -
4.2.2	Vitamin E Uptake and Oxidative Stress Measurements-	133 -
4.2.3	Effect of feed supplementation and in vitro polymer addition on sperm quality .....	- 141 -
4.2.4	Sex Sorted Semen.....	- 145 -
4.2.5	Fluorescent polymers.....	- 151 -
4.3	Conclusions .....	- 167 -
4.4	Experimental.....	- 168 -
4.4.1	Materials and Instrumentation.....	- 168 -
4.4.2	Semen Quality .....	- 169 -
4.4.3	Synthesis of poly[2-( $\beta$ -D-galactosyloxyl)ethyl methacrylate- ter-hostasol methacrylate-ter-2-(dimethylamino)ethyl acrylate] ( <b>15</b> ) .....	- 174 -
4.4.4	Synthesis of poly[methyl methacrylate-ter-hostasol methacrylate-ter-2-(dimethylamino)ethyl acrylate] ( <b>16</b> )..... .....	- 174 -
4.4.5	Vitamin E analysis.....	- 175 -
4.4.6	Confocal Microscopy.....	- 176 -
4.5	References .....	- 177 -
<b>5</b>	<b>DHA polymer synthesis .....</b>	<b>- 179 -</b>
5.1	Introduction .....	- 179 -
5.2	Results and discussion.....	- 182 -
5.2.1	Concluding comments .....	- 196 -
5.3	Experimental.....	- 197 -
5.3.1	Materials .....	- 197 -
5.3.2	Instrumentation.....	- 197 -
5.3.3	2-Azido ethanol ( <b>17</b> ).....	- 197 -
5.3.4	2-(2', 3', 4', 6'-tetra- <i>O</i> -acetyl- $\beta$ -D-galactosyloxyl)ethyl azide ( <b>18</b> ) .....	- 198 -

5.3.5 Docosa-4, 7, 10, 13, 16, 19-hexaenoic acid 2-azido-ethyl ester ( <b>19</b> ) .....	- 199 -
5.3.6 Docosa-4, 7, 10, 13, 16, 19-hexaenoic acid 2-amino-ethyl ester ( <b>20</b> ) .....	- 200 -
5.3.7 Poly[2-( $\beta$ -D-galactosyloxyl)ethyl methacrylate-ter-N-acryloyloxysuccinimide-ter-2-(dimethylamino)ethyl acrylate Galema/NASI/DMAEA Terpolymer ( <b>21</b> ).....	- 201 -
5.3.8 Coupling of <b>20</b> to <b>21</b> .....	- 202 -
5.4 References .....	- 203 -

# **1 Introduction**

## ***1.1 Cells***

### **1.1.1 Cell Membranes**

In order to begin to understand ligand-cell surface interaction(s), one must first appreciate the basic structure of the cell membrane itself.<sup>1, 2</sup> The cell membrane is the interface between the cell surface and the external environment, and as such provides the perfect location and physical platform for interactions, (phospholipids, which make up the membrane bilayer, contribute to the operation of cell surface receptors.) One popular concept of membrane structure is the “Fluid Mosaic” model, postulated by Singer & Nicolson.<sup>3</sup>

The fluid mosaic model has two key features:

- i) Membrane proteins and glycoproteins are asymmetrically embedded in the lipid bilayer.
- ii) The lipid forms the “matrix” of the membrane and provides a viscous medium which permits lateral mobility or diffusion of the protein molecules, which are therefore free to interact over relatively large distances.

In addition to these “standard” membrane regions, specialised regions can be formed which have a particular function or importance, for example, the acrosomal and tail regions of spermatozoa.

A schematic of the fluid mosaic model is shown Figure 1.1 in below.



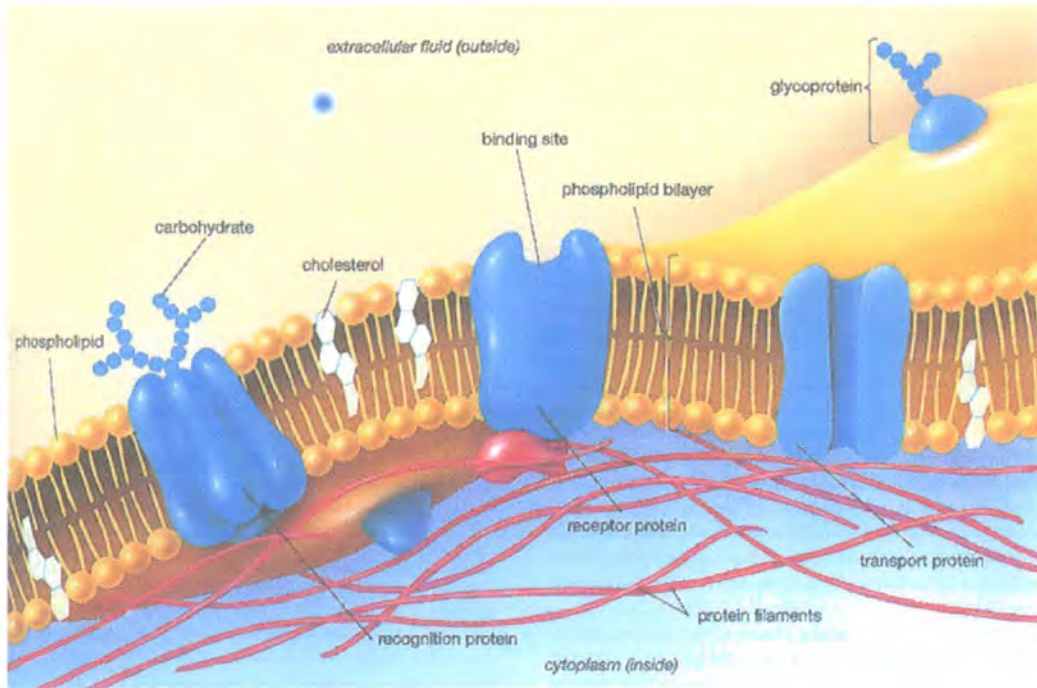


**Figure 1.1 - The Fluid Mosaic Model<sup>4</sup>**

This model can be applied to many different cell types but in the context of this thesis, the interactions of the sperm cell membrane are of particular importance.

### 1.1.2 Mammalian Spermatozoa<sup>5</sup>

The male gamete – the spermatozoon (or sperm cell) is an unusual and unique cell. It is produced in the testis through a complex process known as spermatogenesis, where it undergoes many important changes before it is fully “matured”. Once matured it cannot go through any further differentiation or division. Its principal purpose at this stage is to provide the male pronucleus for a fertilised egg, which of course requires both male and female haploid pronuclei.

Although visually different in some cases (see Figure 1.2 below), sperm cells - across a range of species – share the same key components:

- The acrosome-covered head that contains the DNA, is crucial in the penetration of the female egg, and subsequent fertilisation to produce a zygote.
- The neck containing the centriole is essential for cell division of the zygote.

- The tail, essential for propulsion of the sperm cell, powered by the mitochondria of the mid-piece.

As with all other mammalian cell types, it is covered by a plasma membrane, which undergoes changes depending on its environment (*i.e.* during maturation, post-ejaculation, pre-fertilisation *etc.*).

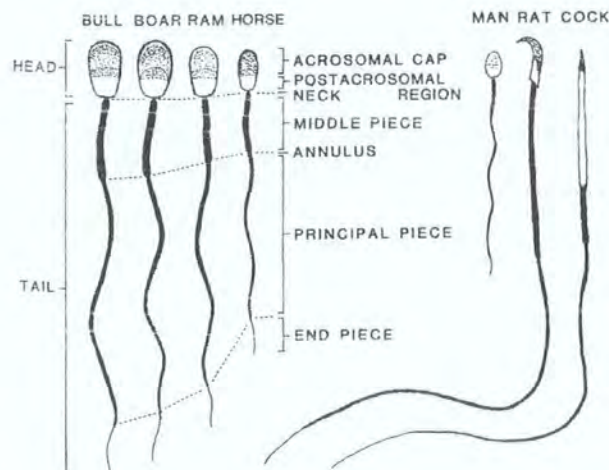


Figure 1.2 - Examples of Mammalian Spermatozoa<sup>6</sup>

### 1.1.3 Sperm Morphology

The appearance of sperm cells was first reported more than 300 years ago, and despite improvements in microscopy over this time, little more was understood about the complex internal structure until the advent of transmission electron microscopy in the 1950s. In general terms the sperm cell can be divided into two main components – the flagellum and the head. These can be further subdivided into a number of key parts, all of which will be discussed below.

#### 1.1.3.1 Head

The primary functions of the sperm head are to enclose and protect the DNA until it is delivered during fertilisation. This requires the DNA to be preserved in a stable form

until the formation of the male pronucleus. Furthermore the head must facilitate the penetration of the egg and possess a means of species-specific sperm-egg recognition. It is essential that the head be able to undergo membrane fusion, otherwise fertilisation would not be possible. Despite the relatively large number of functions required of the head, it has a limited number of structures available with which to perform these tasks. Essentially the structure of all mammalian sperm heads are the same in terms of structural content, however the size and shape differs greatly from species to species (Figure 1.2).

### ***1.1.3.2 Acrosome***

The acrosome is a cap-like covering over the frontal part of the nucleus. Between the outer acrosomal membrane (which is immediately beneath the plasma membrane) and the inner acrosomal membrane is a narrow cavity filled by the acrosomal matrix, which consists of a number of enzymes (*e.g.* hyaluronidase, acrosin, acid phosphatase, phospholipases, N-acetylglucosaminidase, *etc.*) as well as being rich in carbohydrates. Towards the back of the sperm head is the equatorial segment. This region is very stable and is devoid of the enzymes present in the anterior section. This section remains intact after the acrosome reaction\*. The plasma membrane that is on top of the equatorial section is the site of sperm-egg recognition and membrane fusion.

### ***1.1.3.3 Perinuclear material***

Immediately below the acrosome is a thin layer of perinuclear material which separates the acrosome and the nucleus. This structure is stabilised by disulphide bridges and appears to glue the two together. Towards the rear of the head this material forms the post-acrosomal sheath. This has a seemingly complex structure yet its functional significance is not clear.

---

\* The acrosome reaction takes place when the sperm cell comes into proximity with the egg. This is a precursor to fertilisation.

#### ***1.1.3.4 Nucleus***

The nucleus consists of densely packed chromatin, which is made up of DNA complexed to highly basic proteins, known as protamines. These protamines are rich in cysteine and arginine and it is the high level of cysteine that leads to the formation of disulphide bridges between free thiols. This crosslinking imparts great stability to the nucleus. The DNA, which exists in the beta form, is completely inactive until it is inside the egg.

#### ***1.1.3.5 Flagellum (tail)***

It is this region that is responsible for both energy production and propulsion. In order for fertilisation to occur, cellular motility is essential<sup>†</sup>. However motility is not only important in terms of penetrating the egg. Prior to this final stage, the cells must travel to the egg, often (depending on the species) negotiating cervical mucus along the way.

The structure of the tail is complex and will be discussed in detail below. However common to each piece of the tail is the axoneme, which runs throughout the length of the tail. This will be considered in more detail before considering each section of the tail.

#### ***1.1.3.6 Axoneme***

The axial filament (or axoneme) extends the entire length of the flagellum. The structure of the axoneme is not dissimilar to the cilia or flagella of all eukaryotic cells, (the existing knowledge of how the flagella of lower organisms move was applied directly to sperm cells). It consists of 9 evenly spaced microtubular doublets that surround 2 central microtubules. Each of the 9 doublets consists of 2 sub-units (A & B). “A” type subunits are complete microtubules 26 nm in diameter. The “B” type

---

<sup>†</sup> Principally referring to natural fertilisation as a result of sexual intercourse, or artificial insemination, however clearly techniques such as Intracytoplasmic Sperm Injection (ICSI) do not require motile sperm cells in order to achieve fertilisation.

subunits are “C-shaped” and are attached by their free edges to their corresponding A tubules (see Figure 1.3 & Figure 1.4 below).

These microtubules are composed mainly of a protein called tubulin. There is a high degree of heterogeneity both within and between microtubules, which is due to tubulin existing in both alpha and beta forms, in addition to differences in electrophoretic mobility, amino acid composition and phosphorylation sites between the two forms.

The tubulin molecules are arranged in rows to form protofilaments. These are aligned side-by-side to form the microtubule walls. As for both of the central microtubules, the A tubules are composed of 13 protofilaments. However, B tubules are made up of 10 protofilaments.

Each A tubule has projections or “arms” pointing towards the adjacent B tubule. These are 24 nm apart and are designated as inner or outer depending on their position. These play an essential role in flagellar movement. They are principally composed of a  $\text{Ca}^{2+}$  and  $\text{Mg}^{2+}$  dependent ATPase isomer of the protein dynein. These dynein arms enable adjacent doublets to slide relative to one another (*c.f.* sliding filaments in muscle contraction). This is what generates the flagellar movement.

The nine outer doublets are connected to their neighbouring doublets by links composed of the protein nexin. These are situated along the length of the tubule doublets (96 nm apart) and it is thought that they act as an elastic element. These help to regulate shear forces and retain the symmetry of the axoneme structure.

The central microtubules which are interconnected by a series of evenly spaced linkages, are also surrounded by a pair of spiral fibres attached to the microtubules at the levels of the connecting links.

The function of the central pair and the sheath is unclear.

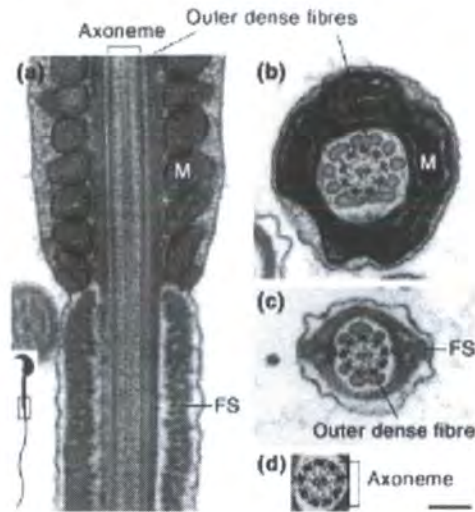


Figure 1.3 – Electron Micrographs<sup>‡</sup> of Mammalian (mouse) Sperm Cell<sup>7</sup>

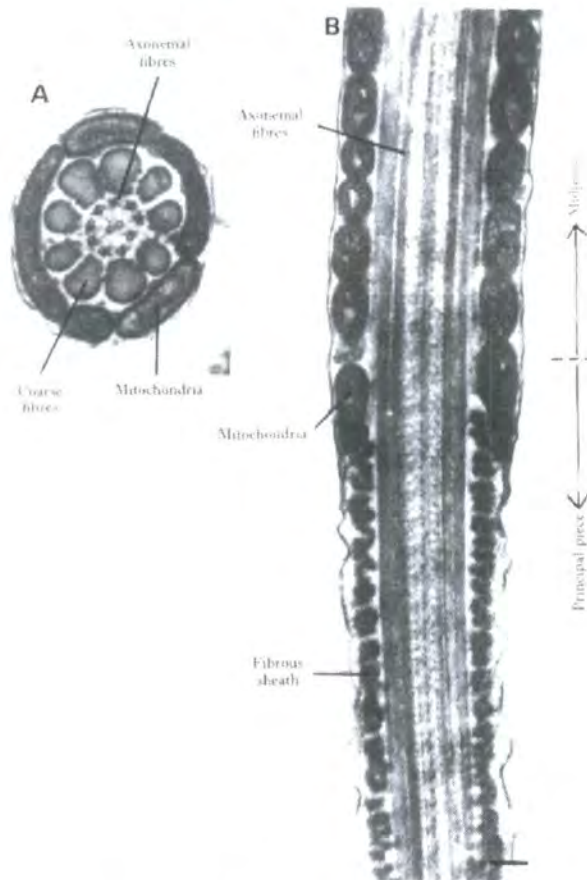


Figure 1.4 – Electron Micrograph<sup>§</sup> of Mammalian (bull) Sperm Cell Flagellum<sup>8</sup>

<sup>‡</sup> (a) Longitudinal section of the junction of the midpiece and principal piece of a mouse spermatozoon (boxed area shown in inset). The axoneme, consisting of microtubules, dynein ATPase and associated proteins, is in the core of the flagellum. It is surrounded by outer dense fibres and mitochondria (M) in the midpiece, and by fibrous sheath (FS) in the principal piece. (b,c) Cross-sections of the midpiece and principal piece, respectively. (d) Cross-section of the axoneme alone, showing the typical ‘9+2’ pattern, with a central pair of microtubules surrounded by nine sets of doublets. Scale bar = 200 nm.

### ***1.1.3.7 Connecting Piece***

As the name suggests, this part is the link between the head and the tail, and is approximately 0.5  $\mu\text{m}$  in length. The structure consists mainly of the capitulum (a dense dome-shaped fibrous structure) and the segmented columns. Although the arrangement of the segmented columns is quite complex, thus far it has not been shown to provide anything more than a simple structural connection.

### ***1.1.3.8 Outer Dense Fibres***

The outer dense fibres surround the axoneme of eutherian spermatozoa. This complex structure is not seen in the flagella of simple invertebrate species. Each one of the 9 microtubule doublets is associated with an outer dense fibre. These fibres start from the back of the connecting piece and end at variable points along the principal piece. The size and thickness of these fibres varies from species to species. The fibres consist of a dense core surrounded partially by a cortex which is not present on the side closest to its respective microtubule doublet. The core consists of a keratin-like protein, which being rich in cysteine, is stabilised by disulphide bridges; the outer cortex is not as stable.

The outer dense fibres tend to be of varying lengths. They seem to have the effect of stiffening a portion of the tail, since in invertebrate species, which do not have these outer dense fibres, the tail can achieve maximum curvature close to the head, while generally in mammalian sperm this is not possible. However, beyond this observation, there is no consensus as to any other potential function(s) they may have.

---

§ (A) Electron micrograph of a cross section of the midpiece of a bull sperm flagellum, showing the axonemal inner fibres, the coarse fibres, and the mitochondrial sheath surrounding the coarse fibres (courtesy of the Biophysical Journal). (B) Longitudinal section of a bull sperm flagellum in the area of the midpiece junction. Scale bar = 0.1  $\mu\text{m}$ .

### **1.1.3.9 Midpiece**

The midpiece refers to the section of the tail which stretches from the connecting piece to the annulus (the junction of the midpiece and principal piece). A characteristic of the midpiece is a helical sheath of mitochondria around the axoneme. The number of mitochondria varies depending on the species.

In terms of their internal structure, the mitochondria are similar to those seen in other cell types; however the outer membrane stability of sperm mitochondria is much greater (than other cell types). This stability is exemplified through their resistance to *e.g.* osmotic changes, and may be attributed to the presence of disulphide bonds, although its functional significance is unclear.

The location of the mitochondrial sheath is perfect for supplying ATP to the axoneme, thus providing motility. Eutherian sperm have many more mitochondria than some invertebrate sperm, and whilst the reason for this is not fully understood, the extra potential energy may be required due to the complexities of internal fertilisation.

### **1.1.3.10 Principal Piece**

This section is the longest part of the flagellum. It extends from the midpiece to the terminal piece. The main feature of the principal piece is the so-called fibrous sheath, which consists of two columns in the plane of the central microtubule pair, connected together around the circumference by a series of closely packed filaments.

It has been suggested that the function of the fibrous sheath is similar to that of the outer dense fibres. It is extremely stable and, like other areas of the sperm cell, it contains many disulphide bridges. In some species, disruption of this sheath has resulted in severely impaired motility, suggesting that it is very important.

### **1.1.3.11 Terminal Piece**

As the name suggests, this is the end of the flagellum. This is where the microtubules terminate, going down in number gradually until the tip of the flagellum is reached.

## **1.1.4 Sperm Cell Plasma Membrane**

As with other cell types, the sperm plasma membrane is the boundary responsible for protecting the cell, ensuring that it remains intact, as well as forming a dynamic interface between the cell and its surroundings. In contrast to other cell types, its structure and function are heterogeneous. The evidence for this is physical, chemical and immunological. These differing domains also undergo reorganisation at various stages of the cell's "life time", notably during capacitation \*\*.

There are five major membrane regions; two distinct regions on the tail, and three on the head. Each one is specifically involved with different aspects of the cell function. These regions differ in their binding affinity to lectins<sup>††</sup> as well as having different lipid compositions. There are also areas of differing surface charge.

The benefit of these unique regions is that the underlying compartments can interact independently with their external environment. Exactly how these different membrane domains are established and maintained is not fully understood. However, the fact that cell apoptosis (death) is accompanied by loss of domain structure is indicative that the maintenance of these domains is an active process.

### **1.1.4.1 Midpiece Region**

The plasma membrane in this region must permit the passage of substrates to the mitochondrial sheath. It is probably that changes in this membrane help to mediate the changes in cell metabolism during capacitation.

---

\*\* Capacitation is a change in mammalian sperm that occurs after exposure to the female genital tract which allows the sperm cell to undergo the acrosome reaction.

†† A lectin is a protein which can bind to a sugar(s) with good affinity and specificity.

#### ***1.1.4.2 Principal Piece Region***

This is the area responsible for generating the cell's movement. Its efficiency hinges on the plasma membrane being attached to the axonemal complex, rather than them moving independently.

The annulus divides the membranes of the midpiece and principal piece, and seems to behave as a physical barrier which restricts the movement of particles between the two domains.

#### ***1.1.4.3 Frontal Acrosomal Region***

The plasma membrane in this region is pivotal in two critical processes: recognition and binding to the zona pellucida (of the egg); and fusion with the outer acrosomal membrane during the exocytotic acrosome reaction.

The binding to the zona pellucida is mediated by glycoconjugates present in the membrane.

#### ***1.1.4.4 Equatorial Region***

As previously mentioned, this region is where fusion with the egg occurs. This is only possible after the acrosome reaction has occurred. This section of the membrane is very stable and appears to act as a barrier, preventing diffusion of particles between the anterior/post-acrosomal domains.

#### **1.1.5 Boar Semen**

As with other mammals, the cellular suspension containing the sperm cells is known as semen. Semen is made from secretions from the accessory organs of the male reproductive tract, and this liquid component of the semen is known as seminal plasma.

The chemical components and characteristics of the semen vary (often greatly) from species to species. A typical set of characteristics and components for boar semen is shown in Table 1.1 & Table 1.2.

**Table 1.1- Characteristics of boar semen<sup>6</sup>**

Ejaculate Volume (ml)	150-250
Sperm concentration ( $10^6$ /ml)	200-300
Motility (%)	50-80
Normal morphology (%)	70-90
pH	7.3-7.8

**Table 1.2 – Chemical components of boar semen<sup>6</sup>**

<b>Component</b>	<b>Concentration (mg/ml)</b>
Na <sup>+</sup>	5.87
K <sup>+</sup>	1.97
Ca <sup>2+</sup>	0.06
Mg <sup>2+</sup>	0.05-0.14
Cl <sup>-</sup>	2.6-4.3
Fructose	0.09
Sorbitol	0.06-0.18
Citric Acid	1.73
Inositol	3.8-6.3
Glyceryl phosphoryl choline	1.1-2.4
Ergothioneine	0.17

Spermatozoa are primarily made up of nucleic acids, proteins and lipids, with approximately a third of the dry weight of the cell made up by the nucleus.

### 1.1.6 Evaluation of Semen

The fertility of breeding males is generally assessed by examination of the semen. This is more practical than directly assessing their ability to produce a pregnancy.

In the case of boars, this analysis involves examining one or more ejaculates using a number of standard protocols. The general minimum requirements for a fertile boar are as follows:

Motility  $\geq 65\%^{\dagger\dagger}$

Morphological abnormalities  $\leq 20\%$

Ejaculate volume between 60-75 ml (sperm rich fraction)

Concentration of cells in ejaculate of  $\geq 100 \times 10^6$  cells/ml

The boar ejaculate consists of several fractions. The initial fraction, known as the *pre-sperm* fraction, is a translucent fluid which can be easily identified by the person collecting the sample. The second fraction is the *sperm-rich* fraction which is a more viscous, whitish, opaque fluid. For the purposes of semen evaluation and ultimately successful artificial insemination (AI), only this fraction is collected (although normally the total volume of the ejaculate is recorded).

After the *sperm-rich* fraction there is a final fraction – the *post-sperm* fraction – which is similar in appearance to the *pre-sperm* fraction.

The total volume of the ejaculate (normally around 240-250 ml) is affected by a large number of factors (age, health, environment, collection procedure, season, frequency of collection, breed, *etc.*).

The concentration of sperm in the sperm-rich fraction is approximately  $6 \times 10^8$  sperm/ml, although this will be diluted substantially prior to AI.

---

<sup>††</sup> Motility refers to any movement by the cell and can be scored either subjectively or by computer assisted methods (CASA).

### 1.1.7 Morphology

The number of sperm cells that have an undamaged acrosome is an important indication of semen quality. There are a number of techniques utilised when assessing sperm morphology. Typically, phase contrast microscopy of “fixed” sperm cells is employed to assess the integrity of the membranes; a number of staining techniques are also used to assess cellular morphology and viability.

### 1.1.8 Semen Quality

Despite the range of assessment techniques that are available, it remains that the most conclusive method of assessing the fertility of a given boar is to achieve pregnancy and the birth of live young. Even when the results of a lab assessment are positive and suggest good fertility, actual “in field” data can be conflicting.

In light of this, several attempts have been made to establish a single *in vitro* parameter that could predict the fertility of a given boar. These are as follows:

- Zona-free hamster ova penetration assay<sup>9</sup>
- Percoll gradients, isolating high velocity sperm<sup>10</sup>
- Assay for detecting integrity of sperm DNA<sup>11</sup>
- Specific sperm membrane proteins correlated to sperm penetrated zona-free hamster eggs<sup>12</sup>
- Hemizona binding assay: more sperm bound leads to increased fertility<sup>13</sup>
- Male pronucleus formation rate<sup>14</sup>

### 1.1.9 Semen Collection in Boars

Boars are trained to mount a dummy sow so that semen can be collected. A typical set-up is shown in Figure 1.5. Once the boar has mounted the “sow” it will begin thrusting: At this stage it is necessary for the technician to grasp firmly the end of the boar’s penis

in order to provide the necessary stimulus for ejaculation. As alluded to earlier, the frequency of collection will influence the concentration of sperm in the ejaculate, so care should be taken not to collect semen from animals too often.



**Figure 1.5- Boar mounting the dummy sow**

## ***1.2 Pig Artificial Insemination (AI)***

Artificial insemination of pigs was first attempted in the late 1920s by Ivanov.<sup>15</sup> This work was investigated further during the 1930s by Milovanov *et al.*<sup>15</sup> It was at this time that the first diluent components were suggested. From the original studies it was clear that only a portion of the cells stored actually survived either during liquid storage, or cryopreservation. Reducing temperatures has a tendency to interfere with membrane integrity, structure and the cell's biochemistry.

Over the last two decades, the use of preserved semen for AI has more than tripled. Statistics suggest that >99% of an estimated 19 million inseminations carried out globally, use semen which has been extended and either used on the same day or within 1-5 days (stored at 15-20°C).<sup>15</sup>

Since 1975, frozen boar semen has been available commercially, however it accounts for less than 1% of all inseminations. Freezing is generally used as a method of storing and ultimately supplying a particular genetic line.

AI in pigs offers many advantages over natural breeding; these include:

- Genetically superior boars can be used.
- Fewer boars require to be kept.
- Time is saved in a synchronised group.
- Cross-breeding programmes are facilitated.
- Good record keeping is encouraged.
- Sub-fertile boars can be identified.

However, as with any process, there are a number of disadvantages associated with using AI:

- Some training is required.
- It must be well managed.
- It is more labour intensive (heat detection, sanitation *etc.*)
- Semen has a limited shelf life (undiluted ~ 2 hours, extended between 3-7 days)

Although the technique is widely used and well established, research in and around the area of AI continues with vigour. There are many areas that could be improved and new technologies are emerging. Improvements in the insemination catheter design, improvements in the insemination techniques<sup>16, 17</sup> (*e.g.* deep uterine insemination, low dose insemination *etc.*), and new diluents/diluent additives<sup>15</sup> that may improve the viability of semen over time are just some examples of the areas which are being researched and improved.

### **1.2.1 Liquid storage**

Commercially, liquid storage is the area of most importance because the majority of farmers and AI stations are using this technology already and are trusting of it, unlike the use of thawed frozen semen which is expensive and not well established. Unlike in

the case of bull semen for example, boar semen cannot be routinely cryopreserved and sold in such a way as to be commercially viable. Additionally, it is the liquid storage of boar semen that is of particular relevance in the context of this thesis.

There are two key factors that affect sperm cell function post-ejaculation:

- i) temperature of collection and storage
- ii) conditions of the diluent

#### ***1.2.1.1 Cold shock***

It is well known that boar sperm are extremely susceptible to cold shock. If fresh semen is cooled too quickly (*i.e.* from body temperature  $\rightarrow$   $<15^{\circ}\text{C}$ ), there will be a sharp decrease in cellular viability. This is exacerbated further if the temperature continues to approach  $0^{\circ}\text{C}$ .

It has been observed that by slowing the rate of cooling from  $35^{\circ}\text{C} \rightarrow 15^{\circ}\text{C}$ , a resistance to cold shock can be established. It has been suggested that the effects of cold shock could be attributed to the lipid composition of the membrane. A reduction in temperature could cause a phase transition in the membrane from liquid to gel. Furthermore, since different lipids have different phase transition temperatures, this could lead to phase separation within the membranes.

The amount of cholesterol present in the membrane is thought to affect the thermotropic behaviour of the membranes.<sup>15</sup> The cholesterol/phospholipids ratio is very low in boar sperm. This leads to an asymmetrical distribution of cholesterol from outer monolayer to inner monolayer. As the membrane components are re-organised as a result of the cold shock, the function of the membrane can be affected in a number of ways (increased permeability, reduced enzymatic activity *etc.*).

### **1.2.1.2 Dilution effect**

During ejaculation, sperm are diluted with fluid from the accessory glands. Under normal circumstances, this would maintain the cells for a few hours. In order to improve on this, it is necessary to reduce the metabolic activity by adding chemical inhibitors or by reducing the temperature.

The problem is that whilst dilution has the effect of initially boosting activity, this is followed by an increase in membrane damage and a loss of motility. There are no definite answers as to why this is the case, however it has been speculated that the dilution of the protective effect of seminal plasma could be a major factor.<sup>15</sup> It has been shown that some of these effects can be countered by inclusion of bovine serum albumin (BSA)<sup>15</sup> – now a common feature of many commercial diluents.

### **1.2.1.3 Diluents**

There are several important factors in the composition of boar semen diluents: pH, ionic strength, type of ions and osmotic pressure. In addition, it is commonplace to include antibiotics to prevent bacterial growth occurring during storage.

Fresh boar semen has a pH of between 7.2-7.5. Motility decreases with decreasing pH. Glucose is often a major component of boar semen diluents. However, since boar sperm are generally stored in plastic tubes, with very little oxygen present, and since the glycolytic metabolism of boar sperm is poor compared to other species, this often leads to a decrease in motility.<sup>15</sup>

There are a couple of methods used to control ionic strength. Older diluents used salts (*e.g.* sodium bicarbonate, sodium citrate) to control the ionic strength, however it is more common now to rely on zwitterionic buffers such as TES & HEPES.

One of the most widely used extenders is the Beltsville Thawing Solution (BTS). This was (as the name suggests) originally used for thawing frozen boar sperm and has since been adapted for use in liquid storage. Many other diluents exist under various trade

names, and are designed for use as either short or long term diluents. BTS is typically regarded as a short term diluent, while Androhep for example is a long term diluent (see Table 1.3). The concentration of sperm cells used for insemination purposes is usually between  $2 \times 10^9$  and  $3 \times 10^9$  cells – this helps to ensure that the number of live births is commercially viable.

**Table 1.3 – Typical boar semen extender components<sup>15</sup>**

<i>Substance</i>	<i>Concentration (g/L) in H<sub>2</sub>O</i>	
	<b>Androhep</b>	<b>BTS</b>
Tri-sodium citrate dehydrate	8.0	6.0
EDTA	2.4	1.25
BSA	2.5	-
Sodium Hydrogen Carbonate	1.2	1.25
HEPES	9.0	-
Glucose monohydrate	26.0	37.0
Potassium chloride	-	0.75
Gentamycin sulfate	-	0.3
Dihydrostreptomycinsulfate	0.81	-
Penicillin-G Sodium salt	0.30	-

#### **1.2.1.4 Duration of storage**

Sperm cells age during liquid storage which leads to a drop in fertility. Even so-called “long-term” diluents cannot totally prevent this, although components such as BSA (found in Androhep for example) do reduce the effect of ageing.<sup>15</sup>

Despite this, numerous experiments have demonstrated that a decrease in fertility due to *in vitro* ageing is inevitable. Furthermore, it is important to match insemination time with ovulation as *in vivo* ageing of sperm is also a consideration.

### 1.3 Carbohydrates

It is widely acknowledged that the Earth's most abundant biomolecules are carbohydrates. They are unrivalled in the density of information that they are able to convey. Plants are able to synthesise cellulose (and other materials) from large quantities<sup>§§</sup> of CO<sub>2</sub> and H<sub>2</sub>O using photosynthesis. Starches and sugars form part of people's diets around the world, while the oxidation of carbohydrates to provide energy is the most important method in non-photosynthetic cells.

In plants, insoluble carbohydrate polymers often serve as structural components. Other such polymers help to lubricate skeletal joints and are involved in cellular recognition processes. Indeed carbohydrate polymers bound to lipids/proteins (known as glycoconjugates) act as signalling species.

Typically carbohydrates have the empirical formula (CH<sub>2</sub>O)<sub>n</sub>, although this is not universally true, since some contain other elements such as phosphorus, nitrogen and sulphur.

Carbohydrates can be split in to 3 main genres: monosaccharides, oligosaccharides and polysaccharides<sup>\*\*\*</sup>, with glucose being the most abundant monosaccharide. Oligosaccharides are short chains of monosaccharide units linked together by glycosidic bonds. The most abundant oligosaccharides are the disaccharides (for example sucrose which consists of D-glucose and D-fructose). Within cells, oligosaccharides which have 3 or more units tend to be joined to other molecules (*e.g.* proteins/lipids) as glycoconjugates.

Polysaccharides are those with more than 20 sugar units, but often have many hundreds or thousands of units. These can be linear (in the case of cellulose for example) or branched (*e.g.* glycogen). The majority of carbohydrates found in nature are polysaccharides.

---

<sup>§§</sup> Approximately 100 billion tonnes per year.

<sup>\*\*\*</sup> Saccharide: from the Greek *sakcharon* – meaning sugar.

The polysaccharides can themselves be sub-divided into two categories: homopolysaccharides and heteropolysaccharides. Homopolysaccharides serve as structural elements within cells/exoskeletons (*e.g.* cellulose and chitin), but can also act as energy stores of monosaccharides. In some animal tissues, heteropolysaccharides act as a matrix for cells/tissues/organs providing protection.

Polysaccharides tend not to have monodisperse, well defined molecular weights, mainly due to their synthesis, which is not as well controlled as the synthesis of proteins which are templated *via* messenger RNA (mRNA). Nevertheless, it is their ability to store and carry information that is of particular interest. They are able to guide proteins to the correct destination, mediate intercellular interactions, as well as interactions between cells and the extracellular matrix.

As alluded to earlier, a protein or lipid covalently bound to a carbohydrate is a biologically active compound known as a glycoconjugate. The structure of glycoconjugates is such that the bulk of the structure is made up of the carbohydrate moiety, and is therefore often the main site of biological activity, since there are multiple binding sites and potential for many H-bonding and electrostatic interactions. Two examples of glycoconjugates are glycoproteins and glycolipids.

The saccharide part of glycoproteins is rich in information and contains highly specific sites for recognition and high-affinity binding. Glycolipids are membrane components where the hydrophilic head groups are composed of oligosaccharides and, as with glycoproteins, act as specific sites for recognition by carbohydrate binding proteins. This area of study, known as glycobiology, is today one of the most exciting and active areas of cell biology/biochemistry.

### **1.3.1 Glycobiology**

This area encompasses the biological aspects of carbohydrates, *i.e.* how they are involved in biological functions. Due to the development of highly sophisticated techniques for the analysis of carbohydrate-mediated cellular functions and interactions, a greater understanding of these processes has been developed. The synthesis of

oligosaccharides and glycoconjugates have been essential for glycobiology studies, providing a correlation between structure and function.<sup>18</sup> Any such oligosaccharides or glycoconjugates must be structurally well-defined; therefore robust synthetic routes are essential. The synthesis of oligosaccharides is particularly difficult as it requires regiochemical and stereochemical control when forming the glycosidic linkage. The Koenigs-Knorr glycosylation<sup>19</sup> was the first viable method reported (in 1901), and while other methods have since been established,<sup>20</sup> vigorous research continues in the search for alternative strategies.<sup>18</sup> Whilst such synthetic methods offer a viable route to oligosaccharide synthesis, it is of particular interest in the context of this thesis to exploit these routes to produce so called glycomonomers, which in turn can be polymerised, resulting in glycopolymers. This concept will be discussed in more detail within. Nevertheless, the ability to synthesis oligosaccharides, glyconjugates or glycopolymers for that matter, allows the interactions between receptors and carbohydrates, examples of which can be found in the literature.<sup>18</sup>

The interaction between lectins and carbohydrates is complex, so many synthetic carbohydrate polymers are being synthesised so that these interactions can be investigated.<sup>21-25</sup> Such materials are referred to as glycopolymers (see later). Glycopolymers also have applications in other areas as surfactants,<sup>26</sup> detergents,<sup>27</sup> food additives, drug delivery,<sup>28, 29</sup> scaffolds for tissue engineering,<sup>30-32</sup> treatment of infectious diseases<sup>33</sup> and the treatment of HIV.<sup>34</sup>

### 1.3.2 The sugar code<sup>35, 36</sup>

When the word 'code' is used in reference to biological systems, one can be forgiven for assuming it is in reference to the genetic code. However, the ability of sugars to perform the task of information storage should not be underestimated. The power of sugars over amino acids or nucleotides emanates from the fact that sugars are not restricted to a single linkage point, but instead the presence of numerous hydroxyl groups can facilitate a whole array of possible linkages (*e.g.* 1-2, 1-3, 1-4, 1-6). Moreover, there is further variation possible through the type of linkage at the anomeric position ( $\alpha$  or  $\beta$ ).

If one considers that 20 amino acids can yield a total of  $6.4 \times 10^7$  hexapeptide isomers, this begins to seem insignificant when, for the same number of sugars, the total is  $1.4 \times 10^{15}$  oligosaccharides. This fact only serves to reinforce the importance of sugars in many aspects of life.

## 1.4 Lectins

A lectin is a protein molecule which can bind to carbohydrates with high specificity and affinity. Lectins can easily distinguish between very similar sugars due to the placement of H-bonding partners in the carbohydrate recognition domain of the lectin. Lectins are crucial in a wide range of cell-cell recognition processes. Lectins are present in all organisms; although they were first discovered more than 100 years ago in plants<sup>37</sup>, they have subsequently been identified in all other life forms (sometimes referred to by other names such as toxins, adhesins and hemagglutinins). Species-specific recognition was discovered after monitoring the phenomenon of re-aggregation of dissociated marine sponge cells – which itself is a carbohydrate mediated interaction. Other relatively simple species such as arachnids and crustaceans showed evidence of red cell agglutination activity (due to the presence of hemagglutinins). It was not until the 1960s that interactions such as this were known in complex multicellular animals such as vertebrates. Early indicators of this came as a result of the work of Ginsburg *et al.*<sup>38</sup> who looked at the treatment of blood leukocytes (from the rat), with bacterial glycosidases. The lack of sufficient tools at that time meant that a full interpretation of results was not possible; however it remains likely that their results were indicative of the presence of an endogenous lectin(s).

Direct evidence for mammalian lectins was serendipitously discovered by Ashwell *et al.*<sup>39</sup> While monitoring the turnover of glycoproteins in the blood using two tritium-labelled glycoproteins (one with and one without terminal sialic acid groups), they observed stark differences in their circulation half-lives. The sialic acid terminated proteins remained in circulation for days, while those without sialic acid groups were gone within several minutes. These desialyated glycoproteins appeared to be

accumulating in the liver. This observation established the existence of the “asialoglycoprotein<sup>†††</sup> receptor (ASGPR)”. This mechanism has since been observed through other experiments, for example ceruloplasmin is a glycoprotein responsible for transporting copper. It contains several oligosaccharide chains terminated with sialic acid. When the enzyme sialidase removes these residues, the proteins are then able to bind to hepatocytes, and are endocytosed and destroyed. This mechanism is similar to that which removes old erythrocytes from the mammalian bloodstream.

Of particular interest in this report is a galactose binding protein (GBP) present on the surface of mammalian spermatozoa,<sup>40</sup> which has a similar structure to the well-characterised asialoglycoprotein receptor<sup>39</sup> of hepatic cells. These receptor types are specific to  $\beta$ -linked galactose or GalNAc residues. A diagram showing the carbohydrate recognition domain (CRD) of a subunit of the human hepatic ASGPR is depicted below.

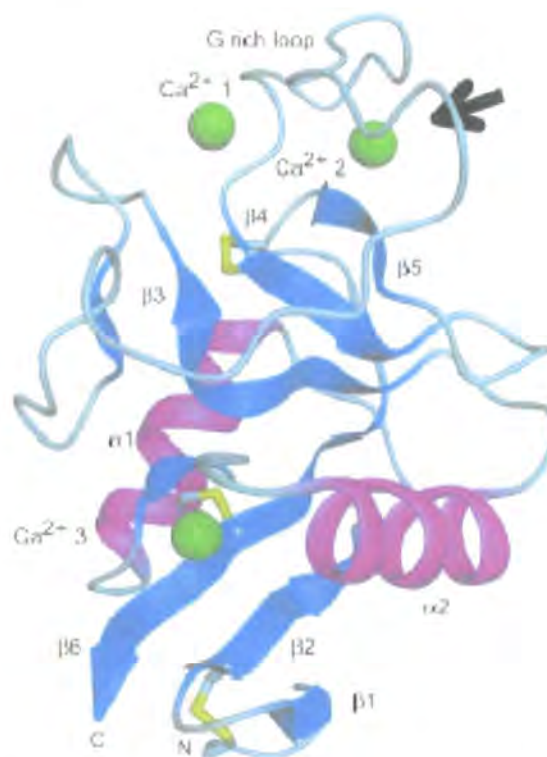


**Figure 1.6 - Ribbon diagram of the H1-CRD<sup>41</sup>**

<sup>†††</sup> *Asialo* – meaning without sialic acid.

The image contains several key components. The  $\alpha$ -helices are shown in purple, the  $\beta$ -strands in blue, the disulphide bridges in yellow and the calcium ions in green. The binding position of the sugar is indicated by the arrow.<sup>41</sup>

### 1.4.1 Classification of Animal Lectins

Historically, animal lectins were classified by the carbohydrate sequences to which they showed the highest affinity (*e.g.*  $\beta$ -galactoside-binding lectins). Due to modern molecular cloning techniques, a more systematic approach to nomenclature now exists. Work by Drickamer<sup>42</sup> suggested two classes of lectins:

- C-type lectins – so-named due to their requirement of calcium for recognition
- S-type lectins – since they required thiols

Since this initial study, further classes have been identified, such as P-type lectins, which recognise Man-6-P.

### 1.4.2 Lectin-Ligand Interactions

The binding constants for monosaccharide interactions with lectins are small, typically  $10^3$ - $10^6$   $M^{-1}$ . However, there is an increase in binding affinity with the number of saccharide units due to the multivalent or “cluster effect”.<sup>43</sup> Affinities of up to  $10^{16}$   $M^{-1}$  have been reported.<sup>21, 44</sup> This occurs when more than one sugar residue of the correct type and orientation are clustered together on the ligand. The number and arrangement of these sugars has a significant bearing on the interaction between the lectin and the sugar.<sup>45</sup> The selectivity of these interactions is largely based on H-bonding and Van der Waals forces. Further selectivity can occur through bridging cations or water molecules. In general, interactions between animal lectins and carbohydrates have been found to be multivalent, either due to having multiple carbohydrate binding sites, or due to the presentation of multiple carbohydrate residues by the ligand, or both. Work has been undertaken to gain a better understanding of multivalent ligand/receptor interactions. Work by Kiessling *et al*,<sup>46</sup> has focussed on the use of synthetic multivalent

ligands as probes of signal transduction. It is suggested that this approach is significantly more valuable than merely studying the function of individual proteins (as was the case historically) when attempting to elucidate receptor function. A multivalent ligand consists of a central scaffold with multiple copies of a recognition element attached. The recognition element of a multivalent ligand can assume a range of forms, *e.g.* peptides, carbohydrates, proteins or any moiety that is able to bind to a specific receptor. It is noteworthy that the structure of the scaffold is also important since factors such as flexibility, shape, size or orientation of the recognition elements *etc.* can have an impact on the biological activity of the multivalent ligand. Furthermore, the architecture of the scaffold can play a significant role in the biological response observed upon binding to the receptor. It is typical to refer to bioactive monovalent entities as agonists or antagonist (*e.g.* they activate or inhibit a response). However, while a single recognition element may be an agonist or antagonist, it is possible for a multivalent ligand to induce the opposite effect depending on the structure of the scaffold and how the binding affects *e.g.* the clustering of receptors.<sup>46</sup>

A number of different scaffold morphologies exist that can be used to study receptor function, examples of which can be seen in Figure 1.7. Synthetic organic chemistry offers routes to a wide variety of well-defined multivalent ligand architectures. As such it is possible to examine the change in biological effect based on the structure of the multivalent ligand.

Whilst multivalent ligands serve as powerful tools for the study and elucidation of complex multireceptor networks, they may also be applicable as treatments of disease. A study by Whitesides *et al* investigated the use of multivalent ligands as inhibitors of the anthrax toxin,<sup>47</sup> suggesting that multivalent ligands may not only serve as useful biological probes, but may actually have viable and worth-while therapeutic applications.

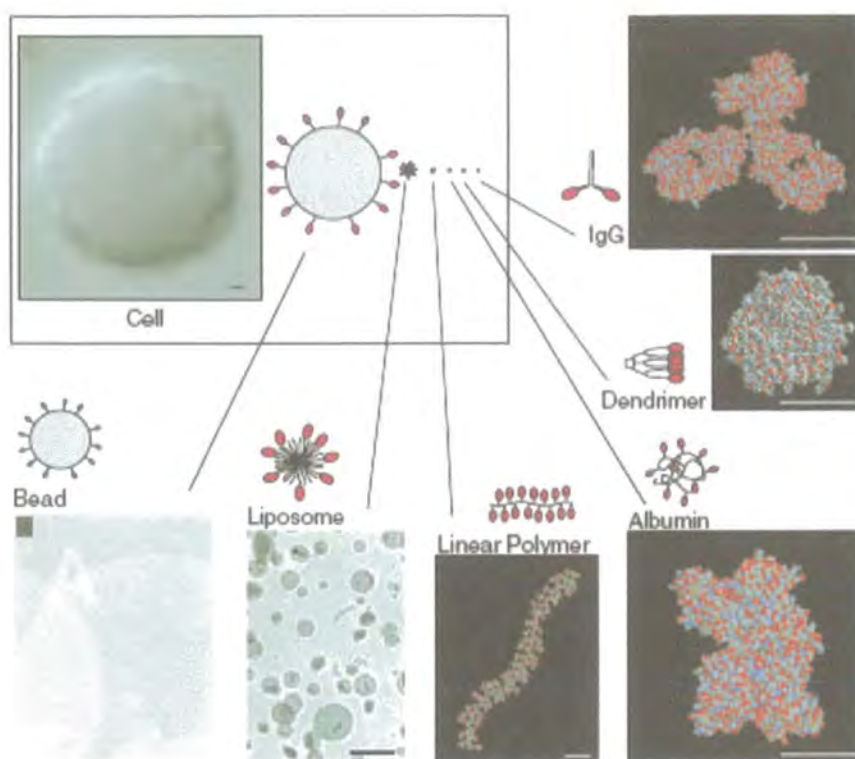


Figure 1.7 - Diagram showing examples of multivalent ligands<sup>46†††</sup>

In an attempt to mimic nature, much work has focused on synthetic materials rich in carbohydrates that can interact with specific lectins.<sup>48</sup> This is complimented by the fact that most lectins have several CRDs – thus increasing the potential binding strength. Recent work by Chung *et al* investigated the specific interaction of mannosylated glycopolymers with macrophage cells mediated by the mannose receptor. They were able to demonstrate (*via* fluorescent microscopy of FITC-labelled polymers containing mannosyl, glucosyl and glucoamidyl moieties), that only the mannosylated glycopolymers exhibited strong binding to the macrophage cell line carrying mannose receptors.<sup>48</sup>

### 1.4.3 Sperm-Egg Binding

Carbohydrate-lectin interactions dominate the fertilisation process in many vertebrate and invertebrate species. For example, in mice, the addition of UDP-Gal or GDP-Fuc

††† The ligands are compared in size to a mammalian lymphocyte. Scale bars are as follows: bead & cell 1 mm; liposome & polymer 0.5 mm; antibody, dendrimer and albumin 0.05 mm.

polymers blocked sperm egg binding.<sup>5</sup> Recently work by Fang *et al* has investigated the interactions of sperm lectins using carbohydrate modified quantum dots.<sup>49</sup> As has been discussed, monovalent interactions are weak and subsequently a number of carbohydrate carriers (*e.g.* dendrimers, polymers, liposomes and nanoparticles) have been developed in order to take advantage of multivalency. As such, the use of quantum dots encapsulated with the biologically important  $\beta$ -*N*-acetylglucosamine (GlcNAc – see Figure 1.8) were used to investigate interactions on the surface of sea-urchin sperm cells. In addition, mannose-encapsulated quantum dots were used to investigate interactions on the surface of mouse sperm cells.

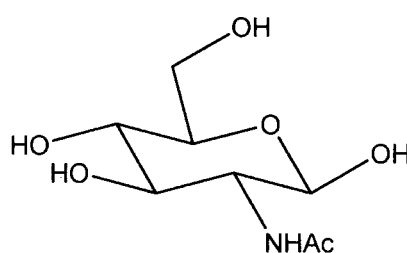


Figure 1.8 - Structure of *N*-acetylglucosamine (GlcNAc)

It was tentatively concluded from fluorescence microscopy studies that GlcNAc and Mannose receptors are distributed differently across the sperm surface since the GlcNAc labelled quantum dots were shown to bind selectively to the sperm heads, whereas the mannose-encapsulated quantum dots were distributed throughout the head and tail of the sperm cell. Fang *et al* also demonstrated binding of GlcNAc encapsulated quantum dots to live pig sperm *via* flow cytometry.<sup>49</sup>

## 1.5 Lipids

Lipids (or fats) are water insoluble biological molecules of much importance. They can be divided into two major groups based on their ability to be hydrolysed by strong bases – saponifiable and nonsaponifiable<sup>§§§</sup>. Lipids are as diverse in biological function as they are in their chemistry. They can act as stored energy within biological systems, be part of structural elements of membranes, *etc.* (*e.g.* phospholipids/sterols), as well as

---

<sup>§§§</sup> Saponification is the process where fatty acids are hydrolysed by base from their equivalent ester.

being electron carriers, hormones, intracellular messengers, to mention a limited subset.

Fatty acids and phospholipids are amphiphilic in nature, that is, they have both hydrophilic and hydrophobic character. In schematic terms one can represent a fatty acid as shown in Figure 1.9. Similarly, phospholipids are amphiphilic and can be represented schematically as illustrated in Figure 1.9.

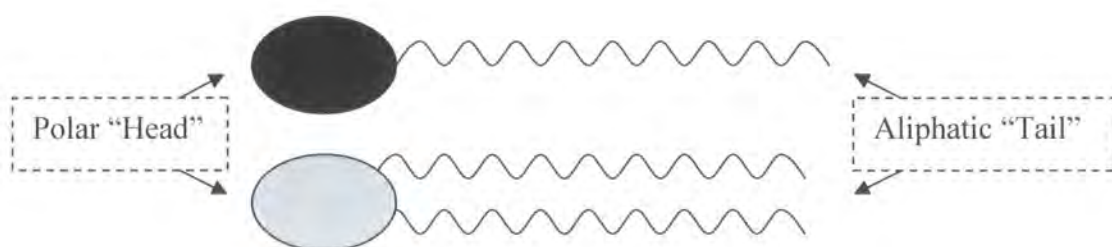


**Figure 1.9 - Cartoon representation of a fatty acid (black) and a phospholipid (grey)**

Within organisms, lipids used to store energy are in the form of fatty acid derivatives. This is essentially akin to burning fossil fuels in an engine, since the fatty acids are converted into  $\text{CO}_2$  and  $\text{H}_2\text{O}^{****}$ . Essentially a fatty acid is a carboxylic acid with a hydrocarbon chain (from  $\text{C}_4$  to  $\text{C}_{36}$ ). The compositions vary from fully saturated (*i.e.* no double bonds) to having one or more double bonds. In addition, the saturated chains can be either linear or branched.

Saturated fatty acids tend to be solids, with the melting point increasing with increasing chain length, whereas unsaturated fatty acids tend to be liquids at room temperature. This can be explained by considering the structure of both saturated and unsaturated fatty acids, and how they are able to pack. The inclusion of only one double bond introduces a kink in the aliphatic chain which leads to inefficient packing.

In general, fatty acids are numbered from the carbonyl carbon and their nomenclature can be simplified by giving the number of carbon atoms followed by the number of double bonds, separated by a colon, so *e.g.* docosaheaxaenoic acid is 22:6 (22 carbon

\*\*\*\* It is noteworthy that sugars provide around half of the energy per mole, compared to fats (18.8 kJ/mol v 37.7 kJ/mol).

atoms, 6 double bonds). In addition, the position of the double bonds can be given by superscript numbers following the symbol  $\Delta$ , (e.g. 4,7,10,13,16,19-docosahexaenoic acid (DHA) would be represented as 22:6( $\Delta^{4,7,10,13,16,19}$ )). One alternative nomenclature is to give the position of the first double bond based on numbering the chain from the opposite end of the chain from the carbonyl carbon (e.g. DHA would be represented as 22:6(n-3) or 22:6( $\omega$ -3)). In fatty acids where there are multiple double bonds, the double bonds are almost never conjugated and most of the fatty acids found in nature are in the *cis* configuration.

The composition of fatty acids varies depending on the organism of origin. Fish have 25-30% of fatty acids containing 20-22 carbon atoms, while mammals only have 5-7% naturally present. Furthermore fish have 15-30% of fatty acids containing 5-6 double bonds, while plants only have 5-6% and mammals less than 1%. Since fatty acids such as DHA & EPA are deemed to be important in mammalian nutrition,<sup>50</sup> and have benefits in reproductive health,<sup>51, 52</sup> it is obvious that food supplementation is important in order to gain the necessary amounts of essential fatty acids. It has been suggested that deficiencies in these essential fatty acids can lead to cognitive disorders like ADHD, dementia and dyslexia.

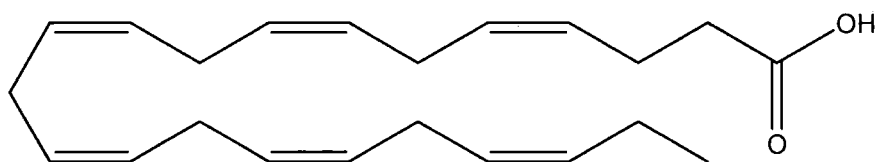


Figure 1.10 - *cis*-4,7,10,13,16,19-docosahexaenoic acid

## 1.6 Vitamin E

The term “vitamin E” was first coined around 90 years ago to describe a constituent of animal feed thought at the time to be important for reproduction.<sup>53, 54</sup> During the mid 1930s it started to become apparent that vitamin E consisted of more than one component, when two compounds of similar activity were isolated and characterised.<sup>53</sup>

These were designated as  $\alpha$ - and  $\beta$ -tocopherol<sup>††††</sup>. During subsequent years a further two tocopherol compounds were discovered ( $\gamma$ - and  $\delta$ -tocopherol), as well as four tocotrienols ( $\alpha$ -,  $\beta$ -,  $\gamma$ -, and  $\delta$ -tocotrienol).<sup>53</sup> Collectively these compounds make up natural vitamin E. These compounds are highly potent, fat-soluble, chain breaking (biological) antioxidants. Their hydrophobic nature means that they tend to associate with cell membranes, lipids, *etc.*

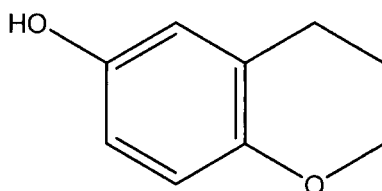


Figure 1.11 – Structure of 6-chromanol

All of the above compounds are derivatives of 6-chromanol (Figure 1.11). The tocopherols are derivatives of tocol and contain a saturated C<sub>16</sub>-side chain (Figure 1.12).

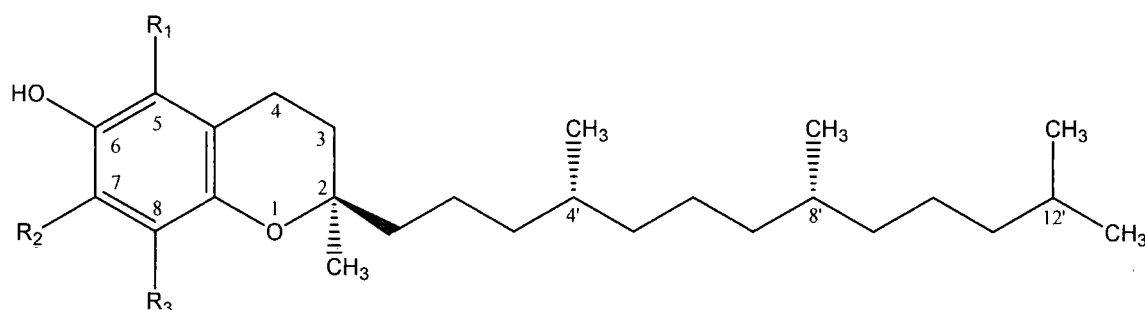


Figure 1.12 - General structure of the tocopherols

Table 1.4 – The tocopherols

<i>-Tocopherol</i>	<i>-Tocol</i>	$R_1$	$R_2$	$R_3$
$\alpha$	5,7,8-trimethyl	CH <sub>3</sub>	CH <sub>3</sub>	CH <sub>3</sub>
$\beta$	5,8-dimethyl	CH <sub>3</sub>	H	CH <sub>3</sub>
$\gamma$	7,8-dimethyl	H	CH <sub>3</sub>	CH <sub>3</sub>
$\delta$	8-methyl	H	H	CH <sub>3</sub>
–	Tocol	H	H	H

<sup>††††</sup> Tocopherol is derived from the Greek words *tocos* (childbirth) and *pherein* (to bring forth) due to the important role it plays in mammalian reproduction.<sup>53</sup>

The second series is derived from tocotrienol (Figure 1.13, Table 1.5), and have a triply unsaturated side chain at positions 3', 7' and 11'.

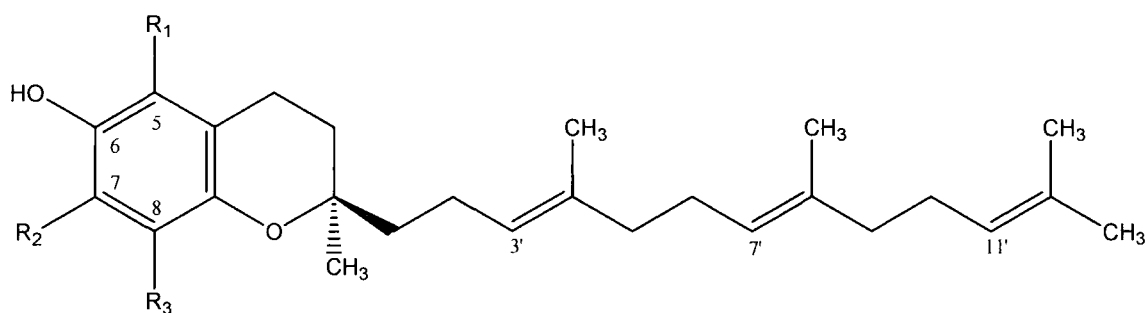


Figure 1.13 - General structure of the tocotrienols

Table 1.5 – The tocotrienols

	<i>-tocotrienol</i>	$R_1$	$R_2$	$R_3$
$\alpha$	5,7,8-trimethyl	CH <sub>3</sub>	CH <sub>3</sub>	CH <sub>3</sub>
$\beta$	5,8-dimethyl	CH <sub>3</sub>	H	CH <sub>3</sub>
$\gamma$	7,8-dimethyl	H	CH <sub>3</sub>	CH <sub>3</sub>
$\delta$	8-methyl	H	H	CH <sub>3</sub>
-	Tocotrienol	H	H	H

Although these 8 compounds exist and are well characterised, it remains the case that the most biologically active and subsequently the most commercially important of all these compounds, is  $\alpha$ -tocopherol.  $\alpha$ -Tocopherol is essential in the body to prevent cellular damage from free radicals.<sup>55</sup> It cannot be synthesised in mammalian systems and therefore must be supplied through feeding and supplementation.<sup>53</sup> Its main function is to prevent the peroxidation of membrane phospholipids, thus preventing membrane damage.<sup>54, 55</sup> If left unchecked, the damage to cell membranes will ultimately lead to apoptosis.<sup>56</sup> In multicellular organisms, this may not be fatal to the entire organism, if cell regeneration is occurring, however in the case of sperm cells (especially post ejaculate) the issue is much more serious.<sup>56</sup> Since  $\alpha$ -tocopherol is highly lipophilic, it tends to associate with the interior of the cell membrane bilayers.<sup>55</sup>

In general the radical trapping mechanism of  $\alpha$ -tocopherol can be considered as shown below.<sup>57, 58</sup>

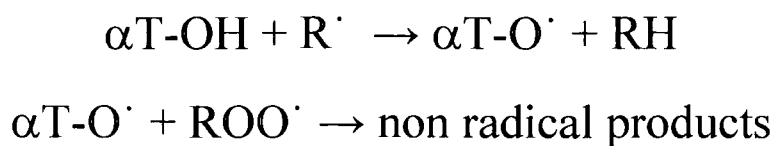
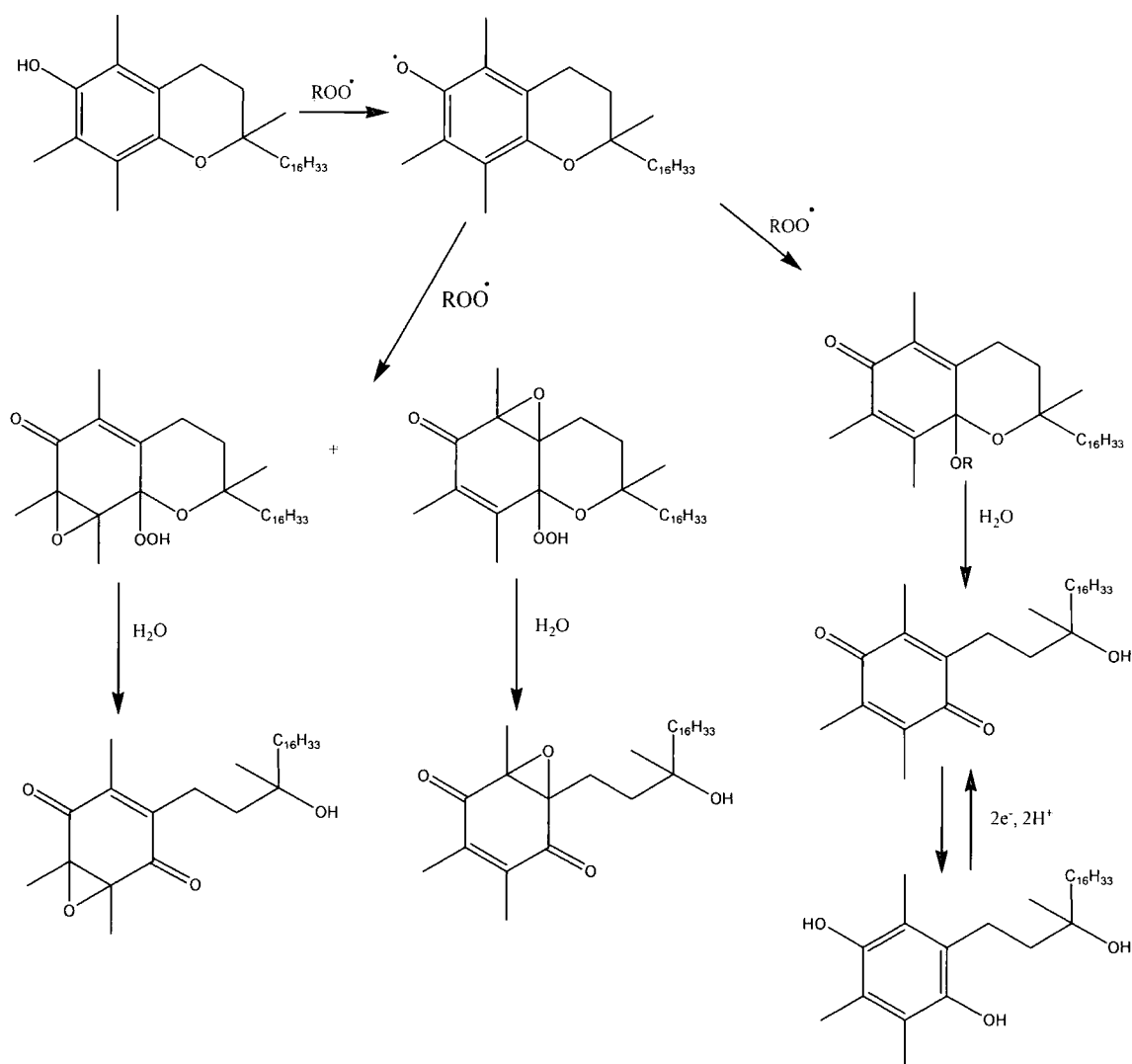


Figure 1.14 – General radical trapping mechanism

Elaborating further, a typical radical oxidative reaction scheme for  $\alpha$ -tocopherol is depicted in Figure 1.15.

Figure 1.15 - Oxidation products of  $\alpha$ -tocopherol<sup>54, 58</sup>

It has been shown that the structure of the  $\alpha$ -tocopheroxyl radical is stabilised by resonance. This is due in part to the structure of the chromanol ring and also to the presence of electron donating substituents on the ring (*e.g.* methyl groups).<sup>53</sup>

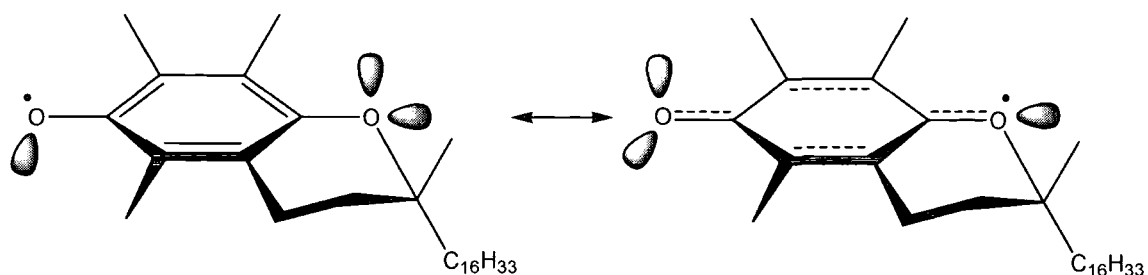


Figure 1.16 - Resonance forms of the  $\alpha$ -tocopheroxyl radical<sup>53</sup>

$\alpha$ -Tocopherol can also act as an anti-oxidant through non-radical pathways to yield a variety of different products.

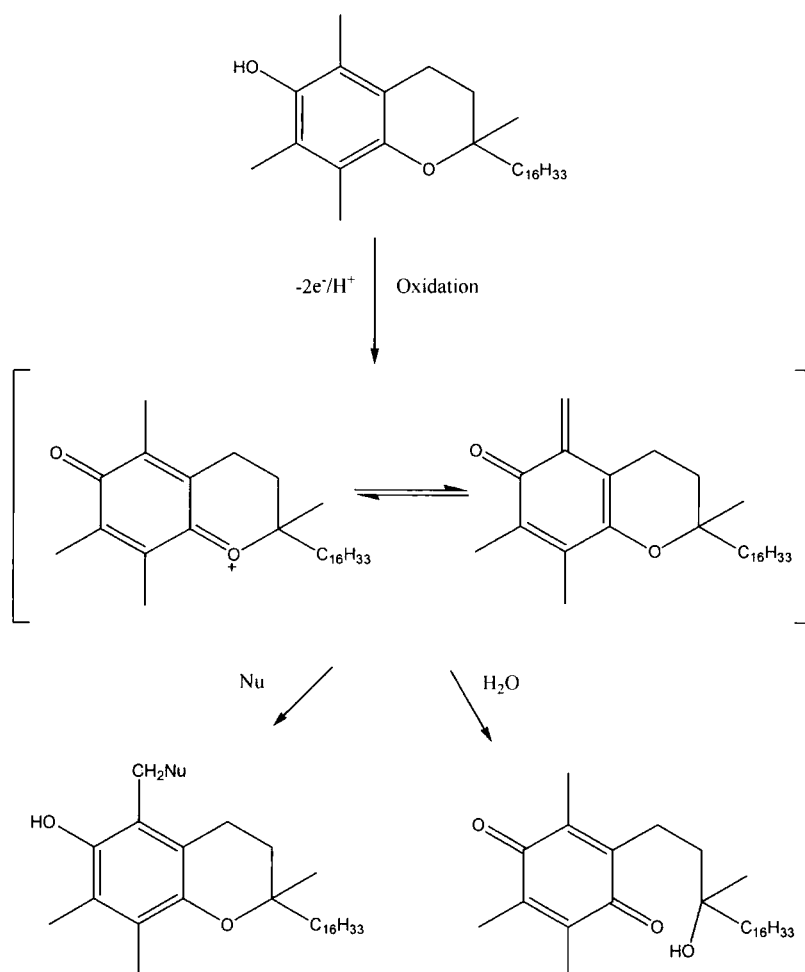


Figure 1.17 - Non-radical oxidation pathway of  $\alpha$ -tocopherol<sup>53</sup>

It is noteworthy that natural and synthetic vitamin E are not exactly the same. In naturally occurring vitamin E, the most abundant form is RRR- $\alpha$ -tocopherol, however

in contrast, the synthetic form is *all-rac- $\alpha$ -tocopherol*, *i.e.* it contains all 8 stereoisomers.

Logically, one might expect that since, in theory, all stereoisomers have the same antioxidant properties, their biological performance would be similar, however this is not the case.<sup>53</sup> This tends to suggest that it is not merely the antioxidant activity of  $\alpha$ -tocopherol that is of importance but that structural aspects are equally or perhaps of greater importance. As a result, structural features (or the lack of them), such as methyl groups on the ring, stereochemistry of the chiral centres, *etc.*, are of significance in terms of biological activity.

It has been shown that the configuration at C-2 has a significant effect on the 3D structure of the molecule. For example, changing the configuration from R to S at C-2 results in the angle between the chromanol ring and the phytyl chain being inverted. This in turn affects the biological activity.<sup>53</sup>

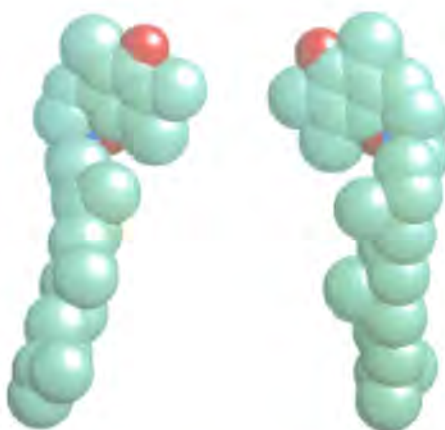


Figure 1.18 – Space-filling diagram showing RRR- $\alpha$ -tocopherol (left) and the synthetic SRR- $\alpha$ -tocopherol (right). Grey = carbon atoms, Blue = C-2, Red = Oxygen.

## 1.7 Drug Delivery

Drug delivery is of immense importance and research in this area has been gaining momentum over the last decade. In particular, the area of polymer therapeutics has come to the fore and is an area of intensive research. As discussed recently by Duncan

*et al*, recent years have seen a shift in how polymers are used in biomedical applications.<sup>59</sup> Previously their applications were limited to biomedical material type uses such as prostheses, medical devices, contact lenses, dental materials and pharmaceutical excipients. It is only in recent years that polymer-based medicines have found their way into routine clinical practice.<sup>59-61</sup> Fortunately and importantly scientific research has demonstrated that many polymer-based therapeutics previously consigned to the scrap heap can in fact pass both regulatory and industrial development scrutiny. It is now widely accepted that *e.g.* synthetic polymers offer a potential route towards more effective treatments of life threatening or debilitating diseases.<sup>59, 62</sup>

In essence, much of the motivation behind the study of targeted delivery techniques stems from the desire to reduce the doses of administered drugs. In no field is this more important than in cancer therapy. The Holy Grail in this area is to deliver a highly cytotoxic drug to the cancer cells and for only those cells to be destroyed. To date there have been many publications detailing targeted delivery techniques for various applications such as the treatment of hepatitis,<sup>63</sup> gene therapy<sup>64, 65</sup> and for treating liver tumours.<sup>66, 67</sup>

It is desirable, in the context of this thesis, to be able to produce linear polymers which will be site-specific to a receptor on the surface of sperm cells. Among the most effective recognition species are moieties such as antibodies, hormones and sugars.<sup>68</sup> Before this concept is discussed in more detail, it is worth considering a more passive approach to drug targeting.

### **1.7.1 The Enhanced Permeability and Retention (EPR) Effect**

Although (as mentioned earlier) this thesis will consider an active targeting approach, other studies have focussed on passive targeting – exploiting the “enhanced permeability and retention effect” (EPR effect). This phenomenon was discovered by Maeda *et al* while working on therapies designed to treat liver cancer.<sup>67, 69, 70</sup>

The EPR effect is the focus of many groups aiming for novel cancer therapies suitable for treating common solid tumours such as breast, prostate, lung and colon cancers<sup>66</sup> (in

the UK in 1998 more people died of cancer than any other disease;<sup>66</sup> in 2006, cancer affects one in three people in the UK and kills one in four<sup>71</sup>). Primary and secondary metastatic tumours arise from a single abnormal cell. As the tumour grows and exceeds a size of around 150-200  $\mu\text{m}$ , vascularisation must be increased.<sup>66</sup> It has subsequently become apparent that tumour vessels have irregular architectures compared with normal cells. Tumour cells are poorly formed with thin walls, and are inherently 'leaky' which in turn can lead to extravasation of macromolecular and liposomal drug carriers.<sup>66</sup>

This phenomenon of accumulation of macromolecules (or other nanoparticles) within solid tumours was largely overlooked for several years, and only the pioneering work of Maeda *et al*<sup>70, 72</sup> (mentioned above) as well as work by Jain *et al*,<sup>73</sup> started to change this.<sup>74</sup> These studies provided a detailed insight into the characteristics of angiogenesis *i.e.* hypervascularity, defective vascular architecture, and impaired lymphatic drainage.<sup>59, 66, 71, 74</sup>

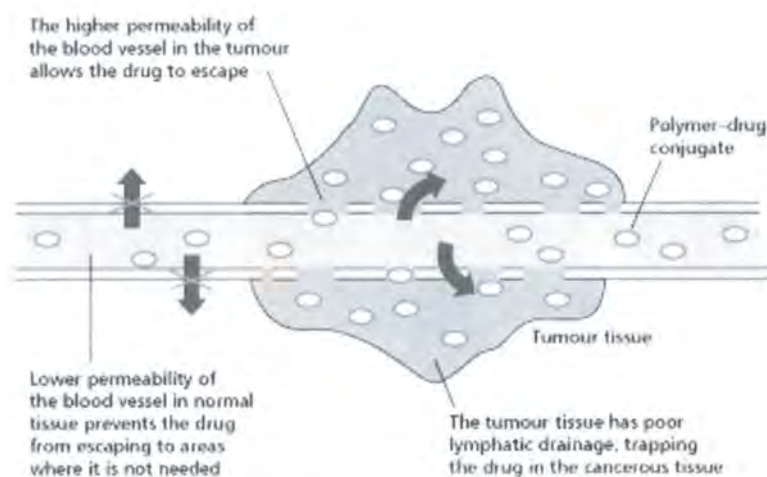


Figure 1.19 - Diagram illustrating the 'enhanced permeability and retention' (EPR) effect<sup>75</sup>

Generally, low molecular weight entities can diffuse within both normal and tumour tissues, *via* the blood capillaries. However, while macromolecules are unable to pass into normal tissue, they are able to enter tumour tissues, in part due to their 'leakiness' (see Figure 1.19). The inherent poor lymphatic drainage (alluded to earlier) means that not only are macromolecules able to enter the tumour tissue, but also tend to accumulate there.<sup>59, 66, 71, 74</sup>

The size of macromolecular drugs/drug carriers is therefore of fundamental importance, and it has been demonstrated that their molecular weights must exceed 20 kDa (most work in recent years has focussed on materials with molecular weights ranging from 20 – 200 kDa).<sup>74</sup> Plasma circulation time is also an important factor, not to mention renal clearance (the threshold of renal clearance is typically 30 – 50 kDa). Indeed some pre-clinical studies have shown that factors such as the molecular weight, charge, conformation, hydrophobicity *etc.* are highly influential in the degree of accumulation within the tumour and on its pharmacokinetic profile.<sup>74</sup> Pre-clinical studies have also demonstrated a correlation between tumour size and uptake of polymers; it appears that smaller tumours accumulate more polymer than larger tumours.<sup>74, 76</sup>

Nevertheless, there is still much to be understood about the influence of the many different factors affecting EPR-mediated uptake. Generally however, polymers should have a neutral charge and a molecular weight above *c.a.* 30 kDa since this ensures a long plasma half-life which is of particular importance to ensure significant accumulation in the tumour.<sup>59, 71, 74</sup>

This simple passive targeting is in contrast to the research being addressed by many others (and indeed this author) on specific targeting, be that *via* antibodies, carbohydrates, peptides *etc.* Although there is some hope that these two approaches (EPR/specific targeting *i.e.* passive and active targeting) can be combined.<sup>71</sup> So far, only one polymer of this type has progressed to clinical trials.<sup>77</sup>

It is noteworthy that at the turn of the last century, the work by Paul Ehrlich on the use of synthetic small molecules as chemotherapy was initially treated with much scepticism. A similar degree of scepticism has initially greeted researchers focussing on polymer-based products over the last 20 or so years. However it has been observed recently that the tide may have turned, since in 2002/03 the FDA approved more macromolecular drugs and drug delivery systems than small molecules as new medicines.<sup>59</sup>

### **1.7.2 Polymeric Drug Delivery<sup>78</sup>**

The importance of active drug targeting has been recognised for almost a century.<sup>78</sup> Since then, the conjugation of drugs to other non-active compounds, in order to improve the efficacy by affecting their physiochemical and pharmacokinetic properties, has been considered.<sup>79</sup> This was taken a stage further in the 1970s when Ringsdorf proposed the idea of polymeric drug delivery.<sup>80</sup> Initially, many of these ideas and concepts were regarded with scepticism, however nowadays “polymeric prodrug” is a popular term and the area is of increasing interest across a range of scientific disciplines.

There are a number of reasons for the increasing interest in polymeric drugs/prodrugs. The main interest is because they can overcome many of the problems associated with conventional drugs. From the time that a (low molecular weight) drug is administered, until it is excreted from the body, it will encounter many physiological processes that will have effects on its concentration and interaction within the body. It may undergo biotransformation(s) or may become bound to tissues, and regardless of whether the drug is free or protein bound, it will ultimately become distributed throughout the body rather than being concentrated solely at the site of action. Consequently, one must increase the dose above the therapeutic level in order to achieve the required therapeutic effect.

A useful, although perhaps over-simplified, model for polymeric drugs was postulated in 1975 by Ringsdorf.<sup>80</sup> In general terms, Ringsdorf’s model describes the polymeric carriers discussed herein, and these will be examined in more detail in later chapters. The model can be considered schematically as shown in Figure 1.20.

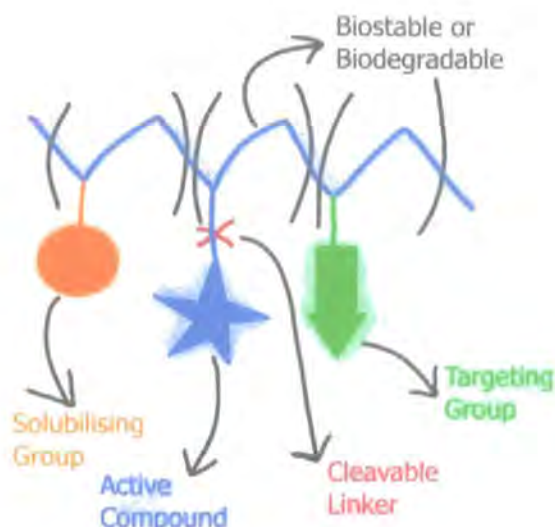


Figure 1.20 – Components of a polymeric drug as proposed by Ringsdorf<sup>80</sup>

Such polymers can be synthesised by statistical terpolymerisation or indeed by block copolymerisation (it will be discussed later why terpolymerisation can be advantageous).

We can consider each of the three components in turn.

- (1) Solubiliser: this part of the polymer can be tuned to give water<sup>††††</sup> or lipid<sup>§§§§</sup> solubility. Often water solubility is preferred so that the polymer is soluble in aqueous physiological media.
- (2) Drug: this must be fixed in such a way as not to affect adversely the activity but also so that it can be cleaved easily and the drug regenerated *in situ*.
- (3) Homing Device: this is the key to delivering the drug with high specificity. However, the homing device can be substituted with a non-specific resorption enhancer that helps to control the distribution of the polymer within the system.

Ultimately, polymeric drug delivery systems can be categorised into two discrete groups – ‘controlled drug release systems’ and ‘targeted drug delivery systems’. These

<sup>††††</sup> Achieved by using monomers such as N-vinylpyrrolidone, acrylamides, sulphoxide containing acrylates, *etc.*

<sup>§§§§</sup> Monomer units bearing long alkyl chains.

categories arise from the difference between the site of drug release and the site of drug action. Generally a 'controlled drug release system' would deliver the drug into the system in a controlled fashion, at a rate controlled by some physical or chemical response to an action, for example, the use of hydrogels to regulate insulin levels in patients with diabetes. As a result of this, the site of drug release and that of drug action are different. On the contrary, 'targeted delivery systems' (which are of relevance in this thesis) can deliver the active drug directly (or very close) to the site of action, avoiding distribution of the active component throughout the whole system, thus allowing lower dosage levels to be administered.

By lowering dosage, one can expect a reduction in adverse side effects or toxicity, and indeed low molecular weight drug compounds which were previously too toxic due to the dosage levels required to produce a therapeutic effect, could be reconsidered as potential drug candidates.<sup>81</sup>

### 1.7.3 Receptor Mediated Endocytosis<sup>82, 83</sup>

Cells uptake extracellular material *via* endocytosis and phagocytosis. Endocytosis can be split into several categories:

- Fluid phase endocytosis (or pinocytosis)
- Recapture
- Receptor mediated endocytosis

It is the latter that is of interest in this text.

Receptor mediated endocytosis (RME) is responsible for the uptake of a number of species, including: metabolic ligands; opportunistic ligands (*e.g.* protein toxins and viruses); growth factors; lysosomal hydrolases; immunoglobulins & asialoglycoproteins; the uptake of particles is by phagocytosis.

The ligand in question can either be destined for lysosomal hydrolysis, or diacytosis (return to the cell surface) for delivery to storage granules or for transcellular transport

(transcytosis). The receptor itself can follow a similar fate pattern in that it can end up in the lysosome where it will be destroyed, return to the surface to mediate further internalisations, or become involved in transcellular transport.

A typical cycle of ligands and receptors is shown below (Figure 1.21) where:

(R) = Receptor

(L) = Ligand

L = Lysosome

Subscripts 's', 'ex', & 'i' = surface, external, & internal respectively.

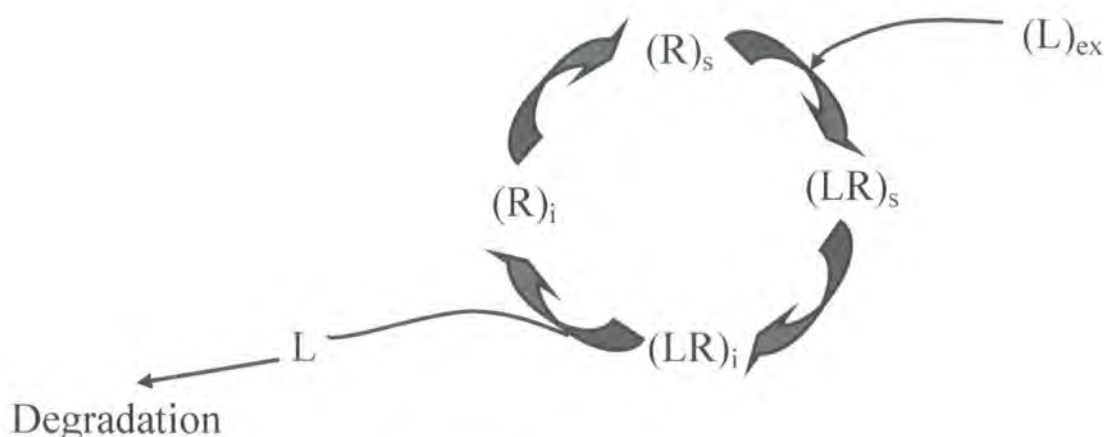


Figure 1.21 - Typical ligand/receptor cycle

Large molecules, *e.g.* proteins (or polymers), mainly enter cells *via* RME.<sup>84</sup> It is a multi-stage process and is sensitive to environmental factors such as temperature. Cells maintained between 0-4°C do not internalise significant amounts of ligands, however when cells are at elevated temperatures (*e.g.* 37°C) internalisation occurs much more rapidly.<sup>84</sup> As mentioned, the endocytic pathway is multi-step and in the first instance relies on the existence of receptors on the cell surface.

Surface receptors do not only facilitate the first stage of internalisation, they also do so with high specificity. The efficiency of cell receptors is dependent upon the quality of the ligand binding. The interaction of a binding site and a ligand will be non-covalent, however still of relatively high affinity. Therefore, it follows that there must be configurational complementarity between the two, *i.e.* the interaction is stereo-specific.

This concept was the brain-child of Emile Fischer, who proposed the “Schloss und Schussel” (lock & key) analogy, and has subsequently been cited on many occasions.<sup>35, 85-89</sup>

There are three important factors of both the receptor and the ligand for selective binding to take place:

- i) molecular geometry
- ii) reactive group positioning
- iii) configurational flexibility

Typically the forces involved in the interaction will be Van der Waals forces, hydrogen bonds and ionic interactions (or more generally electrostatic interactions). Although these do not themselves ensure high specificity - they do help - since as the distance between the ligand and the receptor decreases, the attractive forces will increase.

The importance of the flexibility of the ligand should not be underestimated, since the “docking” of the two will not be quite as straightforward as the “lock and key” principle.

Once a ligand has docked with a surface receptor, the internalisation process continues. The ligand-receptor complex enters so called (clathrin) “coated pits” on the cell surface and the cell membrane closes around the docked species to form an enclosed vesicle. This is then invaginated and forms the “early endosome” (see Figure 1.22). When several of these are fused together, the endosome (or mature endosome) is created. Initially these endosomes may still be clathrin coated, however they quickly lose this coating. Endosomes typically have a pH of between 5 and 6, and are deficient in acid hydrolase content. From the endosomes the ligand-receptor complex then moves to the lysosome. The mechanism by which this happens has been studied in the context of macrophages and two models have been proposed<sup>90</sup>. The first model proposes that the content of the endosome is concentrated, perhaps by membrane withdrawal, and then acquires lysosomal hydrolases by fusion with lysosomes. The second model suggests that lysosomes and endosomes communicate with each other *via* the passage of vesicle populations from one to the next. Regardless of which model is correct, it is evident that the transfer of material does occur. This must necessitate that membrane

withdrawal occurs yet only very small amounts of lysosomal hydrolases are found to leak into the surrounding medium, which is very surprising.

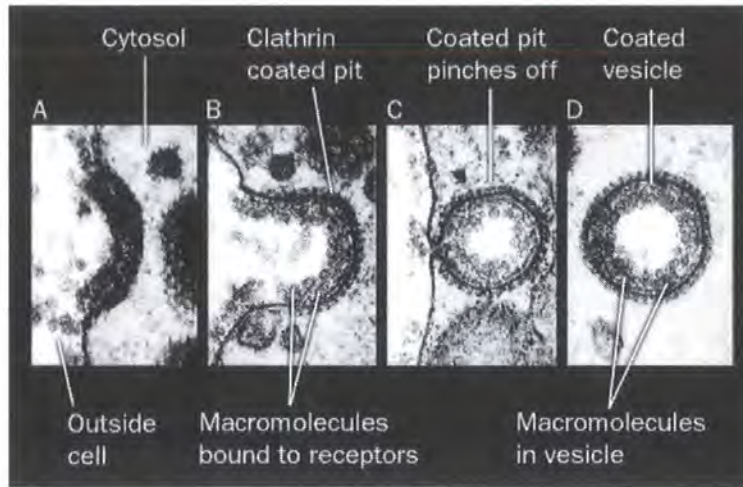


Figure 1.22 - Formation of coated pits during endocytosis<sup>91</sup>

Once the endocytosed material has entered the lysosome, it can be digested. Lysosomes typically have a lower pH than endosomes (4.5-5) and are rich in enzymes (*e.g.* esterases, phosphatases, peptidases, glycosidases, oxidoreductases, *etc.*).

As mentioned earlier, the receptor can either be recycled, or destroyed. One of the best characterised scenarios is that of the asialoglycoprotein receptor.<sup>39, 40, 92</sup> Here, both the ligand and the receptor are internalised to endosomes. Due to the acidity they are then separated; the receptor is conveyed back to the surface and the ligand is sent on to the lysosome.

A simplified diagram depicting a typical RME cycle is shown below in Figure 1.23.

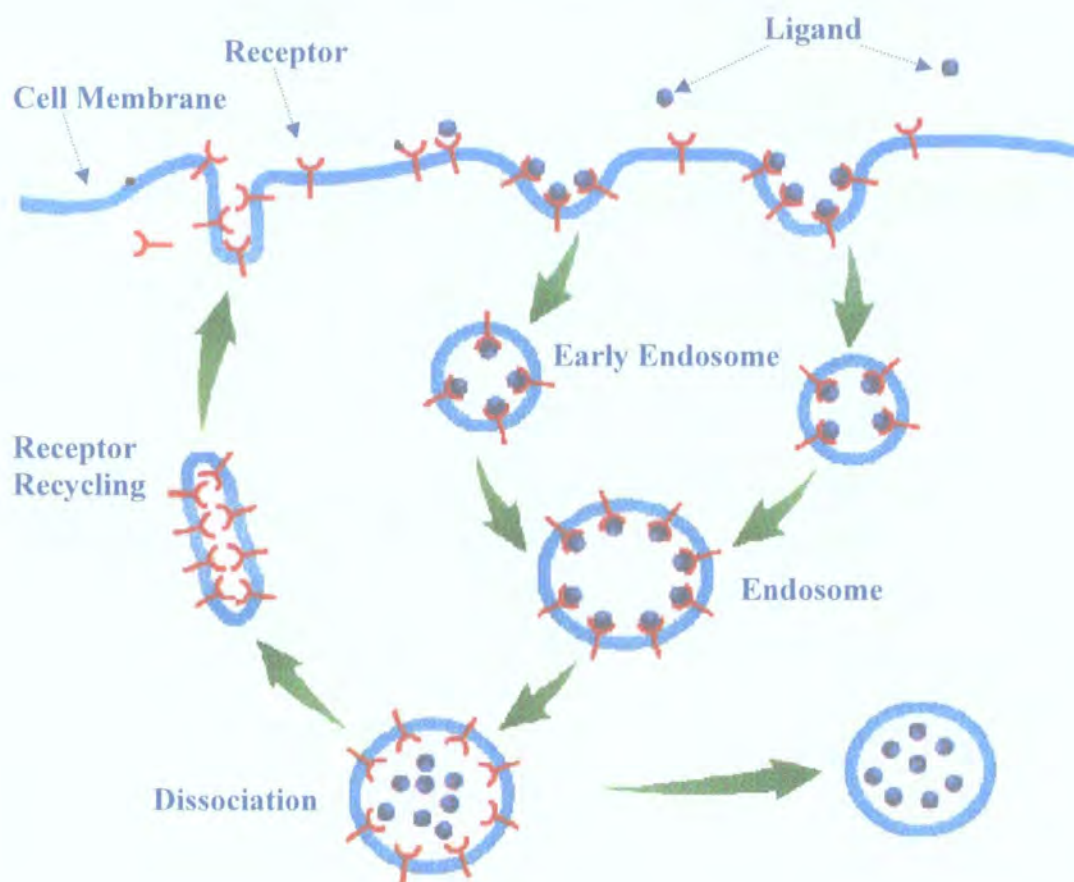


Figure 1.23 - Receptor Mediated Endocytosis<sup>21</sup>

#### 1.7.4 Glycodendrimers

This thesis largely focuses on the use of linear glycopolymers, however this research area is thriving, and a number of fascinating morphologies exist. One such example is that of dendrimers. These are branched synthetic polymers that have shown potential in a number of biomedical applications.<sup>93, 94</sup> The properties of dendrimers are substantially different from their linear counterparts and as such their uses/behaviour should be considered independently. Indeed aspects such as pharmacokinetics or biocompatibility can be tuned carefully through regulation of their synthesis, allowing composition/molecular weight to be regulated.<sup>94</sup>

Structurally, dendrimers are tree like (*dendra* – Greek for tree), having multiple perfect branches emanating from a central core, and can be synthesised *via* a divergent or convergent approach (see Figure 1.24).

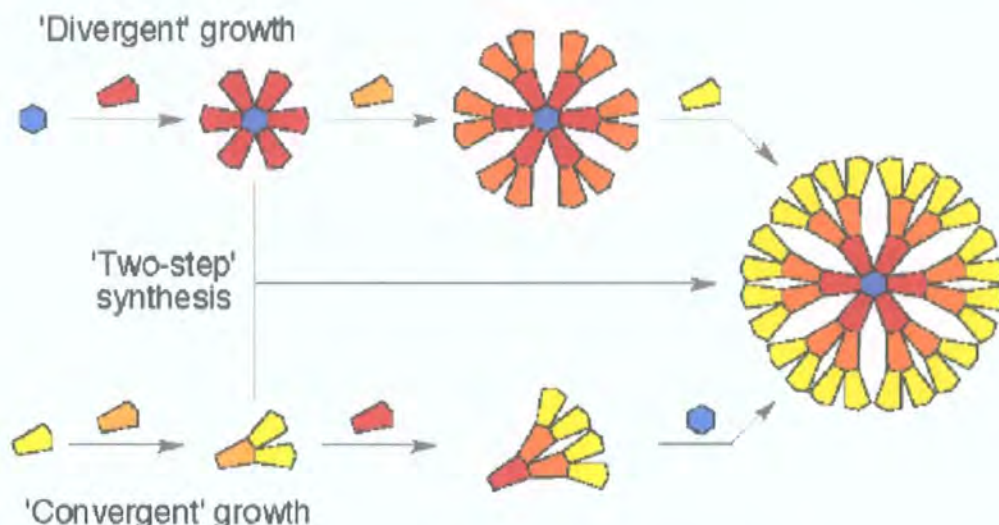


Figure 1.24 - Schematic showing dendrimer formation *via* divergent and convergent growth<sup>95</sup>

Dendrimers can be based on a wide range of chemistries, which can in turn influence factors such as solubility, biological activity *etc.* Since the properties of dendrimers often differ significantly from linear polymer properties, they do have several beneficial attributes for biomedical applications,<sup>94</sup> *e.g.*:

- Tuneable pharmacokinetic/biodistribution properties through control of dendrimer size and conformation.
- High ligand density – as dendrimer generation increases so does the multivalent ligand density at the surface. This can strengthen ligand-receptor binding and improve targeting.
- High structural/chemical homogeneity. This facilitates reproducibility of data (pharmacokinetic and material characterisation).
- Can be functionalised with multiple copies of drugs *etc.*, allowing drug loading to be altered precisely.
- Controlled degradation achieved *via* careful choice of dendrimer chemistry.

Dendrimers may themselves exhibit therapeutic properties, *e.g.* as described by Supattapone *et al*, where polyamidoamine (PAMAM) dendrimers were shown to stimulate the removal of prion proteins present in infected cells.<sup>96</sup> Careful construction of dendritic materials can also afford materials displaying multivalent ligands on the dendritic polymer surface. Such materials have been shown to inhibit multivalent

binding between *e.g.* cells, viruses, bacteria *etc.*<sup>94</sup> Of particular interest however is the work by Davis *et al*, on glycodendrimers, and ultimately on a new class of materials – ‘glycodendriproteins’.

Glycodendriproteins are synthetic glycoprotein mimic enzymes, which in work described by Davis *et al*, are capable of inhibiting bacterial aggregation.<sup>97</sup> Small molecules are not viable as blockers of bacterial adhesive events since as monovalent carbohydrate ligands are poorly recognised by lectins, the therapeutic concentrations required would be unrealistically high.<sup>97</sup> It has been shown that glycodendrimers can mimic the branched carbohydrates found on glycoproteins. When such entities are subsequently attached to a protein, this gives rise to the class of materials ‘glycodendriproteins’ mentioned earlier.<sup>97</sup>

Glycodendriproteins were constructed by first synthesising carbohydrate bearing dendrons which were then attached *via* a cysteine group in the protein-degrading proteinase, subtilisin (from *Bacillus lentus* (SBL)).<sup>93, 97</sup> The pathogen being targeted (*Actinomyces naeslundii*) binds to  $\beta$ -D-galactose, therefore galactose was the carbohydrate of choice attached to the glycodendriprotein.<sup>93, 97</sup> These galactose bearing synthetic glycoproteins were first tested using a peanut agglutinin (PNA) model to mimic the display of surface lectins found on the bacterial surface. Increasing galactose antennae correlated with increasing affinity.<sup>97</sup>

Davis *et al*, went on to demonstrate the ability to inhibit the function of the galactose-binding pathogen (Gram-positive *A. naeslundii*),<sup>93, 97</sup> which has been shown to aggressively colonise oral cavities,<sup>98</sup> surgical prostheses<sup>99</sup> and internal cavities.<sup>97, 100</sup> Studies demonstrated that a bi-antennary carbohydrate structure was most effective at inhibiting bacterial binding. Three properties were found to be key in ensuring optimal inhibition: (i) the protein-degrading activity of the construct, (ii) multi-antennary carbohydrate display, and (iii) galactose presentation. Glycodendriproteins can also be easily modified with alternative carbohydrates for alternative lectin or pathogen targets.<sup>93, 97</sup>

Other similar examples have been reported for the treatment of hyperglycaemia in diabetic patients<sup>101</sup> and for the potential treatment of influenza.<sup>102</sup>

### 1.7.5 Glycopolymers

The interest in carbohydrate containing polymers, known as glycopolymers has been increasing rapidly in recent years. The term *glycopolymers* can be used to describe both natural and synthetic carbohydrate containing polymers. They are in many ways analogous to polysaccharides, but there is a fundamental difference between the two. Glycopolymers consist of a polymer backbone with sugar side groups, whereas polysaccharides have sugars in the backbone. Some examples of naturally occurring polysaccharides include: starch, chitin, cellulose *etc.* Carbohydrates are essential components of life, not simply as sources of energy, but as biomolecules involved in specific recognition events. Their intrinsic properties such as hydrophilicity and biocompatibility make their use in the preparation of biocompatible polymers, with pharmacological and biological properties, almost inevitable.<sup>103, 104</sup>

Glycopolymers can be synthesised in a number of ways. One method is simply to couple a polymerisable group (*e.g.* a vinyl functional compound) to a sugar. This tends to require the protection of the sugar hydroxyl groups. However, there have been other methods reported, which use linkers between the saccharide and the vinyl functionality which allow preparation of the monomer without the need for protecting groups. The advantage of this method is that the syntheses tend to be less time consuming and less expensive.<sup>105</sup>

Glycopolymers have a number of potential uses commercially. They can be used as thickeners, flocculants, polymeric detergents and if crosslinkers are introduced, they can be used as so called “superabsorbers”.<sup>27</sup>

It is, however, the properties of biocompatibility, recognition and hydrophilicity that are attractive for the application discussed herein. These properties make glycopolymers suitable for biomedical applications such as drug delivery.<sup>106</sup>

Below are some examples of how synthetic glycopolymers can be prepared.

### 1.7.5.1 Free radical polymerisation

The advantage of free radical polymerisation is that it is a well established, robust technique. There is wide scope for the use of various solvents/monomers and the initiators are generally inexpensive and readily available. However, there are a number of drawbacks. The polymers tend to be very polydisperse ( $PD > 2$ ), end groups are not easily controlled, and it is difficult to produce materials of a specific architecture. Despite these problems, a large number of glycopolymers have been synthesised in this way.<sup>35, 107</sup>

The first such synthesis reported was in 1978 by Horejsi and co-workers.<sup>108</sup> They synthesised copolymers of acrylamide and allyl glycosides which showed similar binding activities to natural polysaccharides.

In the early 1990s, Kitazawa *et al.* described a method for producing acrylic monomers with pendant saccharide moieties. These were easily polymerised by standard free radical methods.<sup>109</sup>

During the ensuing years, a large number of monomers containing mono, di and trisaccharides suitable for free radical polymerisation have been synthesised and their properties investigated.<sup>35, 107</sup>

More recently, the synthesis of polymethacrylates bearing  $\beta$ -glucose and  $\beta$ -galactose moieties by free radical polymerisation has been reported.<sup>22, 103, 104, 109-111</sup> The synthesis of these monomers *via* the acetyl protected sugars ensures total  $\beta$ -selectivity due to neighbouring group participation of the acetyl groups at O-2. Both pre-polymerisation and post-polymerisation de-acetylation reactions were described, with the former giving better defined materials.

There are many other examples in the literature and this area is likely to continue to develop.

### 1.7.5.2 Ionic polymerisation

Living ionic polymerisation (either cationic or anionic) offers many advantages over conventional free radical polymerisation, and it is no surprise that many glycopolymers have been synthesised in this way.<sup>35, 107</sup> The attractiveness of being able to synthesise polymers of narrow PD ( $<1.2$ ), with well defined architectures and pre-determined molecular weights, is huge. Despite these benefits, both techniques are littered with drawbacks. Anionic polymerisation suffers from a need for very dry solvents, high purity reagents, monomers that are free of acidic protons or electrophilic substituents, sensitivity to oxygen and low reaction temperatures. Cationic polymerisation suffers from similar problems, in addition to being unstable due to side reactions. Nevertheless there have been many successful reactions reported in the literature.<sup>35, 107</sup>

### 1.7.5.3 Ring opening polymerisation (ROP)

The ring opening polymerisation of heterocyclic compounds, by either anionic or cationic routes, is a feasible method of glycopolymer synthesis.

To date the only group to have published examples of anionic ROP (AROP) of glycomonomers is that of Aoi *et al.*<sup>112</sup> They used glycosylated N-carboxyanhydrides (NCAs) to produce glycopolymers.

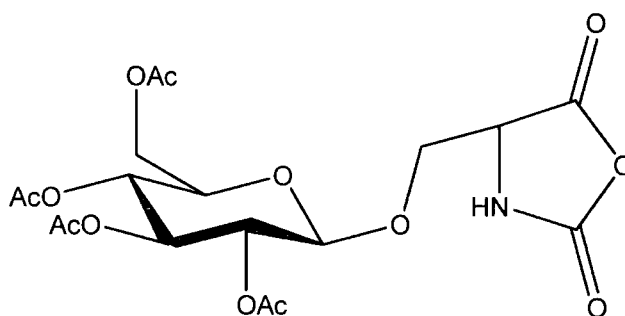


Figure 1.25 - Glycosylated NCA<sup>35</sup>

Such monomers have also been polymerised *via* cationic ROP (CROP).<sup>35</sup>

#### 1.7.5.4 Ring opening metathesis polymerisation (ROMP)

The attraction of ROMP is its ability to produce well-defined polymers with varying architectures. It is also possible, by using Grubbs' catalyst, to have a living polymerisation. Nevertheless, there are a number of drawbacks to this method: it is sensitive to both  $N_2$  and  $O_2$  gases; there are only a few suitable monomers currently available; and the removal of the transition metal catalyst could be an issue (especially for biological applications).

Grubbs and Fraser have demonstrated the synthesis of several sugar bearing copolymers *via* ROMP. Polymerisations were carried out at  $50^\circ C$ , which yielded polymers of narrow PD.<sup>113</sup>

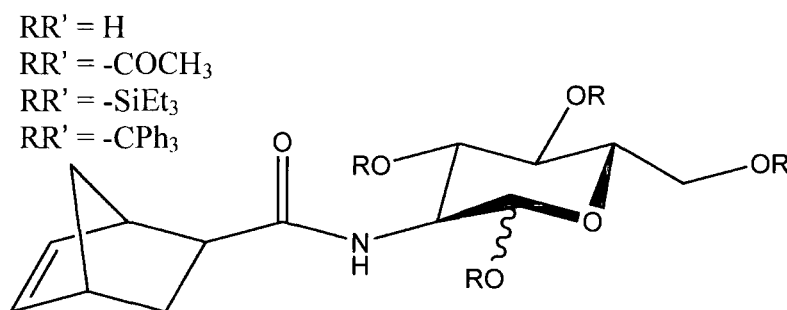


Figure 1.26 - Glycosylated norbornene derivatives<sup>35</sup>

Glucose derivatives of 7-oxanorbornene have been synthesised by Mortell *et al.*<sup>114-116</sup> and have been shown to bind to the lectin Concanavalin A.

#### 1.7.5.5 Nitroxide mediated radical polymerisation (NMRP)

Thus far there have been only a few examples in the literature of glycopolymers synthesised *via* NMRP. The first example of this was from Ohno *et al.*<sup>117</sup> who synthesised two glycomonomers suitable for NMRP.

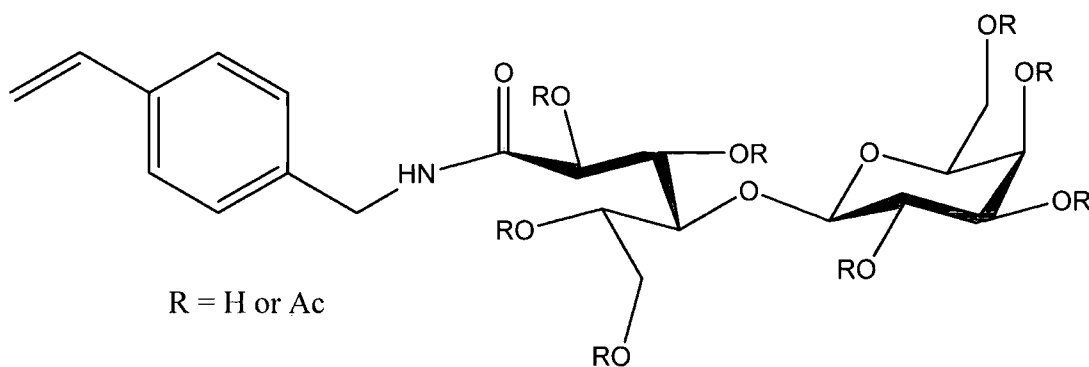


Figure 1.27 - Glycosylated monomer for NMRP<sup>35</sup>

The polymerisation of the unprotected monomer was found to be controlled, however it did not proceed to high conversion. In contrast, the acetylated monomer was also controlled and had a conversion of ~90%. The difference between the two was attributed to retardative transfer to the hydroxyl groups of the unprotected monomer during polymerisation.

Other groups continue to research the area of NMRP of glycosylated monomers.

#### 1.7.5.6 Copper-mediated living radical polymerisation (CMLRP)

As in the case of NMRP, there have not been many examples of glycopolymers produced using this technique. Work by Ohno *et al.*<sup>118</sup> resulted in controlled polymerisation of 3-*O*-methacryloyl-1,2:5,6-di-*O*-isopropylidene-D-glucofuranose (MAIpGlc).

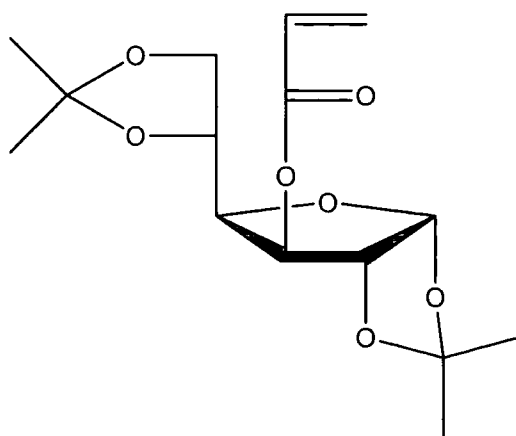


Figure 1.28 - Glycosylated monomer for CMLRP<sup>35</sup>

However, in the context of this report, the work of Li *et al.*<sup>103, 110</sup> who reported the controlled polymerisation of 2-(2',3',4',6'-tetra-*O*-acetyl- $\beta$ -D-glucopyranosyloxy)ethyl acrylate (AcGlcEMA) is of greater relevance. After polymerisation the polymer was deprotected using sodium methoxide, and found to have a PD of 1.4.

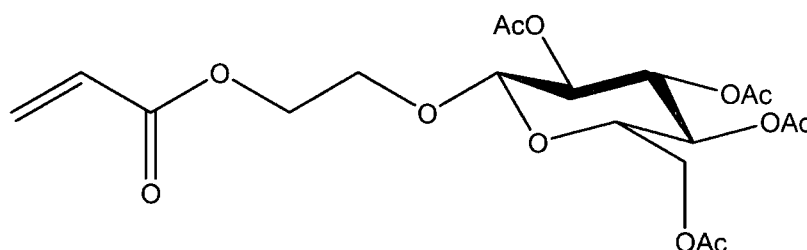


Figure 1.29 - 2-(2',3',4',6'-tetra-*O*-acetyl- $\beta$ -D-glucopyranosyloxy)ethyl acrylate (AcGlcEMA)<sup>35</sup>

The first example of CMLRP of unprotected sugar monomers was reported by Narain and Armes,<sup>119</sup> using 2-gluconamidoethyl methacrylate. This monomer was polymerised under aqueous conditions at ambient temperatures, and delivered well-defined materials of low PD (~1.5).

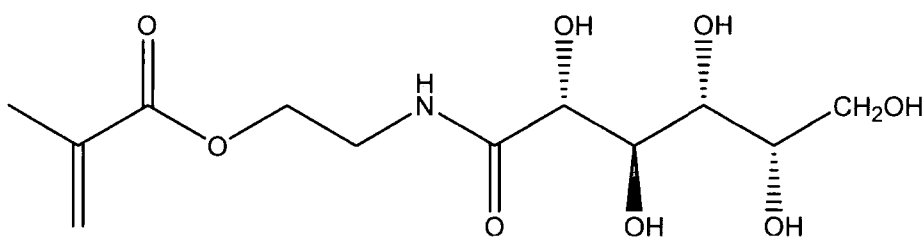


Figure 1.30 - 2-Gluconamidoethyl methacrylate (GAMA)<sup>35</sup>

#### 1.7.5.7 Reversible addition-fragmentation chain transfer (RAFT) polymerisation

In general terms, RAFT polymerisation has been a very versatile technique suitable for a wide range of monomers, functionality, and conditions – even in aqueous media.

Lowe *et al.*<sup>120</sup> reported the RAFT polymerisation of 2-methacryloxyethyl glucoside under aqueous conditions and without the use of protecting group chemistry. They achieved a well defined material of controlled molecular weight and low PD.

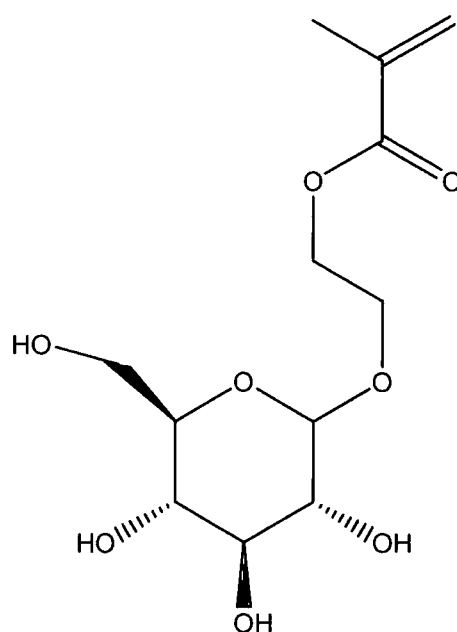


Figure 1.31 - 2-methacryloxyethyl glucoside (mixture of anomers)

They were also able to synthesise block copolymers, indicating that re-initiation was possible and hence that the polymerisation had living character.

## 1.8 Summary

The area of targeted delivery is an increasingly important one, across a range of applications and scientific disciplines. Whilst the majority of examples cited in the literature focus on targeting cells within a host biological system, such as the human body, this report focuses on a more unusual choice of cell type.

Glycopolymers are only one solution to cell targeting, and many other examples of targeted delivery use alternative strategies such as anti-bodies or polypeptides exist.

The aim of this research project was to design a glycopolymer containing vitamin E moieties that was capable of delivering vitamin E to boar spermatozoa through receptor mediated endocytosis. Once internalised the polymer would be attacked by cellular enzymes, releasing vitamin E molecules within the cells. It was hoped and expected that this enhanced cellular concentration of vitamin E should result in the cells

exhibiting an increased resistance to oxidation. Such an invention is desirable for several reasons:

- Cellular oxidation ultimately leads to apoptosis
- Vitamin E is insoluble in aqueous media (boar spermatozoa are suspended in an aqueous based medium)
- Lectin-sugar interactions can be highly specific resulting in targeted uptake

The results of this research project are detailed throughout the remaining chapters of this thesis.

## 1.9 References

1. Singer, J. *Annu. Rev. Biochem.* **1974**, 43, 805.
2. Wallach, D. F. H., *The Plasma Membrane: dynamic perspectives, genetics and pathology*. English Universities Press: London, **1972**.
3. Singer, S. J.; Nicolson, G. L. *Science* **1972**, 175, (4023), 720-.
4. Geibel, G. (1999) *The Cell Membrane*, [http://sun.menloschool.org/~cweaver/cells/c/cell\\_membrane/](http://sun.menloschool.org/~cweaver/cells/c/cell_membrane/), [Accessed 2006]
5. Yovich, J. L., Grudzinskas, J.G., *Gametes - The Spermatozoon*. Cambridge University Press: Cambridge, **1995**.
6. Hafez, E. S. E., Hafez, B., *Reproduction in Farm Animals*. 7th ed.; Lippincott Williams & Wilkins: Baltimore, **2000**.
7. Ho, H. C.; Suarez, S. S. *Reproduction* **2001**, 122, (4), 519-526.
8. Rikmenspoel, R. *J. Exp. Biol.* **1984**, 108, (Jan), 205-230.
9. Clarke, R. N.; Johnson, L. A. *Gamete Res.* **1987**, 16, (3), 193-204.
10. Grant, S. A.; Long, S. E.; Parkinson, T. J. *J. Reprod. Fertil.* **1994**, 100, (2), 477-83.
11. Evenson, D. P.; Thompson, L.; Jost, L. *Theriogenology* **1994**, 41, (3), 637-651.
12. Ash, K. L.; Berger, T.; Horner, C. M.; Famula, T. R. *Theriogenology* **1994**, 42, (7), 1217-1226.
13. Fazeli, A. R.; Holt, C.; Steenweg, W.; Bevers, M. M.; Holt, W. V.; Colenbrander, B. *Theriogenology* **1995**, 44, (1), 17-27.
14. Xu, X.; Foxcroft, G. R. *Reprod. Domestic Anim.* **1996**, 31, (1), 31-36.
15. Johnson, L. A.; Weitze, K. F.; Fiser, P.; Maxwell, W. M. C. *Anim. Reprod. Sci.* **2000**, 62, (1-3), 143-172.
16. Krueger, C.; Rath, D.; Johnson, L. A. *Theriogenology* **1999**, 52, (8), 1363-1373.
17. Rath, D., *Personal Communication*. Fleming, C., **2002**
18. Bertozzi, C. R.; Kiessling, L. L. *Science* **2001**, 291, (5512), 2357-2364.
19. Koenigs, W., Knorr, E. *Berichte* **1901**, 34, 957.
20. Davis, B. G. *J. Chem. Soc., Perkin Trans. 1* **2000**, (14), 2137-2160.
21. Ambrosi, M., *PhD Thesis*, University of Durham, **2002**

22. Ambrosi, M.; Batsanov, A. S.; Cameron, N. R.; Davis, B. G.; Howard, J. A. K.; Hunter, R. *J. Chem. Soc., Perkin Trans. 1* **2002**, (1), 45-52.
23. Cho, C. W.; Cho, Y. S.; Lee, H. K.; Yeom, Y. I.; Park, S. N.; Yoon, D. Y. *Biotechnol. Appl. Biochem.* **2000**, 32, (1), 21-26.
24. Lee, R. T.; Shinohara, Y.; Hasegawa, Y.; Lee, Y. C. *Biosci. Rep.* **1999**, 19, (4), 283-292.
25. Neumann, D.; Lehr, C. M.; Lenhof, H. P.; Kohlbacher, O. *Adv. Drug Delivery Rev.* **2004**, 56, (4), 437-457.
26. Klein, J.; Kunz, M.; Kowalczyk, J. *Makromol. Chem.* **1990**, 191, (3), 517-28.
27. Wulff, G.; Schmid, J.; Venhoff, T. *Macromol. Chem. Phys.* **1996**, 197, (1), 259-274.
28. Kopecek, J.; Kopeckova, P.; Brondsted, H.; Rathi, R.; Rihova, B.; Yeh, P. Y.; Ikesue, K. *J. Controlled Release* **1992**, 19, (1-3), 121-30.
29. Murata, J.-i.; Ohya, Y.; Ouchi, T. *Carbohydr. Polym.* **1996**, 29, (1), 69-74.
30. Bahulekar, R.; Tokiwa, T.; Kano, J.; Matsumura, T.; Kojima, I.; Kodama, M. *Carbohydr. Polym.* **1998**, 37, (1), 71-78.
31. Francis Suh, J. K.; Matthew, H. W. *Biomaterials* **2000**, 21, (24), 2589-2598.
32. Kim, S. H.; Goto, M.; Cho, C. S.; Akaike, T. *Biotechnol. Lett.* **2000**, 22, (13), 1049-1057.
33. Petronio, M. G.; Mansi, A.; Gallinelli, C.; Pisani, S.; Seganti, L.; Chiarini, F. *Chemotherapy* **1997**, 43, (3), 211-217.
34. Yoshida, T.; Akasaka, T.; Choi, Y.; Hattori, K.; Yu, B.; Mimura, T.; Kaneko, Y.; Nakashima, H.; Aragaki, E.; Premanathan, M. *J. Polym. Sci., Part A: Polym. Chem.* **1999**, 37, (6), 789-800.
35. Ladmiral, V.; Melia, E.; Haddleton, D. M. *Eur. Polym. J.* **2004**, 40, (3), 431-449.
36. Yamazaki, N.; Kojima, S.; Bovin, N. V.; Andre, S.; Gabius, S.; Gabius, H. J. *Adv. Drug Delivery Rev.* **2000**, 43, (2-3), 225-244.
37. Varki A., e. a., *Essentials of Glycobiology*. Cold Spring Harbor Lab. Press: New York, **1999**.
38. Gesner, B. M.; Ginsburg, V. *Proc. Natl. Acad. Sci. U. S. A.* **1964**, 52, (3), 750-5.
39. Ashwell, G.; Morell, A. G. *Adv. Enzymol. Relat. Areas Mol. Biol.* **1974**, 41, 99-128.
40. Abdullah, M.; Widgren, E. E.; Orand, M. G. *Mol. Cell. Biochem.* **1991**, 103, (2), 155-161.

41. Meier, M.; Bider, M. D.; Malashkevich, V. N.; Spiess, M.; Burkhard, P. *J. Mol. Biol.* **2000**, 300, (4), 857-865.
42. Drickamer, K. *J. Biol. Chem.* **1988**, 263, 9557-9560.
43. Yuan, C. L. *Carbohydr. Res.* **1978**, 67, (2), 509-514.
44. Rao, M.; Rao, M. N. *J. Pharm. Pharmacol.* **1998**, 50, (6), 687-91.
45. Hashida, M.; Hirabayashi, H.; Nishikawa, M.; Takakura, Y. *J. Controlled Release* **1997**, 46, (1/2), 129-137.
46. Kiessling, L. L.; Gestwicki, J. E.; Strong, L. E. *Angew. Chem., Int. Ed. Engl.* **2006**, 45, (15), 2348-2368.
47. Mourez, M.; Kane, R. S.; Mogridge, J.; Metallo, S.; Deschatelets, P.; Sellman, B. R.; Whitesides, G. M.; Collier, R. J. *Nat. Biotechnol.* **2001**, 19, (10), 958-961.
48. Park, K. H.; Sung, W. J.; Kim, S. W.; Kim, D. H.; Akaike, T.; Chung, H. M. *J. Biosci. Bioeng.* **2005**, 99, (3), 285-289.
49. Robinson, A.; Fang, J. M.; Chou, P. T.; Liao, K. W.; Chu, R. M.; Lee, S. J. *Chembiochem* **2005**, 6, (10), 1899-1905.
50. Sidhu, K. S. *Regul. Toxicol. Pharmacol.* **2003**, 38, (3), 336-344.
51. Rooke, J. A.; Shao, C. C.; Speake, B. K. *Reproduction* **2001**, 121, (2), 315-322.
52. Zanini, S. F.; Torres, C. A. A.; Bragagnolo, N.; Turatti, J. M.; Silva, M. G.; Zanini, M. S. *Archives of Animal Nutrition* **2003**, 57, (6), 429-442.
53. Azzi, A.; Stocker, A. *Prog. Lipid Res.* **2000**, 39, (3), 231-255.
54. Brigelius-Flohe, R.; Traber, M. G. *FASEB J.* **1999**, 13, (10), 1145-1156.
55. Wain, A. J.; Wadhawan, J. D.; France, R. R.; Compton, R. G. *Phys. Chem. Chem. Phys.* **2004**, 6, 836-842.
56. Storey, B. T. *Mol. Hum. Reprod.* **1997**, 3, (3), 203-214.
57. Al-Malaika, S. *Macromol. Symp.* **2001**, 176, (1st International Conference on Polymer Modification, Degradation and Stabilisation, 2000), 107-117.
58. Liebler, D. C.; Burr, J. A.; Philips, L.; Ham, A. J. L. *Anal. Biochem.* **1996**, 236, (1), 27-34.
59. Duncan, R.; Ringsdorf, H.; Satchi-Fainaro, R. *J. Drug Target.* **2006**, 14, (6), 337-341.
60. Duncan, R. *Nat. Rev. Drug Discov.* **2003**, 2, (5), 347-360.
61. Harris, J. M.; Chess, R. B. *Nat. Rev. Drug Discov.* **2003**, 2, (3), 214-221.
62. Ferrari, M. *Nat. Rev. Cancer* **2005**, 5, (3), 161-171.

63. Hashida, M.; Akamatsu, K.; Nishikawa, M.; Yamashita, F.; Takakura, Y. *J. Controlled Release* **1999**, *62*, (1-2), 253-262.
64. Davis, B. G. *J. Chem. Soc., Perkin Trans. 1* **1999**, (22), 3215-3238.
65. van de Wetering, P.; Schuurmans-Nieuwenbroek, N. M. E.; van Steenberghe, M. J.; Crommelin, D. J. A.; Hennink, W. E. *J. Controlled Release* **2000**, *64*, (1-3), 193-203.
66. Duncan, R. *Pharma. Sci. Tech. Today* **1999**, *2*, (11), 441-449.
67. Tsuchiya, K.; Uchida, T.; Kobayashi, M.; Maeda, H.; Konno, T.; Yamanaka, H. *Urology* **2000**, *55*, (4), 495-500.
68. Lohmann, D. *Macromol. Symp.* **1995**, *100*, 25-30.
69. Maeda, H. *Adv. Drug Delivery Rev.* **1991**, *6*, (2), 181-202.
70. Matsumura, Y.; Maeda, H. *Cancer Res.* **1986**, *46*, (12), 6387-6392.
71. Vicent, M. J.; Duncan, R. *Trends Biotechnol.* **2006**, *24*, (1), 39-47.
72. Maeda, H.; Wu, J.; Sawa, T.; Matsumura, Y.; Hori, K. *J. Controlled Release* **2000**, *65*, (1-2), 271-284.
73. Jain, R. K. *Cancer Res.* **1987**, *47*, (12), 3039-3051.
74. Haag, R.; Kratz, F. *Angew. Chem., Int. Ed. Engl.* **2006**, *45*, (8), 1198-1215.
75. Duncan, R., O'Driscoll, C. (2000) *Stealth drugs take off* [http://www.chemsoc.org/chembytes/ezone/2000/odriscoll\\_nov00.htm](http://www.chemsoc.org/chembytes/ezone/2000/odriscoll_nov00.htm), [Accessed 2006]
76. Satchi-Fainaro, R. *J. Drug Target.* **2002**, *10*, (7), 529-533.
77. Seymour, L. W.; Ferry, D. R.; Anderson, D.; Hesslewood, S.; Julyan, P. J.; Poyner, R.; Doran, J.; Young, A. M.; Burtles, S.; Kerr, D. J. *J. Clin. Oncol.* **2002**, *20*, (6), 1668-1676.
78. San Roman, J.; Gallardo, A.; Levenfeld, B. *Adv. Mater. (Weinheim, Fed. Repub. Ger.)* **1995**, *7*, (2), 203-208.
79. Albert, A. *Nature* **1958**, *182*, (4633), 421-2.
80. Ringsdorf, H. *J. Polym. Sci., Polym. Symp.* **1975**, *51*, (Int. Symp. Macromol. Honor Professor Herman F. Mark), 135-53.
81. Maeda, H.; Seymour, L. W.; Miyamoto, Y. *Bioconjug. Chem.* **1992**, *3*, (5), 351-362.
82. Mukherjee, S.; Ghosh, R. N.; Maxfield, F. R. *Physiol. Rev.* **1997**, *77*, (3), 759-804.
83. Russell-Jones, G. J. *Adv. Drug Delivery Rev.* **2001**, *46*, (1-3), 59-73.
84. Willingham, M. C.; Pastan, I. H., Receptor Mediated Endocytosis: General Considerations and Morphological Approaches. In *Receptor Mediated Endocytosis*,

- Cuatrecasas, P.; Roth, T., Eds. Chapman and Hall: London, New York, 1983; Vol. 15, Series B, p 3.
85. Albert Eschenmoser. *Angew. Chem., Int. Ed. Engl.* **1995**, 33, (23-24), 2363.
86. Cramer, F. *Pharm. Acta Helv.* **1995**, 69, (4), 193.
87. Kubinyi, H. *Pharm. Acta Helv.* **1995**, 69, (4), 259.
88. Lehn, J. M. *Pharm. Acta Helv.* **1995**, 69, (4), 205.
89. Meyer, E. F. *Pharm. Acta Helv.* **1995**, 69, (4), 177.
90. Helenius, A.; Mellman, I.; Wall, D.; Hubbard, A. *Trends Biochem. Sci.* **1983**, 8, 245-250.
91. Terry, T. M. (2002) *Clathrin-coated Pit Formation*, <http://www.sp.uconn.edu/~bi107vc/images/cell/clathrin.jpg>, [Accessed 2004]
92. Davis, B. G.; Robinson, M. A. *Curr. Opin. Drug Disc. Dev.* **2002**, 5, (2), 279-288.
93. Doores, K. J.; Gamblin, D. P.; Davis, B. G. *Chem. Eur. J.* **2006**, 12, (3), 656-665.
94. Lee, C. C.; MacKay, J. A.; Frechet, J. M. J.; Szoka, F. C. *Nat. Biotechnol.* **2005**, 23, (12), 1517-1526.
95. Shipway, A. N. (1997) *Dendrimers - Technical Terms, A Review, Diagrams, and Links*, <http://www.ninger.com/dendrimer/>, [Accessed 2006]
96. Supattapone, S.; Nguyen, H. O. B.; Cohen, F. E.; Prusiner, S. B.; Scott, M. R. *Proc. Natl. Acad. Sci. U. S. A.* **1999**, 96, (25), 14529-14534.
97. Rendle, P. M.; Seger, A.; Rodrigues, J.; Oldham, N. J.; Bott, R. R.; Jones, J. B.; Cowan, M. M.; Davis, B. G. *J. Am. Chem. Soc.* **2004**, 126, (15), 4750-4751.
98. Ruhl, S.; Cisar, J. O.; Sandberg, A. L. *Infect. Immun.* **2000**, 68, (11), 6346-6354.
99. Wust, J.; Steiger, U.; Vuong, H.; Zbinden, R. *J. Clin. Microbiol.* **2000**, 38, (2), 929-930.
100. Ormsby, A. H.; Bauer, T. W.; Hall, G. S. *Pathology (Phila).* **1998**, 30, (1), 65-67.
101. Sato, M.; Sadamoto, R.; Niikura, K.; Monde, K.; Kondo, H.; Nishimura, S. I. *Angew. Chem., Int. Ed. Engl.* **2004**, 43, (12), 1516-1520.
102. Ohta, T.; Miura, N.; Fujitani, N.; Nakajima, F.; Niikura, K.; Sadamoto, R.; Guo, C. T.; Suzuki, T.; Suzuki, Y.; Monde, K.; Nishimura, S. I. *Angew. Chem., Int. Ed. Engl.* **2003**, 42, (42), 5186-5189.

103. Liang, Y. Z.; Li, Z. C.; Chen, G. Q.; Li, F. M. *Polym. Int.* **1999**, 48, (9), 739-742.
104. Liang, Y.-Z.; Li, Z.-C.; Li, F.-M. *J. Colloid Interface Sci.* **2000**, 224, (1), 84-90.
105. Wulff, G.; Clarkson, G. *Macromol. Chem. Phys.* **1994**, 195, (7), 2603-2610.
106. Nakamae, K. *Trends Polym. Sci.* **1997**, 5, (6), 198-206.
107. Okada, M. *Prog. Polym. Sci.* **2001**, 26, (1), 67-104.
108. Horejsi, V.; Smolek, P.; Kocourek, J. *Biochim. Biophys. Acta* **1978**, 538, (2), 293-8.
109. Kitazawa, S.; Okumura, M.; Kinomura, K.; Sakakibara, T. *Chem. Lett.* **1990**, (9), 1733-6.
110. Li, Z. C.; Liang, Y. Z.; Chen, G. Q.; Li, F. M. *Macromol. Rapid Commun.* **2000**, 21, (7), 375-380.
111. Nakaya, T.; Nishio, K.; Memita, M.; Imoto, M. *Makromol. Chem., Rapid Commun.* **1993**, 14, (2), 77.
112. Aoi, K.; Tsutsumiuchi, K.; Okada, M. *Macromolecules* **1994**, 27, (3), 875.
113. Fraser, C.; Grubbs, R. H. *Macromolecules* **1995**, 28, (21), 7248-55.
114. Mortell, K. H.; Gingras, M.; Kiessling, L. L. *J. Am. Chem. Soc.* **1994**, 116, (26), 12053-4.
115. Mortell, K. H.; Weatherman, R. V.; Kiessling, L. L. *J Am Chem Soc* **1996**, 118, (9), 2297-8.
116. Schuster, M. C.; Mortell, K. H.; Hegeman, A. D.; Kiessling, L. L. *J. Mol. Catal. A: Chem.* **1997**, 116, (1-2), 209-216.
117. Ohno, K.; Tsujii, Y.; Miyamoto, T.; Fukuda, T.; Goto, M.; Kobayashi, K.; Akaike, T. *Macromolecules* **1998**, 31, (4), 1064-1069.
118. Ohno, K.; Tsujii, Y.; Fukuda, T. *J. Polym. Sci., Part A: Polym. Chem.* **1998**, 36, (14a), 2473-2481.
119. Narain, R.; Armes, S. P. *Chem. Comm.* **2002**, (23), 2776-2777.
120. Lowe, A. B.; Sumerlin, B. S.; McCormick, C. L. *Polymer* **2003**, 44, (22), 6761-6765.

## 2 Vitamin E polymer synthesis

### 2.1 Introduction

The use of vitamin E has been described for several completely different areas of polymer synthesis. Work by Johnston *et al.* focuses on the use of vitamin E as an antioxidant to inhibit polymerisation of monomers in storage.<sup>1</sup> A second application, discussed by Al-Malaika, is the inclusion of vitamin E in polymer melts during processing to help the stability of the product.<sup>2</sup> However, it is the third application that is of most relevance to this report: the derivatisation of  $\alpha$ -tocopherol to produce monomers suitable for radical polymerisation/co-polymerisation; to produce novel polymeric materials of biological significance.

This area has not been explored widely, or at least there have not been many publications involving the polymerisation of vitamin E monomers reported in the literature. Nevertheless, there are some examples worthy of mention.

In 1985 Nakaya *et al.* reported the synthesis of a methacrylate based derivative of  $\alpha$ -tocopherol containing a phospholipid analogue. This monomer was homopolymerised in an attempt to create a polymethacrylic phospholipid analogue.<sup>3</sup> Studies then had focussed on creating such structures that mimicked biological membranes. It was hoped the inclusion of a vitamin E analogue would also help afford protection to these artificial membranes in the same manner that vitamin E is essential for the maintenance of biological membranes.

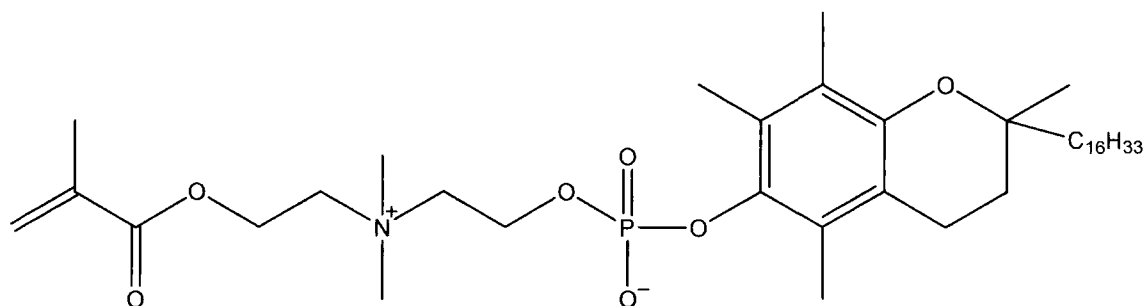


Figure 2.1 - Methacrylate monomer containing vitamin E moiety

A decade or so later a similar material, this time based on an acrylamide functionality was reported.<sup>4</sup> A novel monomer containing vitamin E and an analogue of phosphatidylcholine was synthesised, and was found to form bilayer structures similar to phospholipids. They used these materials to study systems that behave similarly to biological membranes.

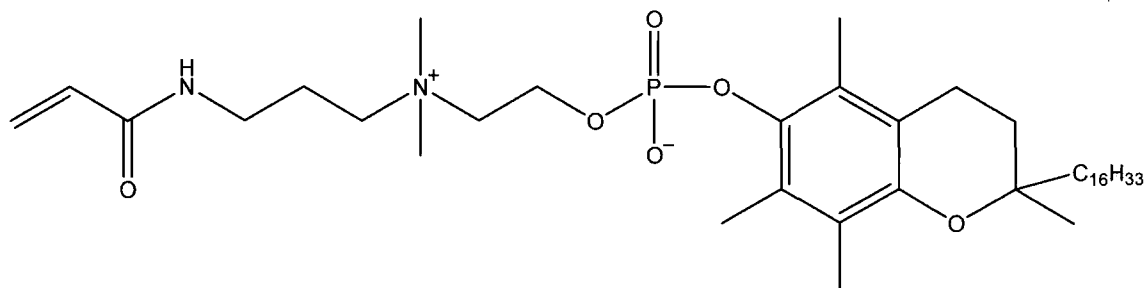


Figure 2.2 - Acrylamide monomer containing vitamin E moiety

The formation of bilayer type structures formed by polymers of this monomer was confirmed by X-ray diffraction analysis.

More recently still, and perhaps of greater relevance, is the work by San Román *et al.* who synthesised and polymerised a methacrylic derivative of vitamin E.<sup>5</sup> Since then, the use of this monomer in the synthesis of hydrogels with HEMA as a co-monomer has been described.<sup>6</sup> These were shown to have beneficial effects in the treatment of damaged tendons.<sup>7</sup> Ortiz *et al* conducted experiments on damaged Achilles' tendons, and the results were impressive. In the groups treated with hydrogels containing vitamin E moieties cell proliferation after 10 days was significantly greater than that of the control group. The group concluded that since no evidence of foreign body reaction was detected in the treated group, such hydrogels could be used and indeed improved by including specific growth factors within the hydrogels.

Further work by this group has highlighted the use of this monomer in the preparation of acrylic bone cements (used in hip replacements for example).<sup>8</sup> These materials were found to be more biocompatible than conventional materials (*e.g.* PMMA) and cells were able to adhere to them, retain their morphology and proliferate.

As far as the author can ascertain, these examples represent a comprehensive list of the literature currently available on the polymerisation of vitamin E derivatives. Furthermore, to the best of this author's knowledge, the work reported herein represents the first example of glycopolymers containing vitamin E moieties. This work is described in a European patent application,<sup>9</sup> briefly in a recent preprint,<sup>10</sup> and in this article<sup>11</sup>.

## 2.2 Results and discussion

### 2.2.1 Glycomonomers

The acetyl protected monomers AcGalEA (**1a**) and AcGalEMA (**1b**) were synthesised by coupling the glycosyl donor 1,2,3,4,6-tetra-*O*-acetyl- $\beta$ -D-galactopyranose with the glycosyl acceptors 2-hydroxyethyl acrylate and 2-hydroxyethyl methacrylate respectively, in anhydrous dichloromethane (DCM) using boron trifluoride diethyl etherate ( $\text{BF}_3\text{Et}_2\text{O}$ ) as the Lewis acid glycosidation promoter.<sup>12-15</sup> There are a number of other effective promoters reported in the literature (e.g. trimethylsilyl trifluoromethanesulfonate (TMSOTf),<sup>16, 17</sup> tin chloride ( $\text{SnCl}_4$ )<sup>18, 19</sup> and iron chloride ( $\text{FeCl}_3$ )<sup>20, 21</sup>). The reaction between the acetylated sugar and the alcohol is specific for the  $\beta$ -anomer due to neighbouring group participation of the 2-OAc group. The reaction proceeds as follows:

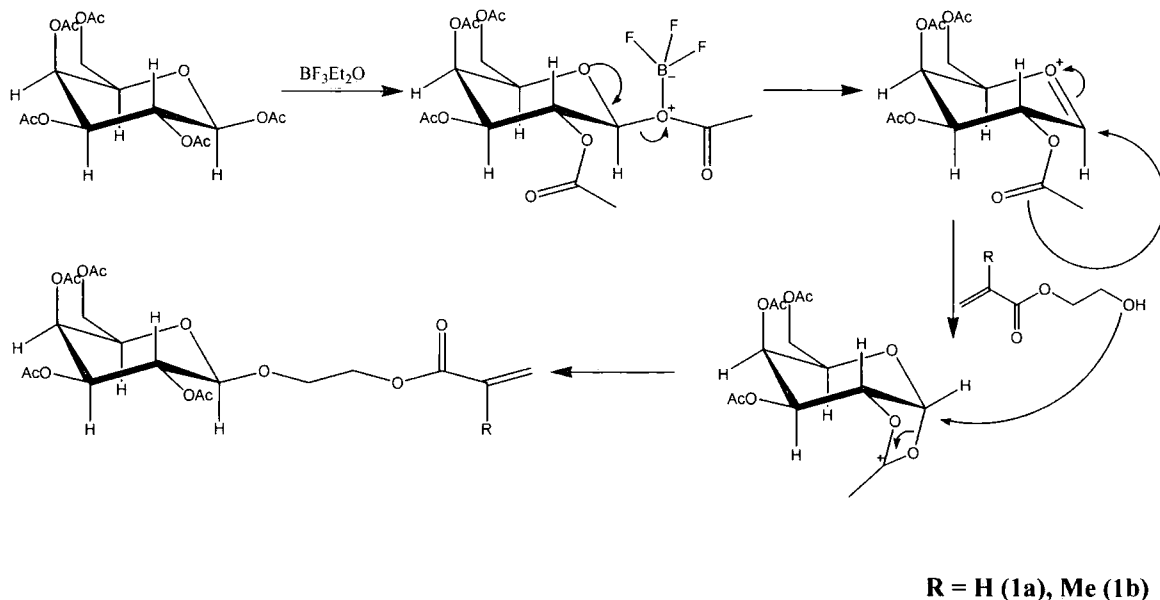
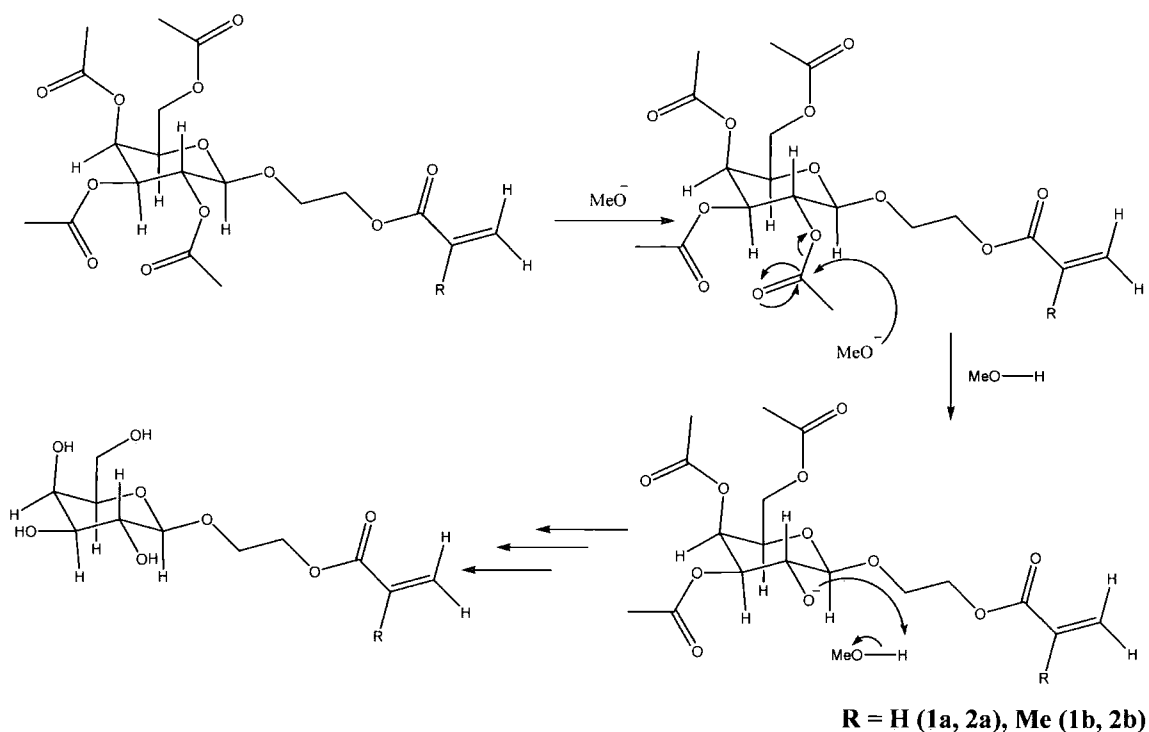


Figure 2.3 - Glycosidation of galactose pentaacetate

Monomers **1a** and **1b** were purified by flash column chromatography. Product **1a** was recovered as a colourless white solid, while product **1b** was a colourless viscous oil, both in reasonable yield (44 and 41% respectively). Both products were characterised

by IR and NMR spectroscopy, mass spectrometry, elemental analysis and polarimetry. Both monomers were soluble in a range of organic solvents.



**Figure 2.4 - De-acetylation of galactosyl monomers**

The de-acetylation of monomers **1a** and **1b** was achieved by addition of catalytic quantities of sodium methoxide in methanol (see Figure 2.4). Despite monitoring the reaction closely by TLC (acetonitrile:water, 9:1), it was not possible to achieve quantitative yields as there is a tendency for the acrylic ester to cleave during the reaction. The de-acetylated products both have  $R_f$  values of  $\sim 0.5$ , while the cleavage product has an  $R_f = 0.2$ . The mechanism for cleavage is shown below in Figure 2.5.

When the evolution of the spot for the cleaved product was observed by TLC, the reaction was stopped by adding the cation exchange resin (DOWEX® 50WX2-200). This results in a mixture of products ranging from a small amount of fully acetylated product, through partially acetylated, fully de-acetylated and cleaved product and therefore necessitated purification by flash column chromatography (chloroform:methanol, 8:2). This yielded products **2a** and **2b** as clear colourless oils (72% and 92% respectively). It is noteworthy that it was possible to recover these monomers by freeze-drying from aqueous solution, however for reasons that are not

entirely apparent the product yielded is generally insoluble in any solvent. It appears that during the freeze-drying process the monomers either polymerise or become highly crosslinked due to hydrogen bonding interactions. Attempts to solubilise these materials in the presence of urea (known to disperse H-bonded networks) were unsuccessful.

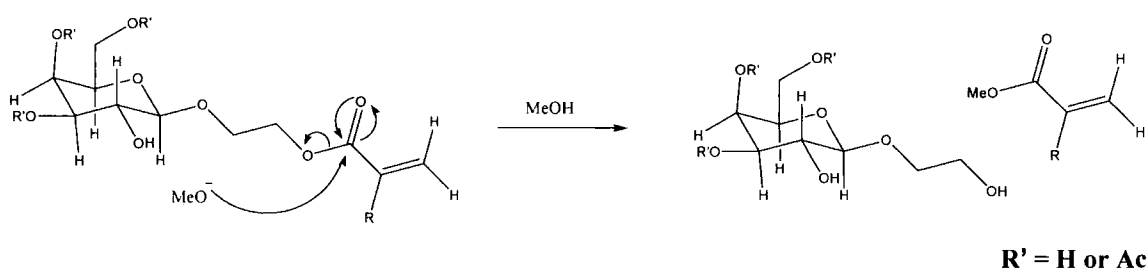


**Figure 2.5 - Cleavage of galactosyl monomers**

These monomers were fully characterised by NMR and IR spectroscopy, mass spectrometry, elemental analysis and polarimetry. There was no evidence of protecting groups from either  $^1\text{H}$  or  $^{13}\text{C}$  NMR spectra. In addition the absence of the carbonyl absorption bands in the region  $1760\text{-}1745\text{ cm}^{-1}$  of the IR spectra supported this.

### 2.2.2 $\alpha$ -Tocopheryl monomers

The synthesis of monomers **3a** and **3b** (see Figure 2.6 - Structures of  $\alpha$ -tocopheryl monomers below), based on the anti-oxidant molecule  $\alpha$ -tocopherol was achieved by reaction of  $\alpha$ -tocopherol with acryloyl or methacryloyl chloride<sup>5</sup> respectively, in anhydrous DCM in the presence of base (triethylamine). The reactions were monitored using TLC ( $R_f = 0.66$ , DCM) and both products were purified by flash column chromatography (DCM) to yield yellow viscous oils in good yields (86 and 78% respectively). Both monomers were fully characterised by IR and NMR spectroscopy, mass spectrometry and elemental analysis.

The synthesis of such molecules for use in free radical polymerisation may initially appear counter intuitive, since the presence of anti-oxidants in a free radical polymerisation could retard or inhibit the polymerisation. Indeed the use of  $\alpha$ -tocopherol for such a purpose is the subject of a US patent application<sup>1</sup>. In the case of

$\alpha$ -tocopherol, its anti-oxidant mechanism requires the phenolic alcohol, and so the monomer can be considered as a “protected” anti-oxidant.

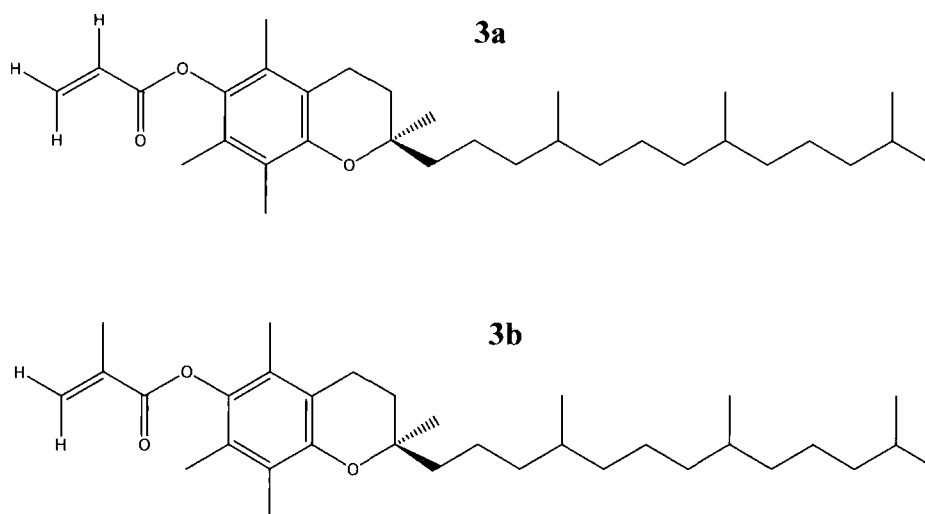


Figure 2.6 - Structures of  $\alpha$ -tocopheryl monomers

### 2.2.3 Scale-up

It is noteworthy that the synthesis of both the galactose and vitamin E bearing monomers has been successfully scaled to >50 g scale in house and during the course of the project was scaled-up further by an external company. The reaction proceeded well and yields were notably high. In these examples, however, the product was not purified further by flash chromatography prior to use. In this case the ability to crystallise these monomers would have been very useful as this would have offered an easier method from which highly pure monomers could be obtained, but to date this has only been shown for a glucose monomer (AcGlcEMA).<sup>13, 22</sup>

### 2.2.4 Polymers

The primary objective of the polymer synthesis was to obtain water soluble polymers containing  $\beta$ -D-galactose and  $\alpha$ -tocopherol residues. A large number of copolymer syntheses were attempted, initially focussing on polymers of AcGalE(M)A and VE(M)A and deprotecting these materials post-polymerisation. Unfortunately this was fraught with difficulties and although some copolymers were synthesised, none of these

had the required water solubility. As such, further characterisation of these materials was not conducted.

However, in addition to the problems associated with product solubility, a number of other factors were highlighted during these reactions. Work by Ortiz *et al.* demonstrated the synthesis of  $\alpha$ -tocopheryl methacrylate and showed that it could be homopolymerised, albeit not to high conversion (ca. 40%).<sup>5</sup> They have also demonstrated the synthesis of copolymers of VEMA with HEMA. Their work indicated that based on the reactivity ratios of these two monomers, VEMA is more likely to react with HEMA than with itself, leading to the conclusion the VHV triads are far more likely than VVV or VVH for example.<sup>5,7</sup>

Having achieved little success with copolymers, focus turned to terpolymer systems which contained sugar and vitamin E moieties, in addition to a third hydrophilic monomer, aimed at imparting the required aqueous solubility. The initial choice of this third monomer was HEMA. Rather surprisingly, this work was not very successful, as the materials obtained were not only insoluble in water but, in many cases, were also insoluble in any solvent. In order to understand the reason(s) for this, two homopolymerisations of HEMA were attempted in parallel, one using a commercially available sample and the other using HEMA that was distilled prior to use. The monomers were dissolved in acetone with AIBN (1.5 wt%) and heated at 50°C for 24 hours. Both reactions yielded seemingly identical but insoluble white solids, although the material obtained from the sample of distilled HEMA did appear to swell slightly in water. It was suggested that this could be a result of transesterification,<sup>23</sup> which was resulting in the *in situ* generation of dimethacrylates which were in turn cross-linking the polymers and rendering them insoluble.

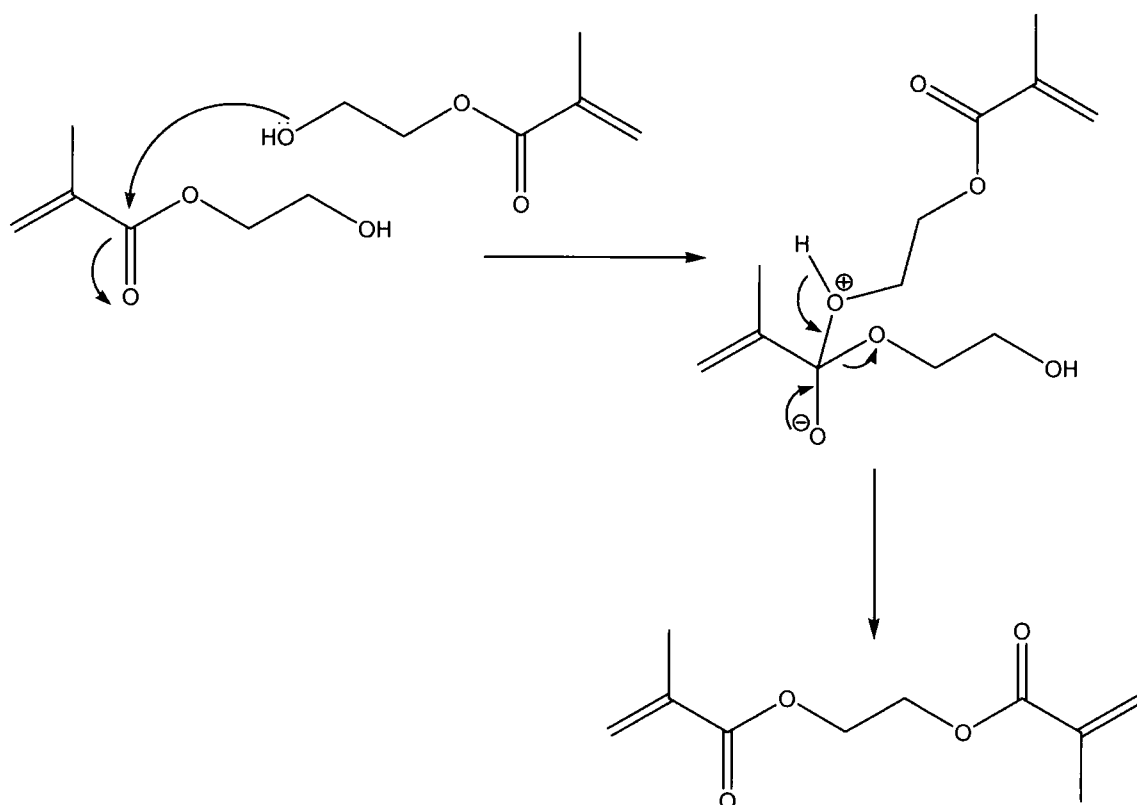


Figure 2.7 - Mechanism of dimethacrylate formation from HEMA

The mechanism above demonstrates clearly that purification of HEMA prior to use may not be sufficient to avoid such impurities being present as they can form spontaneously. Indeed the problem is not limited to HEMA but can occur as an intermolecular reaction between HEMA and AcGalE(M)A or GalE(M)A or indeed between two sugar monomers (see Figure 2.8 & Figure 2.9).

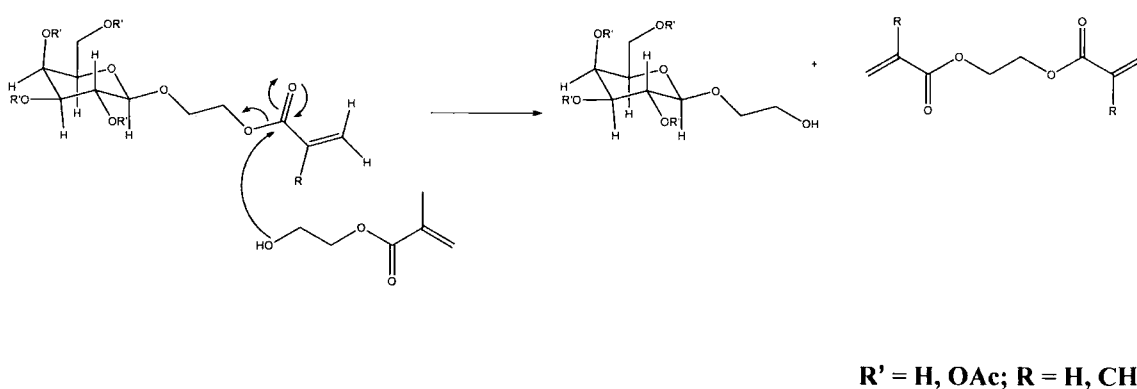
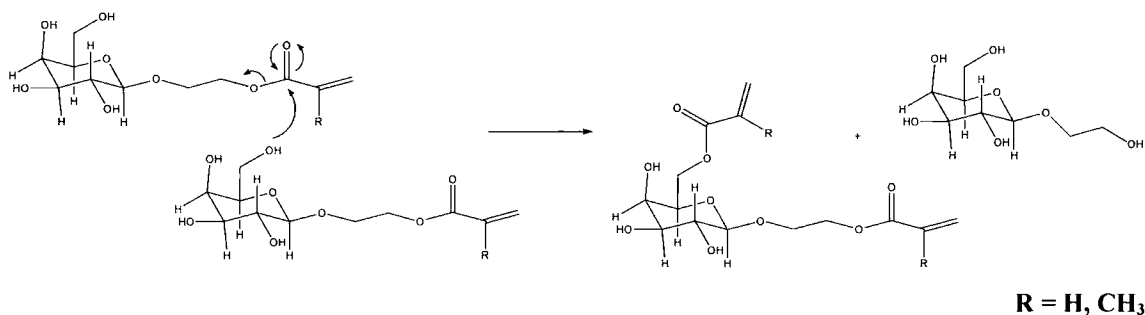


Figure 2.8 - Transesterification of HEMA with sugar monomers



**Figure 2.9 - Intermolecular transesterification of sugar monomers**

These reactions go some way to explaining the insolubility of some of the polymers.

Avoiding transesterification may not be possible; however it is possible to avoid the generation of di-functional monomers, and thus avoid crosslinking of the polymer, by adding methanol as a co-solvent during polymerisation. The methanol becomes involved in the transesterification reactions instead of other monomer molecules, which in turn results in the formation of methyl (meth)acrylate as shown in Figure 2.10.

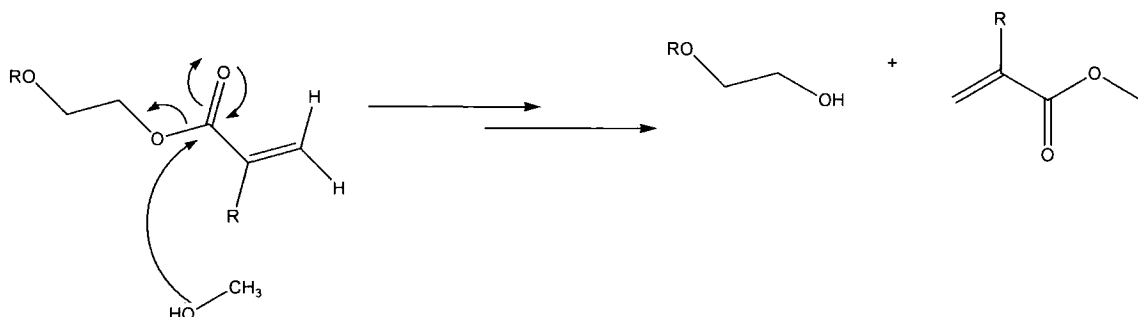


**Figure 2.10 - "Trick" to avoid formation of di-functional monomers**

Having overcome the problems associated with crosslinking, the preparation of a series of terpolymers **4a-12a** (poly[2-(2'3'4'6'-tetra-*O*-acetyl- $\beta$ -D-galactosyloxy)ethyl acrylate-*ter*- $\alpha$ -tocopheryl acrylate-*ter*-2-(dimethylamino)ethyl acrylate]) was attempted. These polymers contained DMAEA as the solubility promoter, in place of HEMA, since DMAEA can become protonated in aqueous conditions and thus aid solubility. These were obtained as off-white powders by polymerisation of **1a**, **3a** and DMAEA at various ratios (Table 2.1) with AIBN in DMF at 50°C for 24 hours. The use of methanol as a co-solvent in the polymerisation was not employed in these reactions,

since the protected sugars are not able to trans-esterify.  $^1\text{H}$  and  $^{13}\text{C}$  NMR spectra of these materials proved that there were no vinyl protons or carbons remaining.

	<b>1a</b>		<b>3a</b>		<b>DMAEA</b>	
	<i>(mg)</i>	<i>(mmol)</i>	<i>(mg)</i>	<i>(mmol)</i>	<i>(mg)</i>	<i>(mmol)</i>
<b>4a</b>	15	0.034	15	0.031	270	1.89
<b>5a</b>	30	0.067	15	0.031	255	1.78
<b>6a</b>	60	0.134	15	0.031	225	1.57
<b>7a</b>	15	0.034	30	0.062	255	1.78
<b>8a</b>	30	0.067	30	0.062	240	1.68
<b>9a</b>	60	0.134	30	0.02	210	1.47
<b>10a</b>	15	0.034	60	0.124	225	1.57
<b>11a</b>	30	0.067	60	0.124	210	1.47
<b>12a</b>	60	0.134	60	0.124	180	1.26

**Table 2.1 – Polymer feed ratios for parallel polymer syntheses**

It is important to remember that these polymers are not easily characterised. In general terms, polymers can be more difficult to characterise by conventional means such as  $^1\text{H}$  and  $^{13}\text{C}$  NMR due to their solution behaviour compared to small molecules (*e.g.* long relaxation times, leading to peak broadening and poorer resolution). This is exacerbated for polymers **4a-12a** because they contain three different monomer units. Subsequently peak broadening leads to overlapping peaks, which in turn makes a definitive characterisation difficult. Furthermore, during dialysis an insoluble brown residue was observed in most cases. Some of this was isolated and identified by  $^1\text{H}$  NMR as containing unreacted VEA. Nevertheless, the choice of monomers meant that typically there were areas in the  $^1\text{H}$  NMR spectrum that were unique for each monomer, which enabled a tentative conclusion that all three monomers were incorporated. For polymers **4a-12a** many of the spectra were very similar, which was to be expected, since these materials only differed in the ratio of the three components.

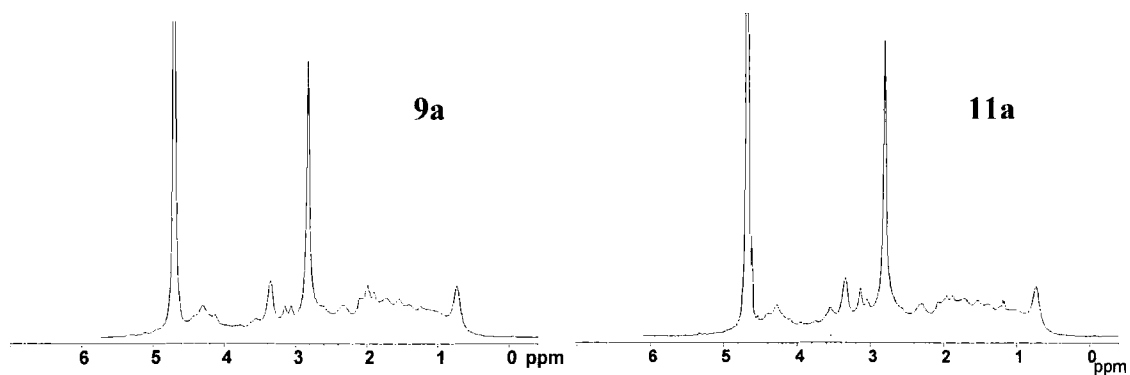


Figure 2.11 -  $^1\text{H}$  NMR spectra of polymers 9a & 11a

However, before these materials could be assessed for their biological activity, it was first necessary to deprotect the sugar moieties. This is not as straightforward as deprotecting the monomer, since the reaction is not easily monitored (TLC is not possible, and  $^1\text{H}$  NMR ambiguous since the methyl acetate by-product of the reaction has peaks in a similar region to residues of the protected sugar). As a result, it is not possible to determine when the polymer has been fully deprotected, which results in an ill-defined polymer. The effect of pre/post-polymerisation deprotection of homoglycopolymers is discussed by Ambrosi *et al.*,<sup>13</sup> where it was concluded that better defined polymers were obtained by deprotecting the monomer rather than the polymer. The extent of deprotection can be assessed qualitatively by weighing the polymer before and after deprotection since there should be a resultant weight loss due to loss of the acetyl groups.

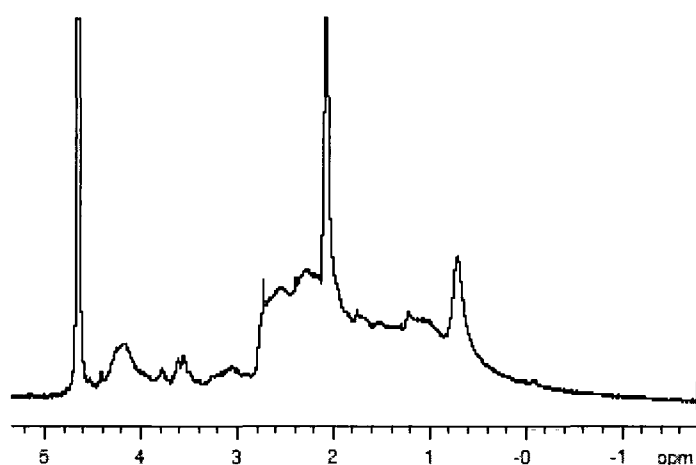
An additional problem associated with this method of glycopolymer synthesis is that, during the deprotection, it is possible to cleave sugar/tocopherol or DMAEA residues from the backbone, since they are all attached by ester linkages, which are susceptible to attack by methoxide. Despite polymers **5b-12b** all being water soluble, yields were low, and there was not sufficient material to perform meaningful biological experiments. Indeed the few experiments that were conducted tentatively suggested that there was very little uptake of vitamin E by the cells. This may be due in part to the fact that many of the sugar residues may still have been mono- or di- acetylated and therefore interaction with cellular receptors was not optimal, or (and possibly just as likely) that there was simply not enough material present initially to give a measurable

amount of vitamin E. These aspects will be discussed in more detail in later chapters. Indeed it is possible that some of the sugar residues were removed during deprotection.

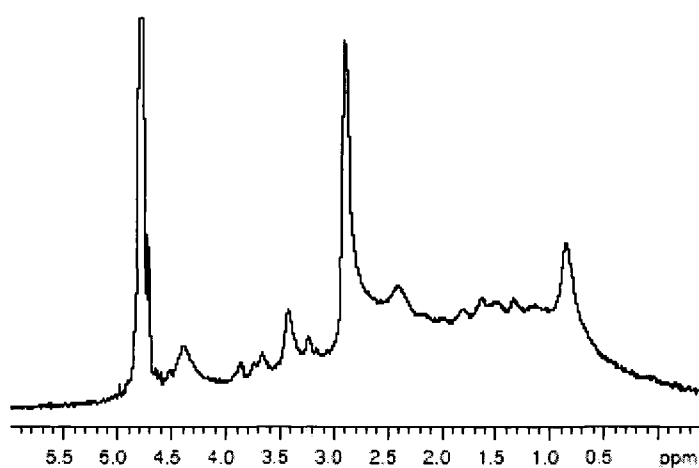
What is noteworthy is that although the sugar residues were acetyl protected, it was possible to dissolve these polymers in water. This vindicates the choice of DMAEA as the solubility enhancing monomer.

In order to avoid the problems associated with post-polymerisation deprotection, polymer **13** was synthesised. Poly[2-( $\beta$ -D-galactosyloxy)ethyl acrylate-*ter*- $\alpha$ -tocopherol acrylate-*ter*-2-(dimethylamino)ethyl acrylate] was obtained by the terpolymerisation of **1a**, **3a** and DMAEA in a mixture of anhydrous DMF and methanol using AIBN as the free radical initiator at 65°C for 24 hours. The crude product was a brown tar, which after purification by dialysis resulted in an off-white solid in good yield (64%). As expected this polymer was readily soluble in water and the  $^1\text{H}$  NMR spectrum indicated that all three monomer components had been incorporated. The broad peak at around 0.7 ppm is due to the methyl protons on the aliphatic chain of the  $\alpha$ -tocopheryl moiety. From 3-3.8 ppm there are broad signals relating to the protons on the ring of the sugar moiety and at around 4.2 ppm there is a broad signal due to one of the  $\text{CH}_2$  groups of the DMAEA, see Figure 2.12.

The result of elemental analysis did not match the expected values based on monomer feed, however this is easily explained. Although all three monomers were acrylates, it is likely that the reactivity ratios of these monomers would be quite different. In addition, the  $\alpha$ -tocopheryl monomer is hindered due to steric factors. As previously mentioned, there was often evidence of unreacted  $\alpha$ -tocopheryl monomer during the dialysis process, manifested as a brown insoluble material which floated on the dialysate. With this in mind, it would perhaps be possible to calculate the composition more accurately, by analysing the insoluble residues after dialysis. The biological activity of this material will be discussed in more detail in a later chapter.

Figure 2.12 -  $^1\text{H}$  NMR spectrum of **13**

Following on from the relative success of polymer **13**, a second analogous material was synthesised (**13** - 13.5 mol% **2a**: 7.9 mol% **3a**: 78.7 mol% DMAEA *c.f.* **14** -14.2% **2b**: 12.9 mol% **3a**: 72.9 mol% DMAEA). The reaction of DMAEA, **3a** and **1b** with AIBN in a mixture of anhydrous DMF and methanol at 70°C for 24 hours gave polymer **14** after purification of the crude material by dialysis and recovery by freeze drying. As expected this material was water soluble and analysis by  $^1\text{H}$  NMR showed many similarities to that of the spectrum of **13**. Once again there were many broad overlapping peaks making a thorough interpretation extremely difficult, however distinctive regions were once again visible.

Figure 2.13 -  $^1\text{H}$  NMR spectrum of **14**

The methyl groups on the aliphatic chain of the  $\alpha$ -tocopheryl residues give rise to the signal at around 0.7 ppm. From  $\sim$ 3-3.8 ppm are peaks resulting from the sugar ring protons, and at 4.30 there is a broad resonance relating to one of the DMAEA CH<sub>2</sub> groups.

The reason why this spectrum is so poorly resolved is doubtless due, to some extent, to the very high molecular weight of this polymer, which is in the order of millions. Aqueous GPC analysis gave the molecular weight values as:  $M_n (8.65 \pm 0.34) \times 10^5$ ;  $M_w (2.73 \pm 0.11) \times 10^6$ ;  $M_z (1.15 \pm 0.14) \times 10^7$ . This is in good agreement with the results of chloroform GPC analysis:  $M_n 9.65 \times 10^5$ ;  $M_w 3.63 \times 10^6$ ;  $M_z 7.64 \times 10^6$ . These results suggest polydispersities of 3.16 and 3.76 respectively, which are also in reasonable agreement. Clearly it is expected that the PD of a random terpolymer prepared by conventional free radical polymerisation would not be narrow, as is illustrated not only by the values but by the shape of the chromatograms.

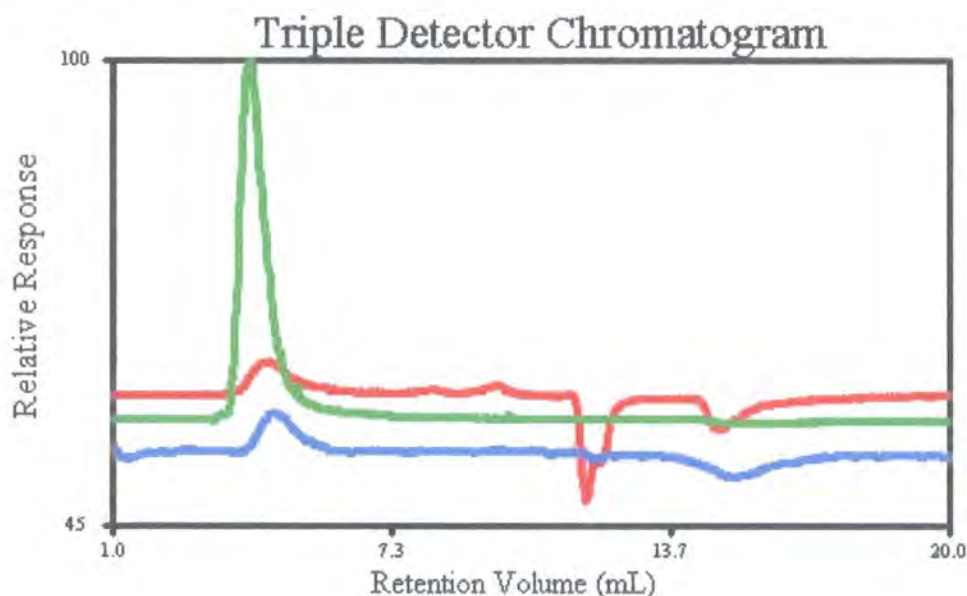


Figure 2.14 - Chromatogram from chloroform GPC: red = refractive index; green = light scattering; blue = differential pressure (viscosity)

Once again the elemental analysis was not exactly as predicted based on the monomer feed; however this is due to the reasons expressed earlier. It would appear that there has been a lesser incorporation of the DMAEA monomer in this material, since the amount of nitrogen found by elemental analysis is lower than expected. In order to gain a better

understanding of the level of Vitamin E present in the polymer, it was studied by UV spectroscopy.

In order to assess the amount of  $\alpha$ -tocopherol present in the polymer, the extinction coefficient of  $\alpha$ -tocopheryl acetate in acetone was established from solutions of known concentration. This was then used to back-calculate the concentration of  $\alpha$ -tocopheryl monomer in the polymer.

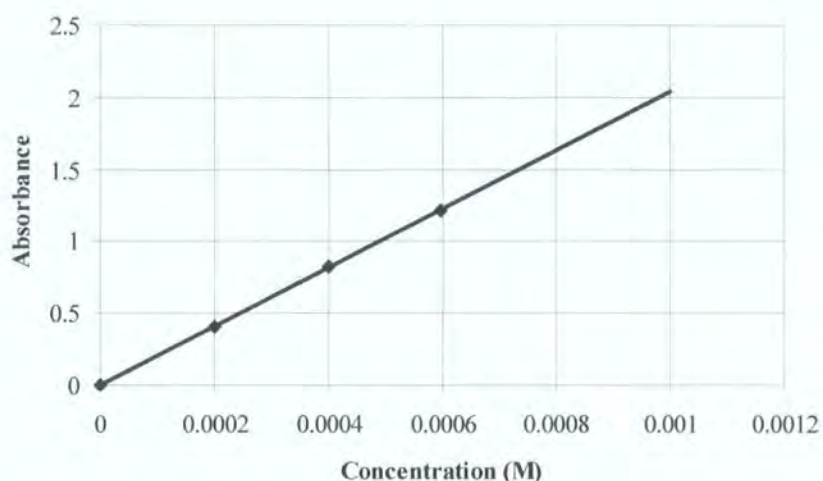


Figure 2.15- Calibration curve for  $\alpha$ -tocopheryl acetate

The equation of the line shown above was found to be  $y = 1960.5x$ . (i.e. the extinction coefficient,  $\epsilon = 1960.5 \text{ g}^{-1} \text{ cm}^{-1} \text{ L}$  since the path length was 1 cm). This equation can be used to calculate the amount of vitamin E present in a solution of the polymer. From a solution of polymer of known concentration and known volume, it is possible to relate an absorbance value to a molar concentration of  $\alpha$ -tocopheryl moiety. This can in turn be converted to a value in terms of weight per unit volume. Using this procedure a value of 36 wt% of Vitamin E in the polymer was calculated. Using this information combined with the elemental analysis information, we can tentatively suggest that the composition was different from the monomer feed, such that the level of incorporation of DMAEA was lower than expected and the level of vitamin E slightly higher than expected. However there are two further complicating factors. Firstly it is possible that despite taking care to ensure that the polymer was rigorously dry prior to elemental analysis, it is possible that the polymer (being so hygroscopic) could have some water

associated with it. Additionally, as described earlier, there is a mechanism by which methyl methacrylate could be formed through the transesterification of methanol and sugar monomer. This could in turn be incorporated into the polymer (albeit in small amounts) meaning that technically the polymer is a quaterpolymer.

Despite these apparent problems it is interesting to note that the incorporation of the vitamin E component remained consistent during subsequent syntheses as is illustrated in Figure 2.16.

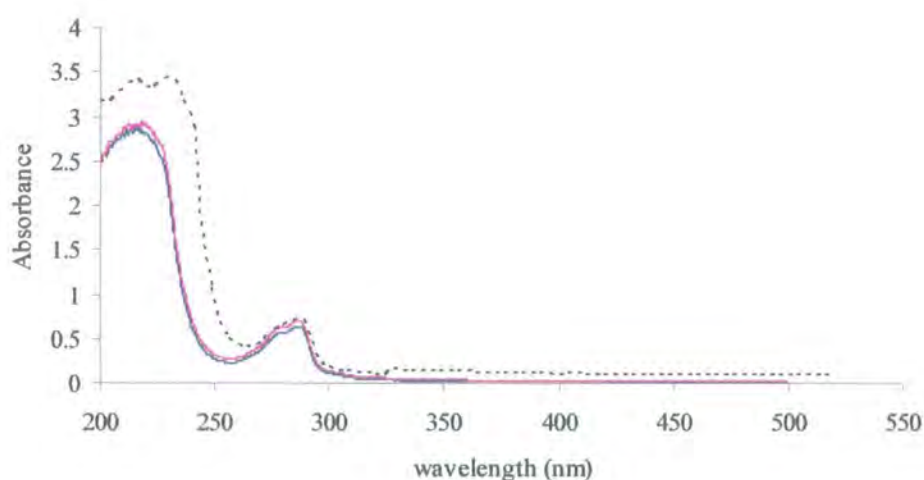


Figure 2.16 - UV absorption curves for 3 different samples of polymer 14\*

As in the case of the sugar and vitamin E monomers, the synthesis and purification of this material was successfully scaled-up to a kilogram scale. Large scale-dialysis was achieved using a continuous circulation flow-through system.

### 2.2.5 Concluding Comments

In summary, monomers of galactose and vitamin E were synthesised according to methods previously described in the literature.<sup>5, 12-15</sup> A range of polymers were synthesised which contained both sugar moieties and vitamin E. Unfortunately, many of these materials were unsuitable for the intended application either due to their

\* The magenta line represents a sample synthesised by the author, the blue line is a sample synthesised in a scaled-up synthesis by an external contractor. The dotted line represents a sample also synthesised by the author but the reading was recorded on a different spectrometer.

inherent insolubility in water, or poor *in vitro* activity. As such these materials were not studied more fully. Two polymers (**13** and **14**) were synthesised which contained the two essential components, and were found to be soluble in a range of solvents, including water. These were analysed by a number of analytical techniques and ultimately assessed for activity within biological systems. The results of the *in vitro/in vivo* work will be discussed in a later chapter.

The ability to synthesise glycopolymers suitable for drug delivery applications has been demonstrated. These systems can be considered as prototypes as there are many potential areas for improvement such as the use of controlled polymerisation techniques to produce materials of defined molecular weight and/or architecture. Research into the controlled polymerisation of glycomonomers is described in a number of literature articles and theses.<sup>24-27</sup>

## 2.3 Experimental

### 2.3.1 Materials

1,2,3,4,6-Penta-*O*-acetyl- $\beta$ -D-galactopyranose (98%),  $\alpha$ -tocopherol ( $\alpha$ -T, 97%), boron trifluoride diethyl etherate (purified, redistilled), 2-hydroxyethyl acrylate (HEA, 96%), 2-hydroxyethyl methacrylate (HEMA, 99+%), acryloyl chloride (98+%), methacryloyl chloride (98+%), 2-dimethylamino ethyl acrylate (DMAEA, 98%), 2-dimethylamino ethyl methacrylate (DMAEMA, 98%), anhydrous methanol (99.8%), anhydrous *N,N*-dimethylformamide (99.8%), and cation exchange resin DOWEX® 50WX2-200 were purchased from Aldrich. Azoisobutyronitrile (AIBN, 97%) was obtained from BDH, and purified by recrystallisation from methanol prior to use. Dichloromethane (DCM) was distilled over calcium hydride under N<sub>2</sub>, HEMA, HEA, acryloyl chloride and methacryloyl chloride had inhibitor removed prior to use by passing through a plug of basic alumina. All other chemicals were used without further purification.

### 2.3.2 Instrumentation

NMR-spectra were recorded on a Varian Unity 300, Varian Mercury 200 or Bruker Avance 400 spectrometers; all chemical shifts were referenced to residual solvent as an internal standard. Infrared (IR) spectra were obtained using a Perkin Elmer 1600 Series FTIR spectrometer with samples prepared as either Nujol mulls or potassium bromide discs. Mass spectra were obtained using a Micromass Platform spectrometer in ionisation mode ES<sup>+</sup>. UV spectra were measured on either a Shimadzu UV-2101PC spectrophotometer, or a ATI Unicam UV/VIS UV2 spectrophotometer, in stoppered quartz cuvettes with a 1 cm path length. Optical rotations were measured on a Jasco P-1020 Polarimeter. Chloroform GPC analyses were carried out using a Viscotek TDA 301 with a Plgel 10  $\mu$  MIXED-B column connected to a triple detection system, with a flow rate of 10 ml min<sup>-1</sup> and an injection volume of 100  $\mu$ l. Samples analysed by aqueous GPC, were determined by aqueous size exclusion chromatography coupled to a Water 410 RI detector and a Wyatt DAWN DSP MALLS, using a TSK GMPW column. The mobile phase consisted of 80% water, 20% methanol, 0.05 M NaNO<sub>3</sub> and

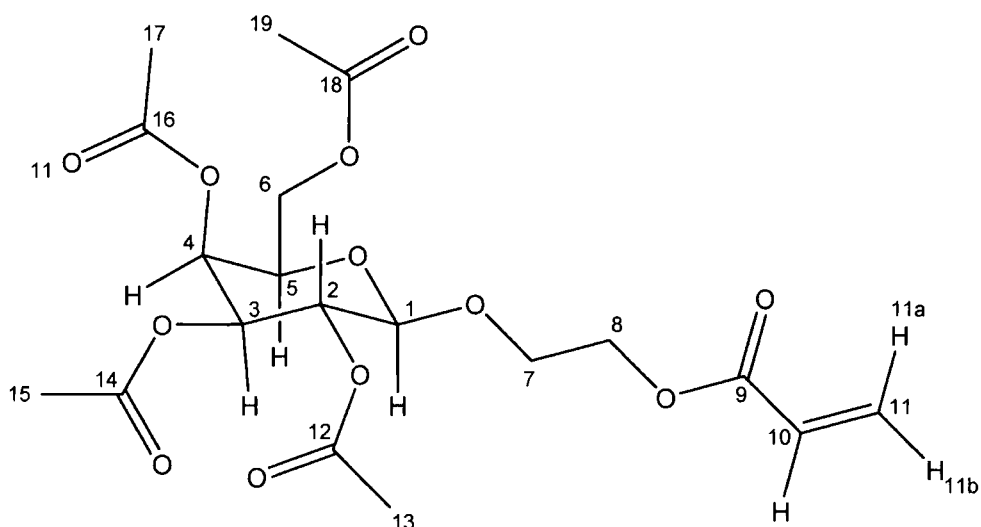
2.5 ml l<sup>-1</sup> 1.0 M NaOH at a flow rate of 0.8 ml min<sup>-1</sup>. Molecular weight averages were calculated using Astra 32 software. Elemental analyses were obtained with an Exeter Analytical Inc. CE-440 Elemental Analyser. Lyophilised products (dialysis membrane MWCO 12-14 kDa) were obtained using a Christ ALPHA-1-4 freeze-dryer with a LDC-1M controller.

### 2.3.3 Synthesis of monomers and polymers

#### 2.3.3.1 2-(2', 3', 4', 6'-tetra-O-acetyl-β-D-galactosyloxy)ethyl acrylate, AcGalEA (1a)

A mixture of 1, 2, 3, 4, 6-β-D-galactose pentaacetate (5 g, 12.8 mmol), 2-hydroxyethyl acrylate (1.5 g, 12.8 mmol), molecular sieves (10 Å, 10 g) in anhydrous dichloromethane (40 ml) was stirred under an atmosphere of nitrogen at 0°C. A solution of boron trifluoride diethyl etherate (10 ml, 78.8 mmol, 6 eq.) in anhydrous dichloromethane (30 ml) was then added drop wise, with stirring, to the reaction mixture. The mixture was then allowed to further react overnight at room temperature under a flowing nitrogen atmosphere.

The solution was subsequently washed with distilled water (3 × 40 ml) and the organic layer dried over magnesium sulphate. After filtration and evaporation, the product was purified by flash chromatography (ethyl acetate:hexane, 2:8, increasing to 4:6), giving product **1a** (2.5 g, 44%) as a white solid.

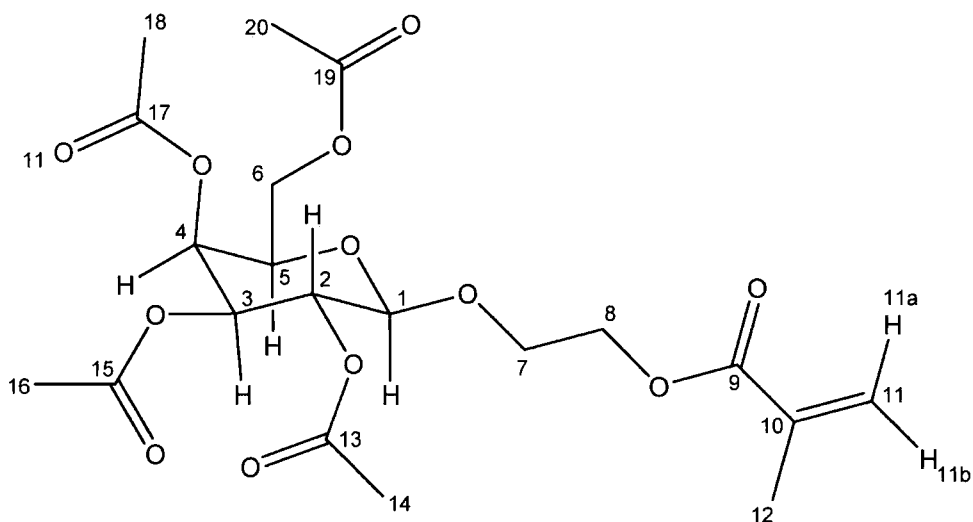


$[\alpha]_D = -6.55$  ( $c = 5.90$ ,  $\text{CHCl}_3$ ), ( $\text{C}_{19}\text{H}_{26}\text{O}_{12}$ , Expected: C 51.12; H 5.87, Found: C 50.96; H 5.76), IR (Nujol mull,  $\text{cm}^{-1}$ ): 3066 (med.) =CH; 2980, 2966, 2887 (med.) –CH; 1747 (sharp) –C=O; 1637 (sharp) –C=C; C-O-C (sharp) 1295, 1220, 1174, 1065.  $^1\text{H}$  NMR ( $\text{CDCl}_3$ , 200 MHz): **1.97-2.14** (4s,  $3\text{H}_{13}$ ,  $3\text{H}_{15}$ ,  $3\text{H}_{17}$ ,  $3\text{H}_{19}$ ), **3.81** (m,  $1\text{H}_7$ ,  $J^3_{7-8} = 5.0$  Hz,  $J^2_5 = 11.6$  Hz), **3.89** (t,  $1\text{H}_5$ ,  $J^3_{5-6} = 6.4$  Hz), **4.0** (m,  $1\text{H}_7$ ,  $J^3_{7-8} = 3.81$  Hz,  $J^2_7 = 11.7$  Hz), **4.10** (m,  $2\text{H}_6$ ,  $J^3_{6-5} = 6.4$  Hz,  $J^2_6 = 12.8$  Hz), **4.30** (m,  $2\text{H}_8$ ,  $J^3_{8-7} = 5.0$  Hz,  $J^2_8 = 10.5$  Hz), **4.50** (d,  $1\text{H}_1$ ,  $J^3_{1-2} = 7.8$  Hz), **4.97** (dd,  $1\text{H}_3$ ,  $J^3_{3-4} = 3.4$  Hz,  $J^3_{3-2} = 10.4$  Hz), **5.17** (dd,  $1\text{H}_2$ ,  $J^3_{2-1} = 7.9$  Hz,  $J^3_{2-3} = 10.4$  Hz), **5.37** (d,  $1\text{H}_4$ ,  $J^3_{4-3} = 3.3$  Hz), **5.83** (d,  $1\text{H}_{11b}$ ,  $J^3_{11b-10} = 10.3$  Hz), **6.10** (dd,  $1\text{H}_{10}$ ,  $J^3_{10-11a} = 17.7$  Hz,  $J^3_{10-11b} = 10.3$  Hz), **6.43** (d,  $1\text{H}_{11a}$ ,  $J^3_{11a-10} = 17.2$  Hz).  $^{13}\text{C}$  NMR ( $\text{CDCl}_3$ , 100 MHz): **20.8-20.9** ( $\text{C}_{13}$ ,  $\text{C}_{15}$ ,  $\text{C}_{17}$ ,  $\text{C}_{19}$ ), **61.5** ( $\text{C}_6$ ), **63.5** ( $\text{C}_8$ ), **67.2** ( $\text{C}_4$ ), **67.6** ( $\text{C}_7$ ), **68.8** ( $\text{C}_2$ ), **70.9** ( $\text{C}_5$ ), **71.0** ( $\text{C}_3$ ), **101.5** ( $\text{C}_1$ ), **128.3** ( $\text{C}_{10}$ ), **131.5** ( $\text{C}_{11}$ ), **166.1** ( $\text{C}_9$ ), **169.5-170.6** ( $\text{C}_{12}$ ,  $\text{C}_{14}$ ,  $\text{C}_{16}$ ,  $\text{C}_{18}$ ). MS (ES<sup>+</sup>):  $m/z = 469$  ( $\text{M}^+ + \text{Na}$ ).

### 2.3.3.2 2-(2', 3', 4', 6'-tetra-O-acetyl- $\beta$ -D-galactosyloxy)ethyl methacrylate, AcGalEMA (1b)

A mixture of 1, 2, 3, 4, 6- $\beta$ -D-galactose pentaacetate (5.00 g, 12.8 mmol), 2-hydroxyethyl methacrylate (1.67 g, 12.8 mmol), molecular sieves (10 Å, 10 g) in anhydrous dichloromethane (40 ml) was stirred under an atmosphere of nitrogen at 0°C. A solution of boron trifluoride diethyl etherate (10 ml, 78.8 mmol, 6 eq.) in anhydrous dichloromethane (30 ml) was then added drop wise, with stirring, to the reaction mixture. The mixture was then allowed to further react overnight at room temperature under a flowing nitrogen atmosphere.

The crude material was purified as described in 2.3.3.1 giving product **1b** (2.4 g, 41%) as a colourless oil.

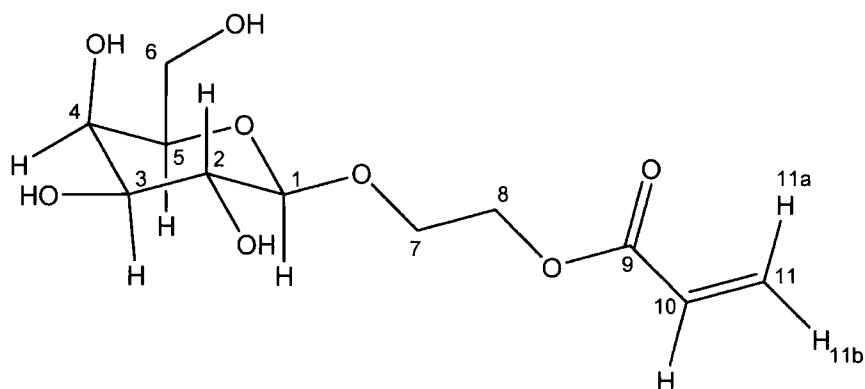


$[\alpha]_D = -0.3$  ( $c = 0.50$ ,  $\text{CHCl}_3$ ), ( $\text{C}_{20}\text{H}_{28}\text{O}_{12}$ , Expected: C 52.17; H 6.13, Found: C 51.70; H 6.10), IR (Nujol mull,  $\text{cm}^{-1}$ ): =C-H (med.) 3066; -C-H (med.) 2980, 2996, 2889; C=O (sharp) 1758, 1744, 1720; C=C (sharp) 1637; C-O-C (sharp) 1246, 1170, 1078, 1056.  $^1\text{H}$  NMR (200 MHz,  $\text{CDCl}_3$ ): **1.94** (s,  $3\text{H}_{12}$ ), **1.97**, **2.00**, **2.03**, **2.14** (s,  $3\text{H}_{14}$ ,  $3\text{H}_{16}$ ,  $3\text{H}_{18}$ ,  $3\text{H}_{20}$ ), **3.79** (m,  $1\text{H}_7$ ,  $J^{3-4} = 4.6$  Hz,  $J^2_7 = 11.3$  Hz), **3.86** (m,  $1\text{H}_5$ ,  $J^{6-5} = 6.2$  Hz), **4.02** (m,  $1\text{H}_7$ ), **4.11** (m,  $2\text{H}_6$ ), **4.27** (m,  $2\text{H}_8$ ,  $J^{8-7} = 4.5$  Hz,  $J^2_8 = 7.6$  Hz), **4.52** (d,  $1\text{H}_1$ ,  $J^{1-2} = 7.8$  Hz), **4.95** (dd,  $1\text{H}_3$ ,  $J^{3-4} = 3.3$  Hz,  $J^{3-2} = 10.3$  Hz), **5.16** (dd,  $1\text{H}_2$ ,  $J^{2-1} = 7.9$  Hz,  $J^{2-3} = 10.4$  Hz), **5.32** (d,  $1\text{H}_4$ ,  $J^{4-3} = 3.3$  Hz), **5.58** (s,  $1\text{H}_{11b}$ ), **6.12** (s,  $1\text{H}_{11a}$ ).  $^{13}\text{C}$  NMR (100 MHz,  $\text{CDCl}_3$ ): **18.16** ( $\text{C}_{12}$ ), **20.55** **20.47** ( $\text{C}_{14}$ ,  $\text{C}_{16}$ ,  $\text{C}_{18}$ ,  $\text{C}_{20}$ ), **61.2** ( $\text{C}_6$ ), **63.4** ( $\text{C}_8$ ), **66.9** ( $\text{C}_4$ ), **67.3** ( $\text{C}_7$ ), **68.6** ( $\text{C}_2$ ), **70.7** ( $\text{C}_5$ ), **70.8** ( $\text{C}_3$ ), **101.2** ( $\text{C}_1$ ), **125.8** ( $\text{C}_{10}$ ), **136.0** ( $\text{C}_{11}$ ), **167.0** ( $\text{C}_9$ ), **169.3**, **170.2**, **170.3**, **170.8** ( $\text{C}_{13}$ ,  $\text{C}_{15}$ ,  $\text{C}_{17}$ ,  $\text{C}_{19}$ ). MS (ES<sup>+</sup>):  $m/z = 483$  ( $\text{M}^+ + \text{Na}$ ).

### 2.3.3.3 2-( $\beta$ -D-galactosyloxy)ethyl acrylate, GalEA (2a)

**1a** (1.0 g, 2.2 mmol) was dissolved in 10 ml of anhydrous methanol, and stirred under  $\text{N}_2$  for approximately 10 minutes. Subsequently, 20 ml of sodium methoxide solution [0.01 M, in MeOH] was added. The solution was stirred at room temperature, and the

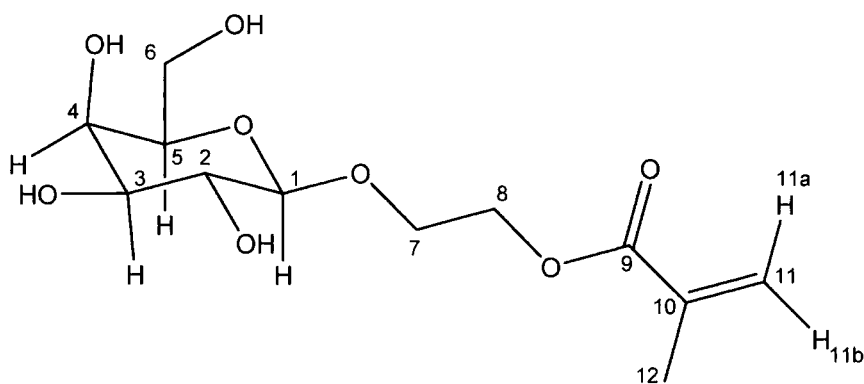
reaction monitored by TLC (acetonitrile:water, 9:1,  $R_f = 0.5$ ). The reaction was stopped after 25 minutes when the formation of a cleavage product was observed ( $R_f = 0.2$ ). Cation-exchange resin (DOWEX 8W50) was added to neutralise the solution. The resin was removed by filtration and the crude product was obtained after evaporation of the solvent. The material was purified by flash chromatography (chloroform:methanol, 8:2) to afford product **2a** (0.45 g, 72%) as a colourless, viscous oil.



$[\alpha]_D = +7.2$  ( $c = 0.29$ ,  $H_2O$ ), ( $C_{11}H_{18}O_8$ , Expected: C 47.48; H 6.52, Found: C 47.56; H 6.42), IR (Nujol mull,  $cm^{-1}$ ): -OH (broad) 3385; =CH (med.) 3304; -CH (sharp) 2935, 2888; -C=O (sharp) 1718; C=C (sharp) 1637; C-O-C (sharp) 1299, 1216, 1146.  $^1H$  NMR (200 MHz,  $CD_3OD$ ): **3.32** (m,  $1H_2$ ,  $J^3_{2-3} = 10.9$  Hz), **3.50** (dd,  $1H_3$ ,  $J^3_{4-3} = 3.1$  Hz,  $J^3_{2-3} = 10.9$  Hz), **3.54** (m,  $1H_5$ ), **3.63** (m,  $2H_6$ ), **3.74** (d,  $1H_4$ ,  $J^3_{4-3} = 3.1$  Hz), **3.82** (m,  $1H_7$ ), **3.97** (m,  $1H_7$ ), **4.24** (m,  $2H_8$ ), **4.30** (d,  $1H_1$ ,  $J^3_{1-2} = 6.6$  Hz), **5.88** (d,  $1H_{11b}$ ,  $J^3_{11b-10} = 10.3$  Hz), **6.16** (dd,  $1H_{10}$ ,  $J^3_{11a-10} = 17.2$  Hz,  $J^3_{11b-10} = 10.3$  Hz), **6.41** (d,  $1H_{11a}$ ,  $J^3_{11a-10} = 17.3$  Hz).  $^{13}C$  NMR ( $D_2O$ , 100 MHz): **61.1** ( $C_6$ ), **64.3** ( $C_8$ ), **67.9** ( $C_7$ ), **68.8** ( $C_4$ ), **71.0** ( $C_2$ ), **72.8** ( $C_5$ ), **75.3** ( $C_3$ ), **103.2** ( $C_1$ ), **127.5** ( $C_{10}$ ), **132.8** ( $C_{11}$ ), **168.5** ( $C_9$ ). MS (ES $^+$ ):  $m/z = 301$  ( $M^+ + Na$ ).

#### 2.3.3.4 2-( $\beta$ -D-galactosyloxy)ethyl methacrylate, GalEMA (**2b**)

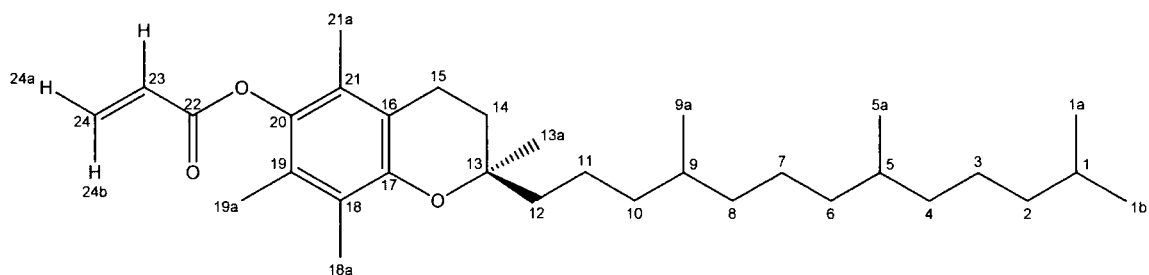
**1b** (1.0 g, 2.2 mmol) was treated as described in section 2.3.3.3, resulting in product **2b** (0.59 g, 92%) as a viscous colourless oil.



$[\alpha]_D = +18$  ( $c = 0.15$ ,  $H_2O$ ), ( $C_{12}H_{20}O_8$ , Expected: C 49.31; H 6.9, Found: C 49.09; H 6.82), IR (Nujol mull,  $cm^{-1}$ ): -OH (broad) 3427; =C-H (med.) 3018; -C-H (med.) 2936, 2897; C=O (sharp) 1718; C=C (sharp) 1636; C-O-C (sharp) 1251, 1162, 1077, 1044.  $^1H$  NMR (200 MHz,  $CD_3OD$ ): **1.93** (s,  $3H_{12}$ ), **3.4** (m,  $1H_2$ ), **3.49** (m,  $1H_3$ ), **3.52** (m,  $1H_5$ ), **3.72** (m,  $2H_6$ ), **3.82** (d,  $1H_4$ ,  $J_{4-3}^3 = 3.1$  Hz), **4.05** (qd,  $2H_7$ ,  $J_{7-8}^3 = 4.1$  Hz,  $J_7^2 = 11.5$  Hz), **4.22** (m,  $2H_8$ ), **4.29** (d,  $1H_1$ ,  $J_{2-1}^3 = 7.8$  Hz), **5.63** (s,  $1H_{11b}$ ), **6.15** (s,  $1H_{11a}$ ).  $^{13}C$  NMR (100 MHz,  $CD_3OD$ ): **17.6** ( $C_{12}$ ), **61.0** ( $C_6$ ), **64.6** ( $C_8$ ), **68.0** ( $C_7$ ), **68.7** ( $C_4$ ), **70.8** ( $C_2$ ), **72.9** ( $C_3$ ), **75.3** ( $C_5$ ), **103.3** ( $C_1$ ), **127.2** ( $C_{10}$ ), **135.9** ( $C_{11}$ ), **169.8** ( $C_9$ ). MS (ES<sup>+</sup>):  $m/z = 315$  ( $M^+ + Na$ ).

### 2.3.3.5 $\alpha$ -Tocopheryl acrylate, VEA (**3a**)

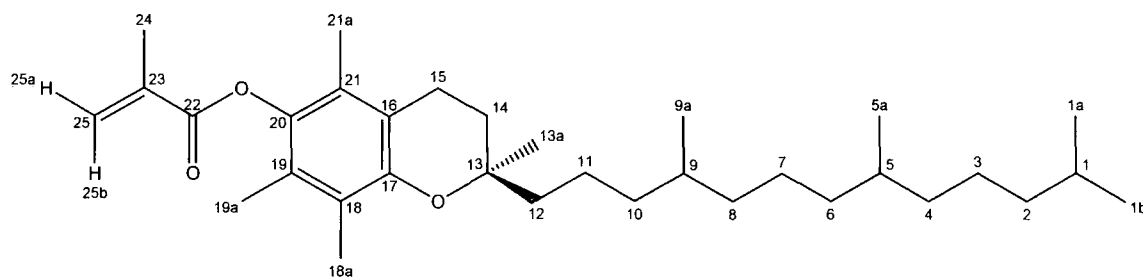
$\alpha$ -Tocopherol (6.20 g, 14.4 mmol) and triethylamine (2.64 ml) were dissolved, with stirring in anhydrous DCM (75 ml) under  $N_2$  and cooled to  $0^\circ C$ . Acryloyl chloride (1.64 ml, 20.2 mmol) was then added dropwise with stirring. The solution was stirred for a further 10 minutes at  $0^\circ C$  and then allowed to reach room temperature. The reaction was monitored by TLC (Rf: 0.66, DCM). Once the reaction was deemed to be complete, the solution was washed (3 x 50 ml 0.1 M NaOH, 3 x 50 ml water), and the organic layer dried over magnesium sulphate, and filtered. The solvent was removed *in vacuo* and the residue purified by flash chromatography (DCM) to yield product **3a** (5.95 g, 86%) as a yellow oil.



(C<sub>32</sub>H<sub>52</sub>O<sub>3</sub>, Expected: C 79.29; H 10.81, Found: C 79.03; H 10.73), IR (Nujol mull, cm<sup>-1</sup>): =C-H (med.) 3055; -C-H (med.) 2925, 2867; C=O (sharp) 1743; C=C (sharp) 1637; C-O-C (sharp) 1232, 1159, 1109, 1081. <sup>1</sup>H NMR (250 MHz, CDCl<sub>3</sub>): **0.82** (m, 3H<sub>1b</sub>, 3H<sub>1a</sub>, 3H<sub>5a</sub>, 3H<sub>9a</sub>), **1.07-1.37** (m, 2H<sub>11</sub>, 2H<sub>10</sub>, 1H<sub>9</sub>, 2H<sub>8</sub>, 2H<sub>7</sub>, 2H<sub>6</sub>, 1H<sub>5</sub>, 2H<sub>4</sub>, 2H<sub>3</sub>, 2H<sub>2</sub>, 1H<sub>1</sub>), **1.4** (m, 3H<sub>13a</sub>), **1.54** (m, 2H<sub>12</sub>, J<sup>3</sup><sub>12-11</sub> = 6.6 Hz), **1.80** (m, 2H<sub>14</sub>, J<sup>3</sup><sub>15-14</sub> = 6.7 Hz), **1.99** (s, 3H<sub>18a</sub>), **2.03** (s, 3H<sub>19a</sub>), **2.10** (s, 3H<sub>21a</sub>), **2.6** (t, 2H<sub>15</sub>, J<sup>3</sup><sub>14-15</sub> = 6.7 Hz), **6.0** (dd, 1H<sub>24a</sub>, J<sup>3</sup><sub>24a-23</sub> = 10.4 Hz, J<sup>2</sup><sub>24a-24b</sub> = 1.4 Hz), **6.3** (dd, 1H<sub>23</sub>, J<sup>3</sup><sub>23-24b</sub> = 17.3 Hz, J<sup>3</sup><sub>23-24a</sub> = 10.4 Hz), **6.6** (dd, 1H<sub>24b</sub>, J<sup>3</sup><sub>24a-23</sub> = 16.8 Hz, J<sup>2</sup><sub>24a-24b</sub> = 1.4 Hz). <sup>13</sup>C NMR (125 MHz, CDCl<sub>3</sub>): **12.1** (C<sub>21a</sub>), **12.3** (C<sub>18a</sub>), **13.2** (C<sub>19a</sub>), **19.9** (C<sub>5a</sub>), **20.0** (C<sub>9a</sub>), **20.6** (C<sub>15</sub>), **21.3** (C<sub>11</sub>), **22.9** (C<sub>1a</sub>), **23.0** (C<sub>1b</sub>), **24.2** (C<sub>13a</sub>), **24.7** (C<sub>7</sub>), **25.1** (C<sub>3</sub>), **28.2** (C<sub>1</sub>), **31.3** (C<sub>14</sub>), **32.9** (C<sub>5</sub>), **33.0** (C<sub>9</sub>), **37.5** (C<sub>4</sub>), **37.6** (C<sub>6</sub>), **37.7** (C<sub>8</sub>), **37.8** (C<sub>10</sub>), **39.6** (C<sub>2</sub>), **40.2** (C<sub>12</sub>), **75.3** (C<sub>13</sub>), **117.7** (C<sub>16</sub>), **123.3** (C<sub>21</sub>), **125.2** (C<sub>19</sub>), **127.0** (C<sub>18</sub>), **128.1** (C<sub>24</sub>), **132.4** (C<sub>23</sub>), **140.5** (C<sub>20</sub>), **149.7** (C<sub>17</sub>), **165.0** (C<sub>22</sub>). MS (ES<sup>+</sup>): m/z = 507 (M<sup>+</sup>+Na). The α-Tocopherol is a racemic mixture, and the assignments were done with reference to the work of Ortiz et al.<sup>5</sup>

### 2.3.3.6 α-Tocopheryl methacrylate, VEMA (3b)

α-Tocopherol (2.5 g, 5.8 mmol) and triethylamine (0.84 ml) were dissolved, with stirring in anhydrous DCM (20 ml) under N<sub>2</sub> and cooled to 0°C. Methacryloyl chloride (0.74 ml, 7.5 mmol) was then added dropwise with stirring. The solution was stirred for a further 10 minutes at 0°C and then allowed to reach room temperature and left to react overnight. Subsequently, the solution was washed (3 x 25 ml 0.1 M NaOH, 3 x 25 ml water), and the organic layer dried over magnesium sulphate, and filtered. The solvent was removed *in vacuo* and the residue purified by flash chromatography (DCM) to yield product **3b** (2.20 g, 78%) as a yellow oil.



(C<sub>33</sub>H<sub>54</sub>O<sub>3</sub>, Expected: C 79.46; H 10.91, Found: C 79.33; H 10.80), IR (Nujol mull, cm<sup>-1</sup>): =C-H (med.) 3052; -C-H (med.) 2954, 2932, 2866; C=O (sharp) 1733; C=C (sharp) 1637; C-O-C (sharp) 1246, 1142, 1107. <sup>1</sup>H NMR (200 MHz, CDCl<sub>3</sub>): **0.88** (m, 3H<sub>1b</sub>, 3H<sub>1a</sub>, 3H<sub>5a</sub>, 3H<sub>9a</sub>), **1.10-1.30** (m, 2H<sub>11</sub>, 2H<sub>10</sub>, 1H<sub>9</sub>, 2H<sub>8</sub>, 2H<sub>7</sub>, 2H<sub>6</sub>, 1H<sub>5</sub>, 2H<sub>4</sub>, 2H<sub>3</sub>, 2H<sub>2</sub>, 1H<sub>1</sub>), **1.38** (m, 3H<sub>13a</sub>), **1.53** (m, 2H<sub>12</sub>), **1.77** (m, 2H<sub>14</sub>, J<sup>3</sup><sub>15-14</sub> = 6.8 Hz), **1.99** (s, 3H<sub>18a</sub>), **2.03** (s, 3H<sub>19a</sub>), **2.10** (s, 3H<sub>21a</sub>), **2.11** (s, 3H<sub>24</sub>), **2.60** (t, 2H<sub>15</sub>, J<sup>3</sup><sub>14-15</sub> = 6.8 Hz), **5.80** (t, 1H<sub>25a</sub>, J<sup>3</sup><sub>25b-25a</sub> = 1.6 Hz), **6.40** (s, 1H<sub>25b</sub>). <sup>13</sup>C NMR (125 MHz, CDCl<sub>3</sub>): **11.8** (C<sub>21a</sub>), **12.1** (C<sub>18a</sub>), **12.9** (C<sub>19a</sub>), **18.5** (C<sub>24</sub>), **19.6** (C<sub>5a</sub>), **19.7** (C<sub>9a</sub>), **20.6** (C<sub>15</sub>), **21.0** (C<sub>11</sub>), **22.6** (C<sub>1a</sub>), **22.7** (C<sub>1b</sub>), **23.9** (C<sub>13a</sub>), **24.4** (C<sub>7</sub>), **24.8** (C<sub>3</sub>), **28.0** (C<sub>1</sub>), **31.0** (C<sub>14</sub>), **32.7** (C<sub>5</sub>), **32.8** (C<sub>9</sub>), **37.2** (C<sub>4</sub>), **37.3** (C<sub>6</sub>), **37.4** (C<sub>8</sub>), **37.5** (C<sub>10</sub>), **39.4** (C<sub>2</sub>), **40.4** (C<sub>12</sub>), **75.0** (C<sub>13</sub>), **117.4** (C<sub>16</sub>), **123.0** (C<sub>21</sub>), **125.0** (C<sub>19</sub>), **126.6** (C<sub>18</sub>), **126.8** (C<sub>25</sub>), **135.9** (C<sub>23</sub>), **140.5** (C<sub>20</sub>), **149.3** (C<sub>17</sub>), **165.9** (C<sub>22</sub>). MS (ES<sup>+</sup>): m/z = 522 (M<sup>+</sup>+Na).<sup>5</sup>

### 2.3.3.7 Poly[2-(2'3'4'6'-tetra-O-acetyl-β-D-galactosyloxy)ethyl acrylate-ter-α-tocopheryl acrylate-ter-2-(dimethylamino)ethyl acrylate] (4a – 12a)

The syntheses of these 9 terpolymers is summarised in Table 2.1. These were synthesised in parallel using a Radley's 12 Station Reaction Carousel mounted on an IKA electronic hotplate stirrer.

The general procedure was as follows:

A solution of **2a** (15 mg, 0.034 mmol), α-tocopheryl acrylate (15 mg, 0.031 mmol), DMAEA (270 mg, 1.89 mmol) and AIBN (4.5 mg, 1.5 wt% w.r.t. monomers) in anhydrous DMF (0.9 ml, 30 wt% monomer solution) was prepared. The solution was

degassed and then heated at 50°C under an atmosphere of nitrogen, with stirring, for 24 hours.

	<b>1a</b>		<b>3a</b>		<b>DMAEA</b>	
	<i>(mg)</i>	<i>(mmol)</i>	<i>(mg)</i>	<i>(mmol)</i>	<i>(mg)</i>	<i>(mmol)</i>
<b>4a</b>	15	0.034	15	0.031	270	1.89
<b>5a</b>	30	0.067	15	0.031	255	1.78
<b>6a</b>	60	0.134	15	0.031	225	1.57
<b>7a</b>	15	0.034	30	0.062	255	1.78
<b>8a</b>	30	0.067	30	0.062	240	1.68
<b>9a</b>	60	0.134	30	0.02	210	1.47
<b>10a</b>	15	0.034	60	0.124	225	1.57
<b>11a</b>	30	0.067	60	0.124	210	1.47
<b>12a</b>	60	0.134	60	0.124	180	1.26

**Table 2.1 – Polymer feed ratios for parallel polymer syntheses**

Subsequently the solvent was removed *in vacuo*, the crude residue was re-dissolved in THF and precipitated into petroleum ether (40°C – 60°C b.p.). The resulting precipitate was collected by filtration, dissolved in distilled water, purified by dialysis against distilled water (using a Dispo-dialyser, MWCO 1000) and lyophilised, giving the polymer as an off-white powder. The product was stored under vacuum in a desiccator over phosphorous pentoxide. <sup>1</sup>H NMR spectra were characteristic of polymer samples, broad over-lapping peaks were evident. The product yields and molecular weights are shown for in Table 2.2.

	Yield		GPC (DMF)	
	(mg)	(%)	$M_n$	$M_w$
<b>5a</b>	81	27	7360	7380
<b>6a</b>	132	44	12700	17600
<b>7a</b>	30	10	12500	13100
<b>8a</b>	159	53	9950	14800
<b>9a</b>	102	34	6350	14500
<b>10a</b>	99	33	5630	9840
<b>11a</b>	39	13	7650	12900
<b>12a</b>	120	40	7580	15500

Table 2.2 – Yield and molecular weight of polymers prepared with carousel reactor

### 2.3.3.8 De-acetylation of terpolymers 5a – 12a (5b – 27b)

The de-acetylation of the polymer series **5a-12a** is summarised in Table 2.3. With the exception of **12a**, all of the de-acetylations were carried out in the Radley's 12 Station Reaction Carousel on an IKA hotplate stirrer.

	(mg)	NaOMe [0.01M] (ml)	Yield	
			(mg)	(%)
<b>5a</b>	38.4	0.1	19.6	51
<b>6a</b>	67.7	0.2	42.7	63
<b>7a</b>	15.1	0.05	2.0	13
<b>8a</b>	65.1	0.1	26.0	40
<b>9a</b>	41.8	0.2	20.9	50
<b>10a</b>	42.8	0.05	15.4	36
<b>11a</b>	13.5	0.1	3.5	26
<b>12a</b>	61.0	0.2	48.0	79

Table 2.3 – Summary of De-acetylations

A general procedure was as follows:

Samples were dissolved in anhydrous methanol (5 ml) to which the sodium methoxide solution was added (at the volume shown in Table 2.1) and stirred under an atmosphere of nitrogen for 2 hours<sup>†</sup>. Subsequently DOWEX® 50WX2-200 cation exchange resin was added to remove Na<sup>+</sup> ions. After stirring for approximately 15 minutes, the solution was filtered and the solvent removed *in vacuo*. The crude polymer was then dissolved in water and lyophilised. This yielded the products as off-white powders.

### 2.3.3.9 Poly[2-( $\beta$ -D-galactosyloxy)ethyl acrylate-ter- $\alpha$ -tocopheryl acrylate-ter-2-(dimethylamino)ethyl acrylate] (13)

A solution of **2a** (150 mg, 0.539 mmol), **3a** (150 mg, 0.309 mmol), DMAEA (450 mg, 3.14 mmol) and AIBN (11.3 mg, 1.5 wt% w.r.t. monomers) in a mixture of anhydrous DMF (1.8 ml) and anhydrous methanol (0.45 ml) was prepared. The solution was degassed (*via* the freeze, pump, thaw method) and then heated at 65°C under an atmosphere of nitrogen, with stirring, for 24 hours.

Subsequently the solvents were removed *in vacuo*, the crude material re-dissolved in distilled water, purified by dialysis against distilled water (1000 MWCO membrane), and lyophilised to yield polymer **13** (674 mg, 64 %) as a cream powder.

(-(**2a**)<sub>13.5</sub>-(**3a**)<sub>7.9</sub>-(DMAEA)<sub>78.7</sub>-, Expected: C 64.4l; H 9.3; N 3.5, Found C 61.5; H 8.7; N 3.9), IR (KBr, cm<sup>-1</sup>): -OH (broad) 3422; -CH (med.) 2946, 2929, 2868; -C=O (sharp) 1734; -CH (sharp) 1459; -CH<sub>3</sub> (med.) 1380. <sup>1</sup>H NMR (200 MHz, D<sub>2</sub>O, significant peaks): **0.71** (broad s, 3H<sub>9a</sub>, 3H<sub>5a</sub>, 3H<sub>1a</sub>, 3H<sub>1b</sub>, tocopheryl group), **3.04-3.80** (sugar ring protons), **4.17** (broad, CH<sub>2</sub>-CH<sub>2</sub>-O-, DMAEA).

### 2.3.3.10 Poly[2-( $\beta$ -D-galactosyloxy)ethyl methacrylate-ter- $\alpha$ -tocopheryl acrylate-ter-2-(dimethylamino)ethyl acrylate] (14)

A solution of **2b** (217 mg, 0.74 mmol), **3a** (325 mg, 0.67 mmol), DMAEA (542 mg, 3.79 mmol) and AIBN (16.3 mg, 1.5wt% w.r.t monomers) in a mixture of anhydrous methanol (0.65 ml) and anhydrous DMF (2.6 ml) was prepared. After degassing, the

<sup>†</sup> CF27 was reacted on its own initially to establish an appropriate duration for the reaction. This reaction was stopped after 1 hour and 15 minutes.

solution was stirred under nitrogen at 70°C for approximately 24 hours. The solvents were removed under vacuum, the residue dissolved in water, purified by dialysis against de-ionised water (1000 MWCO) and lyophilised to yield polymer **2** (820 mg, 76 %).

$[\alpha]_D = -1.7^\circ$  ( $c = 25$ , MeOH),  $(-(\mathbf{2b})_{14.2}-(\mathbf{3a})_{12.9}-(DMAEA)_{72.9})$ , expected C 63.0; H 9.2; N 4.9, Found C 60.71; H 8.9; N 3.7); IR (KBr,  $\text{cm}^{-1}$ ): -OH (broad) 3422; -CH (med.) 2950, 2927, 2867; -C=O (sharp) 1734; -CH (sharp) 1458; -CH<sub>3</sub> (med.) 1380. <sup>1</sup>H NMR (200 MHz, D<sub>2</sub>O, significant peaks): 0.70 (broad s, 3H<sub>9a</sub>, 3H<sub>5a</sub>, 3H<sub>1a</sub>, 3H<sub>1b</sub>, tocopherol group), 3.04-3.82 (sugar ring protons), 4.30 (broad, -CH<sub>2</sub>-CH<sub>2</sub>-O-, DMAEA). GPC (H<sub>2</sub>O): M<sub>n</sub>  $(8.65 \pm 0.34) \times 10^5$ ; PD = 3.2; GPC (CHCl<sub>3</sub>): M<sub>n</sub>  $9.65 \times 10^5$ ; PD = 3.8.

## 2.4 References

1. Johnston, A. D.; Cowperthwaite, G. F. Inhibition of polymerization of methacrylate monomers with  $\alpha$ -tocopherol and compositions containing these materials. US Patent No: 2003191338, **2003**.
2. Al-Malaika, S. *Macromol. Symp.* **2001**, 176, (1st International Conference on Polymer Modification, Degradation and Stabilisation, 2000), 107-117.
3. Yasuzawa, M.; Nakaya, T.; Imoto, M. *Makromol. Chem., Rapid Commun.* **1985**, 6, (11), 727-31.
4. Chen, T.-M.; Wang, Y.-F.; Sakaguchi, T.; Li, Y.-J.; Nakaya, T.; Sakurai, I. *J. Macromol. Sci., Pure Appl. Chem.* **1997**, A34, (3), 451-459.
5. Ortiz, C.; Vazquez, B.; San Roman, J. *Polymer* **1998**, 39, (17), 4107-4114.
6. Ortiz, C.; Vazquez, B.; San Roman, J. *J. Biomed. Mater. Res.* **1999**, 45, (3), 184-191.
7. Plasencia, M. A.; Ortiz, C.; Vazquez, B.; San Roman, J.; Lopez-Bravo, A.; Lopez-Alonso, A. *J. Mater. Sci.: Mater. Med.* **1999**, 10, (10/11), 641-648.
8. Monett, D.; Mendez, J. A.; Abraham, G. A.; Gallardo, A.; San Roman, J. *Macromol. Theory Simul.* **2002**, 11, (5), 525-532.
9. Noble, R. C.; Penny, P. C.; Davis, B. G.; Cameron, N. R.; Maldjian, A.; Fleming, C. Polymeric based complex. UK Patent No: 2003103716, **2003**.
10. Cameron, N. R.; Cunningham, O.; Fleming, C.; Maldjian, A.; Penny, P.; Noble, R. C.; Davis, B. G.; Rullay, A. K.; Haddleton, D. M. *Polym. Mater. Sci. Eng.* **2004**, 90, 249-250.
11. Fleming, C.; Maldjian, A.; Costa, D. D.; Rullay, A. K.; Haddleton, D. M.; St John, J.; Penny, P.; Noble, R. C.; Cameron, N. R.; Davis, B. G. *Nat. Chem. Biol.* **2005**, 1, (5), 270-274.
12. Dahmen, J.; Frejd, T.; Magnusson, G.; Noori, G. *Carbohydr. Res.* **1983**, 114, (2), 328-30.
13. Ambrosi, M.; Batsanov, A. S.; Cameron, N. R.; Davis, B. G.; Howard, J. A. K.; Hunter, R. *J. Chem. Soc., Perkin Trans. 1* **2002**, (1), 45-52.
14. Singh, N. P.; Schmidt, R. R. *J. Carbohydr. Chem.* **1989**, 8, (2), 199-216.
15. Schmidt, R. R. *Angew. Chem.* **1986**, 98, (3), 213-36.

16. Paulsen, H.; Paal, M. *Carbohydr. Res.* **1984**, 135, (1), 53-69.
17. Ogawa, T.; Beppu, K.; Nakabayashi, S. *Carbohydr. Res.* **1981**, 93, (1), C6-C9.
18. Hanessian, S.; Banoub, J. *Carbohydr. Res.* **1977**, 59, (1), 261-7.
19. Hanessian, S.; Banoub, J. *Carbohydr. Res.* **1977**, 53, (1), C13-C16.
20. Kiso, M.; Anderson, L. *Carbohydr. Res.* **1979**, 72, C12-C14.
21. Kiso, M.; Anderson, L. *Carbohydr. Res.* **1979**, 72, C15-C17.
22. Ambrosi, M., *PhD Thesis*, University of Durham, **2002**
23. Armes, S., *Personal Communication*. Cameron, N. R., Fleming, C., **2001**
24. Ladmiral, V.; Melia, E.; Haddleton, D. M. *Eur. Polym. J.* **2004**, 40, (3), 431-449.
25. Okada, M. *Prog. Polym. Sci.* **2001**, 26, (1), 67-104.
26. Watson, H., *MChem Thesis*, University of Durham, **2004**
27. Lowe, A. B.; Sumerlin, B. S.; McCormick, C. L. *Polymer* **2003**, 44, (22), 6761-6765.

### **3 Vitamin E polymer properties**

#### ***3.1 Introduction***

This chapter investigates some of the physical properties of polymer **14**, the preparation of which is described in Chapter 2. Whilst it is primarily the biological properties of this material that are of most interest in the context of this research, some of the physical properties are worthy of mention, and could themselves be relevant in certain biological systems, or indeed provide possible alternative methods to the type of drug delivery system being investigated.

The components of the polymer being studied help to impart certain physical properties. Firstly, the fact that the polymer contains both hydrophilic and hydrophobic components could give rise to micellar behaviour, although one must bear in mind that the polymer was prepared via standard free radical methods and not by controlled radical polymerisation, thus the structure is most likely random in nature and will not possess well-defined blocks. Nevertheless, any observed aggregation of these types of polymers could offer the possibility of micellar drug delivery systems, where metabolites that are not easily modified such that they can be polymerised, could simply be trapped within a polymeric micelle.

There are several characterisation techniques relevant in this area: atomic force microscopy (AFM); light scattering; scanning electron microscopy; and qualitative micellisation studies.

### ***3.2 Results and Discussion***

When preparing aqueous solutions of glycopolymers containing vitamin E, they were observed to froth when agitated. This qualitative observation presented the possibility that these materials may be surface active. Previous work by Ambrosi<sup>1, 2</sup> had reported critical aggregation concentrations (CACs) for surface active homoglycopolymers, therefore it was highly conceivable that terpolymers containing hydrophilic and hydrophobic components could also be surface active. Furthermore, work conducted by this author<sup>3</sup> had indicated that polymers containing DMAEMA were surface active in certain circumstances. Specifically, random copolymers of DMAEMA and MMA at a molar ratio of 50:50 were shown to reduce the surface tension of water from  $0.071 \text{ Nm}^{-1}$  to  $0.061 \text{ Nm}^{-1}$  at  $25^\circ\text{C}$  at a polymer concentration of  $1.8 \text{ gdm}^{-3}$ .

As a result of this observation, and based on the results previously reported, a number of experiments were conducted, which were designed to demonstrate whether or not these materials were also surface active.

Firstly, it was decided to measure the CAC, therefore, a series of solutions of accurate concentration were prepared, and analysed by dynamic light scattering. Each sample was analysed 6 times and an average value taken. The CAC is calculated by monitoring the number of particles counted during each scan. In very dilute solutions, one would expect very few counts to be observed, while in more concentrated solutions, it is more likely that the light will be scattered by aggregated material, and hence the number of counts will be increased. By plotting the number of counts per second against concentration, one can establish the CAC.

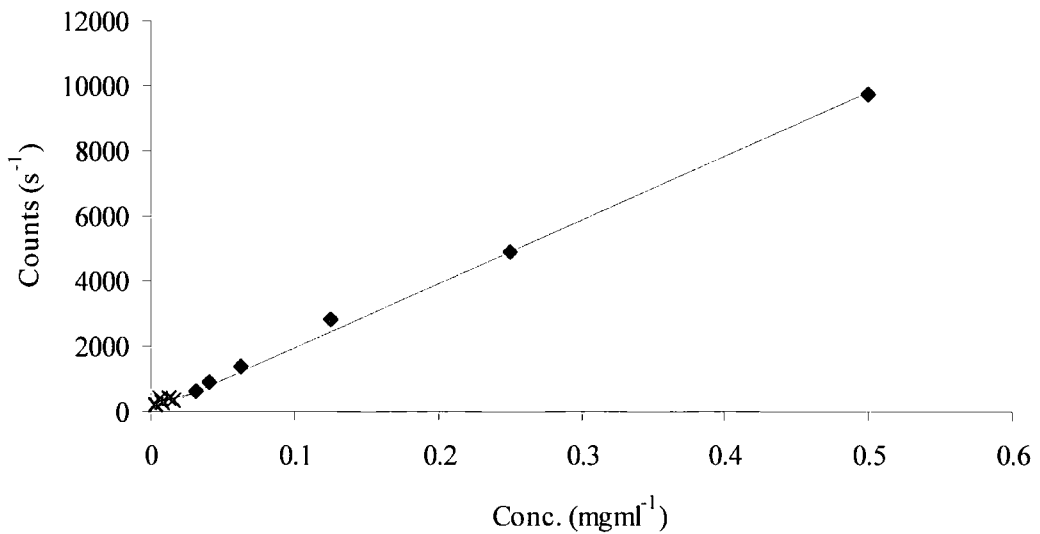


**Figure 3.1 - CAC curve for 14**

Figure 3.1 depicts a plot of counts per second against concentration for polymer 14. At this scale the location of the CAC is not immediately obvious. The CAC can be calculated in two ways. If the graph is plotted accurately then the CAC can be read from the graph as the point where the two lines intersect. Alternatively, the CAC can be obtained by setting the equations of the two lines equal to each other and solving for  $x$ .

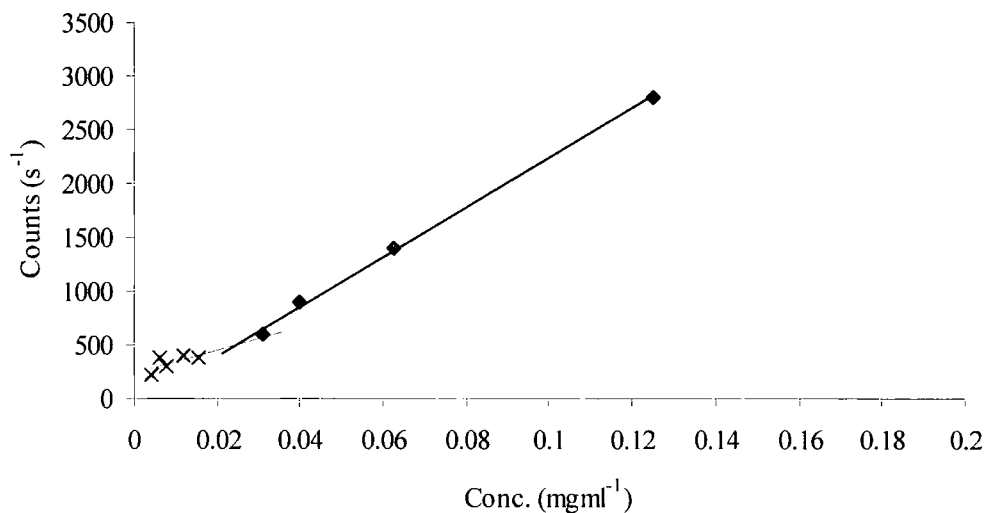


**Figure 3.2 - Intersection of the two lines on the CAC graph for 14**

The CAC of **14** can be obtained approximately by inspecting Figure 3.2. The lines intersect at approximately 0.025 mg/ml. This can be verified and stated more accurately by solving the equations. The equation of the red line is:

$$y = 10.325x + 0.238, \quad (1)$$

The equation of the blue line is:

$$y = 19.626x. \quad (2)$$

Therefore for the same value of  $y$ ,  $x = 0.026$ . This value is in good agreement with the visual interpretation of the graph.

The light scattering experiment not only indicates the CAC but also gives an indication of the size of the aggregates that are present in solution at the various concentrations. Obviously the particle size is not monodisperse, i.e. there is a distribution of particle sizes. This information can be used to gain an average size of the aggregates. The average particle size is obtained from a plot of signal intensity against diameter (nm) on a log scale. This gives a unimodal plot for each concentration, which in turn gives the average particle size. Above the CAC the average particle size was found to be  $\sim 30$  nm (see Figure 3.3 below). This data would suggest that the ESEM images shown later in this chapter (obtained from the spin-coated samples), do not contain any meaningful information.

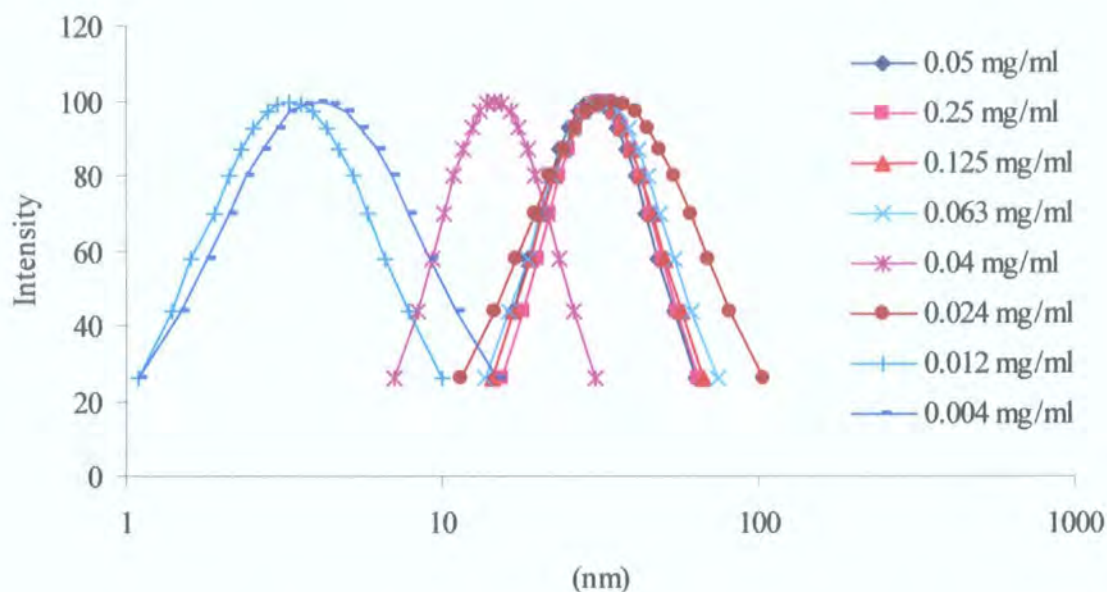


Figure 3.3 - Particle size (nm) distributions for aqueous solutions of 14

### 3.2.1 Micellisation

One area of interest under the heading of drug delivery is the use of micelles or vesicles to deliver drugs to a target cell or organ. The idea is to create a material which has hydrophilic character on the outside of the spherical particle, perhaps with targeting groups attached, and a hydrophobic core. The hydrophobic core is then able to trap a hydrophobic “drug” inside and essentially protect it until it reaches its target, whereupon it is released. In the context of this report, our aims were to produce soluble linear polymers with our “drug”, in this case Vitamin E, bound to the polymer backbone by an enzymatically cleavable linker. However, in light of the results of the CAC measurement which suggest that the polymer forms aggregates in aqueous solution at a concentration above 0.025 mg/ml, it was of interest to assess, at least qualitatively, if such a micellar delivery system was possible.<sup>4-8</sup>

To each of two vials containing approximately 10 ml of water was added approximately 250 mg of Sudan Red dye. One of the vials also had polymer 14 added at a concentration of 0.04 mg/ml. Both vials were stirred/shaken vigorously for 1 hour, then left to settle. This process was repeated for a number of days in order to disperse the solid dye in the aqueous solution, the sealed vials were left at room temperature for 3

weeks. Subsequently, the remaining insoluble material was removed from both vials by filtration, and the two samples were compared. The polymer solution was observed to have solubilised some of the water-insoluble dye, giving a pink colouration to the polymer solution. The vial containing water only was colourless.

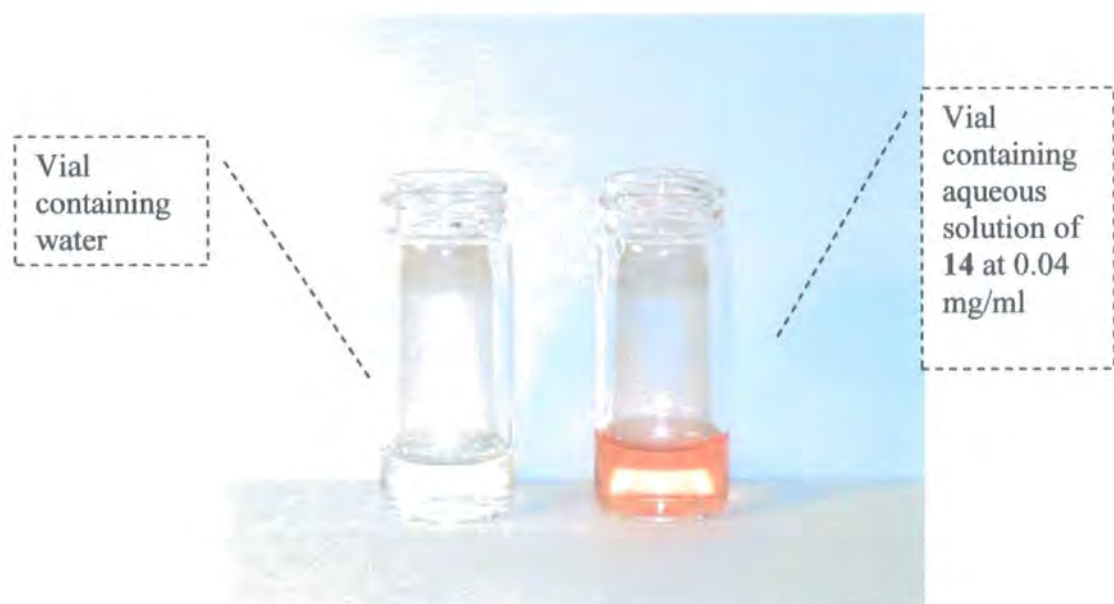


Figure 3.4 - Micellisation of water insoluble dye in solution of 14

Spurred on by the interesting observations obtained from light scattering studies and dye solubilisation it was decided to assess the behaviour of the polymer when concentrated onto a surface. In order to determine whether or not spherical (or approximately) spherical particles were formed, atomic force microscopy (AFM) was attempted. As discussed earlier, the material was soluble in a range of solvents. This afforded the opportunity to use a volatile organic solvent for the purposes of spin coating. Two concentrations of polymer solution (in chloroform) were used to prepare samples. Solutions of 0.1 mg/ml and 0.01 mg/ml of polymer solution were spotted onto the surface of the AFM disks (steel AFM discs coated with HOPG) and spin coated.

These disks were analysed by AFM in tapping mode, to avoid deformation of the material by the AFM tip. In both cases images were obtained which demonstrated the formation of “spherical” aggregates, i.e. shapes either approximating to spheres or spheres further aggregated together. The size of these basic aggregates was found to be in the region of 7-10 nm.

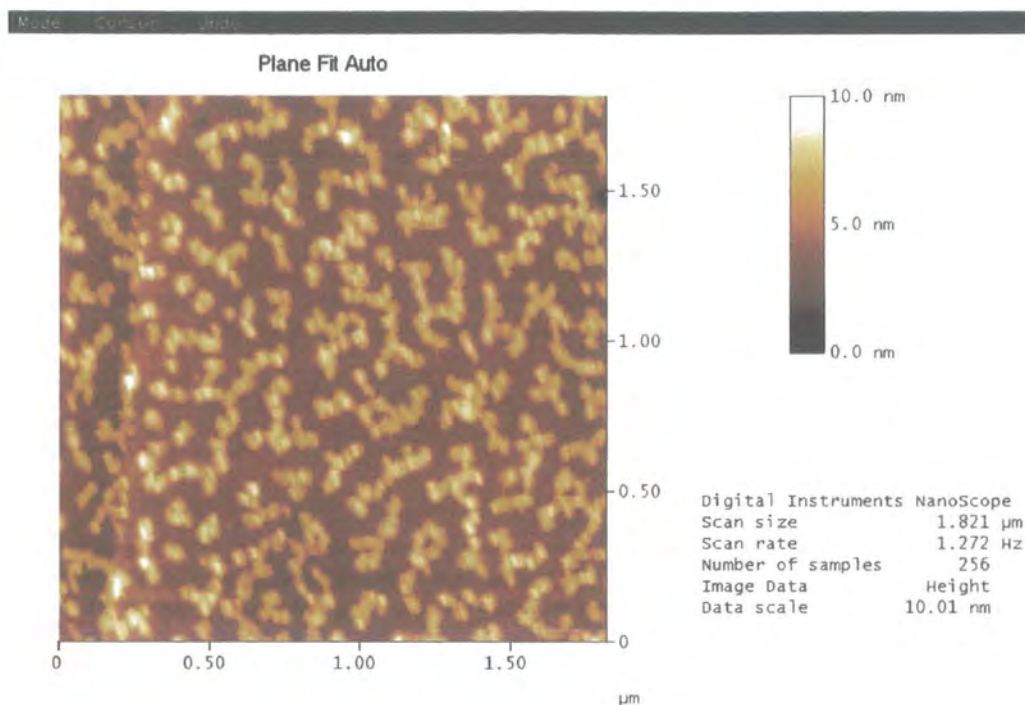


Figure 3.5 - AFM image of 14 at a concentration of 0.1 mg/ml\*

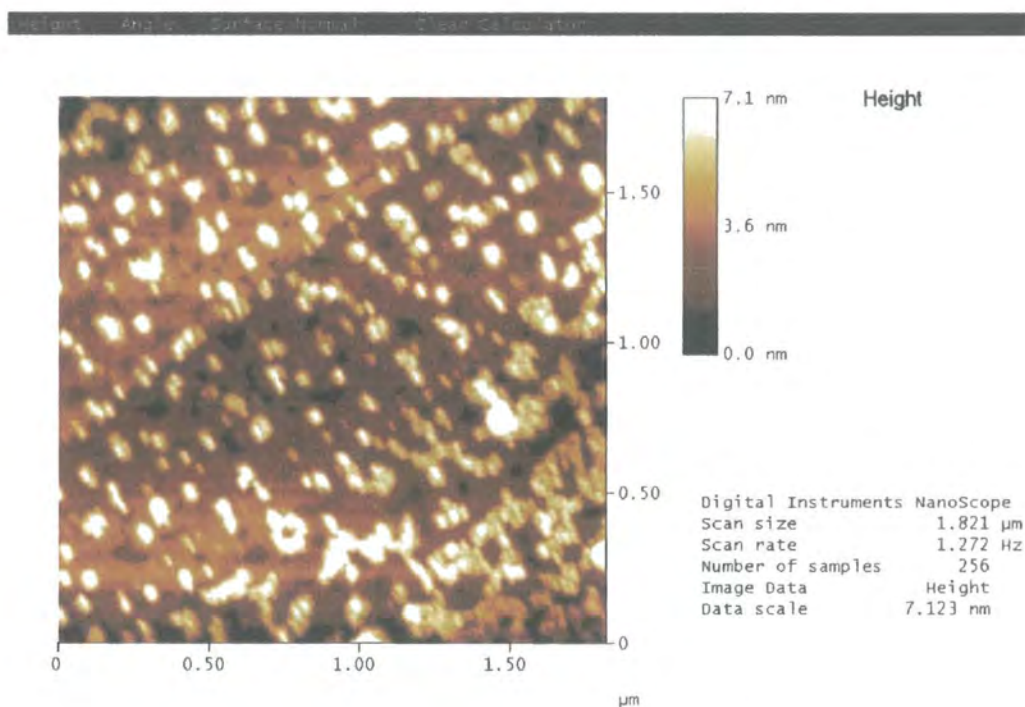


Figure 3.6 - AFM image of 14 at a concentration of 0.01 mg/ml\*

\* Atomic Force Microscopy (AFM) analysis of polymer 14. Samples (from 0.1 mg/ml and 0.01 mg/ml solutions) were measured in tapping mode using an etched silicon probe on a *Nanoscope IV*, spring constant (k): 20-100  $\text{Nm}^{-1}$ , resonant frequency: 200-400 kHz, nominal tip radius of curvature: 5-10 nm, cantilever length: 125 μm, cantilever configuration: single beam, no reflective coating.

The samples used to produce the above images were also examined briefly by environmental scanning electron microscopy, in so-called “low vacuum” mode. This mode avoids the need to sputter samples with gold prior to analysis as the build up of charge on the surface of the sample(s) is dissipated by the low level of water vapour (ca. 0.4 Torr) introduced into the chamber. The images obtained indicated the presence of both large and small aggregates. Work by Ambrosi<sup>1</sup> had suggested that a core-shell type structure could be observed from ESEM images of glycohomopolymers. The ESEM images of this material appeared to show something similar, however whilst such structures may be present it is not possible to draw this conclusion from the images obtained. It is possible that the images observed are a result of glowing of the sample due to electronic bombardment.



a)



b)



**Figure 3.7 – ESEM images of 14 spin coated onto HOPG substrate at, a) 1000x and b) 8000x**

As was previously discussed and will be seen from further data, these images are far too large to represent polymer aggregates and possibly show that there is still water present in the sample. Since analysis of dry, spin-coated samples was inconclusive, samples were subsequently analysed in wet mode.

Since the images obtained in low vacuum mode had been inconclusive, a number of images were also obtained in “wet mode” of the ESEM, using 3 concentrations of **14** in water (40 mg/ml, 1 mg/ml and 0.1 mg/ml). At higher concentrations it appears that the polymer forms a continuous layer rather than discrete spherical particles, although it is conceivable that this layer is composed of closely packed spherical particles (Figure 3.8 & Figure 3.9).



**Figure 3.8 – ESEM image of 14 at a concentration of 40 mg/ml, 1000X magnification**



**Figure 3.9 – ESEM image of 14 at a concentration of 40 mg/ml, 2000X magnification**

Very little structural detail is present in these samples, although it was clear from the analysis which areas of the sample stub contained polymer and which did not, as the metal glows white in the electron beam. Indeed the size of the structural effects observed in the above images is of a similar order of magnitude to those images obtained in low vacuum mode.

At lower concentrations, there is evidence that as the polymer is dehydrated, spherical particles form and these tend to self-associate into larger aggregates (Figure 3.10). This is not entirely surprising, and is in agreement with the results observed by light scattering.

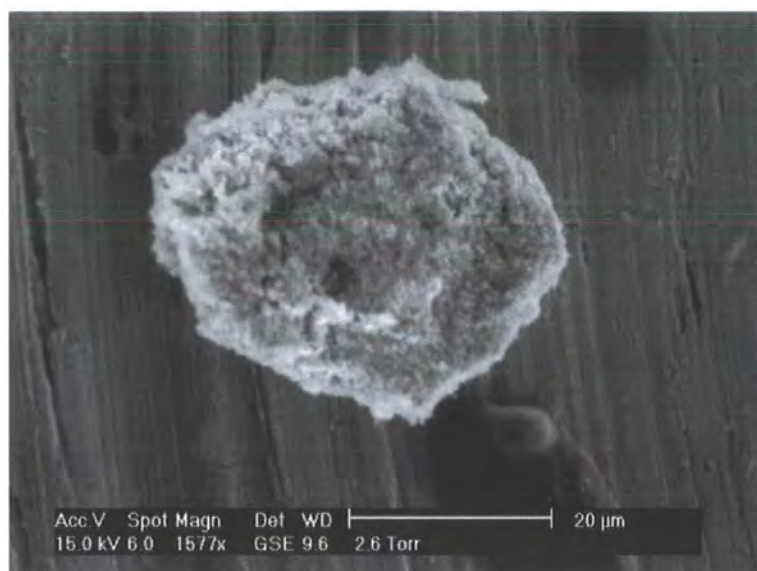


Figure 3.10 – ESEM image of 14 at a concentration of 1 mg/ml, 1577X magnification

This is further illustrated by increasing the magnification as shown in Figure 3.11 and Figure 3.12 below.

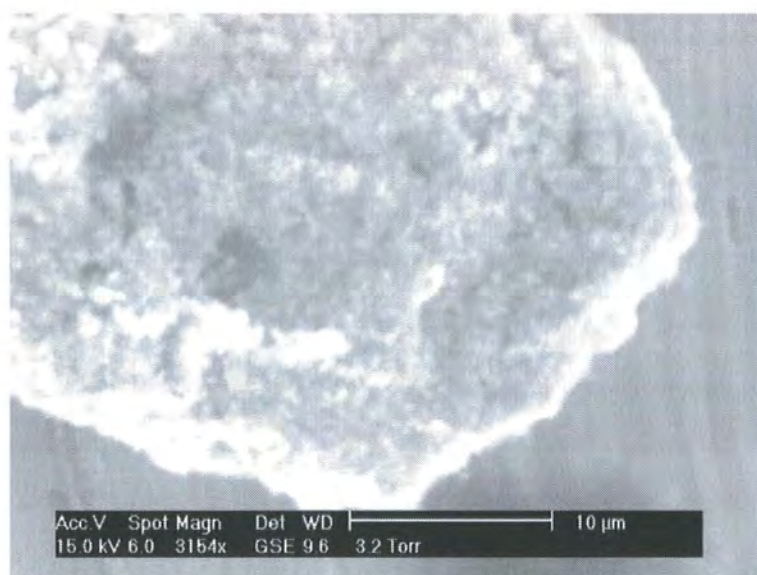
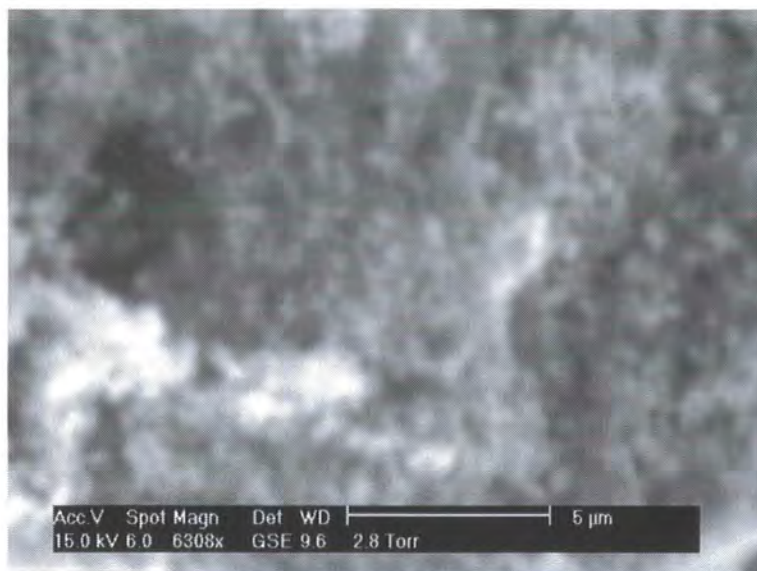


Figure 3.11 – ESEM image of 14 at a concentration of 1 mg/ml, 3154X magnification



**Figure 3.12 – ESEM image of 14 at a concentration of 1 mg/ml, 6308X magnification**

Images such as these are similar to those obtained for glycopolymers investigated by Ambrosi.<sup>1</sup> A further reduction in the initial concentration of polymer solution placed in the sample stub on the Peltier stage did not result in further detail or resolution in the images.

### ***3.3 Concluding remarks***

Whilst the focus of this thesis is on the biological aspects of these types of polymeric species, it is important to investigate their physical properties, which may in some instances be important in their application. Polymer **14** was found to be surface active, which is probably due in part to the presence of a cationic species in the polymer, but may also be attributed to the mixture of both hydrophilic and hydrophobic components along the polymer backbone (i.e. the sugar and vitamin E moieties). The fact that images obtained from more concentrated polymer solutions indicated layers of polymer rather than spherical aggregates is understandable when one considers the effect of allowing a solution of polymer to evaporate in the atmosphere. In this case a waxy residue is formed, which may explain those images. However, by reducing the concentration and keeping some water vapour in the microscope chamber, it was possible to visualise spherical particles. Such images were also obtained for other materials, and will be discussed in detail later.

### 3.4 Experimental

Polymer **14** was prepared as described in Chapter 2. Sudan Red B (dye content 97%) was purchased from Aldrich and was used without further purification. Highly ordered pyrolytic graphite G3389 (10 mm × 10 mm × 2 mm) was purchased from Agar scientific.

#### 3.4.1 Atomic Force Microscopy (AFM)

The instrument used to obtain the AFM images of polymer **14** was the MultiMode™ Nanoscope IV (MM-SPM) manufactured by Digital Instruments. The images were obtained using Tapping Mode AFM.

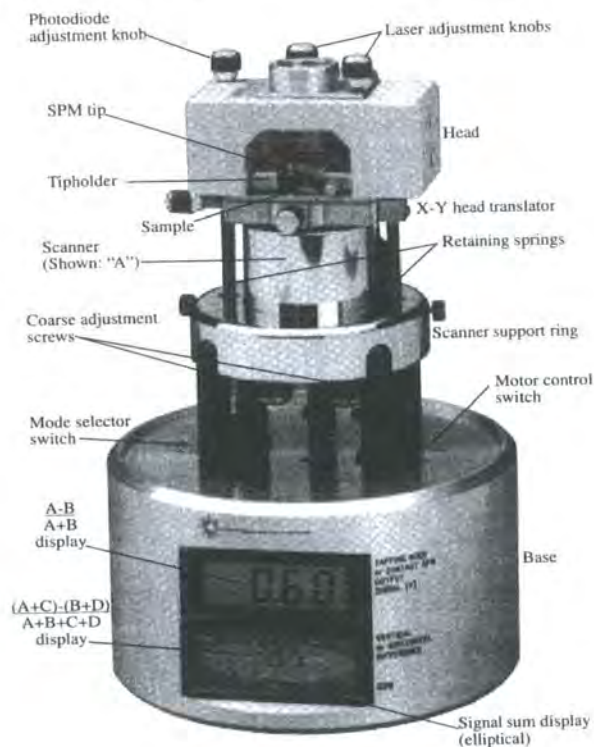


Figure 3.13 – MultiMode™ Nanoscope IV (MM-SPM)

Tapping mode was chosen as the samples are quite soft. In contact mode such samples would easily be deformed, thus giving inaccurate results. Tapping mode AFM uses a stiff crystal silicon probe which is oscillated at its resonant frequency. This gives the tip the required energy to break free of surface tension forces. As the name suggests, in

tapping mode the tip is not in permanent contact with the sample, but only comes into contact with the surface at the lowest point of the tip's oscillation.

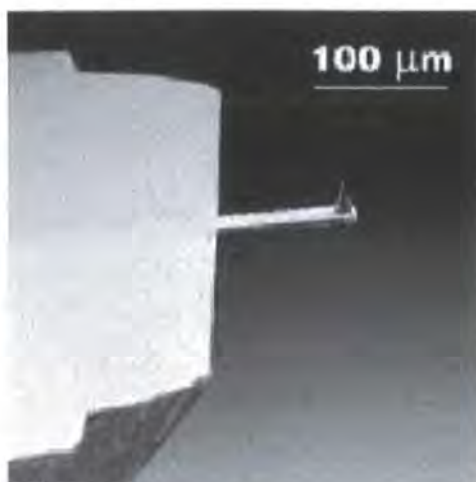


Figure 3.14 – SEM image of a TappingMode AFM crystal silicon tip attached to a vibrating cantilever<sup>9</sup>

However, the tip is very brittle and without care it can easily be broken during use. In order to avoid this, the AFM uses highly sophisticated software with a number of user editable parameters, which must be correctly set in order to ensure safe operation.

#### 3.4.1.1 Sample preparation

Double sided adhesive tape was placed on a steel sample disk (15 mm diameter). On top of this, a piece of HOPG was placed by pressing the two surfaces together (HOPG and adhesive), and then peeling away the HOPG. This leaves a very thin layer of HOPG behind on the steel disk.

The sample was dissolved in chloroform and applied to the HOPG surface by spin coating. It was then mounted onto the magnetic stage and the tip lowered into position electronically.

Obtaining AFM images can be difficult, and is affected by a number of factors *e.g.* choice of substrate, sample concentration, *etc.* The choice of substrate and coating technique came as a result of work previously carried out by Mason<sup>10</sup>. He observed, as had been previously reported,<sup>11, 12</sup> that optimal sample preparation was paramount if

successful visualisation of samples was to be achieved. Initial attempts by Mason, to obtain images from samples coated onto silicon substrate proved fruitless.<sup>10</sup> It was suggested that this was as a result of poor adhesion between the silicon and the polymer, as weak interactions can lead to poor images being obtained.<sup>10</sup> For this reason HOPG was chosen as it was suggested that graphite may interact more strongly with any n-alkyl groups present in the sample. Polymer concentrations of between 0.01 mg/ml and 0.001 mg/ml had proved to be optimal, combined with the use of HOPG as the substrate, therefore the experiments described herein were designed with this insight in mind.

Polymer **14** was dissolved in chloroform at a concentration of 0.01 mg/ml and 0.1 mg/ml. Polymer solutions were applied to the graphite substrate and spin-coated at 2000 rpm for 2-3 minutes. The parameters for AFM measurements were as follows: Atomic Force Microscopy (AFM) analysis of polymer **14**. Samples (from 0.1 mg/ml and 0.01 mg/ml solutions) were measured in tapping mode using an etched silicon probe on a *Nanoscope IV*, spring constant (k): 20-100 Nm<sup>-1</sup>, resonant frequency: 200-400 kHz, nominal tip radius of curvature: 5-10 nm, cantilever length: 125 µm, cantilever configuration: single beam, no reflective coating.

### 3.4.2 Light Scattering

The critical aggregation concentration (CAC) and particle size measurements were measured using a ZetaPlus Zeta Potential Analyser, with BI-MAS Multi Angle Sizing Option, manufactured by Brookhaven Instruments Limited. A series of aqueous solutions was prepared from very low concentration (0.004 mgml<sup>-1</sup>) to “high” concentration (1 mgml<sup>-1</sup>). These were filtered prior to analysis using PALL *Acrodisc*® Syringe Filters (0.2 µm HT Tuffryn® Membrane), in order to remove large dust particles, placed into cuvettes and analysed.

The technique used is called photon correlation spectroscopy (PCS) of quasi-elastically scattered light (QELS), which is based on correlating the fluctuations of the average, scattered laser light intensity. According to the manufacturer, this system offers many advantages:

- Run speed (1 to 2 minutes)
- Accuracy ( $\pm 1\%$  for monodisperse samples)
- No calibration required
- Suitable for measuring particles, polymers, emulsions, colloids *etc.*, in a range of solvents.

The principles behind the measurement are as follows. There is a light detector at a fixed angle with respect to the incident light beam, and at a fixed distance from the scattering sample (*i.e.* the sample containing light scattering particles). The light that is scattered by the particles reaches the detector. The particles will be moving randomly in the liquid (as a result of diffusive Brownian motion), and the distance travelled by the scattered waves from the particle to the detector will vary as a function of time. These waves will either interfere constructively or destructively, depending on the distance travelled. This results in an average intensity with superimposed fluctuations (Figure 3.15). The decay times of these fluctuations are related to the diffusion constants and therefore, the particle size. Small particles lead to faster decaying fluctuations than larger particles. The decay times can be determined by either a spectrum analyser (frequency), or in this case using a correlator (time).

In essence the correlation works by assuming that if two variables are highly correlated, then a change in one can be used to predict a change in the other. The software used is not only able to calculate the particle size based on these correlations but has the advantage of an algorithm to remove erroneous results caused by dust.

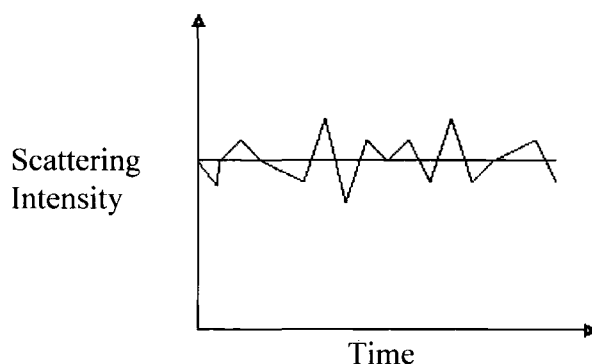


**Figure 3.15 - Fluctuations about the average scattered intensity**

### 3.4.3 ESEM

Environmental scanning electron microscope images were obtained using a FEI Philips XL30 Environmental Scanning Electron Microscope, in low vacuum mode. The samples used in this mode were the same as those used for AFM analysis.

Images were also obtained in “wet mode”. These experiments were carried out using the same microscope, this time with a Peltier sample stage and gaseous secondary electron detector (GSED), to produce the images. Samples were placed in a metallic stub (1 cm diameter, 0.5 cm depth), and the temperature was controlled by the Peltier cooling stage using water/propanol as the coolant. A drop of sample was placed on the stub and the chamber pumped down to a pressure of approximately 4 Torr. The sample was monitored during evacuation by means of the *in situ* CCD camera, and was found to be stable (*i.e.* no boiling of the sample was observed). The samples were cooled to  $\sim 2^{\circ}\text{C}$  and surrounded by water vapour at a pressure of  $\sim 3$  Torr. The accelerating voltage and spot size were 15kV and 5.0 respectively.

### 3.4.4 Solubilisation

Polymer **14** was dissolved in high purity water at a concentration of 0.04 mg/ml. To this solution, Sudan Red (250 mg) was added. This mixture was vortexed and shaken vigorously for several hours each day over a period of 3 weeks, before removing the insoluble dye particles by filtration. The solution was then photographed and compared with a sample of high purity water treated in exactly the same way, with the exception of the addition of polymer.

### 3.5 References

1. Ambrosi, M., *PhD Thesis*, University of Durham, **2002**
2. Ambrosi, M.; Batsanov, A. S.; Cameron, N. R.; Davis, B. G.; Howard, J. A. K.; Hunter, R. J. *J. Chem. Soc., Perkin Trans. 1* **2002**, (1), 45-52.
3. Fleming, C., *BSc Thesis*, University of Strathclyde, **2000**
4. Kataoka, K.; Harada, A.; Nagasaki, Y. *Adv. Drug Delivery Rev.* **2001**, 47, (1), 113-131.
5. Miyata, T.; Nakamae, K. *Trends Polym. Sci.* **1997**, 5, (6), 198-206.
6. Nagasaki, Y.; Yasugi, K.; Yamamoto, Y.; Harada, A.; Kataoka, K. *Biomacromolecules* **2001**, 2, (4), 1067-1070.
7. Yamamoto, Y.; Nagasaki, Y.; Kato, Y.; Sugiyama, Y.; Kataoka, K. *J. Controlled Release* **2001**, 77, (1-2), 27-38.
8. Yasugi, K.; Nakamura, T.; Nagasaki, Y.; Kato, M.; Kataoka, K. *Macromolecules* **1999**, 32, (24), 8024-8032.
9. MULTIMODE (2002) *Operations Notes for the Digital Instruments Multimode AFM*, <http://srv.emunit.unsw.edu.au/pdfs/mmajun02.pdf>, [Accessed 2005]
10. Mason, C., *PhD Thesis*, University of Durham, **2003**
11. Magonov, S. *Visualization of nanoscale architecture of ordered polymers with atomic force microscopy*, Abstracts of Papers, 220th ACS National Meeting, Washington, DC, United States, August 20-24, 2000., pp POLY-002, **2000**.
12. Magonov, S. N.; Kramer, E. J. *Studies of block copolymers with atomic force microscopy*, Abstracts of Papers, 225th ACS National Meeting, New Orleans, LA, United States, March 23-27, 2003., pp PMSE-329, **2003**.

## 4 Biological experiments with multi-component polymers

### 4.1 *Introduction*

It is commonplace in both research laboratories and AI stations to assess the condition of sperm cells at various stages *e.g.* immediately after ejaculation, prior to insemination or at intervals in between. When doing so it is normal to consider the so called “sperm quality parameters” which allow the cells to be benchmarked. These parameters include appearance, assessment of cell motility (including quality of movement<sup>\*</sup>), cell viability, cellular morphology, as well as the volume of the ejaculate and its concentration. The results of these studies provide invaluable information for the commercial user, who does not wish to inseminate with immotile cells, but also provide useful data to the researcher on how the environment or additives affect the cells compared with control samples. Although there are a number of valuable semen evaluation methods/tests widely used, there is no substantial evidence that a particular test (or tests) can predict semen fertility. So whilst predicting poor quality semen is relatively easy, differentiating between medium and high fertility samples is not simple.

In addition to the standard sperm quality parameters, additional analyses were necessary when the cells were incubated with the novel polymer systems. These studies included: vitamin E assays; oxidative stress measurements; confocal microscopy; effect of polymers on the post-thaw motility of bull semen; effect of polymers on post-sort<sup>†</sup> motility; effect of Prosperm<sup>TM</sup> ± polymer on boar semen.

---

<sup>\*</sup> Motility is first scored as a percentage of the cells that are moving. In addition, the quality of this movement is given a score (from 0-4) which further indicates whether or not the cells are swimming, fast and in straight lines (4), or moving slowly on the spot (0). Motility is generally scored subjectively, but can also be measured by computerised systems such as CASA (Computer Assisted Sperm Analysis).

<sup>†</sup> This term refers to semen which has been separated into X and Y chromosome bearing cells using a Cytomation MoFlo<sup>®</sup> flow cytometric sorter.

## ***4.2 Results and discussion***

Two polymers were selected from the range synthesised to be used in the biological assessment of these materials. Ultimately, after a number of experiments this was reduced to one polymer and the focus of the work remained on this material. These polymers contained vitamin E since it had been shown that the inclusion of vitamin E *in vitro* had beneficial effects on the sperm quality parameters<sup>1</sup>. It is worth pointing out that vitamin E cannot be added directly to the ejaculate due to its lack of solubility in the aqueous medium of the extended semen.

### **4.2.1 Motility and viability studies<sup>‡</sup>**

Polymer **13** was assessed in several *in vitro* experiments. Initial experiments focussed on two main aspects, namely cellular motility, and the cells' ability to resist oxidative stress. However, since these systems were entirely novel, the amount of polymer required was unknown, therefore, many initial experiments were needed to optimise fully the concentration of polymer required for effective treatment.

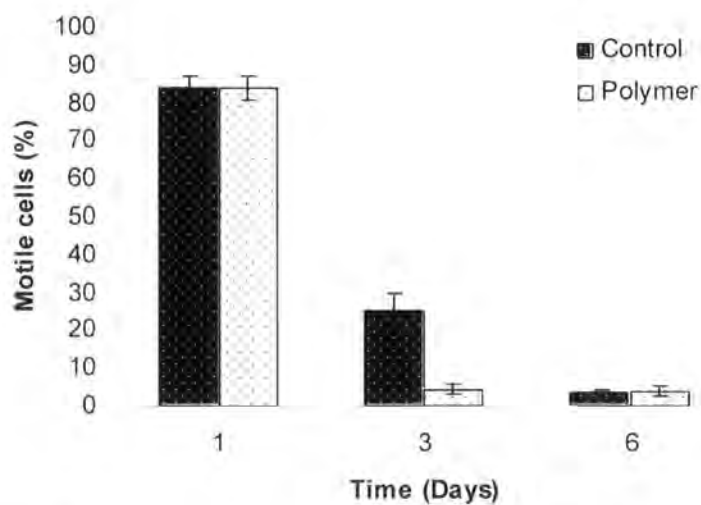
One of the first experiments conducted with polymer **13** monitored the motility and viability of boar sperm cells against untreated control samples, in a commercial diluent (BTS) at 18°C over a 6 day period. The polymer-treated samples had a polymer concentration of 0.2 mg/ml. Unfortunately this resulted in a statistically significant decrease in cellular motility, and although the number of live cells was similar between the two groups, there were statistically more dead cells after 6 days of incubation.

---

<sup>‡</sup> Unless otherwise indicated, biological parameters were assessed by Dr. André Maldjian, Department of Veterinary Medicine, University of Milan.

Table 4.1 - Percentage of motile cells over time  $\pm$  0.2 mg/ml of polymer 13

Day	% Motile	
	Control	Polymer
1	84 $\pm$ 3	84 $\pm$ 3
3	25 $\pm$ 4.7	4.5 $\pm$ 1.3
6	3.2 $\pm$ 1.1	3.9 $\pm$ 1.3

Figure 4.1 - Percentage of motile cells over time  $\pm$  0.2 mg/ml of polymer 13Table 4.2 - Percentage of viable cells  $\pm$  0.2 mg/ml polymer 13 (determined by eosin staining)

Day	Control			Polymer		
	%Live	%Dead	%Damaged	%Live	%Dead	%Damaged
1	71 $\pm$ 2.8	18 $\pm$ 0.9	11 $\pm$ 1.9	71 $\pm$ 2.8	18 $\pm$ 0.9	11 $\pm$ 1.9
3	74 $\pm$ 5.3	12 $\pm$ 2.3	14 $\pm$ 3.7	83 $\pm$ 1.2	10 $\pm$ 1.0	7 $\pm$ 2.2
6	74 $\pm$ 3.0	9 $\pm$ 2.2	17 $\pm$ 1.4	75 $\pm$ 2.5	15 $\pm$ 0.4	10 $\pm$ 2.8

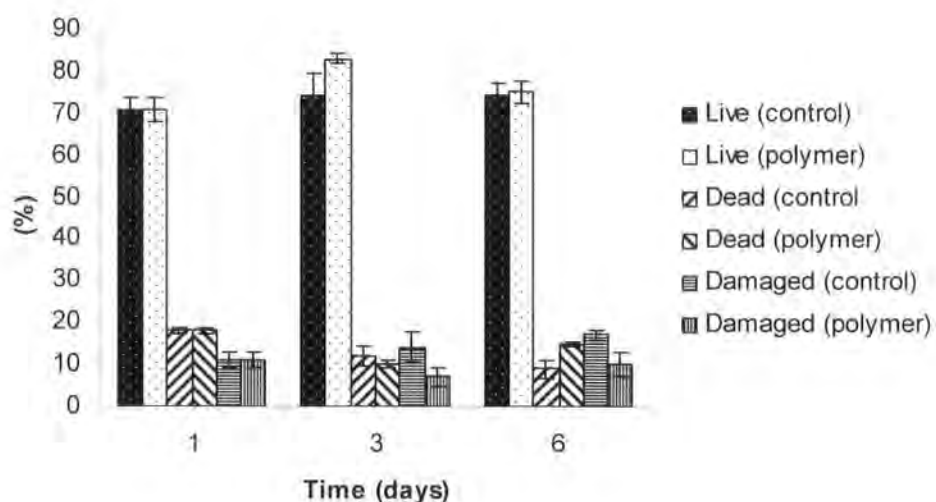
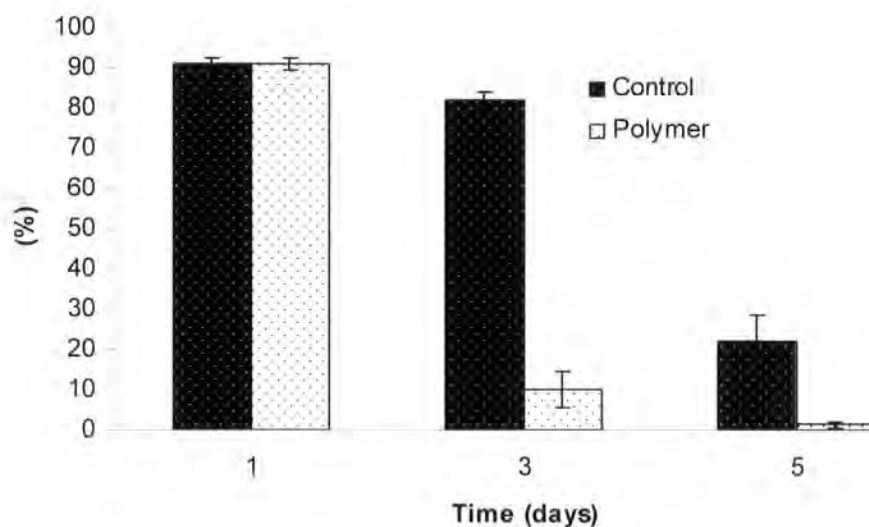


Figure 4.2 - Percentage of viable cells  $\pm$  0.2 mg/ml polymer 13 (determined by eosin staining)

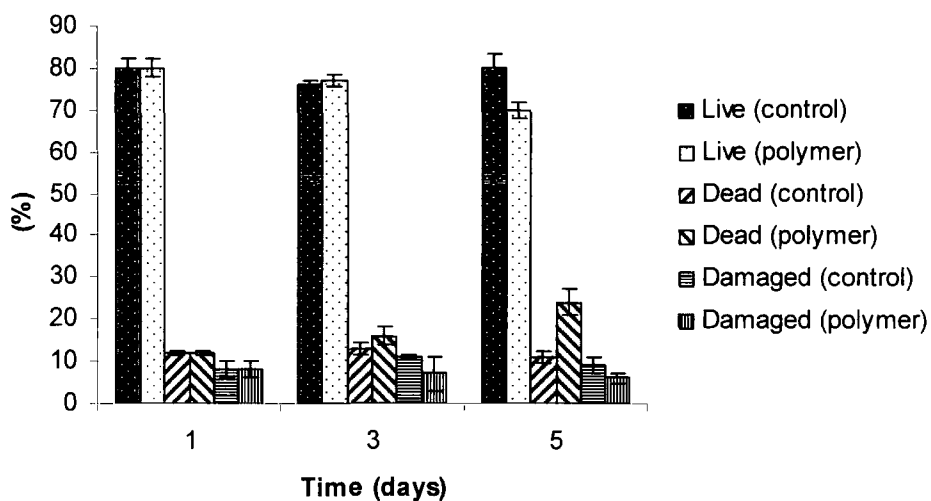
From the results shown in Table 4.1 & Table 4.2, and Figure 4.1 - Percentage of motile cells over time  $\pm$  0.2 mg/ml of polymer 13 & Figure 4.2 it was not clear whether there was too much polymer present in solution or not enough. Too much polymer may have induced negative effects in terms of motility as a result of causing an imbalance in the intracellular osmotic pressure, however since the control samples also showed a fairly rapid decline in cellular motility, it is conceivable that the decrease was due to oxidation perhaps, in which case more polymer may be required. With this in mind a second experiment was conducted, this time using polymer **13** at a concentration of 1 mg/ml. This concentration was chosen as it would deliver the equivalent of approximately 0.2 mg/ml of vitamin E (based on the composition of the polymer). This experiment was conducted over 5 days. Once again the polymer treated cells were found to have lower motility and viability than those of the control samples. It was hypothesised that the reduction in motility could be explained due to the cells being immobilised by polymeric material bound to their outer surface, however washing the cells in physiological buffer and re-suspending them in BTS did not result in a significant improvement in motility (1.3%  $\rightarrow$  3%).

Table 4.3 - Percentage of motile cells  $\pm$  1mg/ml of polymer 13

Day	% Motile	
	Control	Polymer
1	91 $\pm$ 1.6	91 $\pm$ 1.6
3	82 $\pm$ 1.9	10 $\pm$ 4.3
5	22 $\pm$ 6.5	1.3 $\pm$ 0.8

Figure 4.3 - Percentage of motile cells  $\pm$  1mg/ml of polymer 13Table 4.4 - Percentage of viable cells  $\pm$  1 mg/ml of polymer 13

Day	Control			Polymer		
	% Live	% Dead	% Damaged	% Live	% Dead	% Damaged
1	80 $\pm$ 2.2	12 $\pm$ 0.3	8 $\pm$ 1.9	80 $\pm$ 2.2	12 $\pm$ 0.3	8 $\pm$ 1.9
3	76 $\pm$ 1	13 $\pm$ 1.6	11 $\pm$ 0.7	77 $\pm$ 1.6	16 $\pm$ 2.2	7 $\pm$ 3.8
5	80 $\pm$ 3.3	11 $\pm$ 1.4	9 $\pm$ 1.9	70 $\pm$ 2.0	24 $\pm$ 3.1	6 $\pm$ 1.1



**Figure 4.4 - Percentage of viable cells ± 1 mg/ml of polymer 13**

From the results shown in Table 4.3 & Table 4.4 and Figure 4.3 & Figure 4.4 it is obvious that, even at the relatively low concentration of 1 mg/ml, the polymer is detrimental to cellular motility. With this in mind an experiment was conducted with a polymer concentration of 0.02 mg/ml, *i.e.* not only lower than the last experiment but lower than the first attempted concentration of 0.2 mg/ml.

**Table 4.5 - Percentage of motile cells ± 0.02 mg/ml of polymer 13**

Day	% Motile	
	Control	Polymer
1	72 ± 1.5	72 ± 1.5
3	61 ± 3.3	56 ± 3.4
5	28 ± 1.8	28 ± 1.9
8	7 ± 1.2	10 ± 1.5

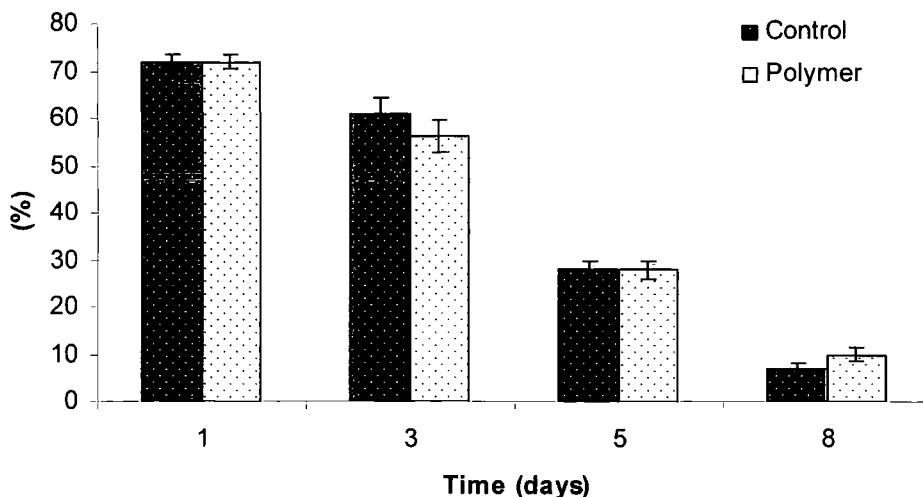


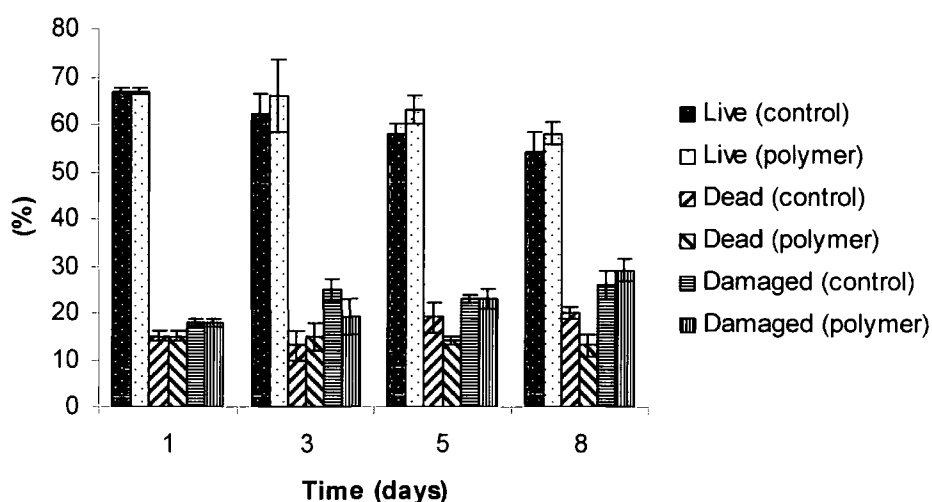
**Figure 4.5 - Percentage of motile cells  $\pm$  0.02 mg/ml of polymer 13**

From the results shown above in Table 4.5 & Figure 4.5 it is evident that the lower concentration of polymer is not having the detrimental effect on motility observed previously for the higher concentrations. The differences between the two groups (control and polymer) were not found to be statistically significant. Obviously it is not possible to compare the motility results exactly from experiment to experiment, not least because they were carried out on different days, but also because there is likely to be natural variation in the performance of the cells, since each sample is clearly unique.

The viability of the cells in the presence of the polymer at 1 mg/ml was lower than control and furthermore, the number of damaged cells was much higher than those in the control samples (see Table 4.4 and Figure 4.4). In this experiment one would expect that since a much lower concentration of polymer was used, this difference should be markedly reduced, or perhaps even show a benefit as a result of the polymer supplementation.

**Table 4.6 - Percentage of viable cells  $\pm$  0.02 mg/ml of polymer 13**

Day	Control			Polymer		
	% Live	% Dead	% Damaged	% Live	% Dead	% Damaged
1	67 $\pm$ 0.6	15 $\pm$ 1	18 $\pm$ 0.8	67 $\pm$ 0.6	15 $\pm$ 1	18 $\pm$ 0.8
3	62 $\pm$ 4.2	13 $\pm$ 3.1	25 $\pm$ 2.3	66 $\pm$ 7.7	15 $\pm$ 3	19 $\pm$ 3.8
5	58 $\pm$ 2.2	19 $\pm$ 3.2	23 $\pm$ 1	63 $\pm$ 3	14 $\pm$ 0.9	23 $\pm$ 2.2
8	54 $\pm$ 4.1	20 $\pm$ 1.2	26 $\pm$ 2.9	58 $\pm$ 2.4	13 $\pm$ 2.4	29 $\pm$ 2.3

**Figure 4.6 - Percentage of viable cells  $\pm$  0.02 mg/ml of polymer 13**

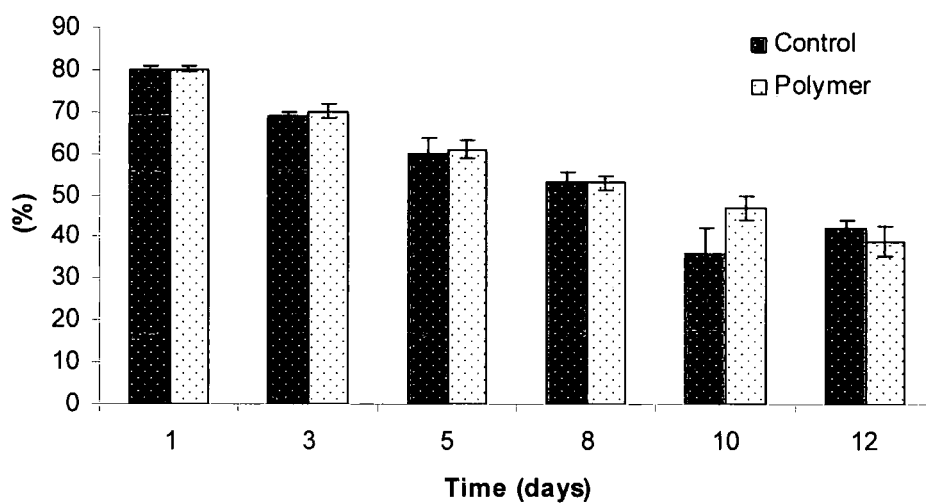
As was expected the lower concentration of polymer resulted in better results in terms of cellular viability. The number of live cells had decreased significantly on day 5 for the control samples, however a significant decrease in live cells was not observed in the polymer treated samples until day 8 (see Table 4.6 and Figure 4.6). Although the number of damaged cells was marginally higher for the polymer treated samples, the number of dead cells was lower than both control and previous experiments.

As alluded to earlier, natural variation between samples can have an effect on results. The incubations with polymer 13 at 0.02 mg/ml were repeated (see Table 4.7 and Figure 4.7) with a different batch of sperm cells and whilst the general trend was the same as the results shown above, the longevity of the cells was markedly increased, although the

temperature of incubation was slightly higher in this case (20°C compared with 18°C previously).

**Table 4.7 - Percentage of motile cells  $\pm$  0.02 mg/ml polymer 13**

<i>Day</i>	% Motile	
	Control	Polymer
<i>1</i>	80 $\pm$ 0.7	80 $\pm$ 0.7
<i>3</i>	69 $\pm$ 0.8	70 $\pm$ 1.7
<i>5</i>	60 $\pm$ 3.6	61 $\pm$ 2.0
<i>8</i>	53 $\pm$ 2.6	53 $\pm$ 1.7
<i>10</i>	36 $\pm$ 5.9	47 $\pm$ 2.9
<i>12</i>	42 $\pm$ 2.0	39 $\pm$ 3.5

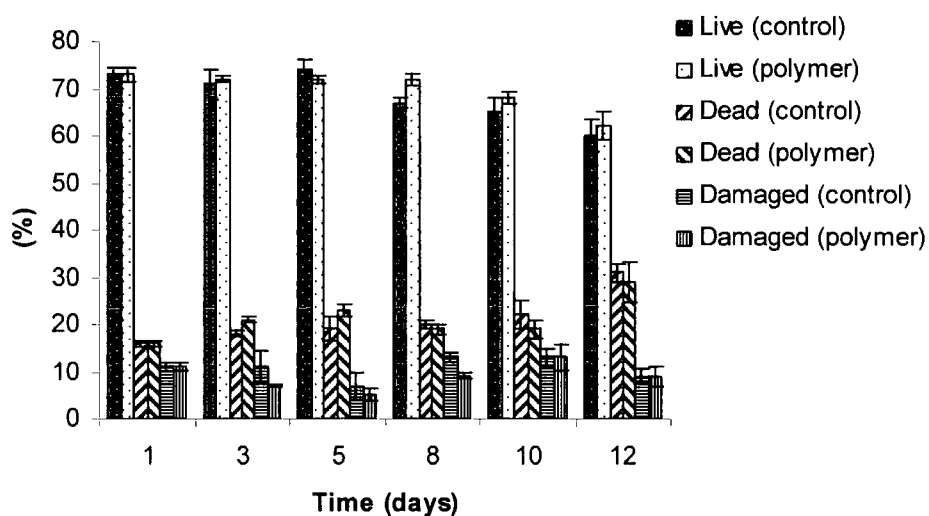


**Figure 4.7 - Percentage of motile cells  $\pm$  0.02 mg/ml polymer 13**

The motility in both groups is very similar and indeed the cells remain motile for an exceptional amount of time compared with typical results. In terms of cellular viability there were significantly more live cells in the treated samples on day 8, and the treated group remained higher than control from day 8 to day 12.

**Table 4.8 - Percentage of viable cells  $\pm$  0.02 mg/ml of polymer 13**

Day	Control			Polymer		
	% Live	% Dead	% Damaged	% Live	% Dead	% Damaged
1	73 $\pm$ 1.4	16 $\pm$ 0.6	11 $\pm$ 0.8	73 $\pm$ 1.4	16 $\pm$ 0.6	11 $\pm$ 0.8
3	71 $\pm$ 3.2	18 $\pm$ 0.7	11 $\pm$ 3.5	72 $\pm$ 0.7	21 $\pm$ 0.5	7 $\pm$ 0.4
5	74 $\pm$ 2.0	19 $\pm$ 2.5	7 $\pm$ 2.7	72 $\pm$ 0.9	23 $\pm$ 1.4	5 $\pm$ 1.3
8	67 $\pm$ 1.0	20 $\pm$ 1.0	13 $\pm$ 1.1	72 $\pm$ 1.4	19 $\pm$ 1.1	9 $\pm$ 0.7
10	65 $\pm$ 3.1	22 $\pm$ 2.9	13 $\pm$ 2.1	68 $\pm$ 1.3	19 $\pm$ 1.8	13 $\pm$ 2.8
12	60 $\pm$ 3.2	31 $\pm$ 1.9	9 $\pm$ 1.5	62 $\pm$ 2.9	29 $\pm$ 4.4	9 $\pm$ 2.2

**Figure 4.8 - Percentage of viable cells  $\pm$  0.02 mg/ml of polymer 13**

Other experiments were conducted at higher concentrations to ensure that the conclusions about the appropriate concentration for a non-detrimental effect on sperm quality parameters were correct. The results of these incubations were in good agreement with those described above.

The effect of polymer concentration on cellular motility over several days can be considered graphically for the polymer 13. These results must be interpreted with caution, since (as has been mentioned already) the fact that the experiments were carried out on separate samples introduces natural heterogeneity.

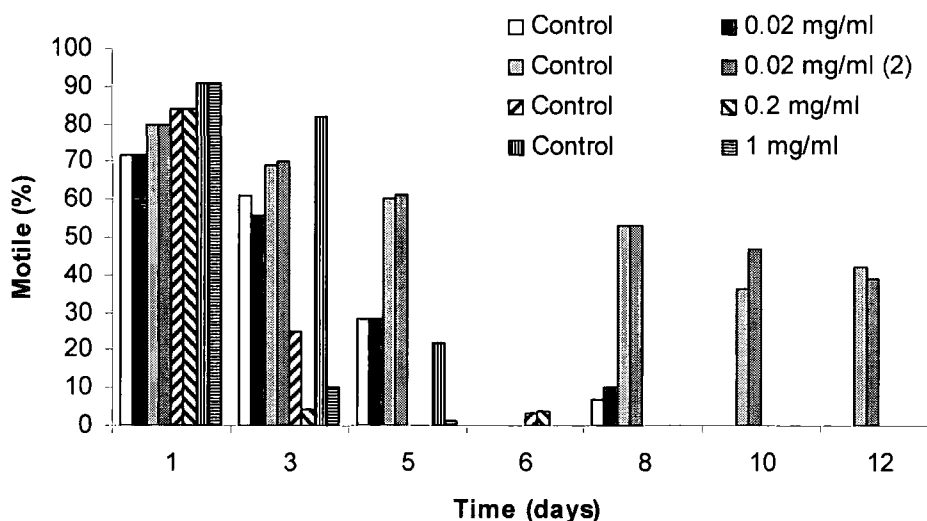


**Figure 4.9 – Summary of cellular motility (%) versus time (days) at various concentrations of polymer 13**

This graph illustrates well the natural variation between samples (see day 1), and also that lower polymer concentrations do tend to produce better motility results, in spite of natural variation.

As mentioned earlier in the chapter, motility can also be given a score which indicates the extent to which the cells are motile. Clearly, for the purposes of fertilisation, a cell which is merely moving on the spot, or swimming in tight circles, is not as “fertile” as a cell swimming in straight lines. The trend in terms of motility score was the same as for motility in general, *i.e.* at higher polymer concentrations the cells had a lower quality of movement compared to control, but at lower concentrations of polymer the motility score was the same and on occasion better than control. This observation may indicate that when the polymer concentration is higher, it is having an influence on the function of the tail, or more particularly an effect on the function of the mid-piece, as this region is critical to cellular motility and any damage to this region would be detrimental to cellular motility.

Cellular viability was improved by using lower concentrations of polymer. However a more interesting point of observation is that the number of damaged cells was generally lower in the samples treated with polymer. The reasons for this are not entirely clear, since the number of dead cells was higher in certain instances. It is conceivable that

damaged cells were adversely affected by the polymer treatment such that they quickly died, and subsequently the number of damaged cells is lower, but the number of dead cells is higher.

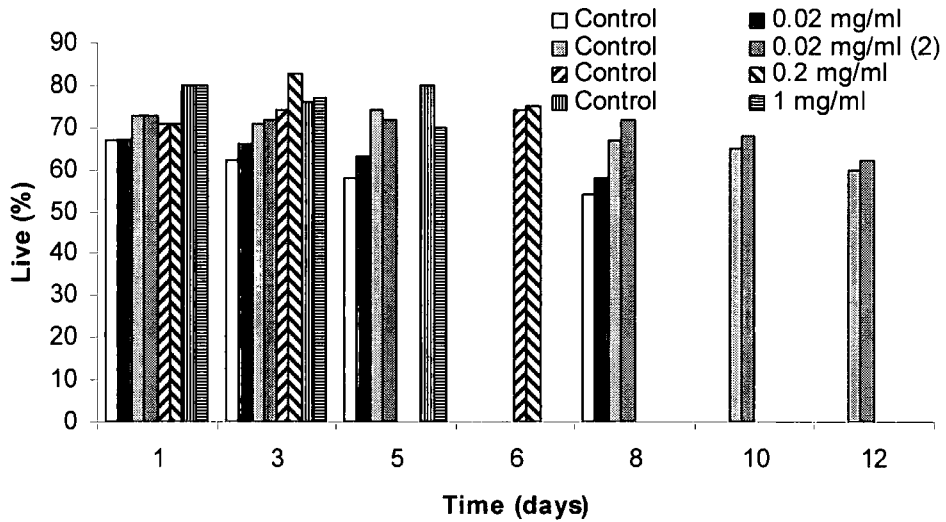


Figure 4.10 - Summary of live cells (%) ± polymer 13 at various concentrations versus time (days)

Although there clearly are differences between the two groups (treated and untreated, see Figure 4.10), they were generally not significant as is clearly illustrated in the figure shown above. Once again the evidence of natural variation is evident from the day 1 time point values.

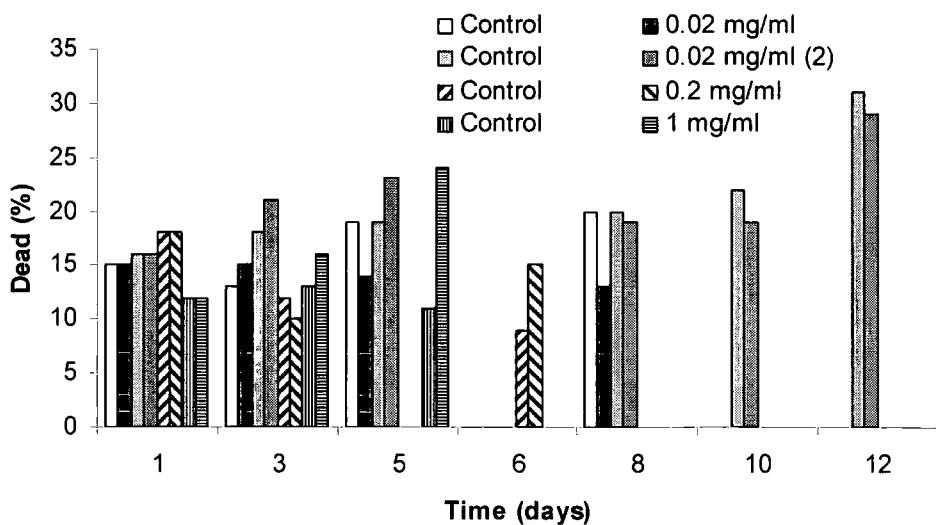


Figure 4.11 - Summary of dead cells (%) ± polymer 13 at various concentrations versus time (days)

In this instance the trend is more obviously polymer concentration dependent. For lower concentrations of polymer in solution, the number of dead cells appears in general to be lower than the control samples (see Figure 4.11), however when higher polymer concentrations were used the trend is reversed. This emphasises the observations made with regard to the effect of polymer concentration on motility.

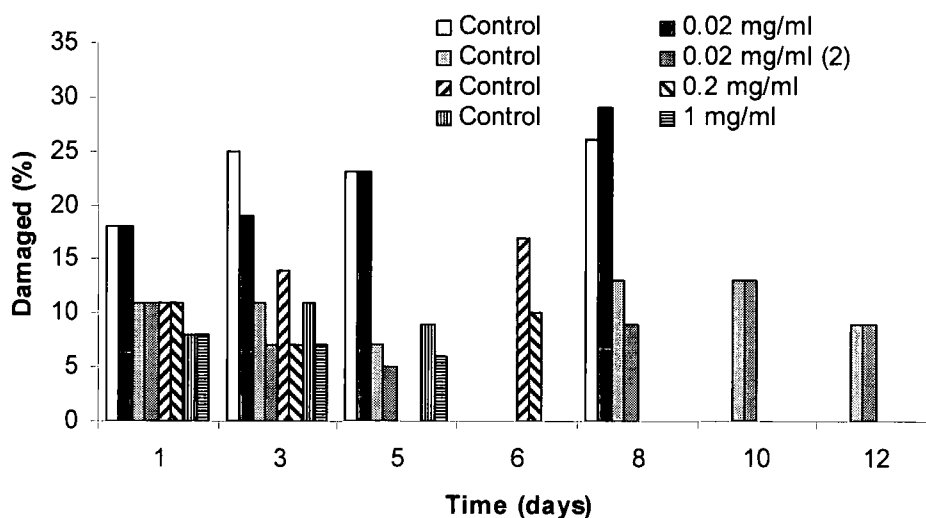


Figure 4.12 – Summary of damaged cells (%) ± polymer 13 at various concentrations versus time (days)

The number of cells damaged appears not only to be influenced by the polymer concentration used, but also on the condition of the sample at day 1. For example, looking at the green bars in Figure 4.12 above, we can see that over 5 days there is little change in the number of damaged cells in both experimental groups, this is also the case for the groups represented by the blue lines. These two groups represent the highest and lowest polymer concentrations respectively, suggesting that the amount of polymer present is not having a noticeable effect on the number of damaged cells.

It is worth reiterating at this stage that the purpose of this particular polymeric material was to prevent oxidative damage to the cells, and that any positive effects on motility or viability would be regarded as an additional benefit. However it was obviously of importance that the use of the polymer in the semen samples did not have any adverse effects on sperm quality parameters, which is why these measurements are of paramount importance.

Polymer **14** was also subjected to *in vitro* testing and initially compared with **13**. It was hypothesised that **14** may perform better than **13** since the former contains more vitamin E moiety per unit weight. An initial experiment to assess the performance **14** in comparison to **13** and control was conducted using polymer concentrations of 0.02 mg/ml (see Table 4.9 and Figure 4.13 below).

**Table 4.9 – Percentage of motile cells  $\pm$  0.02 mg/ml of polymer**

Day	% Motile		
	Control	<b>13</b>	<b>14</b>
1	71 $\pm$ 3.4	71 $\pm$ 3.4	71 $\pm$ 3.4
3	64 $\pm$ 3.0	69 $\pm$ 4.0	76 $\pm$ 2.2
6	10 $\pm$ 1.1	21 $\pm$ 4.6	18 $\pm$ 4.2
8	6 $\pm$ 1.6	6 $\pm$ 3.2	10 $\pm$ 3.8

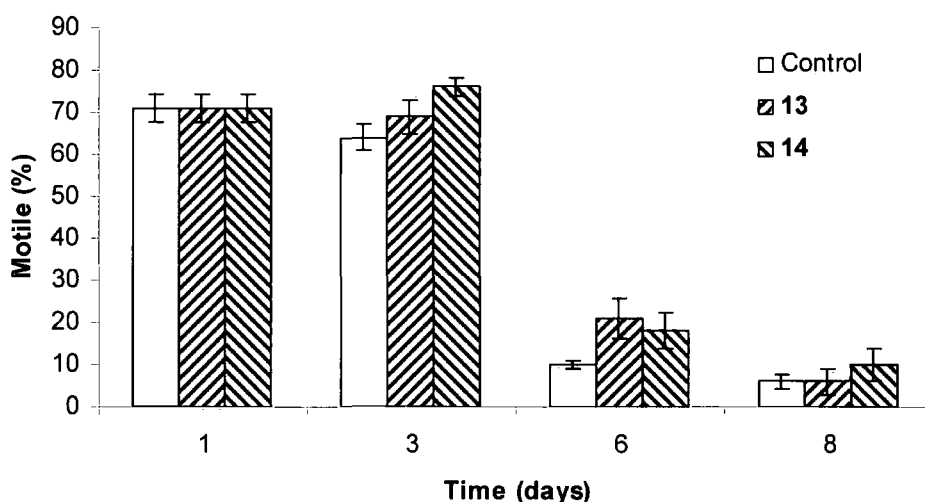


**Figure 4.13 – Percentage of motile cells versus time (days) at polymer concentrations of 0.02 mg/ml**

In general there was not much difference between the groups, although on day 3 the cells treated with polymer **14** were significantly more motile than those of the control group. This was the only time period where a significant difference was observed. In terms of cellular viability there was little difference found between all three groups. In this experiment the cellular viability was assessed by fluorimetry rather than by eosin staining. The former technique is believed to be more accurate, and is based on

recording the number of damaged cells only. The percentage of damaged cells found in each group is shown and illustrated in Table 4.10 & Figure 4.14 below.

**Table 4.10 - Percentage of damaged cells  $\pm$  polymer**

Day	% Damaged		
	Control	13	14
1	11 $\pm$ 0.4	11 $\pm$ 0.4	11 $\pm$ 0.4
3	10 $\pm$ 0.6	10 $\pm$ 0.2	11 $\pm$ 0.3
6	18 $\pm$ 1.3	21 $\pm$ 2.8	23 $\pm$ 1.9
8	26 $\pm$ 0.7	26 $\pm$ 4.7	30 $\pm$ 1.4

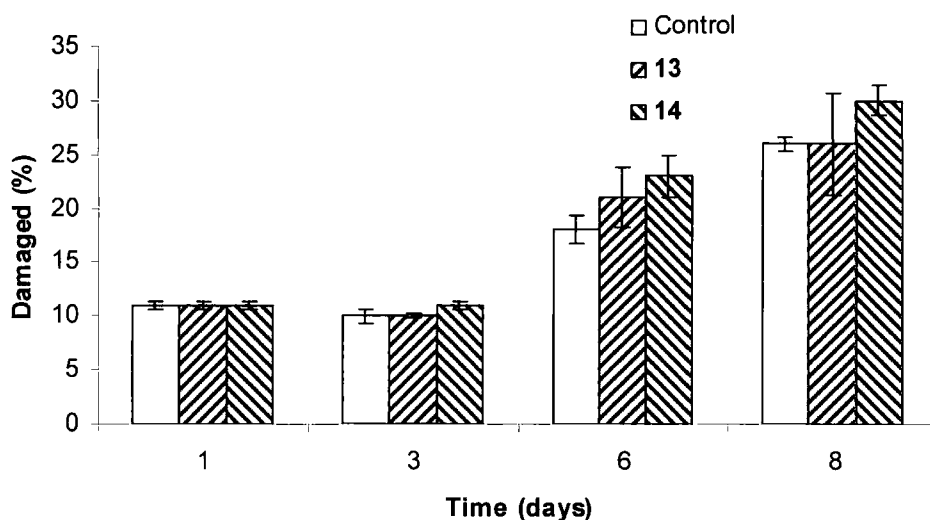


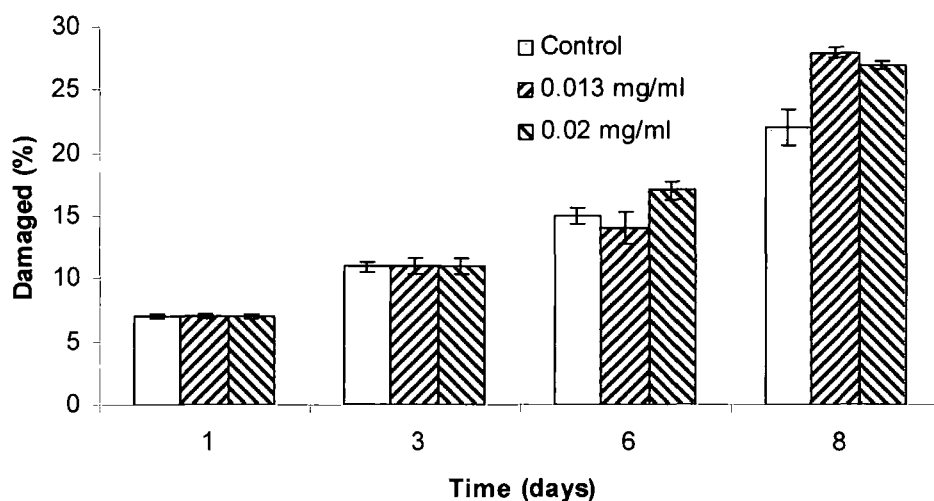
**Figure 4.14 – Comparison of damaged cells (%) versus time for polymers 13 & 14 at 0.02 mg/ml**

These results are encouraging as there would be no reason to suspect that **14** should behave in an entirely different manner to **13**. Nevertheless, there was a preference to continue further *in vitro* studies with **14** rather than **13** due to the additional vitamin E moieties. Results based on vitamin E uptake by the cells will be discussed in more detail later in this chapter.

The “therapeutic” concentration of **14** was reduced further to deliver the same quantity of vitamin E as **13** at 0.02 mg/ml. In this experiment, motility was only assessed until day 3 with the focus being on cellular viability and resistance to oxidation (see later).

**Table 4.11 - Percentage of damaged cells ± polymer 14**

Day	% Damaged		
	Control	0.013 mg/ml	0.02 mg/ml
1	7 ± 0.2	7 ± 0.2	7 ± 0.2
3	11 ± 0.4	11 ± 0.7	11 ± 0.6
6	15 ± 0.6	14 ± 1.3	17 ± 0.7
8	22 ± 1.4	28 ± 0.4	27 ± 0.3

**Figure 4.15 – Comparison of damaged cells (%) after incubation with two concentrations of polymer 14 versus time**

These results (Table 4.11 & Figure 4.15) indicated that there were significantly more damaged cells in both treated groups on day 8 compared to control samples. It was hypothesised that the seemingly more reliable technique of fluorimetry could be artificially increasing the value for the polymer treated samples, due to the inherent fluorescence of the vitamin E species being released inside the cells.

Despite the number of damaged cells appearing higher on day 8 in the experiment described above, it was accepted that the concentration of 0.013 mg/ml seemed to be giving acceptable results in terms of the standard sperm quality parameters. As such similar experiments were repeated to assess their reproducibility. Nevertheless it must

be reiterated that producing a “typical” or “standard” response curve based on a particular polymer concentration is simply not possible due natural variation.

Cells were incubated  $\pm 0.013$  mg/ml of **14** over an 8 day period at 18°C in a commercial diluent (BTS). The results obtained were very encouraging as both motility values and viability values indicated that there were significant benefits in the treated groups at various time points throughout the incubation period.

**Table 4.12 - Percentage motility  $\pm 0.013$  mg/ml of polymer 14**

<i>Day</i>	% Motile	
	Control	<b>14</b>
<i>1</i>	73 $\pm$ 1.7	73 $\pm$ 1.7
<i>3</i>	54 $\pm$ 2.4	66 $\pm$ 0.8
<i>4</i>	54 $\pm$ 3.1	71 $\pm$ 2.4
<i>5</i>	48 $\pm$ 1.4	59 $\pm$ 2.4
<i>6</i>	35 $\pm$ 2.0	39 $\pm$ 3.8
<i>8</i>	2 $\pm$ 0.6	5 $\pm$ 0.5

In this particular experiment the cellular motility was significantly different on days 3-5 and on day 8 (see Table 4.12 & Figure 4.16). Whilst the purpose of this material is not to boost the motility of the cells, it is encouraging that it is not hindering it. The difference is more obvious in the figure shown below.

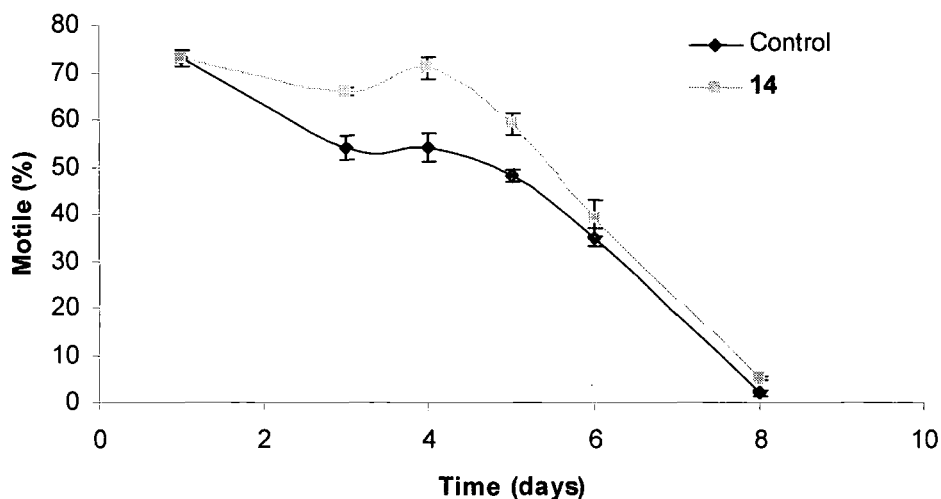


**Figure 4.16 - Cellular motility  $\pm$  polymer 14 versus time**

In addition to showing potential benefits in terms of motility, in this example there were also associated benefits in terms of cellular viability. In contrast to previous results where as time progressed during incubations the number of damaged cells increased more in the treated group, in this example the number of damaged cells was statistically lower from day 6 onwards (see Table 4.13 & Figure 4.17). This makes interpretation of this result difficult.

**Table 4.13 - Percentage of damaged cells  $\pm$  polymer 14**

Day	% Damaged	
	Control	14
1	12 $\pm$ 0.2	12 $\pm$ 0.2
3	12 $\pm$ 0.3	13 $\pm$ 0.3
4	12 $\pm$ 0.4	13 $\pm$ 0.2
5	15 $\pm$ 0.4	15 $\pm$ 0.7
6	18 $\pm$ 0.4	14 $\pm$ 0.3
8	34 $\pm$ 0.6	21 $\pm$ 0.2

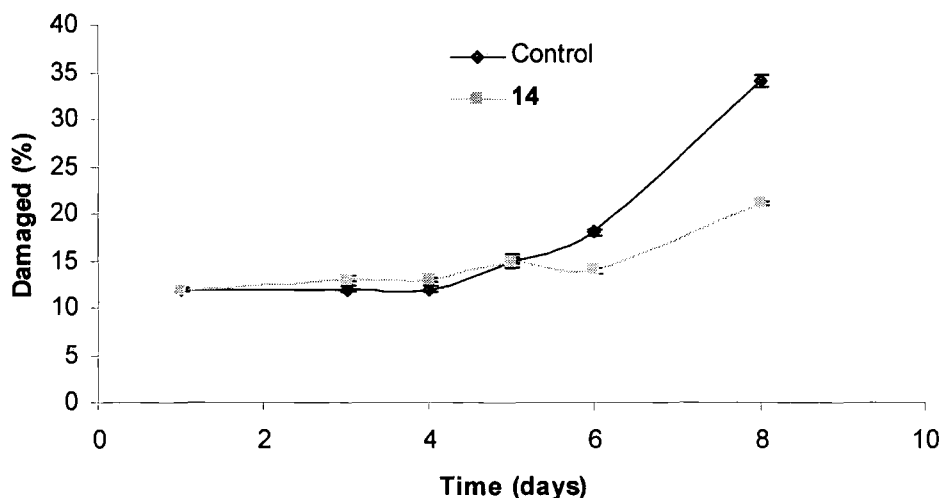


Figure 4.17 – Damaged cells (%) versus time (days) incubating with polymer 14 (0.013 mg/ml)

Another point of consideration was the “shelf-life” of the polymer product and this was investigated for polymer 14. In general, polymer solutions were stored frozen and were thawed prior to use. One area of concern was the possibility that during storage in aqueous solution, some of the ester linkages could be hydrolysed and some of the key components (sugar or vitamin E) could be lost. Although there were some differences found between samples of “old” (*i.e.* frozen and thawed > 10 times) and “new” 14, these were not found to be significant at all time points. The results are summarised in Table 4.14 & Figure 4.18 below.

Table 4.14 - Percentage of motile cells  $\pm$  0.013 mg/ml of 14

Day	% Motile		
	Control	“old”	“new”
1	82 $\pm$ 3.3	82 $\pm$ 3.3	82 $\pm$ 3.3
2	65 $\pm$ 2.9	77 $\pm$ 1.7	73 $\pm$ 1.7
5	45 $\pm$ 2.9	52 $\pm$ 4.4	45 $\pm$ 8.7
7	23 $\pm$ 1.7	36 $\pm$ 0.1	20 $\pm$ 7.6

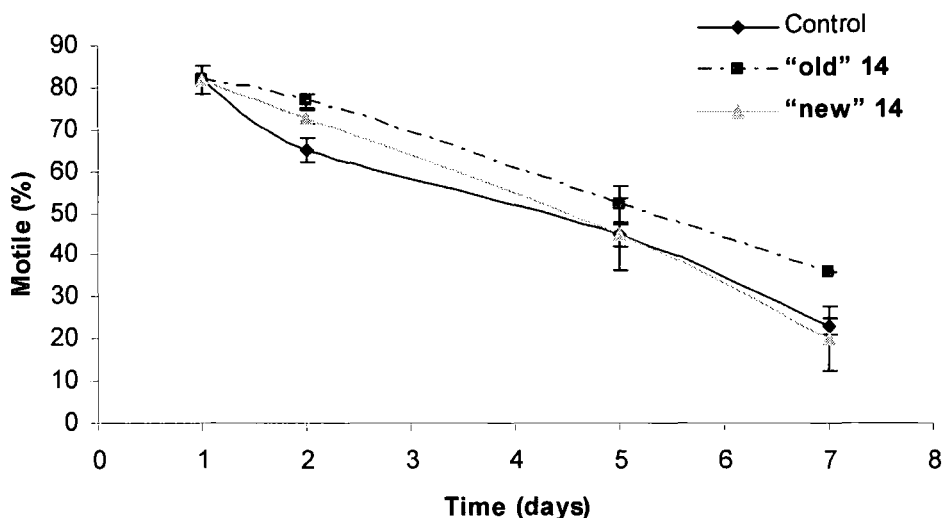


Figure 4.18 – Comparison of “old” and “new” batches of 14 effect on motility versus time

It is interesting to note that although there appeared to be more motile cells in the group treated with “old” polymer, this result was not reflected in the viability results which actually found more damaged cells in this group (although not statistically more – see Table 4.15 &

Figure 4.19). The reasons for this are not clear, but it was accepted that the storage of the material in deep freeze and subsequent thawing and re-freezing was an acceptable protocol.

Table 4.15 - Percentage of damaged cells ± 0.013 mg/ml of 14

Day	% Damaged		
	Control	“old”	“new”
1	22 ± 0.3	22 ± 0.3	22 ± 0.3
2	23 ± 0.9	22 ± 0.3	24 ± 0.3
5	26 ± 1.2	25 ± 0.4	26 ± 0.4
7	22 ± 1.3	25 ± 2.2	16 ± 3.4

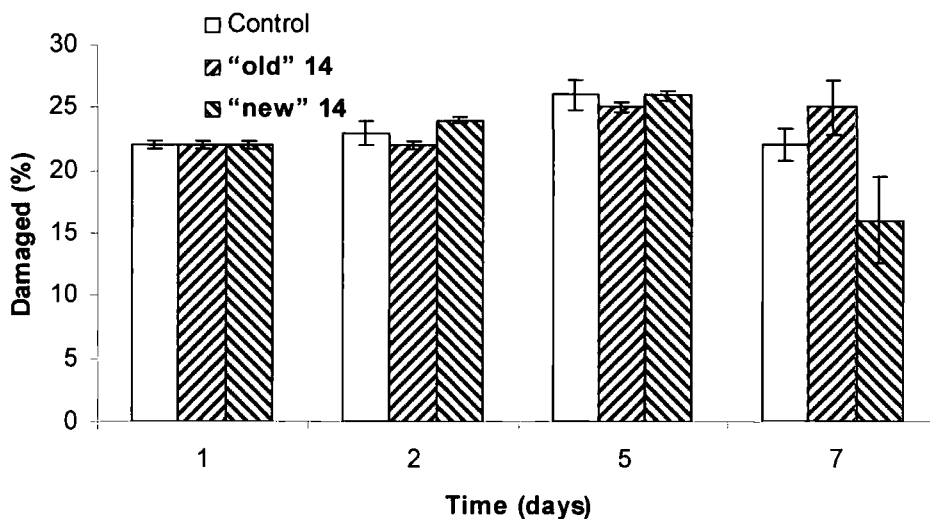


**Figure 4.19 - Comparison of "old" and "new" batches of 14 effect on cell damage versus time**

Several other similar experiments have been conducted using polymer **14** in order to assess the reproducibility of these results. In general terms, incubation of the sperm cells in the presence of this polymer exhibits neither a positive nor negative effect (examples of both have been recorded). This is important but of much greater importance and interest is the ability of the sperm cells to uptake these glycopolymers and make use of the pendant vitamin E groups. These aspects are discussed in more detail below.

#### **4.2.2 Vitamin E Uptake and Oxidative Stress Measurements**

Both polymer **13** and polymer **14** were used to assess the ability of the cells to uptake polymer molecules, release vitamin E and subsequently use this additional vitamin E to protect themselves against iron-induced oxidation. Having conducted many experiments to fine-tune the concentration, the uptake of **13** was measured over a period of several days, using a polymer concentration of 0.02 mg/ml. The concentration of vitamin E present within the cells was determined by removing approximately 750 million cells (15 ml) from incubating samples, washing and subsequently lysing them and analysing the resulting material by HPLC. HPLC analysis was conducted (excitation at 295 nm, emission at 330 nm) on a system fitted with a Hypersil column (250 × 4.6 mm, 5 mm) run with 97% MeOH: 3% water (v:v) as an eluent system. Prior

to analysis spermatozoa were homogenized and tocopherols extracted as described by Dvorska *et al.*<sup>2</sup> In short, a pellet of  $500 \times 10^6$  spermatozoa was obtained after two centrifugations (2000g for 10 min at 5°C), the pellet was washed and resuspended between centrifugations using a physiological solution in order to eliminate all contamination from the polymer remaining in solution. Then the pellet was resuspended in 0.7 ml of NaCl 0.7% (wt:v) and 1 ml of ethanol with 3 ml of hexane were subsequently added and the samples vortexed for 20 s. Samples were centrifuged as described above, the hexane layer containing the tocopherols was collected and left in the dark. The hexane extraction was repeated thrice (3 ml each time). Finally, samples were dried under nitrogen at 40°C, resuspended in methanol and analysed by HPLC.<sup>§</sup>

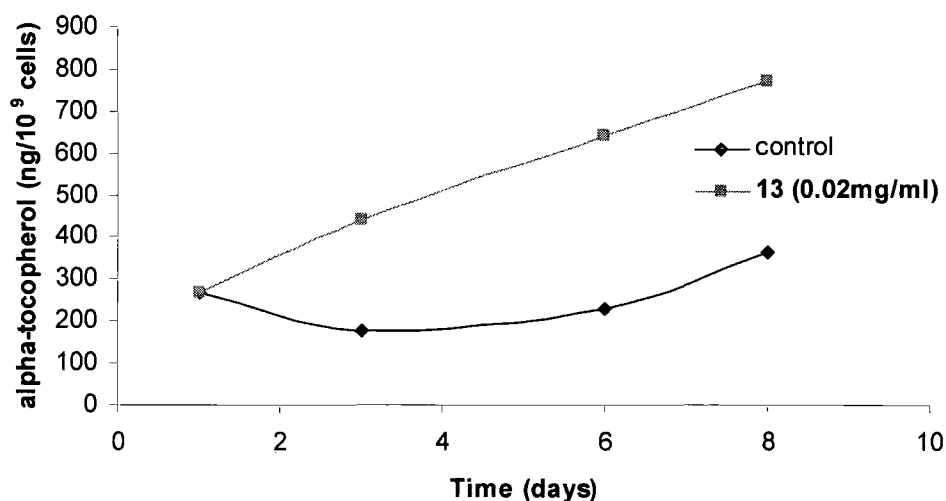


**Figure 4.20 - Uptake of vitamin E versus time ± 13 (0.02 mg/ml) after incubation at 18°C over an 8 day period**

As is clearly visible from Figure 4.20 above, there is a significant and measurable difference in the amount of vitamin E present in cells incubated with and without polymer. There is no suggestion (despite the appearance of the graph) that the uptake is linear, however clearly there is some time related increase for this particular material.

A similar experiment was conducted for polymer 14, which was incubated at the same concentration as 13. As one might expect this led to an even higher concentration of vitamin E present within the cells. Again the lines on the graph are purely to aid the

<sup>§</sup> These analyses were conducted by Dr André Maldjian.

visibility of the points and in no way suggest any particular uptake kinetics (see Figure 4.21).

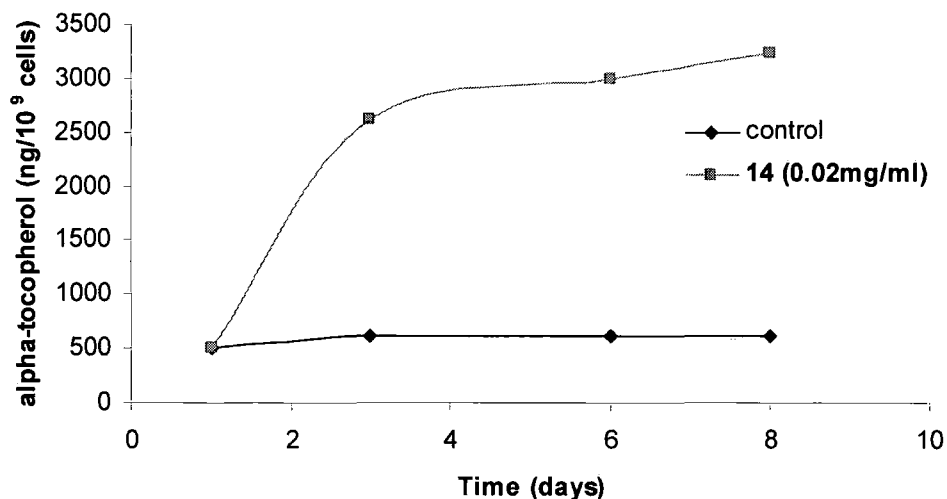


**Figure 4.21 - Uptake of vitamin E versus time  $\pm$  14 (0.02 mg/ml) after incubation at 18°C over an 8 day period**

One of the obvious problems with these data is the small number of data points, however this is almost entirely unavoidable due to the number of cells available for analysis since large numbers are needed for each single analysis and each analysis is done in triplicate (at least). Nevertheless, what is of both interest and value is that these data suggest (qualitatively at least) that the cells are able to internalise the polymer, and release the vitamin E, by enzymatic means. In order to assess this potential further, TBARS<sup>3</sup> assays were conducted. Oxidation of the cells was induced artificially by incubating in the presence of FeSO<sub>4</sub>.

#### **4.2.2.1 Oxidative Stress Measurements**

As already mentioned, the kinetics of uptake are not well understood, and although an appropriate dose concentration has been established, these experiments were conducted

at a number of different polymer concentrations in order to assess the impact on oxidation\*\*.

In this example, there were 3 experimental groups (control, + 0.02 mg/ml of **14**, + 0.1 mg/ml of **14**). These were incubated at 37°C for 2 hours before the addition of FeSO<sub>4</sub> [0.8 mM], and incubated for a further hour. The amount of MDA was then assessed spectrophotometrically<sup>3</sup>.

**Table 4.16 - Oxidation product after incubation of boar sperm cells for 2 hours with polymer 14 at 37°C, followed by 1 hour with FeSO<sub>4</sub> [0.8 mM] at 37°C**

	MDA (ng/10 <sup>9</sup> cells)
Control	3789 ± 491
<b>14</b> (0.02 mg/ml)	3808 ± 227
<b>14</b> (0.1 mg/ml)	2448 ± 232

Over such a relatively short incubation time, it was only the group treated with the higher polymer concentration that was able to reduce significantly the amount of cellular oxidation. Although this concentration is in practice too high, due to the knock-on effects of lower motility and higher cellular damage, it does illustrate that the cells are able to internalise the polymer and release a significant amount of vitamin E over a short period of time.

\*\* Although in general the procedure was the same, a number of variables were used, for example, the amount of time the cells were incubated with polymer prior to oxidation, and the temperature of incubation prior to oxidation.

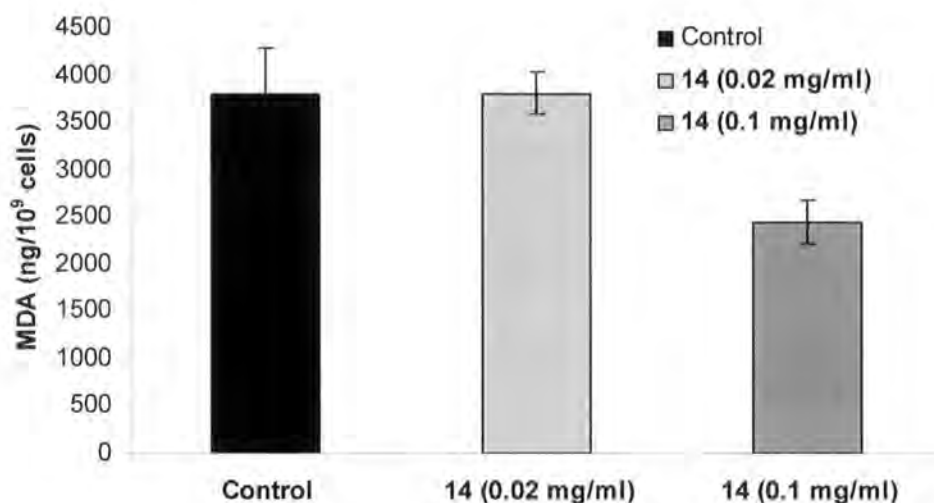


Figure 4.22 - Oxidation product after incubation of boar sperm cell for 2 hours with polymer 14 solutions at 37°C, followed by 1 hour with FeSO<sub>4</sub> [0.8 mM] at 37°C

In addition a second experiment was conducted using the lower polymer concentration (0.02 mg/ml) and lower temperature (18°C) for a longer incubation period (3 days) prior to the oxidative stress. The reason that the higher concentration of polymer was not also tested is that the number of live cells may not have been sufficiently high to achieve meaningful results, as has been shown previously.

Table 4.17 – Oxidation product after incubation of boar sperm cells for 3 days with polymer 14 at 18°C, followed by 1 hour with FeSO<sub>4</sub> [0.8 mM] at 37°C

MDA (ng/10 <sup>9</sup> cells)	
Control	11984 ± 630
<b>14</b> (0.02 mg/ml)	6198 ± 1360

One immediately apparent difference between this set of data and the previous set is the amount of oxidation in the control sample. This would tend to suggest that the cells are much more vulnerable to oxidation after several days of storage than they are shortly after ejaculation. Nevertheless, in the treated group there has been sufficient uptake of polymer and release of vitamin E to reduce significantly the amount of oxidation by approximately half.

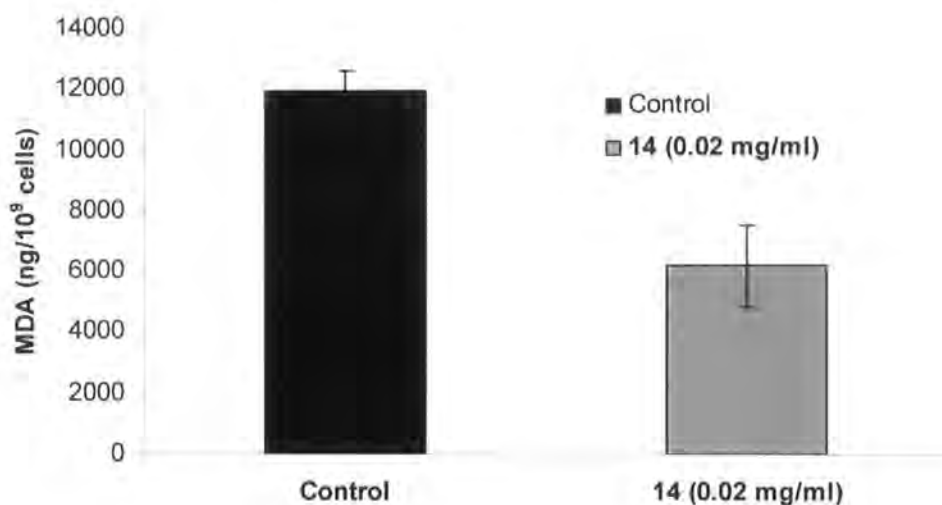


**Figure 4.23 - Oxidation product after incubation of boar sperm cells for 3 days with polymer 14 at 18°C, followed by 1 hour with FeSO<sub>4</sub> [0.8 mM] at 37°C**

This shows that when using a lower polymer concentration, more incubation time is required in order to get a sufficient/significant amount of vitamin E released within the cells. It is likely that the actual incubation time required lies somewhere between 2 hours and 3 days.

Similar experiments were conducted this time using a longer incubation period prior to the addition of FeSO<sub>4</sub>. This yielded some interesting observations, some of which may have been expected, but others which were initially surprising based on previous experiments.

**Table 4.18 - Oxidation product after incubation of boar sperm cells for 8 days with polymer 14 at 18°C, followed by 1 hour with FeSO<sub>4</sub> [0.8 mM] at 37°C**

	MDA (ng/10 <sup>9</sup> cells)
Control	2384 ± 95
<b>14</b> (0.02 mg/ml)	410 ± 9
<b>14</b> (0.013 mg/ml)	1119 ± 279

From these results it is clear that the polymer treatments once again reduce the amount of oxidation occurring. However, contrary to the previous experiments, there appears to be a greater amount of oxidation in the control after 3 days of incubation compared to 8

days. In this example, the overall level of oxidation is comparable with the values obtained for oxidation after short incubation time, and much less than the values measured after 3 days. This once again indicates the problems associated with the natural variation encountered when working with live biological systems.

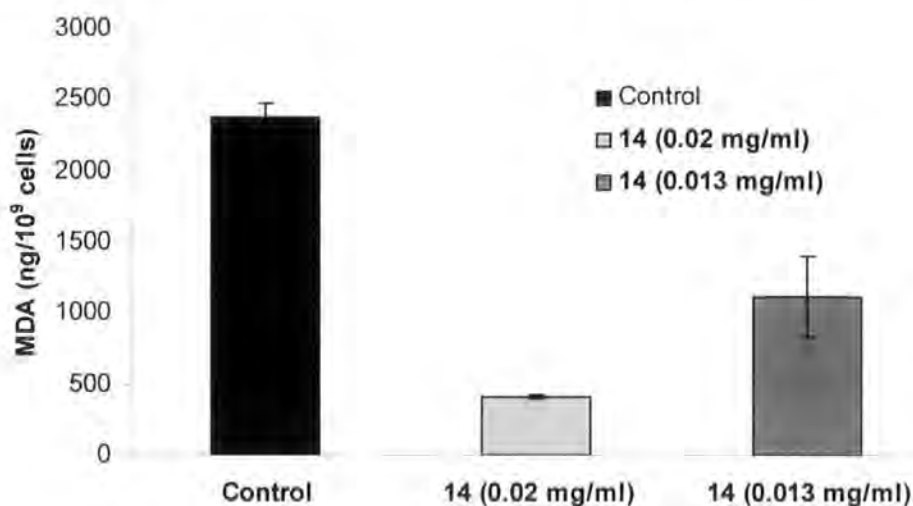


Figure 4.24 - Oxidation product after incubation of boar sperm cells for 8 days with polymer 14 at 18°C, followed by 1 hour with FeSO<sub>4</sub> [0.8 mM] at 37°C

Both polymer treated groups significantly reduced the production of MDA compared to the control group, which is in good agreement with results obtained previously.

This experiment was repeated, this time focussing on the lowest polymer concentration to ensure the best level of reproducibility possible (*i.e.* taking natural variation into consideration). Again there was a significant reduction in the amount of MDA produced after induced oxidation, however once again the overall amount of MDA produced in both groups was significantly different compared with previous experiments.

Table 4.19 - Oxidation product after incubation of boar sperm cells for 8 days with polymer 14 at 18°C, followed by 1 hour with FeSO<sub>4</sub> [0.8 mM] at 37°C

MDA (ng/10 <sup>9</sup> cells)	
Control	5328 ± 421
14 (0.013 mg/ml)	517 ± 43

The polymer reduced the amount of MDA produced to around a tenth of the control value. This was statistically significant, and as previously noted, in good agreement with the trend previously observed in similar experiments of this nature.

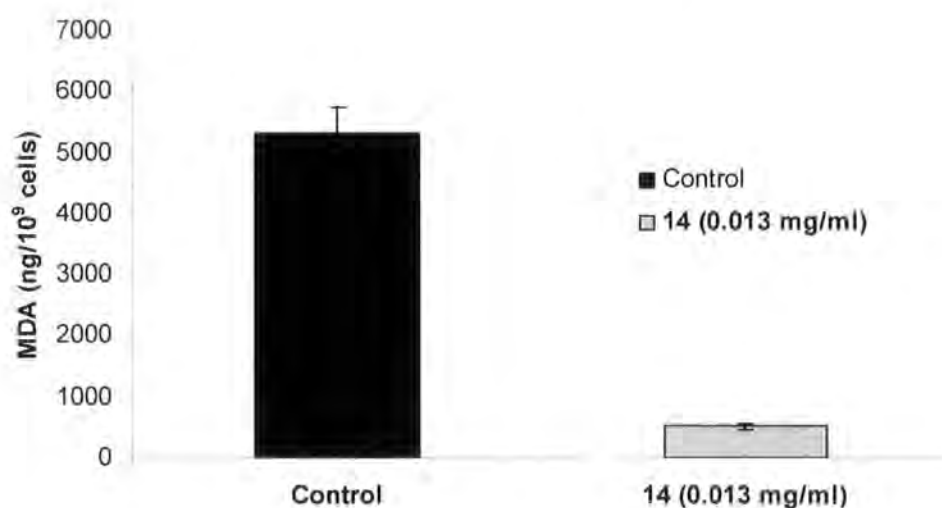


Figure 4.25 - Oxidation product after incubation of boar sperm cells for 8 days with polymer 14 at 18°C, followed by 1 hour with FeSO<sub>4</sub> [0.8 mM] at 37°C

It is of note that, although throughout many experiments comparing the sperm quality parameters of control and polymer-treated samples there have been both positive and negative results in terms of motility and viability, there has never been a poor result in terms of reducing oxidation. This emphasises the actual efficacy of this material *in vitro* – a polymer for the delivery of anti-oxidant to sperm cells.

However there is a bigger picture to consider. As can be observed from earlier data, there is a naturally occurring amount of vitamin E present within boar spermatozoa. Polymeric materials such as **13** or **14** aim to increase this through *in vitro* incubation, however it is possible to manipulate this naturally occurring level through dietary means. In the context of this report, there was a desire to investigate the effect of these polymeric materials on sperm cells that had been enhanced *in vivo* by feeding boars with a specialised food supplement containing a number of essential factors (DHA, selenium and vitamin E for example). Previous work has shown that this food supplement had benefits in terms of sperm quality, and ultimately in terms of fertility.<sup>4-7</sup> With this in mind, studies were conducted to investigate the differences between boars

fed ProSperm™ (the supplement in question) and those on a conventional diet, with and without polymer treatment *in vitro*.

### **4.2.3 Effect of feed supplementation and *in vitro* polymer addition on sperm quality<sup>††</sup>**

A small scale study was conducted using 7 boars. There were 3 boars (Marco, Jörg and Karl) in the control group and 4 boars (Bruno, Norbert, Leo and Ingo)<sup>‡‡</sup> in the ProSperm™ group, although for the purposes of this experiment the ejaculates from the boars in each group were pooled prior to analysis. It is known already<sup>4-7</sup> that this feed supplementation helps to increase the concentration of sperm cells in the ejaculate, as well as improving their motility and viability. Ideally, a positive correlation between the sperm improved by feed supplementation and the subsequent *in vitro* polymer supplementation would be observed. This particular study only focussed on cellular motility and viability, which although not ideal, does form the basis for further future studies.

There were 4 experimental groups, referred to herein as Control ± polymer and ProSperm™ ± polymer. The polymer was included at a concentration of 0.02 mg/ml. The results obtained from this study are encouraging (see Table 4.20 & Figure 4.26).

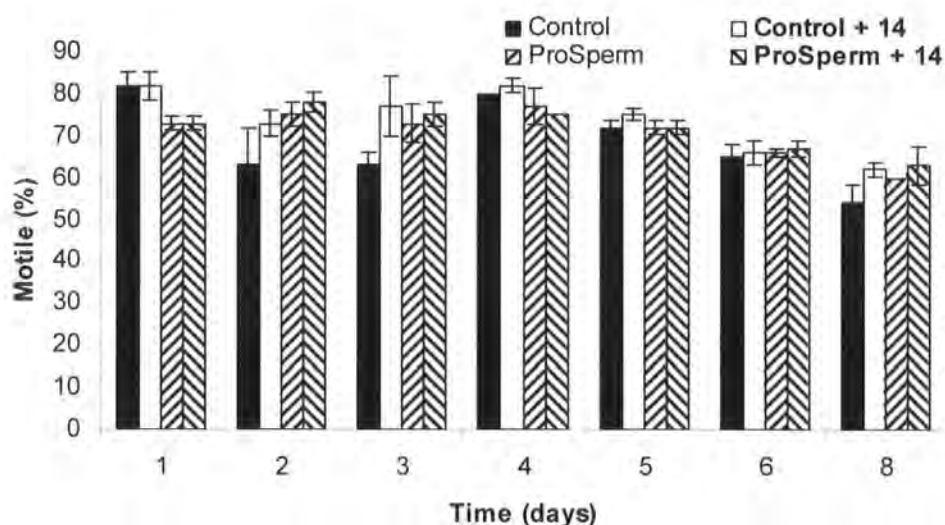
---

<sup>††</sup> Until indicated otherwise, the experiments detailed from this point onwards were conducted by the author.

<sup>‡‡</sup> All ejaculates were obtained from standard commercial breeding boars housed according to UK/EU standards for artificial insemination centres. The boars were between 9 and 14 months of age and of high reproductive capacities.

**Table 4.20 - Percentage motilities measured over 8 days**

Day	Control	Control + 14	ProSperm	ProSperm + 14
1	82 ± 3.3	82 ± 3.3	73 ± 1.7	73 ± 1.7
2	63 ± 8.8	73 ± 3.3	75 ± 2.9	78 ± 2.5
3	63 ± 3.3	77 ± 7.3	73 ± 4.4	75 ± 2.9
4	80 ± 0	82 ± 1.7	77 ± 4.4	75 ± 0
5	72 ± 1.7	75 ± 1.4	72 ± 1.7	72 ± 1.7
6	65 ± 2.9	66 ± 3.0	66 ± 0.8	67 ± 1.7
8	54 ± 4.2	62 ± 1.7	60 ± 0	63 ± 4.4

**Figure 4.26 - Percentage motilities measured over 8 days – comparison of control versus ProSperm +/- polymer 14**

From these data, the average motilities over the entire 8 day period were calculated and found to be as follows.

**Table 4.21 - Average motilities over the 8 day incubation period**

	Motility (%)
Control	69 ± 3.7
Control + 14	74 ± 2.9
ProSperm	71 ± 2.2
ProSperm + 14	72 ± 1.9

Whilst it is acknowledged that these results are not statistically significant, there does appear to be a tentative trend. Furthermore, these results corroborate earlier experiments which identified this polymer concentration as having no negative effect on the sperm quality parameters of motility and viability. What is interesting is that the control group appears to perform marginally better than the ProSperm™ group (although once again the lack of a statistical difference is acknowledged).

Another interesting observation (although it is treated with caution due to the lack of statistical significance) is apparent when plotting the data in Table 4.20 and applying linear trendlines, the two control groups appear to have parallel trend lines, with the polymer treated group being above the standard control. Such an obvious trend is not visible for the ProSperm™ groups, however polymer treated group is again marginally better.

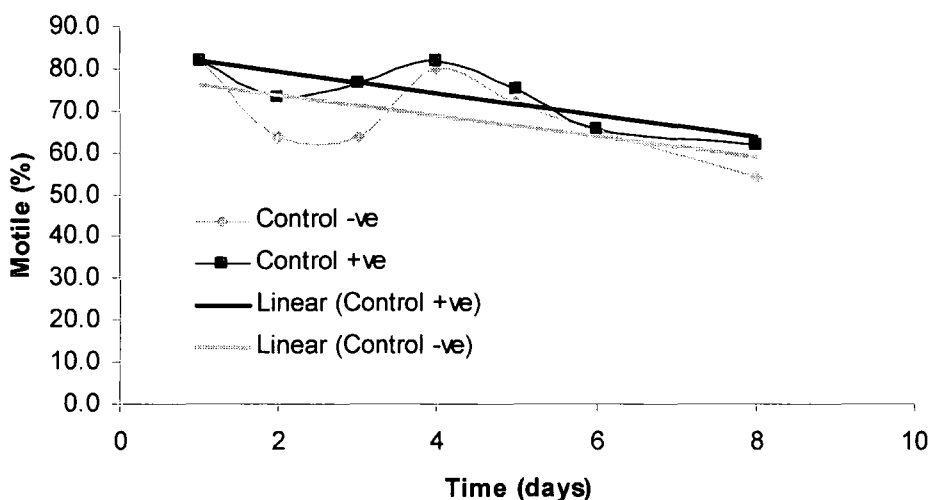


Figure 4.27 - Average motilities versus time showing parallel trend lines

Of course, these trendlines must be regarded with caution, as the loss of motility over time is clearly not linear. Indeed, extrapolation of these lines to zero motility suggests that the cells would be motile for between 32 and 43 days (depending on the experimental group) which is clearly invalid.

In terms of cellular viability, there was no obvious trend in relation to the different treatments. Furthermore, although there were differences in the numbers of live/dead/damaged cells, these were not found to be significant.

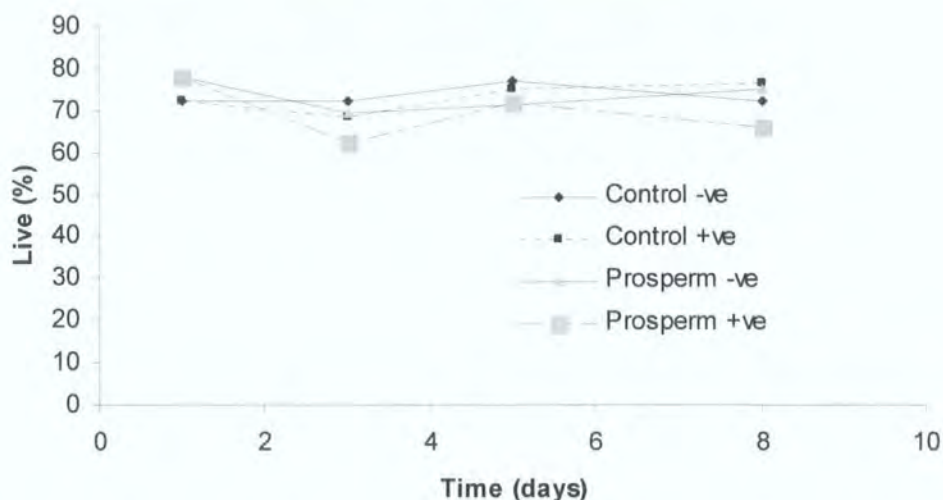


Figure 4.28 – Percentage of live cells during 8 days incubation period +/- polymer 14

Throughout the experiment there are very few differences observed between all of the groups although admittedly the group with the lowest number of live cells on day 8 appears to be the group which had both polymer treatment and ProSperm™. In general however, all four groups remain fairly constant throughout.

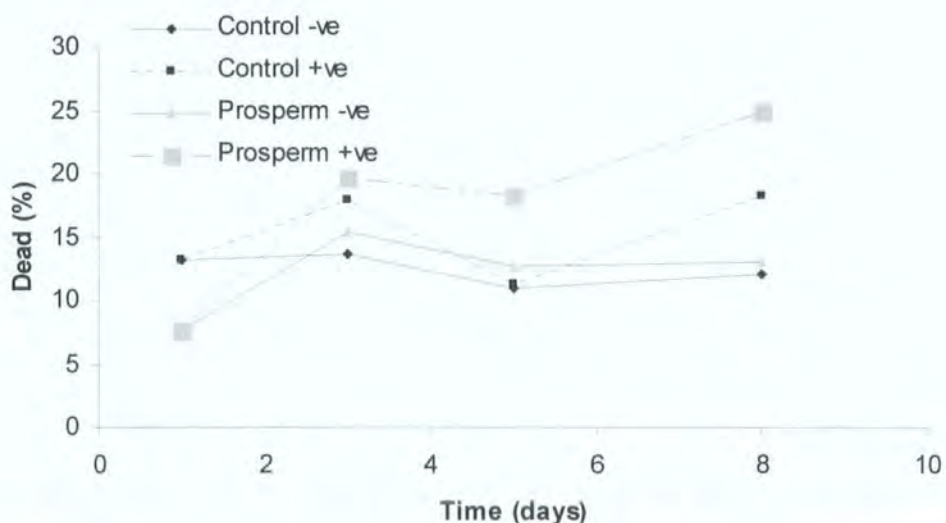


Figure 4.29 - Percentage of dead cells during 8 day incubation period +/- polymer 14

The results shown here tend to mirror those shown for the number of live cells, since the ProSperm™ plus polymer group has the worst result. This is made slightly worse since this group actually started from a lower number of dead cells on day 1. Nevertheless these results must be treated with caution, since they were not found to be statistically significant.

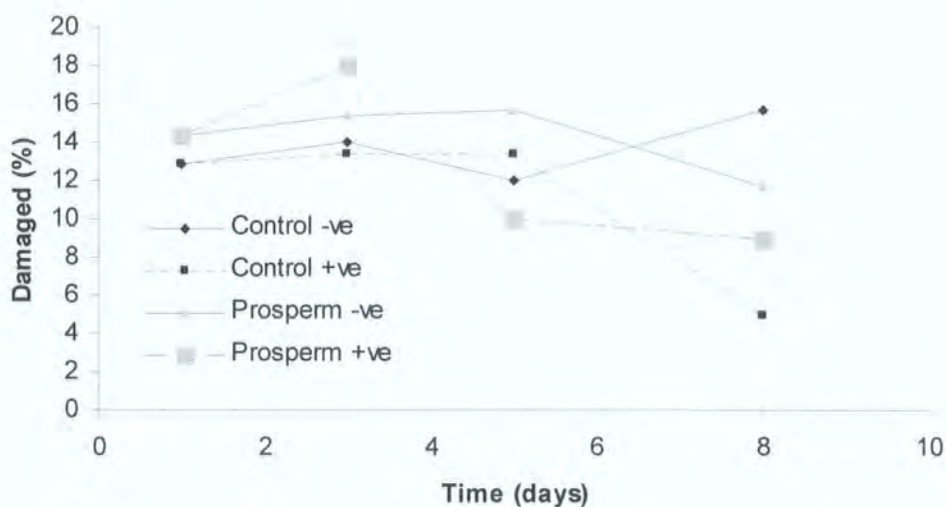


Figure 4.30 - Percentage of damaged cells during 8 day incubation period +/- polymer 14

Finally, if we examine the number of damaged cells recorded during the incubation period, we see a trend similar to that previously noted. The polymer treated groups tend to show fewer damaged cells compared to controls. Interpreting this result optimistically one can suggest that the polymer treatment (and indeed the ProSperm™ in this instance) helps to reduce the number of damaged cells, however it is acknowledged that it can also be interpreted as a knock on effect of the number of dead cells being increased in the treated groups. It is possible that the result reflects a combination of these two factors.

#### 4.2.4 Sex Sorted Semen

In addition to the use of polymers to deliver anti-oxidants and other metabolites to sperm cells for use in standard AI conditions, there were some exploratory studies conducted using sex sorted semen. Commercially the use of sex-sorted boar semen is

not currently viable since it requires 8 hours of sorting to produce enough semen for 1 insemination. However, the process is being exploited commercially in the sale of sex sorted bull semen, which requires less time and has the added benefit of being suitable for cryogenic storage.

In the first instance we investigated the use of the polymer (**14**) containing vitamin E, on sorted bull semen. The experiment was qualitative and certainly preliminary, however the results were interesting and encouraging. Experimentally, two groups were considered. The control samples were sorted as per normal protocols, while the samples treated with polymer were sorted into a mixture of polymer dissolved in BTS and TRIS sheath fluid (0.25 ml of BTS containing polymer **14** at a concentration of 0.02 mg/ml and 0.25 ml of TRIS). After collection, 4 samples from each group were pooled and washed by centrifugation. Samples were assessed for motility at three stages during the procedure: immediately prior to sorting, immediately after sorting, and after 40 hours of storage at 5°C (followed by 25 minutes of incubation at 37°C). The results are described below<sup>§§</sup>.

**Table 4.22 - Effect of polymer 14 on motility of sex sorted bull semen**

<i>Time point</i>	Motility (%)	
	Control	Polymer
<i>Pre-sort</i>	85	85
<i>Post-sort</i>	<10	40-50
<i>40 hrs</i>	20	50-60

These results were encouraging, however it was suggested that the positive effect could be due entirely, or in part to the use of BTS which is not normally included in the collection fluid. With this in mind, the experiment was repeated using a positive control (BTS only). In addition to assessing motility, acrosomal morphology was also investigated.

<sup>§§</sup> In this instance only the Y chromosome-bearing semen were analysed. Motility was assessed subjectively and blind.

Table 4.23 - Acrosomal morphology of Y chromosome-bearing bull semen, 24 hours after sorting

	(%)			
	Normal <sup>***</sup>	Swollen <sup>***</sup>	Dissolving <sup>***</sup>	Dissolved <sup>***</sup>
<i>Control</i>	42	1	0	57
<i>BTS control</i>	55	0	0	45
<i>Polymer 14</i>	64	0	0	36

In terms of acrosomal integrity, there appears to be a slight positive effect from using BTS, which is further enhanced by the inclusion of polymer 14. The results of the motility studies followed a similar pattern although the control was considerably less motile than the other two groups.

Table 4.24 - Motility of bull semen 24 hours after sorting

	(%)
Control	<10
BTS control	60-65
Polymer 14	70

These results are consistent with those discussed above, however as can be seen from the table, there is not a large difference between the BTS control and the polymer sample. This would suggest that the inclusion of BTS does have a positive bearing on the cells. It should be noted again that although these motilities were assessed subjectively, they were assessed blind. Further motility assessments were conducted on day 2 and day 6, the results of which are detailed below.

<sup>\*\*\*</sup> These terms are visual descriptions used to describe the morphology of the acrosomal region of the sperm head under microscopic examination.

**Table 4.25 - Motility of stored, sorted bull semen**

	(%)	
	Day 2	Day 6
Control	0	0
BTS control	40-50	20
Polymer 14	40-50	30

These experiments represent a preliminary study into alternative uses of glycopolymers containing vitamin E, and their use with alternative species. Whilst these results were not the subject of statistical analysis, it seems fair to comment tentatively that the exposure of these highly stressed sperm cells to a polymer containing vitamin E had a positive effect.

A similar experiment was conducted using boar semen in place of bull semen. Again only the Y chromosome-bearing cells were used. On this occasion, due to the length of time required to sort the required number of cells for each group, a positive control was not measured. The cells were collected into the two media (control and BTS/TRIS + polymer as previously described) and washed by centrifugation. They were then incubated at 15°C. Motilities were assessed after 24 hours, firstly at 15°C and subsequently after incubation at 37°C for 15 minutes.

**Table 4.26 - Motility of sorted boar semen after 24 hours**

	(%)	
	15°C	37°C
Control	15	5
Polymer 14	25	5

The difference here is not as stark as in the case of bull semen however there does appear to be a slight beneficial effect. This concept was further explored in experiments conducted by Joanne Leigh.<sup>8</sup> Her experiments demonstrated the deleterious effects of

the DNA binding dye and the laser used in the sex sorting procedure. Experiments were conducted similar to those shown above, where the cells were sorted into a solution containing polymer 14. The results echoed those already described, although somewhat more convincingly since the diluent used in these examples was a long term diluent (Androhep) rather than a short term diluent (BTS).

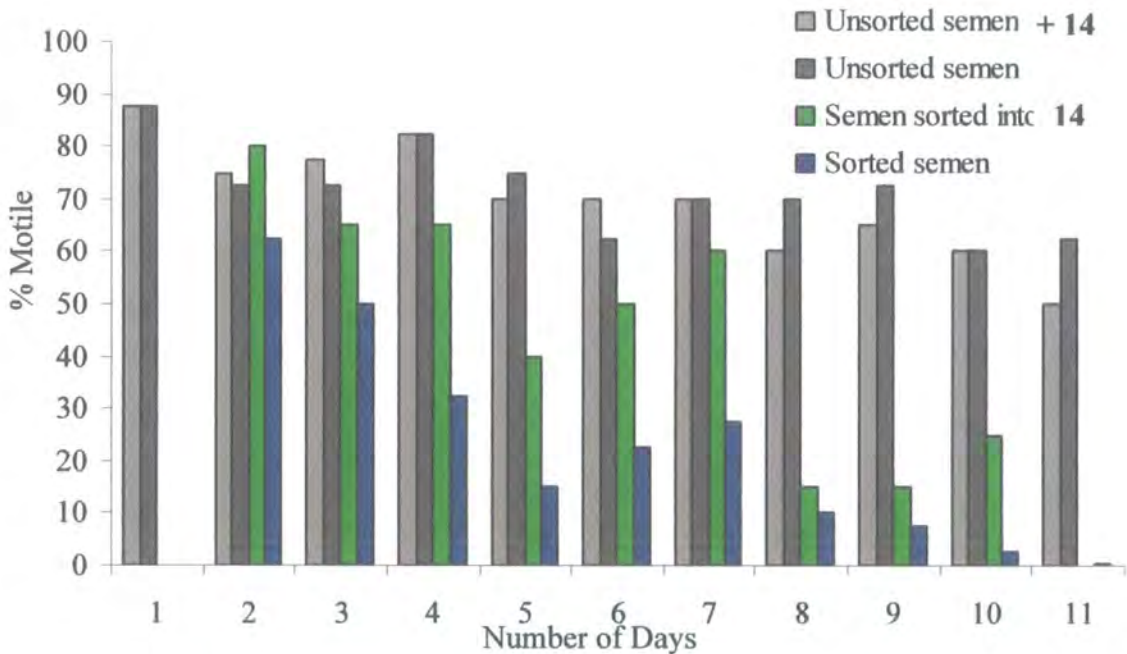


Figure 4.31 – Effect of including polymer 14 in the sorting collection medium (T=24 hrs)

Once again, as shown for both bull and boar semen, including polymer 14 in the medium into which the sorted cells are collected shows an improvement in post-sort cellular motility.

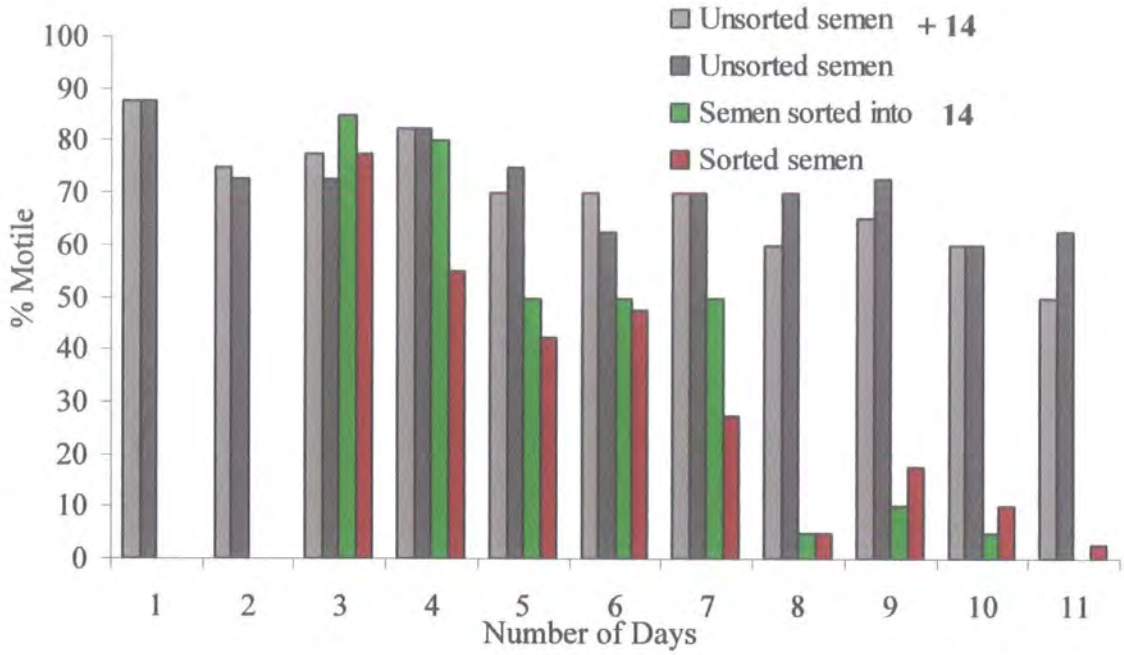


Figure 4.32 - Effect of including polymer 14 in the sorting collection medium (T=48 hrs)

It was subsequently demonstrated that incubating boar sperm cells with polymer 14 (at a concentration of 0.02 mg/ml) prior to sorting had beneficial effects on the post-sort motility. This area is undoubtedly worthy of further research as the preliminary results were very encouraging.

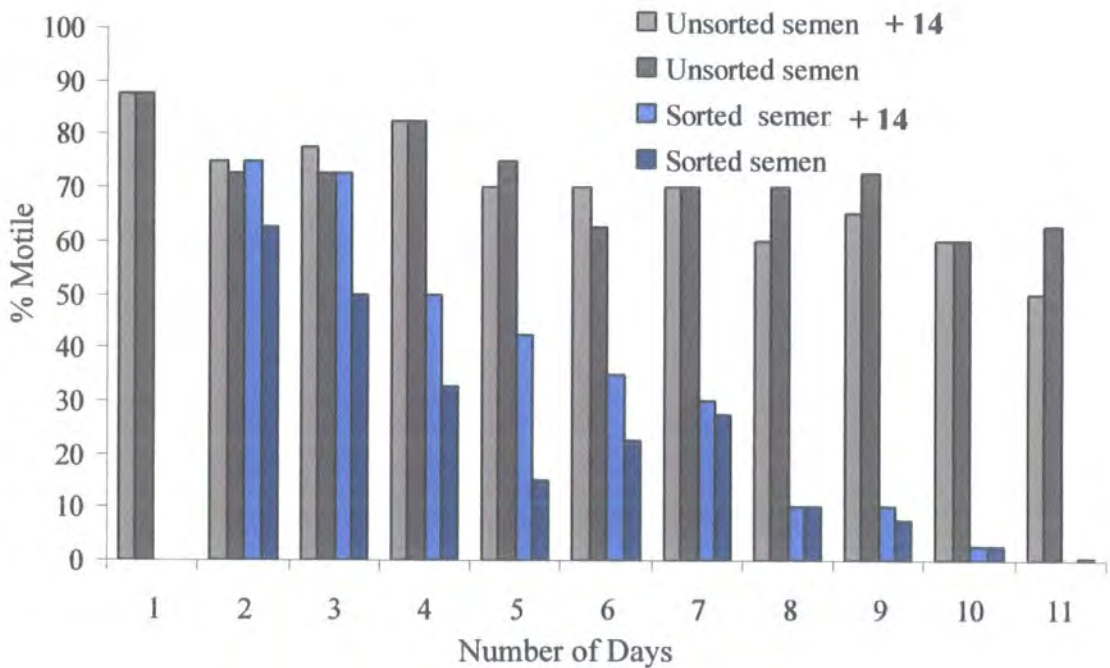


Figure 4.33 - Effect of 24 hour incubation with 14 on post sort motility

Whilst it is obvious that there is a benefit for the first few days after sorting, the difference is much less as time elapses further. Clearly the effect of sex sorting in general can be observed since both unsorted samples remain very motile even after 11 days. The effect is even more significant when the pre-incubation with polymer 14 is extended from 24 hours to 48 hours.

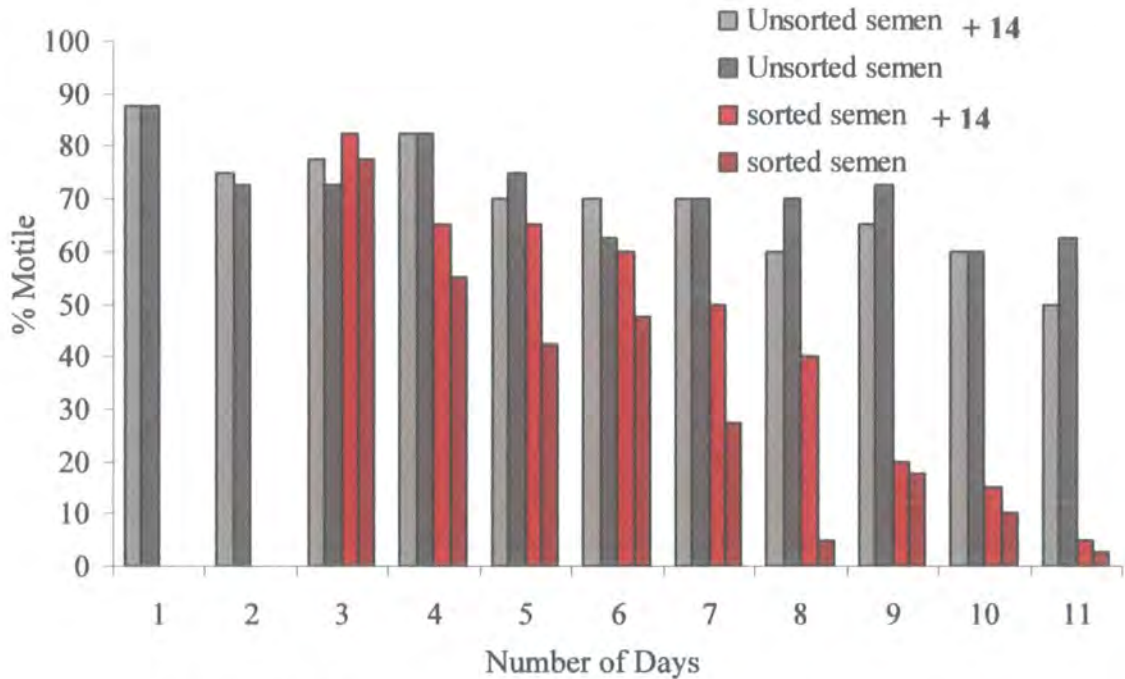


Figure 4.34 - Effect of 24 hour incubation with 14 on post sort motility

The above figure (Figure 4.34) demonstrates that not only is there a benefit associated with pre-incubation with polymer 14, but that pre-incubation in a commercial extender (in this example Androhep was used), can also have a benefit on post-sort motility compared to the standard protocol of sorting almost immediately after semen collection. Of course, what is not clear at this stage is how these pre-sort incubation steps affect the post-sort fertility of the sperm, although motility is generally accepted as a good marker.

#### 4.2.5 Fluorescent polymers

Having established that the treatment of the sperm cells with glycopolymers containing vitamin E results in free vitamin E within the cells, it seemed logical to attempt to

visualise the uptake of polymer into these cells using confocal microscopy. In order to achieve this, a polymer was synthesised which contained a fluorescent species in place of vitamin E. The fluorescent species in question was hostasol. Hostasol is used commercially as a filler to colour plastics.<sup>9</sup> The synthesis of hostasol methacrylate from the hostasol starting material is shown in Figure 4.35.

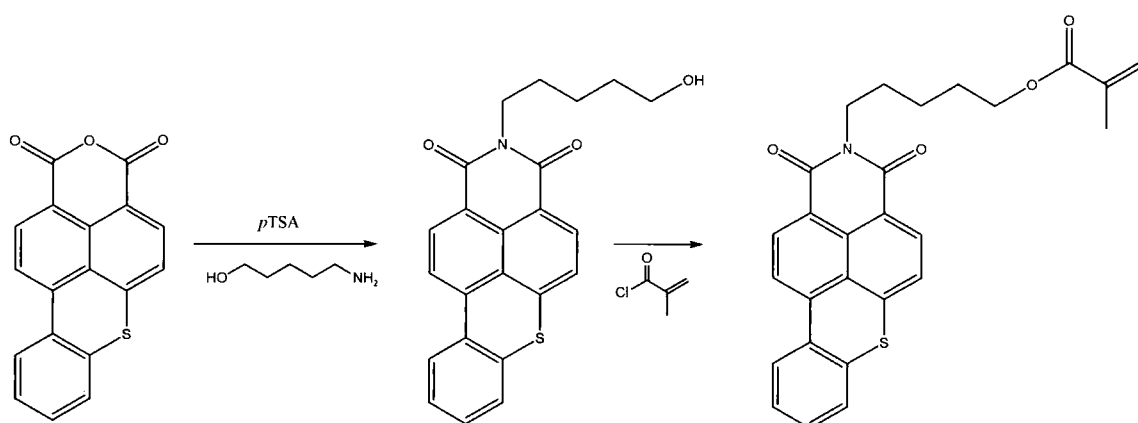


**Figure 4.35 - Synthesis of hostasol methacrylate**

This monomer was supplied by Prof. D Haddleton and although used without further purification, it was analysed by  $^1\text{H}$  NMR spectroscopy prior to use. The monomer was terpolymerised with DMAEA and **2b** in a mixture of methanol/DMF (1:4) using AIBN as the free radical initiator. This yielded a bright orange solid following dialysis and lyophilisation polymer **15**.  $^1\text{H}$  NMR of this material provided limited information due to the molecular weight of the polymer combined with its multi-component nature. Indeed the results of the elemental analysis of the material did suggest that all monomers (both sulphur and nitrogen were detected, indicating the presence of the Hostasol and DMAEA monomers respectively – notwithstanding the polymer's bright orange colour) had been incorporated, but not at the ratios dictated by the monomer feed. This is not entirely surprising since this trend was also observed following the synthesis of polymers **13** and **14** as discussed in Chapter 2. Furthermore the author had no information regarding the reactivity ratios of the three monomers. Nevertheless, despite the random incorporation of the three monomers, the resultant polymer was water soluble – almost certainly due (in part at least) to the use of a cationic monomer (as discussed in Chapter 3).

The UV-vis absorption, emission and excitation spectra for both the monomer and polymer were recorded in various solvents. The absorption spectrum for the hostasol monomer was recorded in DCM. Subsequently the excitation fluorescence spectrum was recorded in both DCM and cyclohexane

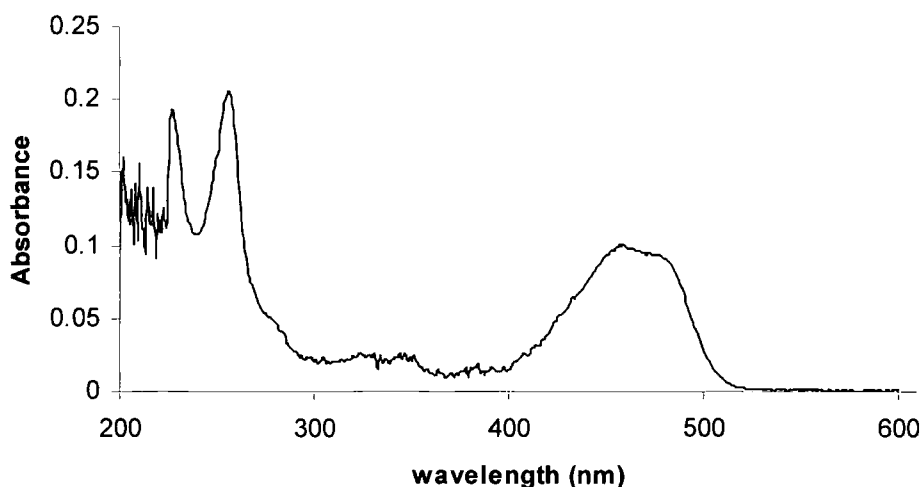


Figure 4.36 - Absorption spectrum of hostasol monomer

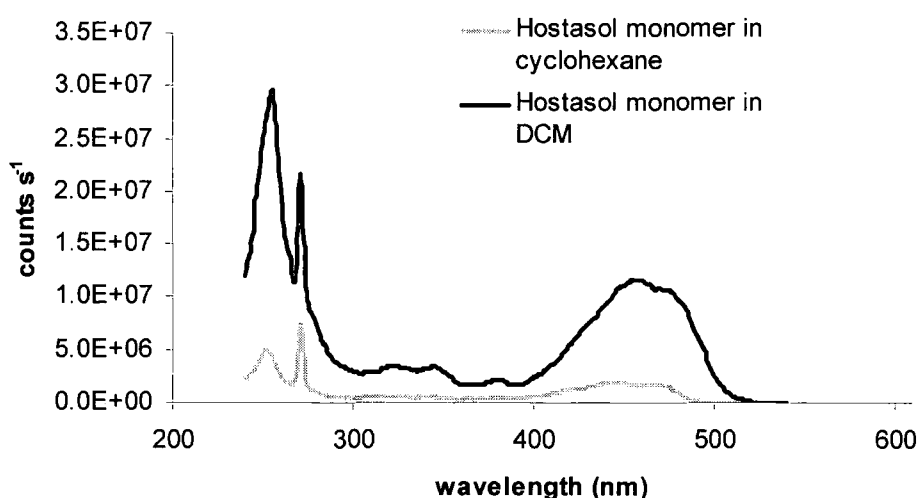


Figure 4.37 – Corrected excitation spectra of hostasol monomer (emission at 545 nm)

The emission spectra for the monomer were recorded in both DCM and cyclohexane (*i.e.* a polar and a non-polar solvent).

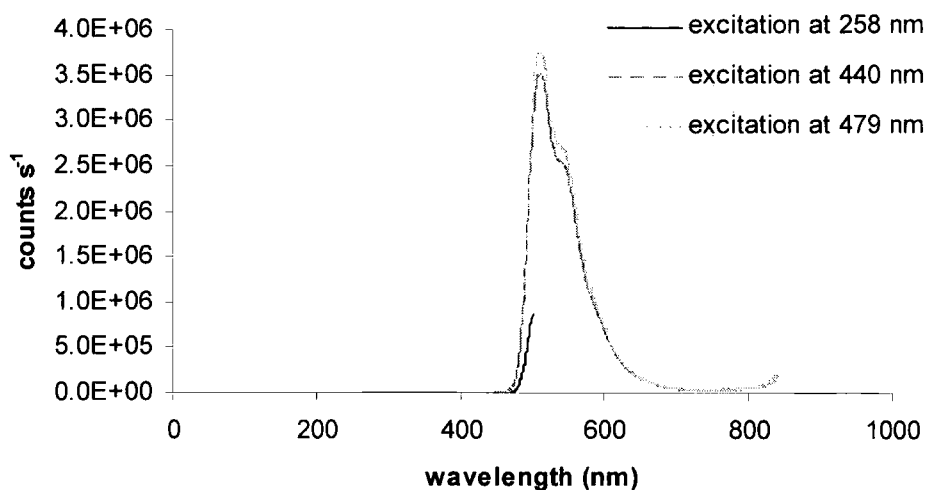


Figure 4.38 - Emission spectra of hostasol monomer in DCM

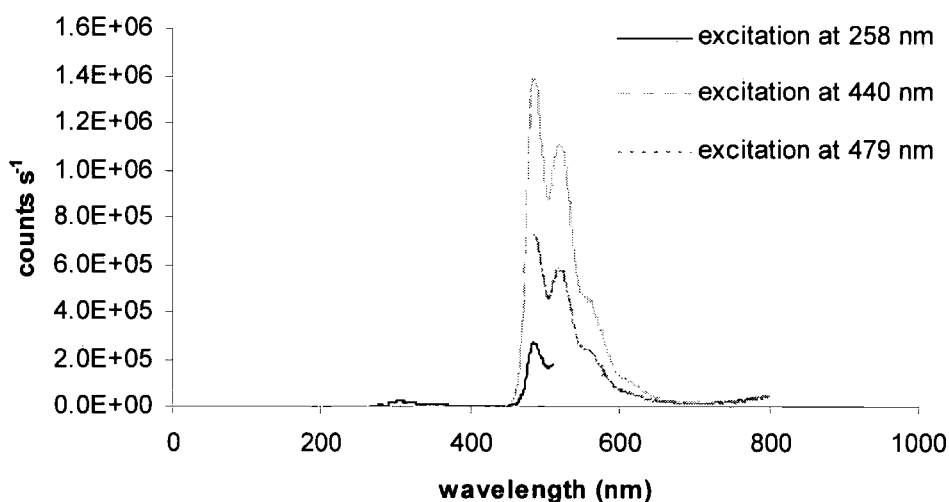


Figure 4.39 - Emission spectra of hostasol monomer in cyclohexane

From these spectra we can see that the monomer was found to emit between approximately 460 nm – 650 nm. It was expected that this would not change after polymerisation since the chromophore should not be affected chemically by polymerisation. The excitation spectra for **15** in water and DCM were measured and found to be in good agreement with the spectra recorded for the monomer, indicating that there was no significant difference in the fluorescence as a result of polymerisation.

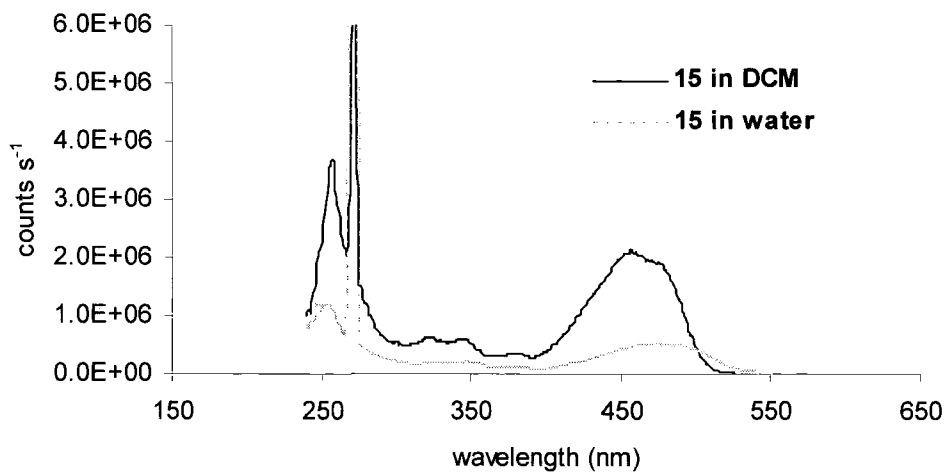


Figure 4.40 – Corrected excitation spectra of **15** (emission at 545 nm)

In addition, the emission spectra for **15** were also measured and compared with those recorded for the monomer. Once again the results were in good agreement; further supporting the assumption that polymerisation of the monomer does not affect its fluorescence.

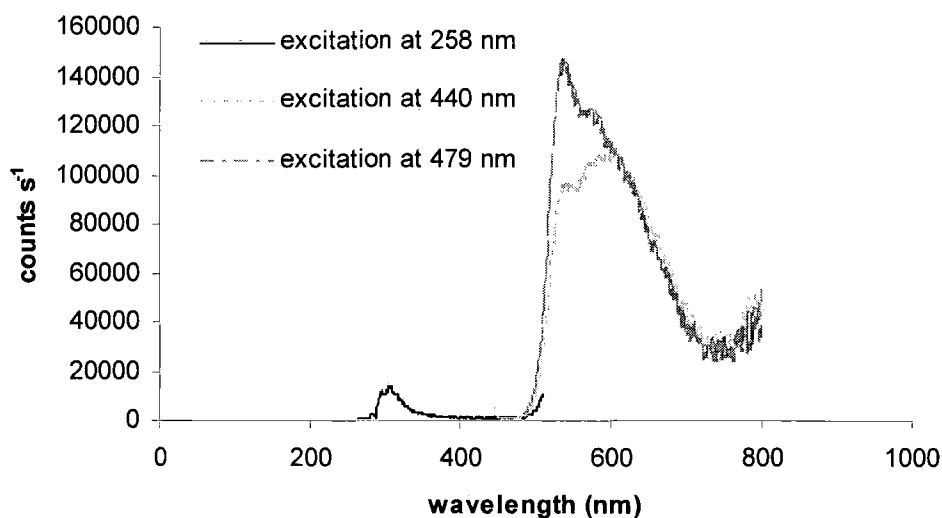


Figure 4.41 - Emission spectra of **15** in water

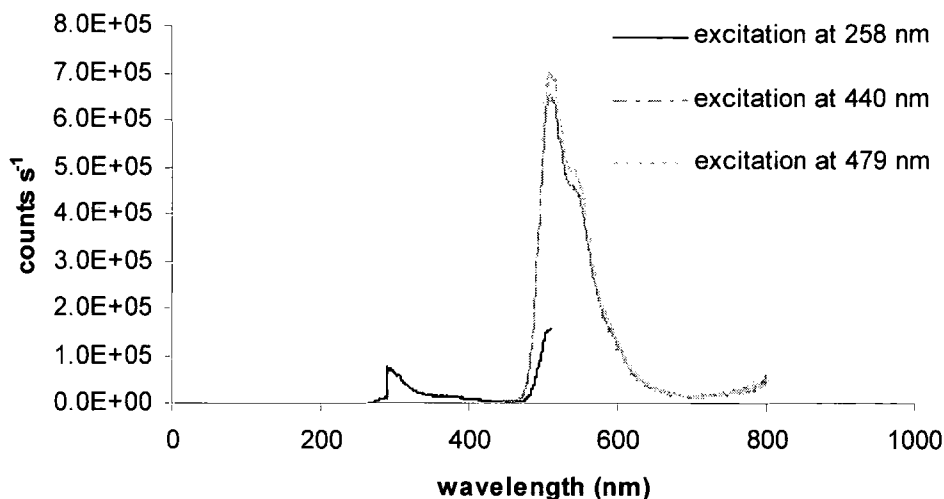


Figure 4.42 - Emission spectra of **15** in DCM

The differences between the spectra recorded in water and those recorded in DCM are largely due to the differences in the concentration of polymer in solution. It is not possible to compare the **15** in water spectra with equivalent spectra for the monomer, since the monomer is not water soluble. However, inspection of Figure 4.38 and Figure 4.42, the emission spectra for monomer and **15** in DCM, show that the difference is in the intensity of the signal – again due to the species being at different concentrations in solution.

These data were subsequently used when analysing the cells treated with the fluorescent polymer **15** by confocal microscopy. There were initially two confocal microscopy experiments conducted using **15** with boar spermatozoa. Solutions of polymer at two concentrations (1 mg/ml and 0.02 mg/ml) were incubated with the cells at 18°C over 5 days. The cells were then washed to remove any residual polymer and fixed onto microscope slides using the DNA binding dye DAPI (see Figure 4.43).

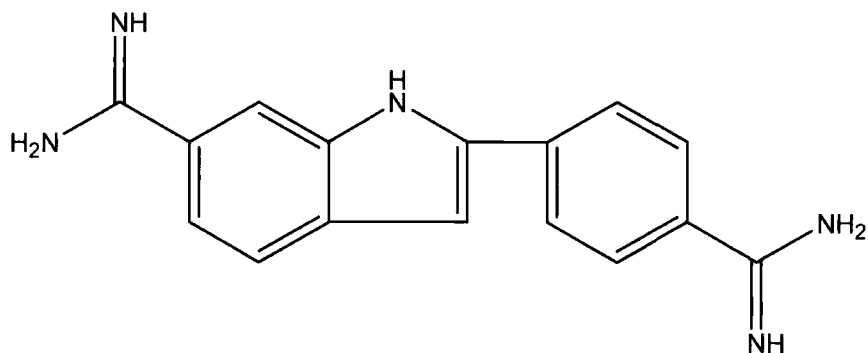
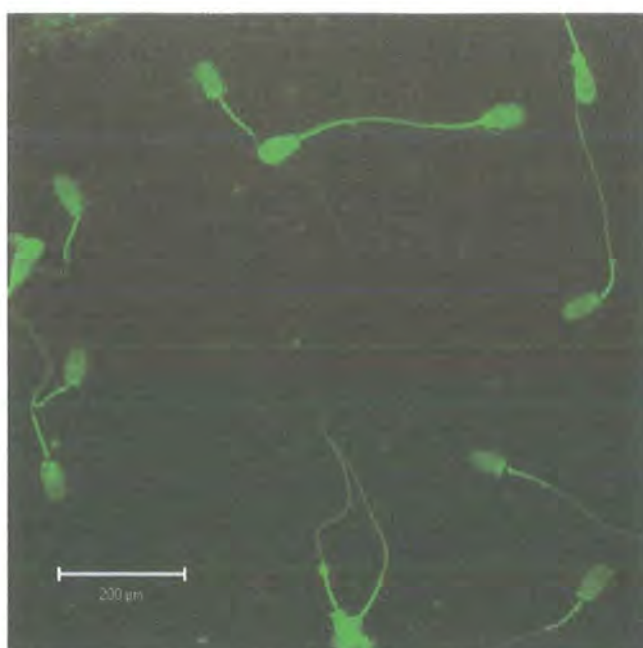


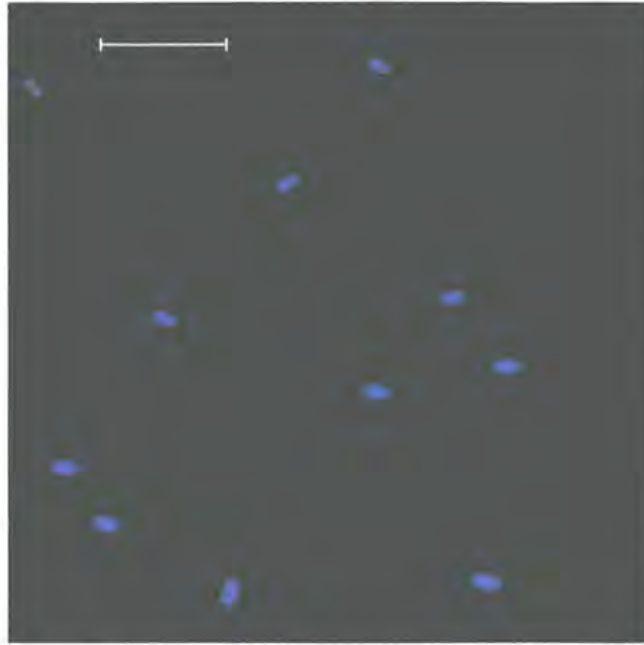
Figure 4.43 - Structure of DAPI

The primary objective of this experiment was to establish how well the cells could be imaged by this method and to arrive at a suitable experimental concentration of polymer in solution. From these experiments it became clear that using a polymer concentration of 1 mg/ml resulted in the fluorescence being far too intense. Indeed even at a 50<sup>th</sup> of the concentration, there was still a relatively high level of background fluorescence. Nevertheless, useful images were obtained. The purpose of the DAPI DNA staining dye was to make initial localisation of the cells more straightforward. For these initial experiments, the excitation wavelength used was 488 nm.



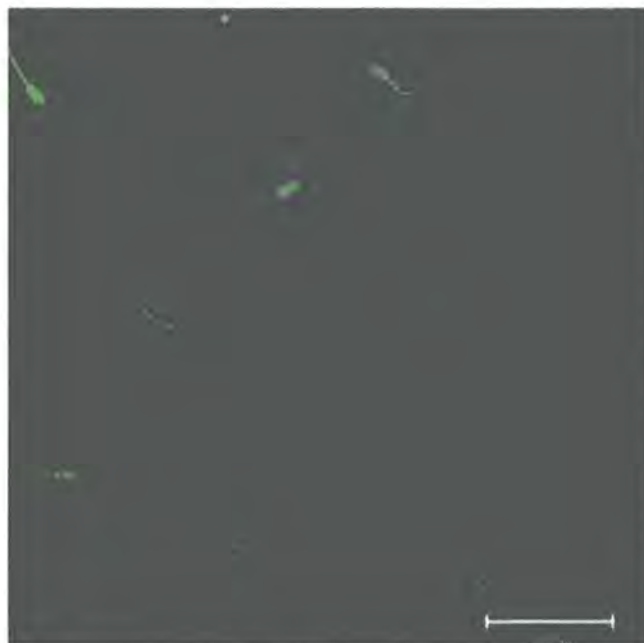
**Figure 4.44 - Cells stained with 15 (1 mg/ml), 63X magnification**

Figure 4.44 demonstrates that images were obtainable even at high polymer concentrations, however these were far more difficult to optimise due to high levels of background fluorescence. As such, the focus of the discussion will be on the lower concentration incubations.



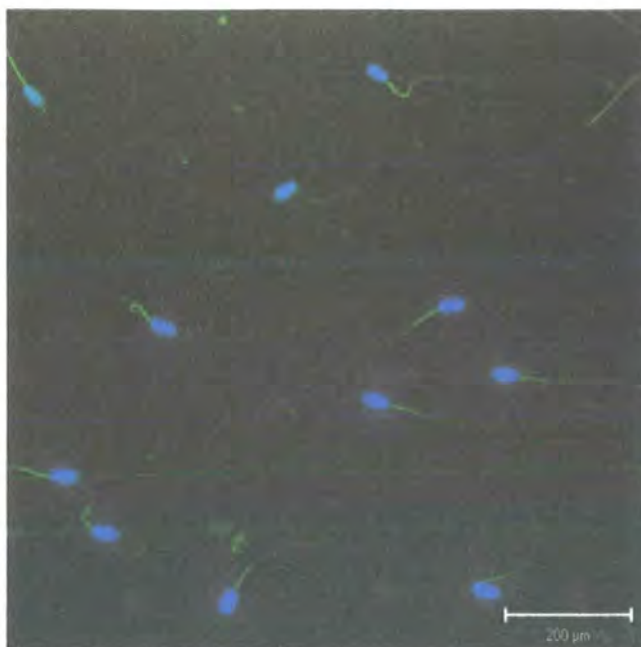
**Figure 4.45 - Sperm cells stained with DAPI, 40X magnification**

It is noteworthy that in Figure 4.45, only the heads of the sperm cells are visible. This is simply due to the fact that DAPI only binds to the DNA of the cell. Since, in the case of sperm cells, the DNA is localised in the head, the tails are not visible.



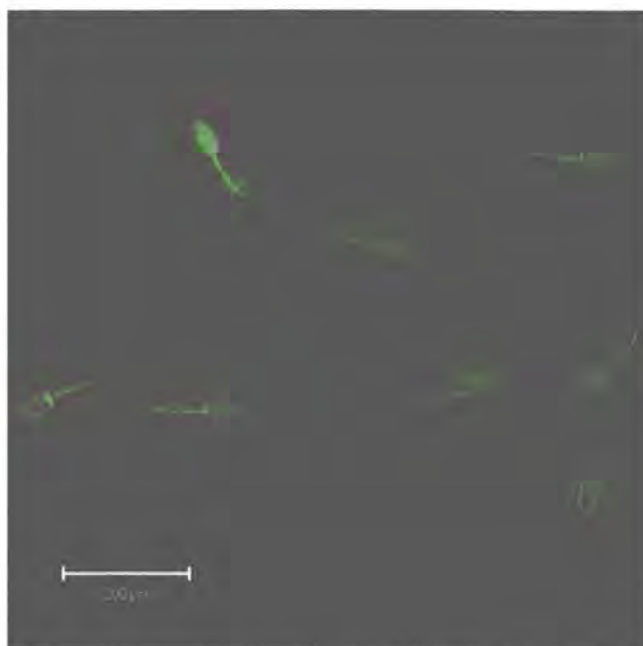
**Figure 4.46 - Sperm cells stained with 15 (0.02 mg/ml), 40X magnification**

Figure 4.46 clearly illustrates that the cells incubated with **15** are stained throughout the head and the tail, since the dye is not specific to any particular cellular compartment. The figure shown below illustrates that not only is the fluorescent polymer present throughout all of the sperm cell, it is also present within all of the cells in the sample, or at the very least, it is visible in all of the cells stained by the DAPI (which it is reasonable to assume will stain all of the sperm cells).



**Figure 4.47 - Overlay of Figure 4.45 and Figure 4.46, showing the presence of the 15 in all of the cells**

These cells were also analysed at higher magnification (63X), an example of such an image is shown in Figure 4.48.



**Figure 4.48 - Sperm cells stained with 15 (0.02 mg/ml), 63X magnification**

In addition to these images, a series of images in the  $z$  plane ( $z$  stacks) was created. These were designed to ascertain if the polymer was simply coated onto the outside of the cell surface or if it had been fully internalised.

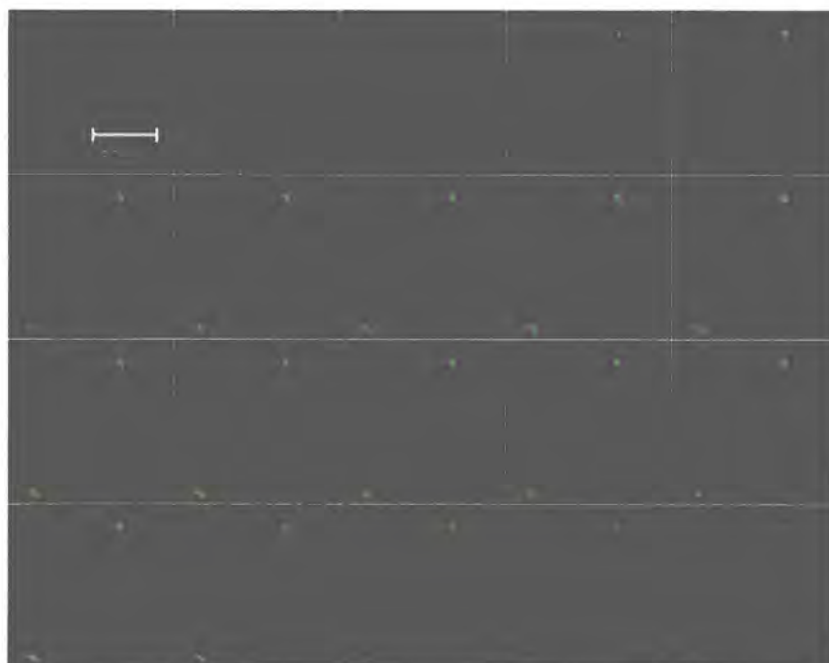


**Figure 4.49 - Montage of  $z$  stack slices of cells incubation with 15 (0.02 mg/ml)**

Each slice is approximately 0.2  $\mu\text{m}$  thick and the sequence shown is from top to bottom (from the top left hand square to the bottom right hand square). This helps to confirm that the glycopolymers are internalised by the sperm cells, although they do not confirm that the process is receptor mediated. However it also suggests that the thickness of the sperms cell heads is around 4  $\mu\text{m}$ . This is not consistent with literature values for this species which suggest thicknesses in the order of 1  $\mu\text{m}$ .<sup>10, 11</sup> However, this exaggeration of depth by confocal microscopy is known and has been discussed in several publications.<sup>12-16</sup>

In order to assess the effect of the galactosyl residues on the polymer, a second fluorescent polymer was synthesised with MMA in place of the sugar residue. As in the case of **15** the resultant polymer was bright orange in appearance and was also water soluble. <sup>1</sup>H NMR analysis of the material proved to be qualitative, and the results of elemental analysis were again not in good agreement with monomer feed ratios, however this is likely to be due to the factors discussed earlier.

This polymer (**16**) was then incubated with the cells in parallel with **15** in order to assess if there was any difference in the amount of material taken up by the cells. One observation from the first set of confocal experiments, was that not only was 0.02 mg/ml a more suitable concentration of polymer, but that 5 days incubation was probably more time than was necessary. Therefore, these experiments were conducted following an incubation period of 8 hours and using polymer concentrations of 0.02 mg/ml. In addition, images were viewed at both 488 nm, and 514 nm, the latter appearing to highlight more structural features of the cells.

The excitation and emission spectra for **16** were measured and found to be similar to that of both the monomer and **15**.

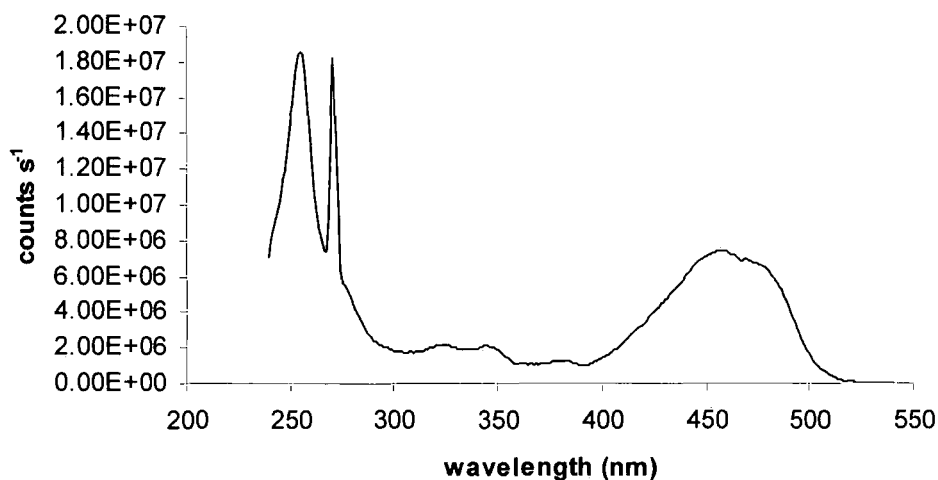


Figure 4.50 - Excitation spectrum of 16 in DCM (excitation at 545 nm)

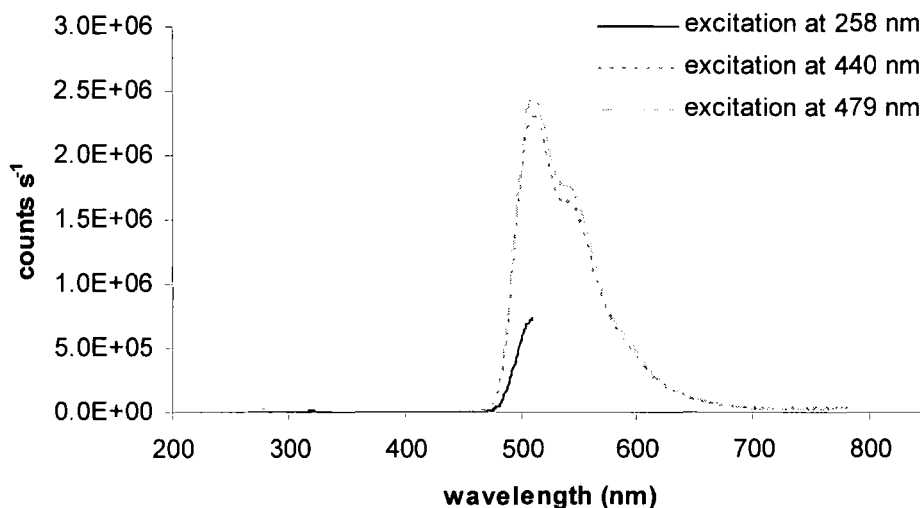
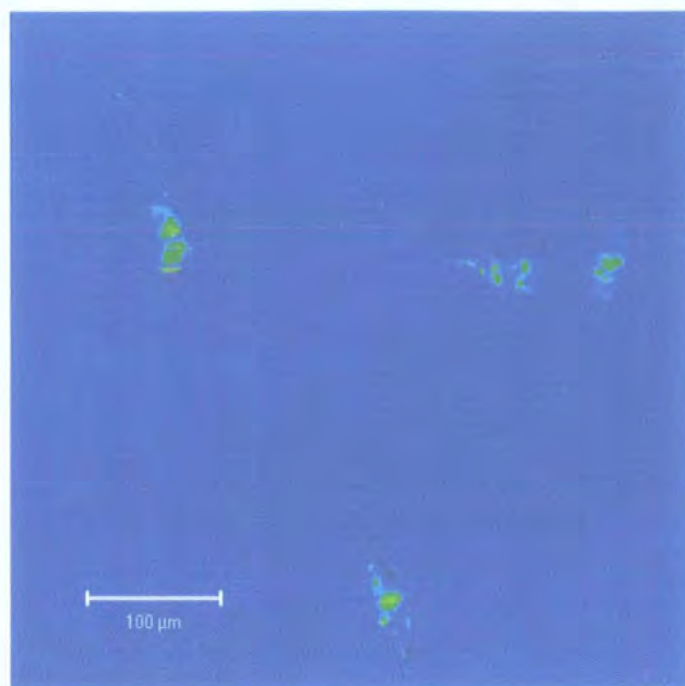


Figure 4.51 - Emission spectra of 16 in DCM

Prior to conducting the confocal microscopy experiment, it had been assumed that the non-glycosylated polymer would show no uptake if the process was sugar-mediated. Initially, observations were therefore rather disappointing. Cells incubated with the sugar-free polymer were also found to be fluorescent.



**Figure 4.52 - Cells incubated with 16 at 0.02 mg/ml for 8 hours, 63X magnification**

This image is presented in a colour map format<sup>†††</sup> which shows the intensity of the fluorescence signal (blue = no signal, red = intense signal). This manipulation makes comparison of different samples measured, using the same experimental parameters and settings, more straightforward than comparing the green images on a black background.

Whilst this result was initially greeted with disappointment, the following image taken of the cells incubated with **15** re-ignited the possibility of a sugar-mediated uptake mechanism being at least partially responsible for internalisation of the polymer.

---

<sup>†††</sup> This format is analogous to an image produced by an infra-red heat detection camera.

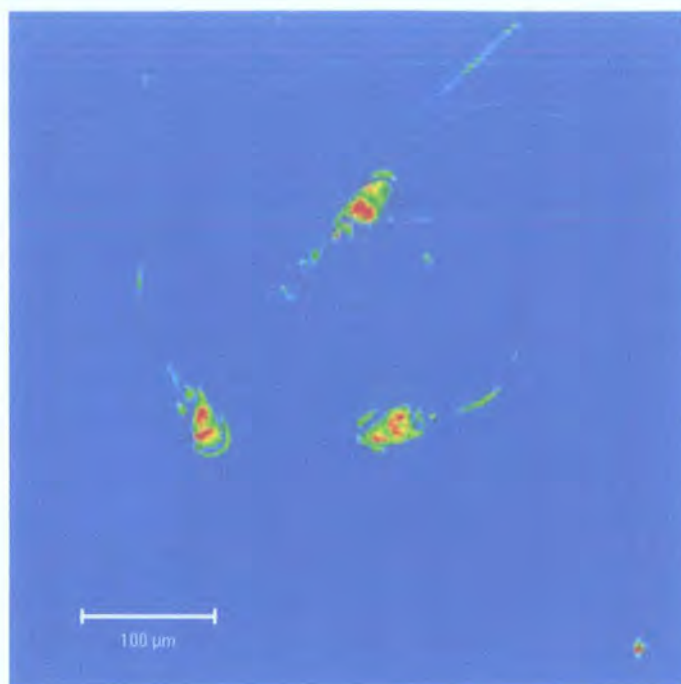


**Figure 4.53 - Cells incubated with 15 at 0.02 mg/ml for 8 hours, 63X magnification**

By comparing Figure 4.52 and Figure 4.53 it is clear that there is more material present in the cells that were incubated with the polymer containing galactose residues. This would tend to suggest that there are at least two mechanisms responsible for the uptake. It seems likely that there is a reasonable amount of polymeric material which enters the cell via a diffusive mechanism, while the presence of sugar on the polymer also provides the opportunity for receptor-mediated uptake to occur. The uptake of material is also relatively fast, since these images were recorded after only 8 hours of incubation with both polymers. Previous *in vitro* studies had suggested that the level of vitamin E within the cells was very low on the first day of incubation, a result which at face value is in contrast to the results with the fluorescent polymers. However, it is the thesis of this author that the uptake has two key steps – i) the uptake of the material itself; ii) subsequently, the release of the active component. Since these polymers will fluoresce regardless of whether the dye is bound to the polymer or not, it is not possible to infer anything regarding the speed of release from these images. Therefore, it has been postulated that the uptake of these glycopolymers is rapid, and the rate limiting step is the hydrolysis of the active component from the polymer.

In order to ascertain if this theory was valid, cells were incubated with **15** (at a concentration of 0.02 mg/ml) over a 5 hour period, and samples were taken at one hour intervals. These samples were washed 3 times by centrifugation, before being spun onto glass slides. These were then analysed in turn using confocal microscopy. The results supported the theory that uptake is extremely rapid as no obvious differences were observed between the samples.

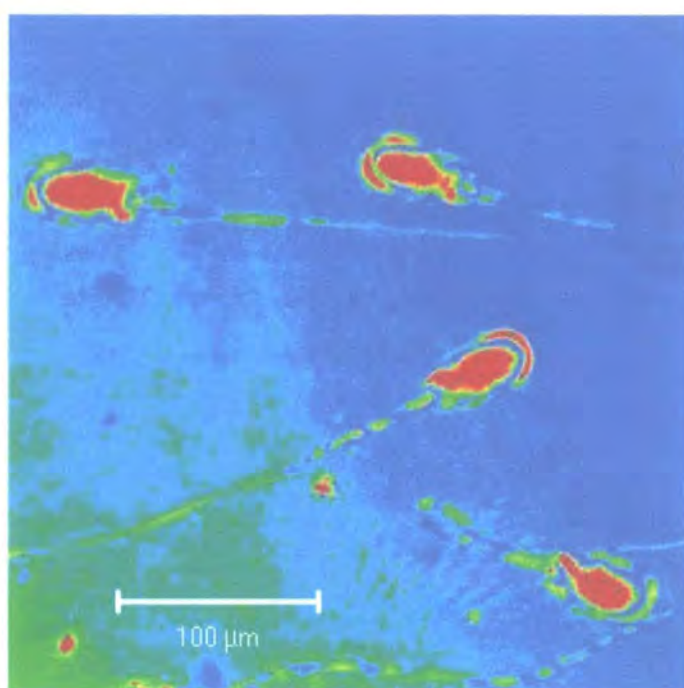


**Figure 4.54 - Cells incubated with 15 for 1 hour**

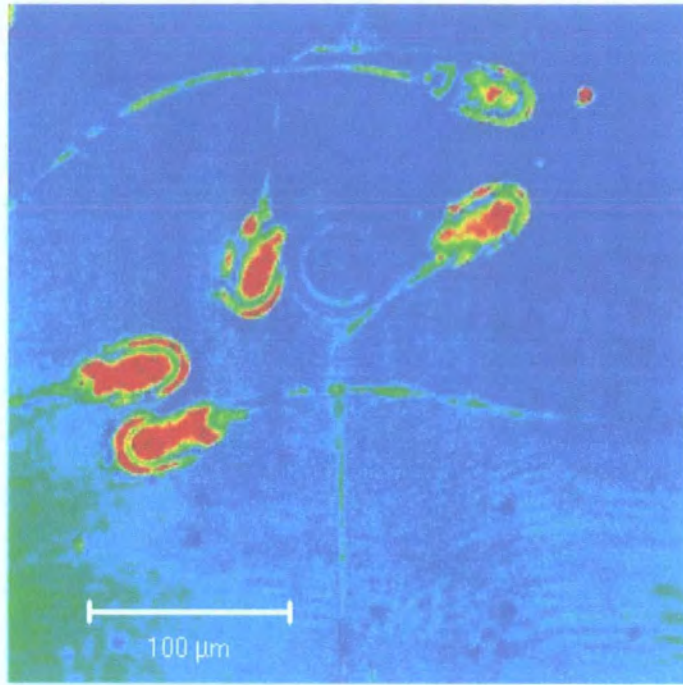


**Figure 4.55 - Cells incubated with 15 for 5 hours**

### ***4.3 Conclusions***

It has been demonstrated that sperm cells incubated in the presence of glycopolymers with pendant vitamin E moieties can significantly reduce cellular oxidation under induced oxidative conditions, without having an adverse effect on key sperm quality parameters. This suggestion was further corroborated by using polymer incubation pre/post sorting – a process which inherently damages cells (presumably not only via oxidative pathways). Numerous experiments focussing on cellular motility and viability demonstrated that when the polymer concentration was lower, there was a neutral impact on sperm quality parameters.

Although the results of induced oxidation experiments *etc.*, tentatively and qualitatively suggested that these polymeric species were being internalised by the sperm cells, further investigations using fluorescently labelled glycopolymers provided more substantial evidence of internalisation. This work has recently been the subject of a publication in *Nature Chemical Biology*.<sup>17</sup>

In summary – sperm cells incubated with glycopolymers containing pendant vitamin E moieties, are significantly less damaged, compared with control samples, during oxidative stress. It is hypothesised that the mechanism for uptake is receptor-mediated via the complementary interaction of the galactose moieties with cellular receptors.

## 4.4 Experimental

### 4.4.1 Materials and Instrumentation

2-Dimethylamino ethyl acrylate (DMAEA, 98%), anhydrous methanol (99.8%) and anhydrous *N,N*-dimethylformamide (99.8%) were purchased from Aldrich. Azobisisobutyronitrile (AIBN, 97%) was obtained from BDH, and purified by recrystallisation from methanol prior to use. DMAEA had inhibitor removed prior to use by passing through a plug of basic alumina. Hostasol monomer was supplied from Prof. D Haddleton's group, at the University of Warwick. Compound **2b** was synthesised as described previously in Chapter 2 section 2.3.3.4. All other chemicals were used without further purification.

NMR-spectra were recorded on a Varian Unity 300, Varian Mercury 200 or Bruker Avance 400 spectrometers; all chemical shifts were referenced to residual solvent as an internal standard. Infrared (IR) spectra were obtained using a Perkin Elmer 1600 Series FTIR spectrometer. UV spectra were measured on an ATI Unicam UV/VIS UV2 spectrophotometer, in stoppered quartz cuvettes with a 1 cm path length. Fluorescence spectra were obtained using a Jobin-Yuon Horba Fluorolog 3-22 Tan-3 spectrofluorimeter with 90° geometry. Samples analysed by aqueous GPC, were determined using a Viscotek TDA 301 with triple detection (refractive index, viscosity and right angle laser light scattering detectors), eluted through two 300 × 7.5 mm ViscoGel GMPW xl columns. The light scattering detector was calibrated using a PEO standard of 82 500 gmol<sup>-1</sup>. The mobile phase consisted of 80% water, 20% methanol, 0.05 M NaNO<sub>3</sub> and 2.5 ml l<sup>-1</sup> 1.0 M NaOH at a flow rate of 0.5 ml min<sup>-1</sup>. Elemental analyses were obtained with an Exeter Analytical Inc. CE-440 Elemental Analyser. Lyophilised products were obtained using a Christ ALPHA-1-4 freeze-dryer with a LDC-1M controller. Confocal and fluorescence microscope images were obtained using a Zeiss LSM 510 microscope fitted with an Argon laser (458, 477, 488 and 514 nm).

## 4.4.2 Semen Quality

### 4.4.2.1 Appearance

The first and perhaps most primitive method of semen evaluation is its physical appearance. Undiluted fresh semen should be a white viscous liquid, whose viscosity is relative to the number of cells present. There should be no associated odour, and indeed any unpleasant odour is often an indication of infection or the presence of urine. Discoloration of the semen may indicate the presence of blood, urine or faeces. The sample may occasionally contain other debris such as mud or straw for example.

Samples which have abnormalities in appearance should not be used for AI.

### 4.4.2.2 Motility<sup>†††</sup>

Motility was assessed using a Computer Assisted Sperm Analyzer (CASA, Hobson Tracking Systems (7V2B)). The sperm cells were diluted in BTS (Beltsville diluent) to a concentration of between 30-50 x 10<sup>6</sup> cells ml<sup>-1</sup>. The samples were then incubated at 37°C for 10 minutes, before a 10 µl drop was deposited on a Makler chamber (which was kept at 37°C on a heating plate). The samples were then read using a Nikon microscope equipped with a heating plate (maintained at 37°C). A video camera (Sony) was connected to the computer. Motility was assessed on 200 tracks per sample.

### 4.4.2.3 Viability

There are a number of standard experimental techniques that can be used to assess cellular viability<sup>18, 19</sup>. Most rely on some form of cell staining, and the number of dead (or live) cells is then counted either manually<sup>§§§</sup> or by an automated fluorescence measurement<sup>†††</sup>.

---

††† Conducted by Dr André Maldjian.

#### **4.4.2.3.1 SYBR14/Propidium Iodide<sup>†††20</sup>**

SYBR 14 was diluted 20 times with DMSO. The semen sample was then diluted to give a final concentration of between 25-40 x 10<sup>6</sup> cells ml<sup>-1</sup>. An aliquot of semen (500 µl) and an aliquot of SYBR 14 solution (4 µl) were mixed together. This was incubated for 10 minutes, before adding propidium iodide solution (5 µl). The sample was then incubated for a further 5 min. Subsequently 5 - 10 µl of sample was spotted onto a slide, and covered with a slip. The slide was then read using a fluorescent microscope (blue light wavelength). Three populations were counted: live (green), dead (red), damaged (green and red) and the results expressed as a percentage.

#### **4.4.2.3.2 Eosin Staining<sup>§§§</sup>**

Semen (~2 µl) and eosin dye (~2 µl) were spotted on a microscope slide. The spots were then smeared quickly across the slide using the edge of a cover slip. The resultant thin film was dried quickly and then observed at high magnification. One hundred cells were counted; those stained with the dye are damaged. The result is expressed as a ratio of percentages (live:dead).

#### **4.4.2.3.3 Lectin Binding<sup>§§§</sup>**

Semen (1 ml, 10 x 10<sup>6</sup> cells ml<sup>-1</sup>) was charged with peanut agglutinin (PNA) (5 µl) and propidium iodide [PI, 1mg ml<sup>-1</sup> in water] (5 µl). The sample was then mixed and incubated at 38°C for 4 minutes. The sample was then divided in two. To one half, para-formaldehyde (10 µl, 1% in water) was added and the cells were counted using fluorescence microscopy. To the other half, LPC (5 µl) was added and the sample was incubated for a further 5 minutes at 38°C, after which para-formaldehyde was added (as above) and the cells were counted as in section 4.4.2.3.1.

---

<sup>§§§</sup> Conducted by the author.

**4.4.2.4 Morphology<sup>SSS</sup>**

Cellular morphology was assessed using high-powered light microscopy (typically 100X); the cells were fixed using Hancock Solution.<sup>21</sup> Key morphological features (see examples in Figures Figure 4.56 Figure 4.57 below) were assessed and the number of cells with/without defects was counted. The results were expressed as percentages.

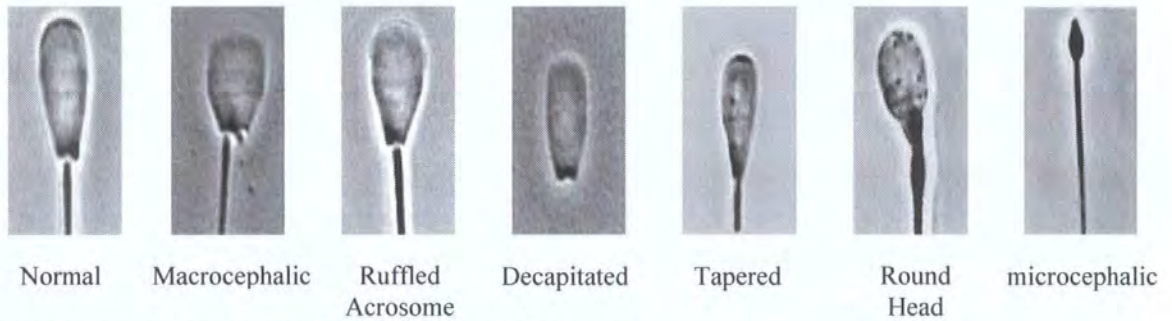


**Figure 4.56 - Morphological abnormalities of the head**

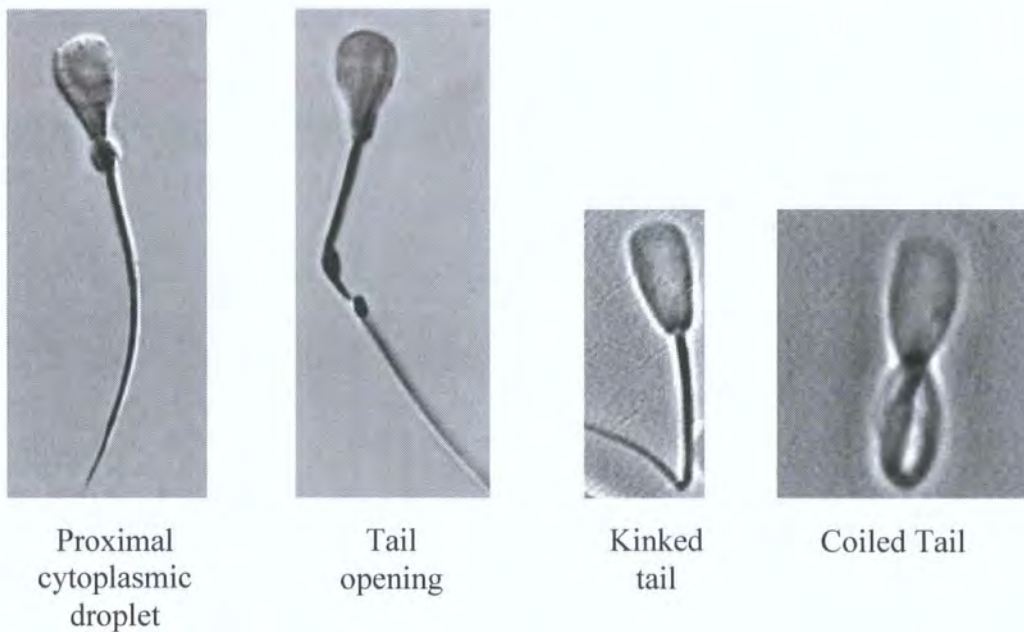


**Figure 4.57 - Morphological abnormalities of the tail**

**4.4.2.5 Enumeration<sup>SSS</sup>**

The concentration of sperm cells in the ejaculate was calculated by counting the number of cells on a Thoma haemocytometer slide. The slide contains 2 grids of 2 x 25 squares and cells within 5 of the 25 squares on each grid are counted (Figure 4.58). The semen

was first diluted with water (5  $\mu\text{l}$  of semen in 10 ml of water); this also serves to immobilise the cells. The total number of cells is multiplied by 5000 (a factor which takes into account the dimensions of the grid and the dilution factor) to give a concentration expressed as millions of cells per millilitre.

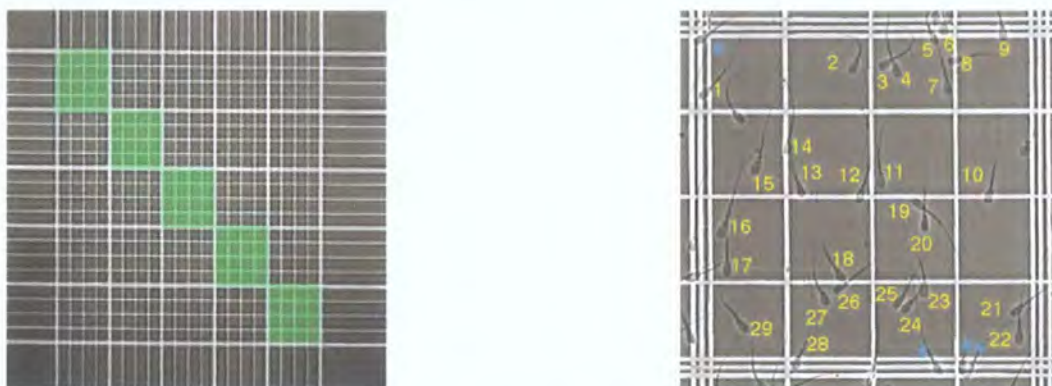


Figure 4.58 – Typical haemocytometer images

#### 4.4.2.6 TBARS Assay<sup>##</sup>

The ability of polymer treated/untreated cells to resist oxidation was assessed using the TBARS assay.<sup>3</sup> Cell pellets were washed after various periods of incubation in the presence of  $\alpha$ -tocopherol containing polymers (2  $\times$  with physiological solution after centrifugation (10 minutes at 5°C)). Pellets were re-suspended in 1 ml of a 1.15% KCl solution, before iron (III) sulphate (0.8 mM) was added to initiate peroxidation (1 hour at 37°C). A solution of BHT (butylated hydroxytoluene) (40 ml, 0.4% w/v in ethanol) was added at the end of the incubation period in order to stop oxidation. Subsequently acetic acid (1.5 ml, 20%, v/v; pH 3.5) and thiobarbituric acid solution (1.5  $\mu\text{l}$ , 0.8% w/v) were added. After homogenisation, samples were incubated at 95°C and analysed for malonyldialdehyde (MDA) according to the method of Ohkawa et al.<sup>3</sup> To establish any potential errors in the assay due to protein-derived materials, additional assays on trichloroacetic acid-precipitated materials were also conducted; however no significant differences were observed.

4.4.2.7 *Sex sorted semen* \*\*\*\*

Semen was diluted to a concentration of  $150 \times 10^6$  cells  $\text{ml}^{-1}$ . It was then stained with a fluorescent dye (Hoechst No. 33342 - 2'-[4-ethoxyphenyl]-5-[4-methyl-1-piperazinyl]-2,5'-bi-1H-benzimidazole) at concentrations ranging between 15 and 30  $\mu\text{l}$  per ml. The stained samples were incubated at 37°C for 1 hour prior to use. The cells were then passed through the sorter and separated based on DNA content into two tubes (X & Y). A basic schematic of the process is shown in Figure 4.59.

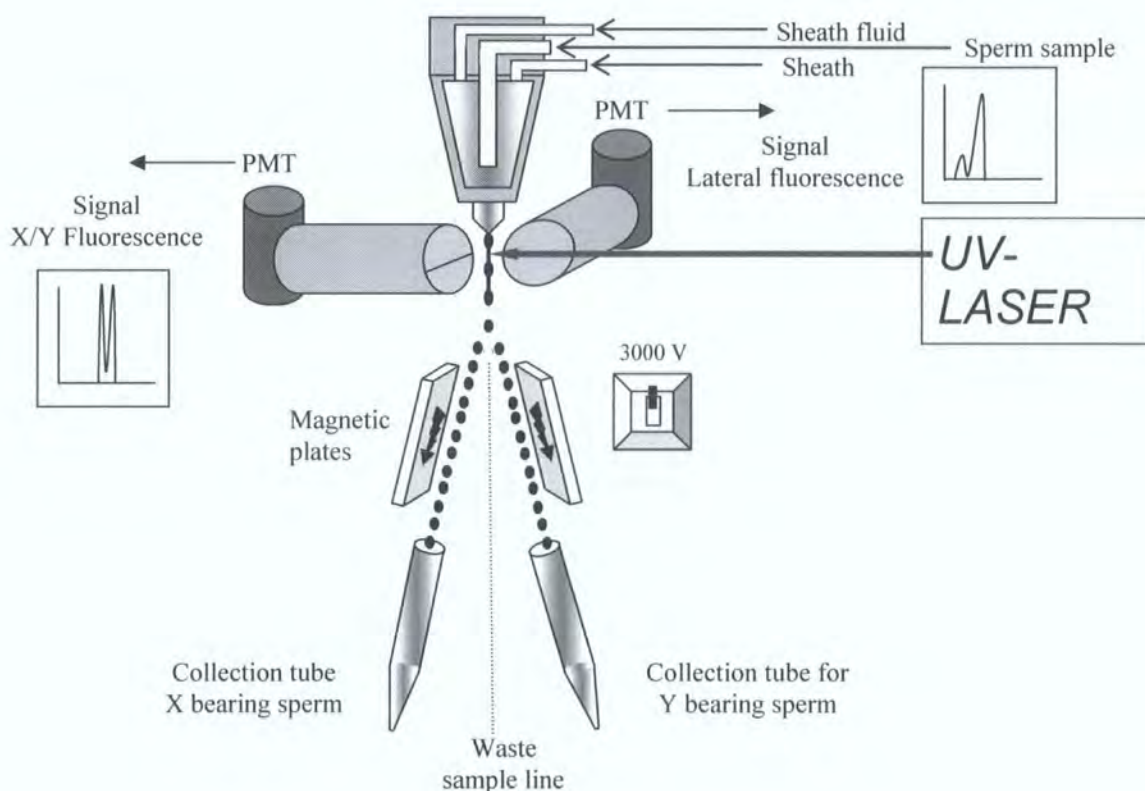


Figure 4.59 – A schematic of the flow cytometer

\*\*\*\* These experiments were conducted by the author, with the assistance of staff at the Institut für Tierzucht und Tierverhalten, Hanover, Germany.

#### 4.4.3 Synthesis of poly[2-( $\beta$ -D-galactosyloxy)ethyl methacrylate-ter-hostasol methacrylate-ter-2-(dimethylamino)ethyl acrylate] (15)

A mixture of hostasol monomer (0.28 g, 0.612 mmol), DMAEA (0.499 g, 3.485 mmol), **2b** (0.20 g, 0.684 mmol) and AIBN (2 mg, 1.5 wt%) were dissolved in DMF (2.6 ml) and methanol (0.65 ml) (4:1). The mixture was degassed (by the freeze pump thaw method) and stirred under nitrogen at 70°C for 24 hours. After this time the solvents were removed under vacuum and the orange/red waxy residue was redissolved in water and recovered by freeze drying. The residue was re-dissolved in water, dialysed against distilled water (MWCO 12-14 kDa), and recovered again by freeze drying. This yielded **15** (730 mg, 73%), however the elemental analysis data measured was not in good agreement with the expected values. This may be due to the monomers having very different reactivity ratios, which in turn impacts on the incorporation of the monomers into the polymer. Since this material is being synthesised by free radical polymerisation, there is very little control over the result of the polymerisation. In addition, there may be some water associated with the polymer, which would also skew these data. The polymer synthesized is analogous to polymer **14**, with vitamin E monomer having been substituted for Hostasol monomer.

(Expected C 60.27; H 7.52; N 5.85; S 2.00 Found C 56.62; H 6.51; N 3.13; S 2.38); IR (KBr,  $\text{cm}^{-1}$ ): -OH (broad) 3402; -CH (med.) 2962, 2936, 2865; -C=O (sharp) 1736, 1720; - aromatic (sharp) 1653, 1642, 1560; CH (sharp) 1458; -CH<sub>3</sub> (med.) 1390; aromatic -CH deformations (sharp) 764. <sup>1</sup>H NMR (200 MHz, D<sub>2</sub>O, significant peaks): 3.04-3.82 (sugar ring protons), 4.30 (broad, -CH<sub>2</sub>-CH<sub>2</sub>-O-, DMAEA), 7.2-8.1 (broad, hostasol aromatic protons). GPC (H<sub>2</sub>O): M<sub>n</sub> 4.19 × 10<sup>5</sup>; M<sub>w</sub> 1.13 × 10<sup>6</sup>, PD = 2.7.

#### 4.4.4 Synthesis of poly[methyl methacrylate-ter-hostasol methacrylate-ter-2-(dimethylamino)ethyl acrylate] (16)

A mixture of hostasol monomer (0.28 g, 0.612 mmol), DMAEA (0.5 g, 3.485 mmol), MMA (0.07 g, 0.684 mmol) and AIBN (0.013 mg, 1.5 wt%) were dissolved in DMF (2.82 ml). The mixture was degassed and stirred under nitrogen at 70°C for 24 hours.

After this time the solvents were removed under vacuum and the orange/red waxy residue was re-dissolved in water and recovered by freeze drying. The residue was re-dissolved in water, dialysed against distilled water (MWCO 12-14 kDa), and recovered again by freeze drying. This yielded **16** (586 mg, 69%) as a bright orange solid. The polymer synthesized is analogous to polymer **15**, with galactose monomer having been substituted for MMA. Once again, analysis of this material was difficult and clearly incorporation of the monomers has not been as desired. The  $^1\text{H}$  NMR spectrum was indicative of a high molecular weight polymer (also shown from the results of GPC analysis). Nevertheless, key areas of the spectrum indicated the presence of the components.

(Expected C 62.9; H 7.7; N 6.8; S 2.3, Found C 42.34; H 5.33; N 3.28; S 1.95); IR (KBr,  $\text{cm}^{-1}$ ): -OH (broad) 3420; -CH (med.) 2949, 2866; -C=O (sharp) 1738, 1724; -CH (sharp) 1458; -CH<sub>3</sub> (med.) 1408; aromatic -CH deformations (sharp) 850, 760.  $^1\text{H}$  NMR (300 MHz,  $\text{CDCl}_3$ , significant peaks): 4.1 (med, -O-CH<sub>3</sub>, MMA), 4.7 (broad, -CH<sub>2</sub>-CH<sub>2</sub>-O-, DMAEA), 7.5-8.4 (broad, hostasol aromatic protons). GPC ( $\text{H}_2\text{O}$ ):  $M_n$   $6.64 \times 10^4$ ;  $M_w$   $1.11 \times 10^6$ , PD = 16.66.

#### 4.4.5 Vitamin E analysis<sup>†††</sup>

HPLC analysis was conducted (excitation at 295 nm, emission at 330 nm) on a system fitted with a Hypersil column (250 × 4.6 mm, 5 mm) run with 97% MeOH: 3% water (v/v) as the eluent system. Prior to analysis spermatozoa were homogenized and tocopherols extracted as described by Dvorska et al<sup>2</sup>. In short, a pellet of  $500 \times 10^6$  spermatozoa was obtained after two centrifugations (2000g for 10 min at 5°C); the pellet was washed and re-suspended between centrifugations using a physiological solution in order to eliminate all contamination from the polymer remaining in solution. Then the pellet was re-suspended in aqueous NaCl (0.7 ml, 0.7% (w/v)). Subsequently ethanol (1 ml) and hexane (3 ml) were added and the samples were mixed by vortexing for 20 s. Samples were centrifuged as described above, the hexane layer containing the tocopherols was collected and left in the dark. The hexane extraction was repeated thrice (3 ml each time). Finally, samples were dried under nitrogen at 40°C, re-suspended in methanol and analysed by HPLC.

#### 4.4.6 Confocal Microscopy

In short, two or more 75 ml tubes of boar semen (supplied by JSR Newsham) were pooled. Each experimental group was conducted in triplicate (20 ml per sample)

Incubations were carried out over a prescribed time period at 20°C. Following incubation, the cells were centrifuged (300 g, 5 minutes at 20°C), the supernatant removed and the cells re-suspended in BTS (15 ml). The cells were then centrifuged again (300 g, 5 minutes at 20°C) a further two times in order to ensure any polymer remaining in solution was discarded.

Following the final wash the cells were re-suspended in BTS (15 ml). An aliquot (25 µl) was removed from each sample and made up to 500 µl with BTS. These samples were then centrifuged in a CYTOSPIN centrifuge, which deposited the cells as a thin layer on a microscope slide. The cover slip was then “glued” to the slide using an adhesive that contains the DNA binding dye (DAPI).

The samples were then analysed by laser scanning confocal microscopy (excitation 488 & 514 nm). Images were taken at 40x and 63x magnification, and a 3D picture of the cells was built up using 0.2µm image stacks. The confocal images showed the dye to be inside, and not outside the cell, supporting the theory of RME.

## 4.5 References

1. Cerolini, S.; Maldjian, A.; Surai, P.; Noble, R. *Anim. Reprod. Sci.* **2000**, *58*, (1,2), 99-111.
2. Dvorska, J. E.; Surai, P. F.; Speake, B. K.; Sparks, N. H. C. *Comp. Biochem. Physiol. C.* **2002**, *131C*, (2), 197-205.
3. Ohkawa, H.; Ohishi, N.; Yagi, K. *Anal. Biochem.* **1979**, *95*, (2), 351-358.
4. Maldjian, A.; Penny, P. C.; Noble, R. C. *Male Fertil. Lipid Metab.* **2003**, 60-72.
5. Noble, R. C. *Supplement containing an admixture of an enriched triacylglycerol source of docosahexaenoic acid (DHA), an antioxidant, selenium, and g-linolenic acid to enhance fertility.* Wo 2001097802, **2001**.
6. Strzezek, J.; Fraser, L.; Kuklinska, M.; Dziekonska, A.; Lecewicz, M. *Reprod. Domest. Anim.* **2003**, *38*, (4), 319-364.
7. Surai, P.; Noble, R. C. *Improvement of male fertility with antioxidants and/or polyunsaturated fatty acids.* WO 9800125, **1998**.
8. Leigh, J. *Year in Industry Report*; University of York: 2003.
9. Clariant (2005) *Dyes for the colouration of resins*, <http://pa.clariant.com/C1256C70004F0C0D/vwWebPagesByID/65C76258408F6ED1C1256C8500594F85>, [Accessed 2005]
10. Gadella, B. M.; Gadella, T. W. J.; Colenbrander, B.; Van Golde, L. M. G. *J. Cell Sci.* **1994**, *107*, (8), 2151.
11. Rath, D., *Personal Communication.* Fleming, C., **2002**
12. Brismar, H.; Patwardhan, A.; Jaremko, G.; Nyengaard, J. *J. Microsc.* **1996**, *184*, (2), 106-116.
13. Everall, N. *Confocal Raman microscopy - Why the depth resolution is much worse than you think! Modelling and measuring the effect of refraction in transparent media.*, International Union of Microbeam Analysis Societies, Kailua-Kona, HI, Jul, Williams, D. B.; Shimizu, R., Eds. Bristol: Kailua-Kona, HI, pp 33-34, **2000**.
14. Everall, N. *J. Appl. Spectrosc.* **2000**, *54*, (10), 1515-1520.
15. Michielsen, S. *J. Appl. Polym. Sci.* **2001**, *81*, (7), 1662-1669.
16. Watson, T. F. *Adv. Dent. Res.* **1997**, *11*, (4), 433-441.

17. Fleming, C.; Maldjian, A.; Costa, D. D.; Rullay, A. K.; Haddleton, D. M.; St John, J.; Penny, P.; Noble, R. C.; Cameron, N. R.; Davis, B. G. *Nat. Chem. Biol.* **2005**, 1, (5), 270-274.
18. Gliozzi, T. M.; Luzi, F.; Cerolini, S. *Theriogenology* **2003**, 60, (4), 635-645.
19. Bilgili, S. F.; Renden, J. A. *Poult. Sci.* **1984**, 63, (11), 2275-2277.
20. Garner, D. L.; Johnson, L. A. *Biol. Reprod.* **1995**, 53, 276-284.
21. Ozturkler, Y.; Baran, A.; Evecen, M.; Ak, K.; Ileri, I. K. *Turk. J. Vet. Anim. Sci.* **2001**, 25, (5), 675-680.

## 5 DHA polymer synthesis

### 5.1 Introduction

DHA is a naturally occurring PUFA found mostly in oily fish such as haddock, tuna, salmon and mackerel.<sup>1</sup> DHA and other PUFAs are recognised as being important constituents of mammalian diets although frequently they are consumed at levels below the recommended values.<sup>1</sup> In the human body DHA is found in the cell membranes in various parts of the body, namely the brain, retina, testes and in sperm cells and it has been suggested that it is an essential component in the development of such cells<sup>1</sup>. Such is the awareness of the importance of these essential PUFAs that many foodstuffs are now available (bread,<sup>2</sup> eggs, spreads, milk, orange juice<sup>3</sup>) that have been enriched with PUFAs through the manipulation of animal feeds.<sup>4</sup> Herein it is the presence and importance of DHA within the cell membranes of spermatozoa that are of greatest importance.

As has been discussed previously, the delivery of antioxidants to spermatozoa is of importance due to the high levels of PUFAs present, since the latter are susceptible to oxidation. As also alluded to earlier, the levels of DHA in boar sperm cells<sup>5</sup> (or indeed the sperm cells of other species<sup>6-8</sup>), can be heightened through dietary means, but what is of further interest, is the delivery of DHA to sperm cells *in vitro*. This could potentially be achieved via two key mechanisms, the merits of which are discussed below. If we consider this problem as a “drug delivery” scenario, then it could be possible to deliver DHA to sperm cells using a targeted delivery method as described for vitamin E in the previous chapters. However, as in the case of some drug delivery examples,<sup>9-13</sup> the delivery of DHA *in vitro* could be achieved by encapsulating DHA inside glycopolymer micelles, thus forgoing the need to chemically bond the DHA molecule to the polymer structure. One potential advantage of this is that the DHA is less likely to be degraded or attacked as may be the case during polymerisation (*e.g.* by free radicals), however the loading of micelles with the “correct” or indeed with an exact amount of DHA is not straightforward. Due to their high degree of unsaturation, PUFAs that have two or more double bonds are highly sensitive to attack by reactive

oxygen species. This is detrimental especially with respect to the PUFAs present within cell membranes. In sperm cells, the generation of reactive oxygen species results in a damage to the cells as a result of the attack on the PUFAs (particularly DHA) that are in abundance within the cell membrane. Mechanistically speaking the process starts with the removal of an allylic hydrogen, thus forming a lipid free radical. This can then in turn react with oxygen to produce lipid alkoxy and peroxy radicals which will subsequently react with other fatty acids producing more stable lipid hydroperoxides as well as more radicals which can then propagate further oxidation. This process will continue un-hindered unless the process is blocked by chain-breaking antioxidants (*e.g.* vitamin E). The structure of DHA, as well as the oxidation pathway of PUFAs, is shown below in Figure 5.1 and Figure 5.2 respectively.

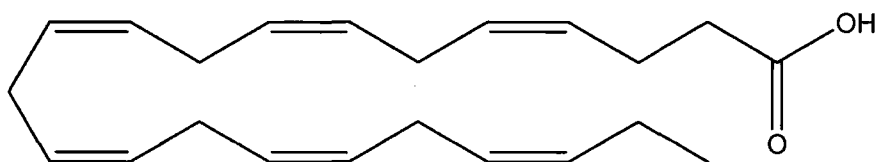


**Figure 5.1 – *cis*-4,7,9,11,13,16,19-docosahexaenoic acid**

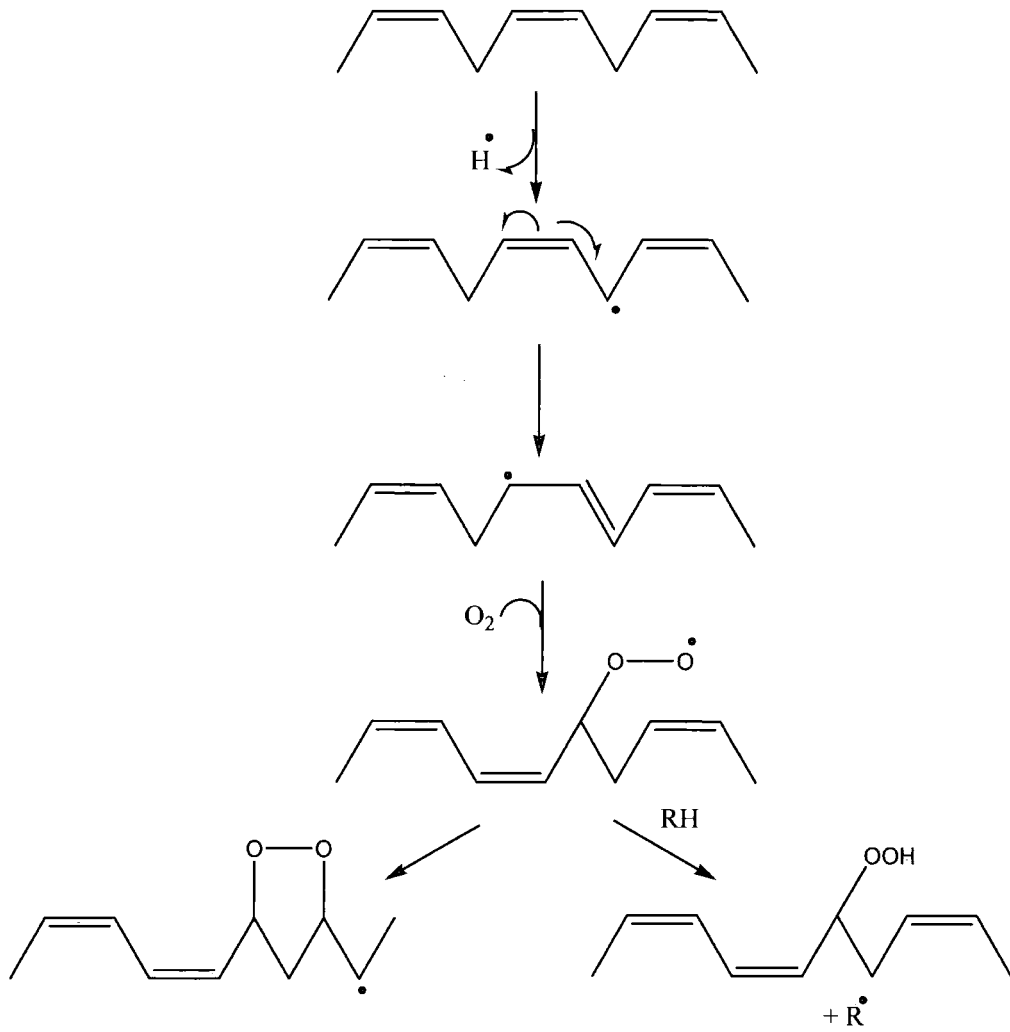


Figure 5.2 - Schematic pathway of peroxidation of PUFAs

## 5.2 Results and discussion

The delivery of DHA *in vitro* offers the possibility of increasing intracellular levels in order to compensate for any lost due to oxidation during the *in vitro* lifetime of the sperm cell. The lipid composition of boar spermatozoa is shown in Table 5.1.

**Table 5.1 – PUFAs as wt% of total fatty acids for spermatozoa**

Linoleic* (18:2 n-6) <sup>†</sup>	2.1 ± 0.12
Alpha-linolenic (18:3 n-3)	0.8 ± 0.02
Arachidonic (20:4 n-6)	3.0 ± 0.21
Docosapentaenoic (22:5 n-6)	24.8 ± 2.3
Docosahexaenoic (22:6 n-3)	33.1 ± 2.9
Total polyunsaturates	63.8 ± 5.01

From this it is obvious that the fatty acid composition of the cells is largely composed of DPA and DHA, meaning that the cell is susceptible to oxidative damage, since both fatty acids have high levels of unsaturation and are inherently susceptible to oxidative damage. Obviously, as discussed in earlier chapters, this can be combated by increasing the levels of anti-oxidants in the feed<sup>5</sup>, or by delivery of anti-oxidants *in vitro* using a polymeric delivery system.<sup>14, 15</sup> However a complementary strategy is to deliver additional DHA to the sperm cells and therefore maintain a high level of this essential fatty acid. It has been suggested that these fatty acids are extremely important in the fertilisation process, not only in pigs but in other animals.<sup>16-25</sup>

For poultry and some mammals, for example bulls, it is possible to include DHA and other lipophilic media directly in the ejaculate, since the ejaculate of these species is largely lipophilic. In the case of porcine semen (as discussed for Vitamin E) this is not as straightforward. It is possible to use seminal plasma to aid the solubility; however

\* Trivial names of PUFAs

<sup>†</sup> Abbreviated nomenclature in the form (x:y n-z) where x = number of carbon atoms, y = number of double bonds, and n-z indicates the position of the first double bond relative to the carbon furthest from the acid functionalised end of the molecule.

this is not appropriate for commercial purposes so it is generally reserved for experimental testing purposes.

One possible method of including DHA in aqueous diluents is to encapsulate the material inside a polymeric micelle or aggregate. As has been discussed in Chapter 3, the polymers containing vitamin E were found to aggregate in aqueous solution and it was demonstrated qualitatively that a water insoluble species (a red dye) could be “solubilised” in an aqueous polymer solution in this way. Some preliminary experiments of this nature were conducted by Joanne Leigh<sup>26</sup> using **14** polymer solution and DHA, however there were a number of prohibitive problems associated with this approach.

Firstly, micellisation of the DHA oil in the aqueous polymer solution is time consuming and difficult to monitor. Often, after vigorous mixing and vortexing the DHA appears to have dissolved and may remain so for 30 minutes or 1 hour, however, over time an oily layer begins to form on the surface of the water indicating that some (or all) of the DHA has not been micellised. This in itself means that it is very difficult to quantify how much (if any) DHA has been encapsulated. Since the double bonds in DHA are not conjugated, there is no strong chromophore for the molecule, ruling out the possibility of monitoring the progress of encapsulation by UV spectroscopy. Nevertheless, some experiments were conducted in this way which investigated the potential benefits of storing sorted bull semen into various collection fluids. From Ms Leigh’s work it was clear that although the control groups had similar morphological integrity compared to the **14**/DHA group, the motility of the latter group 24 hours after sex sorting, was zero compared to ~60% for the control group. This is clearly undesirable and would require further investigation to understand the reason(s) behind this.

Another interesting result was obtained from the fatty acid analysis of sorted boar semen. Previous semen sorting work by the author and analysis by Dr. André Maldjian had shown some interesting changes in the fatty acid composition of boar semen subsequent to the sex sorting procedure. From Table 5.2 it can be seen that there is a dramatic change in the relative fatty acid composition of the sperm cells, apparently as a result of the sorting procedure. DHA (C22:6 n-3) and DPA (C22:5 n-6) levels are

reduced significantly and in turn are “replaced” largely by saturated fatty acids. The lower levels of PUFAs could go some way to explaining why the sperm cells are much less motile and viable after this process. There are many possible reasons why these changes take place, for example the laser light used in the sorting process may accelerate the oxidation of the PUFAs, or perhaps the extremely high electric field used in the sorting process is detrimental to the cells, however the exact mechanisms involved are not obvious. It is the thesis of this author that one of the most probable factors is the use of the high powered laser, as it may result in the fragmentation of large molecules or generate radicals capable of oxidising these PUFAs.

It is perhaps easier to appreciate the differences in pre/post sort relative fatty acid composition by considering the data graphically. Figure 5.3 depicts the pre-sort data against the mean values for both X & Y sorted semen. It is evident from Figure 5.3 that the relative levels of unsaturated fatty acids decrease following the sorting procedure and consequently the saturated fatty acid content increases, ultimately to the detriment of the cell.

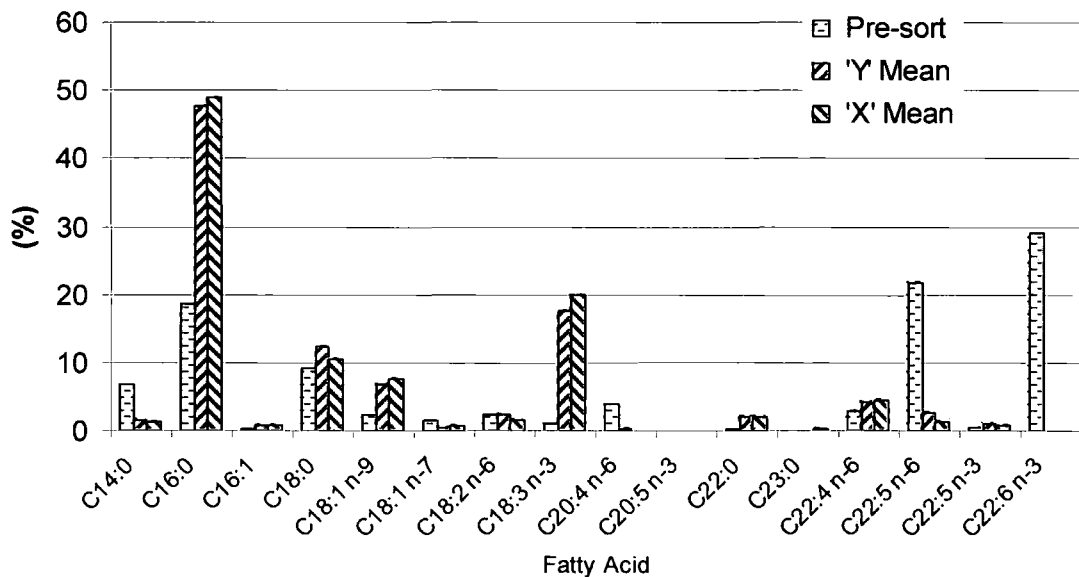


**Figure 5.3 - Comparison of relative fatty acid composition of pre/post sort boar semen**

Having identified this as a significant problem, a series of experiments was carried out by the author and Ms Leigh to establish if including DHA in the sorting medium could

help to counter some of the negative effects, and help to sustain or boost DHA levels within the cells.

Table 5.2 - Percentage of total fatty acids present in unsorted/sorted boar semen

Boar	Sample Type	C14:0	C16:0	C16:1	C18:0	C18:1	C18:1	C18:2	C18:3	C20:4	C20:5	C22:0	C23:0	C22:4	C22:5	C22:5	C22:6
						n-9	n-7	n-6	n-3	n-6	n-3			n-6	n-6	n-3	n-3
Sabo	Pre-sort	6.7	18.5	0.3	9.1	2.3	1.7	2.4	1.0	3.8	0.0	0.2	0.1	2.9	21.7	0.5	29.0
Sabo	Y	1.6	44.8	0.7	10.6	6.8	0.7	4.4	21.5	0.6	0.0	2.3	0.0	0.0	5.0	1.0	0.0
Leo	Y	1.6	53.4	0.6	13.9	5.1	0.4	1.0	20.0	0.0	0.0	2.2	0.4	0.0	0.4	1.2	0.0
Ingo	Y	1.4	45.1	0.9	12.4	8.6	0.6	1.4	11.3	0.0	0.0	1.9	0.0	12.9	2.3	1.2	0.0
	<i>Mean</i>	<i>1.5</i>	<i>47.8</i>	<i>0.7</i>	<i>12.3</i>	<i>6.8</i>	<i>0.6</i>	<i>2.3</i>	<i>17.6</i>	<i>0.2</i>	<i>0.0</i>	<i>2.1</i>	<i>0.1</i>	<i>4.3</i>	<i>2.6</i>	<i>1.1</i>	<i>0.0</i>
Sabo	X	1.2	44.6	1.1	10.3	6.1	0.7	1.6	21.5	0.0	0.0	2.0	0.0	8.8	1.0	0.9	0.0
Leo	X	1.3	53.4	0.3	10.6	8.8	0.7	1.8	18.2	0.0	0.0	2.3	0.4	0.0	1.5	0.9	0.0
Ingo <sup>‡</sup>	X	1.1	37.8	0.4	8.2	4.4	0.3	10.2	18.2	1.7	0.0	1.3	1.8	0.9	10.2	2.0	1.1
	<i>Mean</i>	<i>1.3</i>	<i>49</i>	<i>0.7</i>	<i>10.5</i>	<i>7.5</i>	<i>0.7</i>	<i>1.7</i>	<i>19.9</i>	<i>0</i>	<i>0</i>	<i>2.2</i>	<i>0.2</i>	<i>4.4</i>	<i>1.3</i>	<i>0.9</i>	<i>0</i>

Fatty acid analyses were conducted by Dr. André Maldjian.

<sup>‡</sup> This sample is thought to have been contaminated with bacteria and as such many values were artificially exaggerated. The data is included for completeness but has not been used to calculate the average values.

There were 4 experimental groups considered in order to assess the impact of the DHA. The fatty acid composition of unsorted boar semen was compared with semen sorted into BTS, DHA (2% w/v) solubilised using OEP (Orvus ES paste), **14** (0.02 mg/ml in BTS) or DHA (2% w/v) in **14** (1 mg/ml in BTS). From Table 5.3 and Figure 5.4Figure 5.5 we can see that inclusion of DHA in the sorting medium does seem to have a positive effect on the amount of DHA found during analysis of the cells. Furthermore, the amount of DHA present in the samples collected into the mixture of DHA and **14** was much greater than the samples collected into the DHA micellised using a surfactant. Indeed the amount of DHA measured is approximately at the same level as the pre-sort sample. This difference may be due to the polymer aggregates of the **14** assisting in the delivery of DHA to the cells since these aggregates will have an outer surface containing the galactosyl residues which have been shown to aid in the uptake of material by the cells. It is worth highlighting that the cells are washed thoroughly by repeated centrifugation prior to analysis, so this should rule out errors associated with DHA in solution.

Furthermore, it seemed possible that the inclusion of **14** in the sorting medium helped to reduce the amount of DHA lost immediately post sorting. This again highlights the complexity of the mechanism(s) by which this reduction in PUFAs takes place, but does suggest that it is a process, which left unchecked, will continue after the cells have passed through the cytometer. Nevertheless it is apparent that none of the collection media used completely halted the degradation within the cells. Indeed this would be an extremely interesting and worthwhile area of further study in the future.

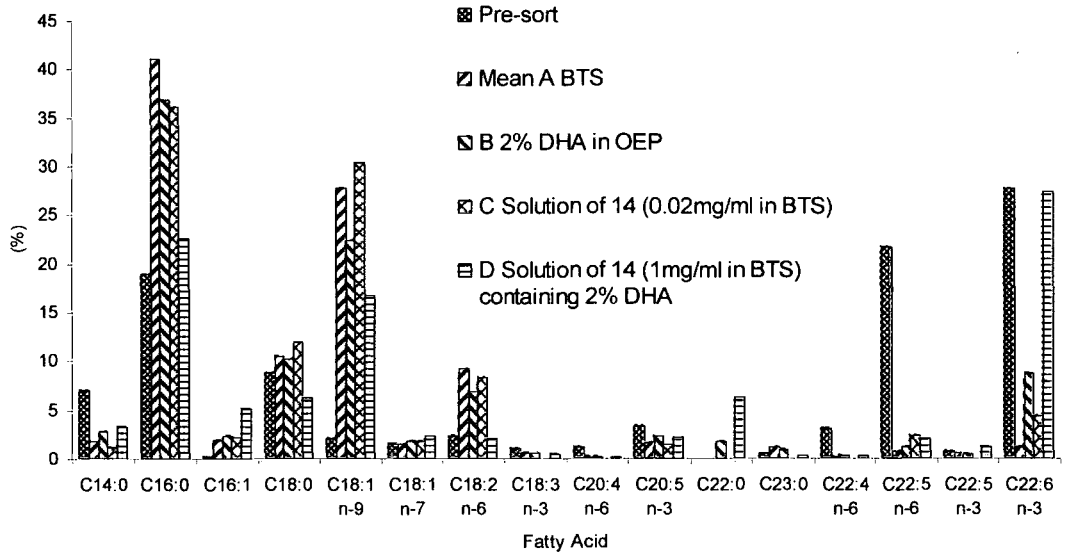


Figure 5.4 - Effect of sorting medium on relative fatty acid composition of sorted semen ('X')

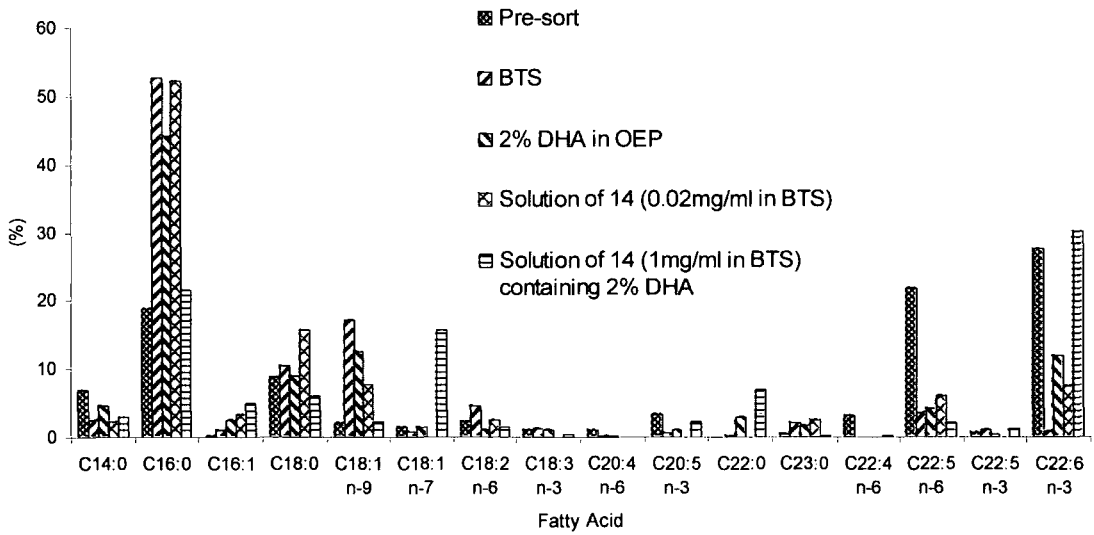


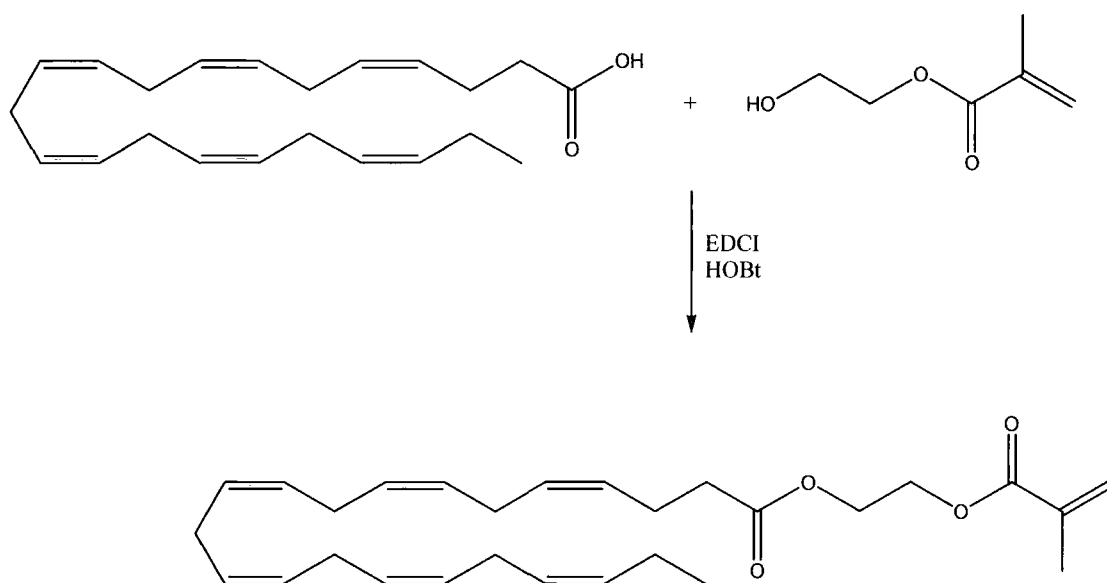
Figure 5.5 - Effect of sorting medium on relative fatty acid composition of sorted semen ('Y')

Table 5.3 - Percentage of total fatty acids present in unsorted/sorted boar semen collected into various media

Medium <sup>§</sup>	Sample Type	C14:0	C16:0	C16:1	C18:0	C18:1 n-9	C18:1 n-7	C18:2 n-6	C18:3 n-3	C20:4 n-6	C20:5 n-3	C22:0	C23:0	C22:4 n-6	C22:5 n-6	C22:5 n-3	C22:6 n-3
	Pre-sort	7.0	18.9	0.2	8.7	2.1	1.4	2.3	1.0	1.1	3.4	0.0	0.4	3.1	21.7	0.7	27.7
A	X	1.6	42.5	1.8	10.6	26.4	1.3	9.1	0.6	0.2	1.7	0.0	1.1	0.1	0.9	0.5	1.0
A	X	1.8	39.5	1.9	10.3	29.2	1.5	9.3	0.6	0.2	1.5	0.0	1.1	0.1	0.6	0.6	1.2
B	X	2.7	36.9	2.4	10.2	22.5	1.7	6.9	0.6	0.2	2.3	1.7	0.9	0.3	1.1	0.4	8.7
C	X	1.1	36.1	2.2	12.0	30.5	1.7	8.3	0.0	0.0	1.4	0.0	0.0	0.0	2.4	0.0	4.3
D	X	3.2	22.6	5.1	6.3	16.8	2.3	2.1	0.4	0.1	2.2	6.3	0.3	0.3	2.0	1.2	27.4
	<i>Mean</i>	<i>2.1</i>	<i>35.5</i>	<i>2.7</i>	<i>9.9</i>	<i>25.1</i>	<i>1.7</i>	<i>7.1</i>	<i>0.4</i>	<i>0.1</i>	<i>1.8</i>	<i>1.6</i>	<i>0.7</i>	<i>0.2</i>	<i>1.4</i>	<i>0.5</i>	<i>8.5</i>
A	Y	1.7	44.6	1.5	10.4	26.3	1.2	8.1	0.8	0.1	1.3	0.0	1.4	0.1	0.5	0.2	0.9
A	Y	3.5	60.8	0.6	10.3	7.8	0.6	1.1	1.7	0.3	0.0	0.3	2.7	0.0	6.7	1.9	0.7
B	Y	4.6	44.1	2.6	8.9	12.5	1.5	1.1	1.1	0.2	1.1	2.9	1.6	0.0	4.2	0.5	11.9
C	Y	2.4	52.2	3.4	15.7	7.8	0.0	2.5	0.0	0.0	0.0	0.0	2.6	0.0	6.0	0.0	7.5
D	Y	3.0	21.6	5.0	6.1	2.3	15.6	1.4	0.4	0.1	2.2	6.9	0.3	0.3	2.0	1.3	30.1
	<i>Mean</i>	<i>3.1</i>	<i>44.6</i>	<i>2.6</i>	<i>10.3</i>	<i>11.3</i>	<i>3.8</i>	<i>2.8</i>	<i>0.8</i>	<i>0.1</i>	<i>0.9</i>	<i>2.0</i>	<i>1.7</i>	<i>0.1</i>	<i>3.9</i>	<i>0.8</i>	<i>10.2</i>

<sup>§</sup> A = BTS, B = 2% DHA in OEP, C = 14 (0.02 mg/ml in BTS), D = 2% DHA in 14 (1 mg/ml in BTS)

Despite these potentially positive results, it remained more in line with the focus of this thesis to synthesise a polymer containing both sugar and DHA, chemically attached – *i.e.* a polymer similar to those synthesised with vitamin E moieties. In principle this appeared to be straightforward and a synthetic route was proposed (see Figure 5.6).



**Figure 5.6 - Synthesis of methacrylate monomer of DHA**

Although this route is feasible, when attempts were made to homo/co/ter polymerise this monomer no reaction occurred. Indeed not only did the DHA monomer not react, but there was no evidence of any polymeric material being formed by any of the co-monomers. In hindsight the reason for this is obvious; the arrangement of the double bonds in DHA is such that there are 10 allylic hydrogens present. These are easily abstracted by free radicals resulting in extremely stable radicals (stabilised by resonance – see Figure 5.7).

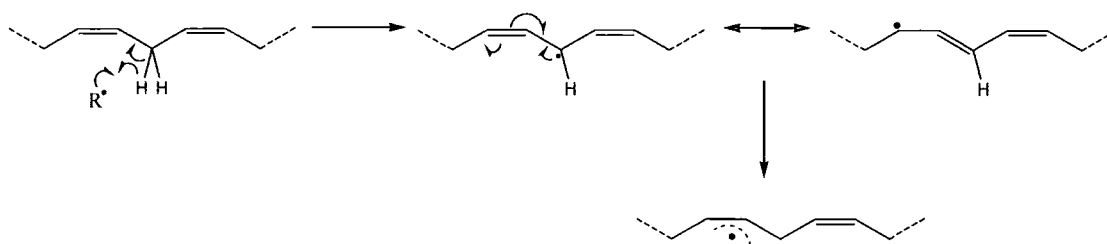


**Figure 5.7 - Stabilisation of radicals following abstraction of allylic hydrogen**

Obviously this process is likely to inhibit a free radical polymerisation and fully explains why there were no polymeric products obtained by following this route.

An alternative strategy was developed by adapting work by Whitesides *et al.*<sup>27</sup> This focused on the use of N-acryloyloxy succinimide (NASI), or more precisely poly-NASI, as a facile way to couple nucleophilic materials to polymers, post polymerisation. The principle being exploited in such examples is the fact that hydroxy succinimide is a good leaving group during nucleophilic attack. It also helps to activate the ester carbonyl, by making the carbon atom of the carbonyl more electropositive due to the electron withdrawing effect of the succinimide residue.

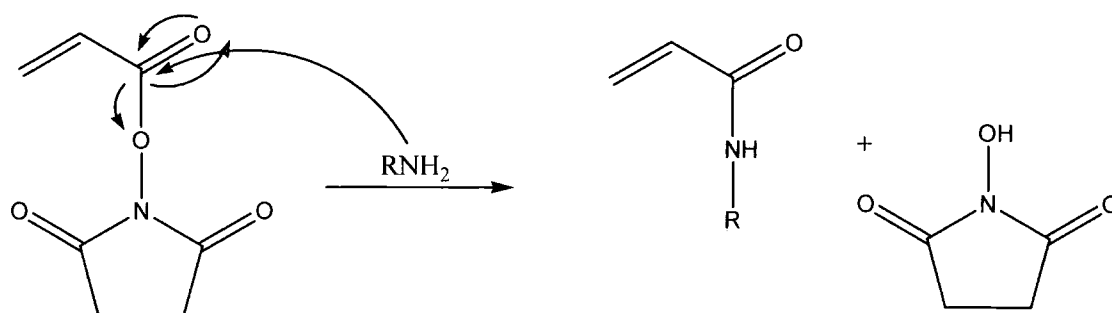


Figure 5.8 - Nucleophilic attack of NASI

This mechanism can also be exploited on poly-NASI or indeed a copolymer containing NASI; as such, nucleophilic species can easily be coupled to NASI functionalised polymers. In this way it was possible to synthesise a polymer containing a DHA residue by first synthesising a functionalised derivative of DHA.

This process involves several steps (see Figure 5.10 below), and although these are documented in the literature (in general terms) and each step is relatively straightforward, yields did decrease throughout. It was first necessary to synthesise azido-ethanol from 2-chloroethanol and sodium azide.<sup>28-31</sup> The two were stirred together with heating for 24 hours before the product was extracted into chloroform. The product was recovered by evaporation and in reasonable yield (78%).

The next stage involved the esterification of DHA with azido-ethanol. This synthesis was designed based on examples of esterification cited in the literature.<sup>32, 33</sup> The two

reactants were stirred overnight with EDCI and HOBt. After several aqueous washes and extraction into chloroform, the product, was recovered by evaporation in good yield (88%). The use of EDCI and HOBt in the reaction can be explained mechanistically, but essentially the carboxylic acid nucleophilically attacks the EDCI, which results in the carbonyl being activated to nucleophilic attack by an alcohol. Theoretically, either the HOBt, or the reactant alcohol can attack at this stage. If the latter occurs then clearly the desired product is formed immediately. However, if the HOBt attacks, the “wrong” ester is formed. This is actually beneficial since the HOBt is a good leaving group and so the preferred alcohol (in this case azido-ethanol) can displace the HOBt and the desired product is formed. Only a catalytic quantity of HOBt is required since (as shown in Figure 5.9) it is regenerated continuously during the reaction.

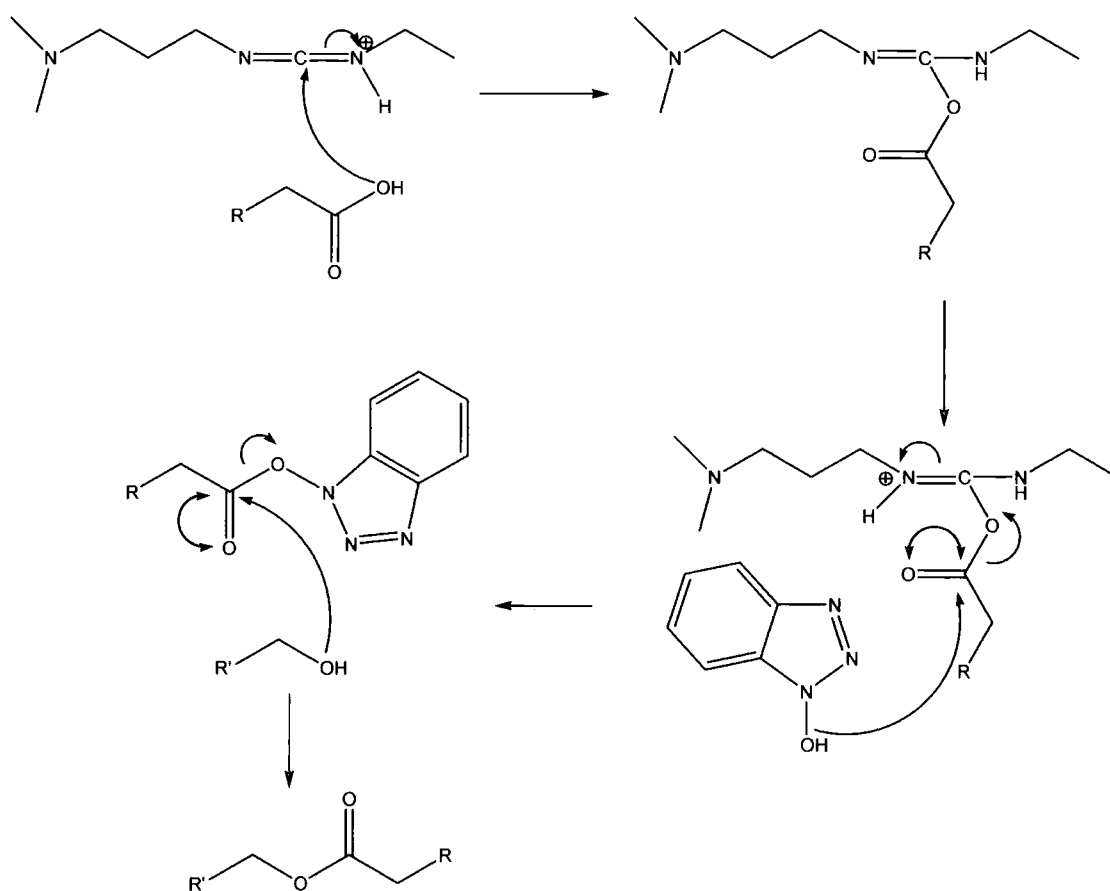


Figure 5.9 - Esterification using EDCI and catalytic HOBt

The analysis of both azido-ethanol, and azido-DHA was limited due to these products potentially being explosive, however in addition to the results obtained from conventional and safe methods of analysis, it was noted that the reaction between

azido-ethanol (a clear, colourless liquid) and DHA (a brown viscous oil) resulted in a brown amorphous solid with a fishy odour. Furthermore, since the DHA starting material contained impurities (as determined by HPLC), and since it is also sensitive to heat and light, there were invariably a considerable number of impurities present through the various reaction steps involving DHA derivatives. Ultimately this resulted in very noisy NMR spectra which were inherently difficult to interpret.

The next stage of this process was to reduce the azide to the primary amine. The reaction utilised in this example was the Staudinger Reaction, of which there are several examples in the literature.<sup>28, 34-40</sup> Clearly it is possible to transform an azide to an amine by hydrogenation, however in this case this would not be practical since it would also result in the saturation of the double bonds of the DHA, *i.e.* resulting in a fully saturated fatty acid derivative, which would be detrimental to the cells.

From the information contained in the literature, an experiment was designed to reduce the azide using triphenylphosphine. Although it appears this reaction was successful, it did result in a large number of bi-products which were difficult to remove by chromatography. Indeed, a solvent system for flash chromatography was not immediately apparent; however some insight was gained from an article by Bezuglov *et al.*,<sup>41</sup> who described the purification of the dimethylamino analogue of amino-DHA. Using their solvent system, it was possible to purify partly the reaction mixture, and a yellow wax was obtained from the crude brown oil. However, this material still contained some triphenylphosphine byproduct in low quantities. Once again this severely hampered the interpretation of NMR spectra, however the target compound was indentified by LC-MS as being present amongst the impurities.

Ultimately the objective of this synthetic procedure was to produce an amine-functionalised derivative of DHA that could be reacted with a glycopolymer containing NASI such that the product of the two would be a glycopolymer containing pendant DHA moieties. This being the case, a glycopolymer was synthesised that contained **GalEMA**, NASI and DMAEA (**21** terpolymer). The polymer was synthesised in the same manner as has been described previously – briefly, the monomers and AIBN were dissolved in a mixture of DMF and methanol (4:1) at heated at 65°C for 24 hours - and was found to be of relatively high molecular weight

with a high polydispersity (5.9). Since the polymer was synthesised via conventional free radical polymerisation, it is not unsurprising that the polydispersity is broad. The polymer was found to be soluble in water and after purification by dialysis (against water, MWCO 12-14 kDa) the polymer was recovered by freeze drying as a pale brown solid. The difference between the predicted and measured elemental analysis values can be explained due to some of the monomers not being incorporated in the polymer (as discussed in previous chapters).

Using the polymer described above a coupling reaction was attempted between the **21** terpolymer and **20**. The reaction conditions were adapted from those described by Whitesides *et al.*<sup>27</sup> Therein it is suggested that the reaction mixture should be heated, however in order to avoid oxidation of the DHA, this was avoided and the reagents were merely stirred at room temperature for 4 days. After this time the solvent was removed and the residue was re-dissolved in water and purified by dialysis (against water, MWCO 12-14 kDa). Subsequently the product was recovered by freeze drying. It was encouraging to note that the residue was soluble in water, which tentatively suggested that the **20** had been successfully coupled, since it in itself is not water soluble. Freeze drying of the solution resulted in a brown powder with a fishy odour. A brief analysis of the material was conducted by <sup>1</sup>H NMR and IR and it is tentatively suggested from these experiments (notably by NMR) that the coupling reaction was successful, although it was also evident that some succinimide moieties remained attached to the polymer. This route therefore offers a relatively facile method of synthesising a water soluble polymer carrying pendant galactosyl and DHA moieties.

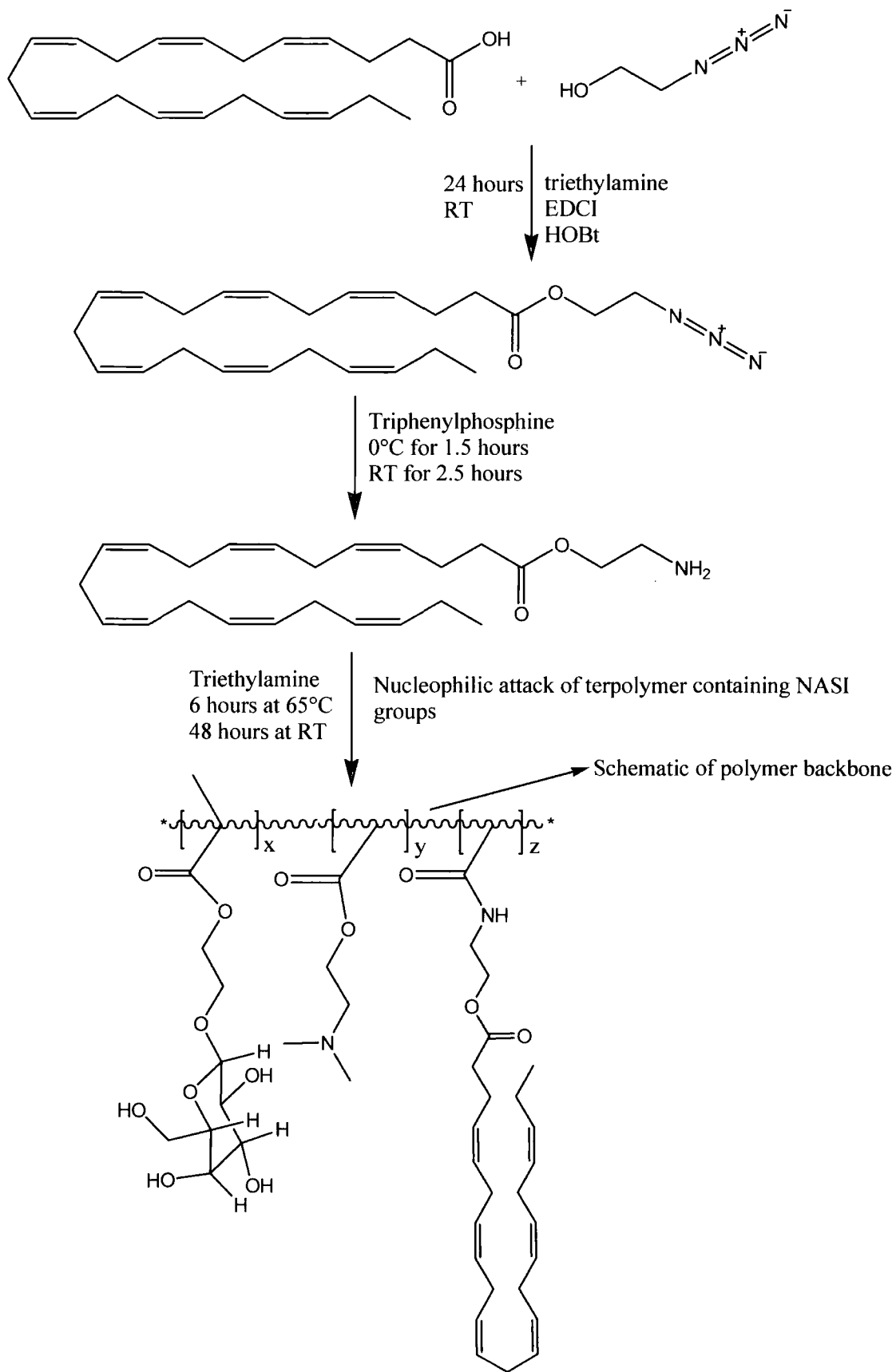


Figure 5.10 - Schematic of proposed route to DHA functionalised glycopolymer

### 5.2.1 Concluding comments

The synthesis of glycopolymers containing DHA moieties is achievable via the route described above. This route has several steps and as such, there are a number of impurities introduced progressively. As such, the analysis of these compounds was increasingly complex. High purity products may be achievable via painstaking purification at each reaction stage, or by selecting an alternative strategy for the reduction of the azide to the primary amine. Whilst the process described above may not have commercial viability, it is possible that the process could be further optimised. Furthermore, it has been demonstrated that hydrophobic materials can be included in aqueous systems either by attachment to hydrophilic polymers, or by micellisation within hydrophilic polymers. Ultimately it has been the primary objective of this thesis to derive methodologies of delivering hydrophobic metabolites to cells in hydrophilic environments, and to this end this has been shown to be feasible.

## 5.3 Experimental

### 5.3.1 Materials

1,2,3,4,6-Penta-*O*-acetyl- $\beta$ -D-galactopyranose (98%), boron trifluoride diethyl etherate (purified, redistilled), 2-chloroethanol (99%), sodium azide (99%), 2-dimethylamino ethyl acrylate (DMAEA, 98%), anhydrous methanol (99.8%) and anhydrous *N,N*-dimethylformamide (99.8%) were purchased from Aldrich. NASI (99%) was purchased from Acros Organics. Azoisobutyronitrile (AIBN, 97%) was obtained from BDH, and purified by recrystallisation from methanol prior to use. DHA (98 %) was purchased from Cayman Chemicals. Dichloromethane (DCM) was distilled over calcium hydride under N<sub>2</sub>. All other chemicals were used without further purification.

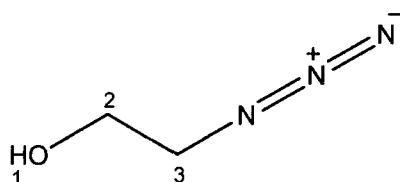
### 5.3.2 Instrumentation

NMR-spectra were recorded on a Varian Unity 300, Varian Mercury 200 or Bruker Avance 400 spectrometers; all chemical shifts were referenced to residual solvent as an internal standard. Infrared (IR) spectra were obtained using a Perkin Elmer 1600 Series FTIR spectrometer. Mass spectra were obtained using a Micromass Platform spectrometer in ionisation mode ES<sup>+</sup>. Aqueous size exclusion chromatography was conducted with a Water 410 RI detector and a Wyatt DAWN DSP MALLS, using a TSK GMPW column. The mobile phase consisted of 80% water, 20% methanol, 0.05 M NaNO<sub>3</sub> and 2.5 ml l<sup>-1</sup> 1.0 M NaOH at a flow rate of 0.8 ml min<sup>-1</sup>. Elemental analyses were obtained with an Exeter Analytical Inc. CE-440 Elemental Analyser. Lyophilised products were obtained using a Christ ALPHA-1-4 freeze-dryer with a LDC-1M controller.

### 5.3.3 2-Azido ethanol (17)<sup>42</sup>

2-Chloroethanol (24.2g, 300 mmol) was added rapidly to a solution of sodium azide (23.5 g, 361 mmol) in 80 ml of water at room temperature. The reaction mixture was

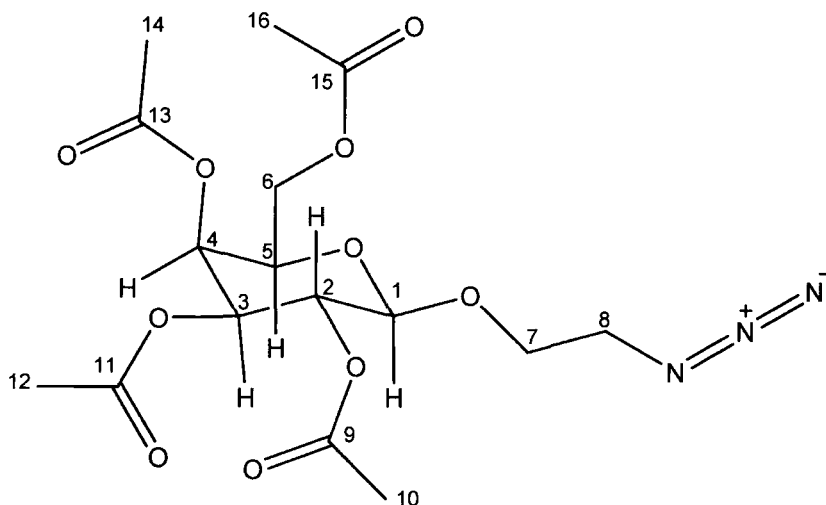
stirred at 30°C for 1 hour, followed by a further 24 hours at 70°C. The solution was then cooled to room temperature, saturated with sodium sulfate, and extracted with chloroform (4 x 40 ml). The combined organic layers were dried over anhydrous sodium sulfate and concentrated to yield product **17** (24.5 g, 78 %) as a colourless liquid.



Elemental analysis and mass spectroscopy could not be completed due to the explosive hazard of azides. IR (cm<sup>-1</sup>): -OH (broad) 3377; -CH<sub>2</sub> (med.) 2927, 2854; N<sub>3</sub> (med.) 2101. <sup>1</sup>H NMR (200 MHz, CDCl<sub>3</sub>): **3.00** (s, 1H<sub>1</sub>), **3.39** (t, 2H<sub>3</sub>, J = 5 Hz), **3.73** (t, 2H<sub>2</sub>, J = 5Hz). <sup>13</sup>C NMR (100 MHz, CDCl<sub>3</sub>): **53.5** (C<sub>3</sub>), **61.7** (C<sub>2</sub>).

#### 5.3.4 2-(2', 3', 4', 6'-Tetra-*O*-acetyl-β-D-galactosyloxy)ethyl azide (**18**)

β-D-Galactose pentaacetate (5 g, 12.81 mmol) was dissolved in 25 ml of anhydrous dichloromethane. To this solution, **17** (2.2 g, 25.61 mmol, 2eq) was added via syringe. The resulting solution was stirred under N<sub>2</sub> and cooled to 0°C. Boron trifluoride diethyl etherate (2.1 ml, 16.65 mmol, 1.3eq) was then added dropwise. The reaction was stirred for 1h at 0°C, then at room temperature overnight. The reaction mixture was then diluted with DCM (25 ml), washed with water (3 x 30 ml) and saturated aqueous NaHCO<sub>3</sub>. The organic phase was dried over anhydrous Na<sub>2</sub>SO<sub>4</sub> and evaporated under reduced pressure. The crude residue was purified by flash chromatography (n-hexane:ethyl Acetate, 1:1), yielding **18** (4.0 g, 76%) as a colourless oil.



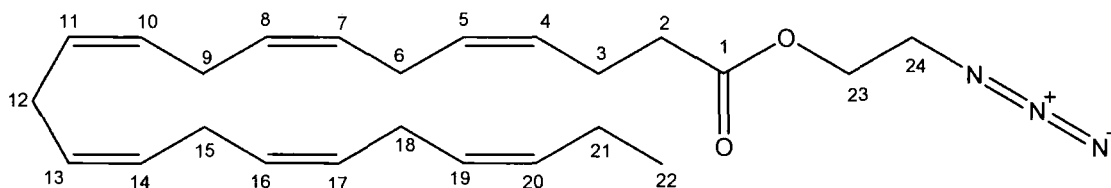
Elemental analysis and mass spectroscopy could not be completed due to the explosive hazard of azides. IR (nujol mull,  $\text{cm}^{-1}$ ): -C-H (med.) 2930, 2850;  $\text{N}_3$  (med) 2100; C=O (sharp) 1758, 1744, 1720; C-O-C (sharp) 1246, 1170, 1078, 1056.  $^1\text{H}$  NMR (400 MHz,  $\text{CDCl}_3$ ): **1.98, 2.05, 2.06, 2.15** (s,  $3\text{H}_{16}$ ,  $3\text{H}_{14}$ ,  $3\text{H}_{12}$ ,  $3\text{H}_{10}$ ), **3.32** (m,  $2\text{H}_8$ ), **3.91** (t,  $1\text{H}_5$ ,  $J = 6.57$  Hz), **4.02** (m,  $1\text{H}_7$ ), **4.10** (m  $2\text{H}_6$ ,  $1\text{H}_7$ ), **4.55** (d,  $1\text{H}_1$ ,  $J^{1-2} = 8.08$  Hz), **5.00** (dd,  $1\text{H}_3$ ,  $J^{3-4} = 3.28$  Hz,  $J^{3-2} = 10.36$  Hz), **5.22** (dd,  $1\text{H}_2$ ,  $J^{2-1} = 8.08$  Hz,  $J^{2-3} = 10.36$  Hz), **5.39** (d,  $1\text{H}_4$ ,  $J^{4-3} = 3.28$  Hz).  $^{13}\text{C}$  NMR (100 MHz,  $\text{CDCl}_3$ ): **20.6-21.0** ( $\text{C}_{10}$ ,  $\text{C}_{12}$ ,  $\text{C}_{14}$ ,  $\text{C}_{16}$ ), **50.5** ( $\text{C}_7$ ), **60.3** ( $\text{C}_6$ ), **61.5** ( $\text{C}_8$ ), **66.9** ( $\text{C}_4$ ), **68.5** ( $\text{C}_2$ ), **70.8** ( $\text{C}_3$ ), **70.7** ( $\text{C}_5$ ), **101.1** ( $\text{C}_1$ ), **169.5-171.1** ( $\text{C}_9$ ,  $\text{C}_{11}$ ,  $\text{C}_{13}$ ,  $\text{C}_{15}$ ).

### 5.3.5 Docosa-4, 7, 10, 13, 16, 19-hexaenoic acid 2-azido-ethyl ester (19)\*\*

17 (264 mg, 3.04 mmol) was dissolved in DMF/THF (20 ml/20 ml). In sequential order DHA (1 g, 3.04 mmol), triethylamine (0.428 ml, 3.04 mmol), EDCI (582 mg, 3.04 mmol), and HOBt (42 mg, 0.46 mmol) were added to the flask at room temperature. The reaction mixture was stirred overnight at room temperature. After this time a precipitate had formed in solution. This was removed by filtration, and the filtrate volume reduced under vacuum. Once the volume had been reduced by ~75%, more precipitate began to form. At this stage the solution was diluted with

\*\* The analysis of products derived from DHA was extremely difficult. As has been discussed in several sections of this thesis, DHA is highly susceptible to oxidation. As such, it was evident from most analyses conducted that any products contained impurities. Further purification seemed to be futile as over time (and possibly during purification), further impurities were formed. Due to time constraints at the end of the project, it was not possible to optimise these systems further.

chloroform, extracted with brine (3x), and the organic layer dried over magnesium sulphate before being evaporated to dryness. NMR studies showed some impurities so the product was redissolved in chloroform and extracted with aqueous sodium hydrogen carbonate (3x), dried over magnesium sulphate and evaporated to dryness, giving 1.06 g (2.67 mmol; 88%) of **19** as a brown amorphous solid.

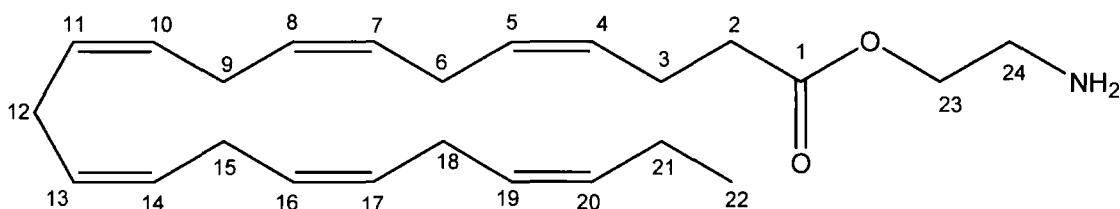


Elemental analysis and mass spectroscopy could not be completed due to the explosive hazard of azides. IR (KBr,  $\text{cm}^{-1}$ ): =C-H (med.) 3014; -C-H (med.) 2966, 2940, 2878; N-CH<sub>2</sub> (med.) 2776; N<sub>3</sub> (s) 2112; C=O (s) 1742; C=C (s) 1662; -C-H (med.) 1460; -CH<sub>3</sub> (s) 1394. <sup>1</sup>H NMR (400 MHz, CDCl<sub>3</sub>): **0.94** (m, 3H<sub>22</sub>), **1.95-2.99** (m, 2H<sub>2</sub>, 2H<sub>3</sub>, 2H<sub>6</sub>, 2H<sub>9</sub>, 2H<sub>12</sub>, 2H<sub>15</sub>, 2H<sub>18</sub>, 2H<sub>21</sub>), **3.18-4.22** (m, 2H<sub>23</sub>, 2H<sub>24</sub>) **5.15-5.40** (m, 1H<sub>4</sub>, 1H<sub>5</sub>, 1H<sub>7</sub>, 1H<sub>8</sub>, 1H<sub>10</sub>, 1H<sub>11</sub>, 1H<sub>13</sub>, 1H<sub>14</sub>, 1H<sub>16</sub>, 1H<sub>17</sub>, 1H<sub>19</sub>, 1H<sub>20</sub>). <sup>13</sup>C NMR (100 MHz, CDCl<sub>3</sub>): **7.6** (C<sub>22</sub>), **13.2** (C<sub>3</sub>), **19.5** (C<sub>21</sub>), **23.8** (C<sub>6</sub>, C<sub>9</sub>, C<sub>12</sub>, C<sub>15</sub>, C<sub>18</sub>), **32.3** (C<sub>2</sub>), **35.4** (C<sub>24</sub>) **44.7** (C<sub>23</sub>), **126.0-131.1** (C<sub>4</sub>, C<sub>5</sub>, C<sub>7</sub>, C<sub>8</sub>, C<sub>10</sub>, C<sub>11</sub>, C<sub>13</sub>, C<sub>14</sub>, C<sub>16</sub>, C<sub>17</sub>, C<sub>19</sub>, C<sub>20</sub>) **162.0** (C<sub>1</sub>).

### 5.3.6 Docosa-4, 7, 10, 13, 16, 19-hexaenoic acid 2-amino-ethyl ester (**20**)\*\*

Compound **19** (500 mg, 1.26 mmol) was dissolved in a solution of THF (40 ml), water (5 ml) and aqueous NaOH (0.5 ml, 1 M). The reaction mixture was cooled in an ice bath, and a solution of triphenylphosphine (330 mg, 1.26 mmol) in THF (10 ml) was added drop-wise. The reaction was stirred at 0°C for 1.5 hours, before being allowed to reach room temperature, and stirred for a further 2.5 hours. Subsequently the solvents were removed *in vacuo*, the crude residue redissolved in ethyl acetate, and washed with a saturated aqueous sodium chloride solution. Analysis by both <sup>1</sup>H NMR and mass spectroscopy indicated the presence of the target molecule; however a large number of impurities remained. This crude product was recovered as a dark

brown viscous oil, which had a fishy odour (400 mg, 85%). A portion of this crude material (150 mg) was purified by flash column chromatography (toluene:acetone, 5:1, rf 0.3) to yield **20** as a yellow wax with a fishy odour (~100 mg), however further analysis established that some additional impurities remained. Nevertheless, the disappearance of the azide signature and appearance of the amine signature in the IR was encouraging qualitative evidence of the reduction.



(Expected C 77.58; H 10.04; N 3.77, Found C 77.26; H 7.19; N 1.37). IR (nujol,  $\text{cm}^{-1}$ ): N-H (med.) 3282; =C-H (med.) 3014; -C-H (med.) 2966, 2930, 2874; C=O (s) 1776; C=C (s) 1660; -NH<sub>2</sub> (med.) 1574; -C-H (med.) 1438; -CH<sub>3</sub> (s) 1388. <sup>1</sup>H NMR (400 MHz, CDCl<sub>3</sub>): **0.90** (m, 3H<sub>22</sub>), **1.90-2.80** (m, 2H<sub>2</sub>, 2H<sub>3</sub>, 2H<sub>6</sub>, 2H<sub>9</sub>, 2H<sub>12</sub>, 2H<sub>15</sub>, 2H<sub>18</sub>, 2H<sub>21</sub>), **3.40-4.35** (m, 2H<sub>23</sub>, 2H<sub>24</sub>), **5.20-5.40** (m, 1H<sub>4</sub>, 1H<sub>5</sub>, 1H<sub>7</sub>, 1H<sub>8</sub>, 1H<sub>10</sub>, 1H<sub>11</sub>, 1H<sub>13</sub>, 1H<sub>14</sub>, 1H<sub>16</sub>, 1H<sub>17</sub>, 1H<sub>19</sub>, 1H<sub>20</sub>). Although <sup>13</sup>C NMR spectroscopy was attempted on this material, there was not sufficient material available to collect a satisfactory spectrum. Even after several hours, the signal to noise ratio was still unsatisfactory, making a thorough assignment extremely difficult.

### 5.3.7 Poly[2-(β-D-galactosyloxy)ethyl methacrylate-ter-N-acryloyloxysuccinimide-ter-2-(dimethylamino)ethyl acrylate Galema/NASI/DMAEA Terpolymer (21)]

A solution of **2b** (300 mg, 1.08 mmol), NASI (122 mg, 0.72 mmol), DMAEA (258 mg, 1.8 mmol) and AIBN (10.2 mg, 1.5 wt% w.r.t. monomers) in DMF (1.8 ml):MeOH (0.45 ml) (4:1) was prepared and purged with nitrogen. The solution was heated at 65°C, with stirring, under nitrogen for 24 hours. The solvent was removed under vacuum and the crude mixture redissolved in water. The crude product was

subsequently purified by dialysis against water (MWCO 12-14 kDa) and recovered by freeze drying to yield a pale brown amorphous solid (150 mg – low yield due to burst dialysis membrane).

(Expected C 52.9; H 9.8; N 5.1, Found C 49.71; H 6.83; N 2.75). IR (KBr,  $\text{cm}^{-1}$ ): -OH (broad) 3414; -CH (med.) 2956, 2926; -C=O (sharp) 1738; tertiary amine (succinimide) (sharp) 1658; -CH (sharp) 1458; -C-O (sharp) 1162, 1076.  $^1\text{H}$  NMR (300 MHz,  $\text{D}_2\text{O}$ , significant peaks): **2.76-2.79** (-RO-**CH<sub>2</sub>-CH<sub>2</sub>**-OR-, NASI), **3.37-3.87** (sugar ring protons), **4.28** (broad, -CH<sub>2</sub>-**CH<sub>2</sub>**-O-, DMAEA). GPC ( $\text{H}_2\text{O}$ ):  $M_n$   $1.05 \times 10^5$ ,  $M_w$   $6.24 \times 10^5$ ; PD = 5.9.

### 5.3.8 Coupling of 20 to 21\*\*

100 mg of **21** (contains approx. 18 mg of NASI) was dissolved in DMF (0.35 ml). To this was added a solution of **20** (50 mg) in triethylamine (6  $\mu\text{l}$ ). The solution was stirred for 96 hours at room temperature.

The reaction mixture was then evaporated to dryness, re-dissolved in water and purified by dialysis against distilled water (MWCO 12-14 kDa). The modified polymer product (**22**) was recovered by freeze drying (approximately 85 mg was recovered).

IR (KBr,  $\text{cm}^{-1}$ ): -OH (broad) 3420; =C-H (med.) 3014; -CH (med.) 2966, 2930, 2878; -C=O (sharp) 1738; C=C (sharp) 1649; -CH (sharp) 1460, 1402; -C-O (sharp) 1164, 1077.  $^1\text{H}$  NMR (300 MHz,  $\text{D}_2\text{O}$ , significant peaks): **2.78** (-RO-**CH<sub>2</sub>-CH<sub>2</sub>**-OR-, NASI), **3.35-3.84** (sugar ring protons), **4.64** (broad, -CH<sub>2</sub>-**CH<sub>2</sub>**-O-, DMAEA), 5.06 (broad, 1H<sub>4</sub>, 1H<sub>5</sub>, 1H<sub>7</sub>, 1H<sub>8</sub>, 1H<sub>10</sub>, 1H<sub>11</sub>, 1H<sub>13</sub>, 1H<sub>14</sub>, 1H<sub>16</sub>, 1H<sub>17</sub>, 1H<sub>19</sub>, 1H<sub>20</sub>, DHA).

## 5.4 References

1. Kroes, R.; Schaefer, E. J.; Squire, R. A.; Williams, G. M. *Food Chem. Toxicol.* **2003**, 41, (11), 1433-1446.
2. Warburtons (2003) *Warburtons Press Release*, <http://www.warburtons.co.uk/cgi-bin/pressrelease.cgi?num=228>, [Accessed 2003]
3. Supajus (2004) *Supajus*, <http://www.supajus.co.uk/>, [Accessed 2004]
4. Sidhu, K. S. *Regul. Toxicol. Pharmacol.* **2003**, 38, (3), 336-344.
5. Noble, R. C. *Supplement containing an admixture of an enriched triacylglycerol source of docosahexaenoic acid (DHA), an antioxidant, selenium, and g-linolenic acid to enhance fertility*. WO 2001097802, **2001**.
6. Arav, A. *Dietary manipulation to increase freezability and hypothermic storage of sperm and eggs*. WO 9966876, **1999**.
7. Blesbois, E.; Douard, V.; Germain, M.; Boniface, P.; Pellet, F. *Theriogenology* **2004**, 61, (2-3), 537-549.
8. Conquer, J. A.; Tekpetey, F. *Male Fertil. Lipid Metab.* **2003**, 41-48.
9. Kataoka, K.; Harada, A.; Nagasaki, Y. *Adv. Drug Delivery Rev.* **2001**, 47, (1), 113-131.
10. Miyata, T.; Nakamae, K. *Trends Polym. Sci.* **1997**, 5, (6), 198-206.
11. Nagasaki, Y.; Yasugi, K.; Yamamoto, Y.; Harada, A.; Kataoka, K. *Biomacromolecules* **2001**, 2, (4), 1067-1070.
12. Yamamoto, Y.; Nagasaki, Y.; Kato, Y.; Sugiyama, Y.; Kataoka, K. *J. Controlled Release* **2001**, 77, (1-2), 27-38.
13. Yasugi, K.; Nakamura, T.; Nagasaki, Y.; Kato, M.; Kataoka, K. *Macromolecules* **1999**, 32, (24), 8024-8032.
14. Cameron, N. R.; Cunningham, O.; Fleming, C.; Maldjian, A.; Penny, P.; Noble, R. C.; Davis, B. G.; Rullay, A. K.; Haddleton, D. M. *Polym. Mater. Sci. Eng.* **2004**, 90, 249-250.
15. Noble, R. C.; Penny, P. C.; Davis, B. G.; Cameron, N. R.; Maldjian, A.; Fleming, C. *Polymeric based complex*. WO 2003103716, **2003**.
16. Cerolini, S.; Gliozzi, T. M.; Pizzi, F.; Parodi, L.; Maldjian, A.; Noble, R. *Prog. Nutr.* **2002**, 4, (2), 151-154.

17. Cerolini, S.; Kelso, K. A.; Noble, R. C.; Speake, B. K.; Pizzi, F.; Cavalchini, L. G. *Biol. Reprod.* **1997**, *57*, (5), 976-980.
18. Cerolini, S.; Maldjian, A.; Surai, P.; Noble, R. *Anim. Reprod. Sci.* **2000**, *58*, (1,2), 99-111.
19. Kelso, K. A.; Cerolini, S.; Noble, R. C.; Sparks, N. H.; Speake, B. K. *Comp. Biochem. Physiol. B. Biochem. Mol. Biol.* **1997**, *118*, (1), 65-9.
20. Kelso, K. A.; Cerolini, S.; Noble, R. C.; Sparks, N. H. C.; Speake, B. K. *J. Reprod. Fertil.* **1996**, *106*, (2), 201-6.
21. Kelso, K. A.; Cerolini, S.; Speake, B. K.; Cavalchini, L. G.; Noble, R. C. *J. Reprod. Fertil.* **1997**, *110*, (1), 53-59.
22. Kelso, K. A.; Redpath, A.; Noble, R. C.; Speake, B. K. *J. Reprod. Fertil.* **1997**, *109*, (1), 1-6.
23. Maldjian, A.; Penny, P. C.; Noble, R. C. *Male Fertil. Lipid Metab.* **2003**, 60-72.
24. Surai, P.; Noble, R. C. *Improvement of male fertility with antioxidants and/or polyunsaturated fatty acids*. WO 9800125, **1998**.
25. Surai, P. F.; Noble, R. C.; Sparks, N. H. C.; Speake, B. K. *J. Reprod. Fertil.* **2000**, *120*, (2), 257-264.
26. Leigh, J. *Year in Industry Report*; University of York: 2003.
27. Sigal, G. B.; Mammen, M.; Dahmann, G.; Whitesides, G. M. *J. Am. Chem. Soc.* **1996**, *118*, (16), 3789-3800.
28. Carboni, B.; Vaultier, M.; Carrie, R. *Tetrahedron* **1987**, *43*, (8), 1799-1810.
29. Pfaendler, H. R.; Weimar, V. *Synthesis* **1996**, (11), 1345-1349.
30. Smith, R. H.; Mehl, A. F.; Shantz, D. L.; Chmurny, G. N.; Michejda, C. J. *J. Org. Chem.* **1988**, *53*, (7), 1467-1471.
31. Sutowardoyo, K. I.; Emziane, M.; Lhoste, P.; Sinou, D. *Tetrahedron* **1991**, *47*, (8), 1435-1446.
32. Frenette, R.; Friesen, R. W. *Tetrahedron Lett.* **1994**, *35*, (49), 9177-9180.
33. Guiles, J. W.; Johnson, S. G.; Murray, W. V. *J. Org. Chem.* **1996**, *61*, (15), 5169-5171.
34. Knouzi, N.; Vaultier, M.; Carrie, R. *Bull. Soc. Chim. Fr.* **1985**, (5), 815-819.
35. Murahashi, S. I.; Taniguchi, Y.; Imada, Y.; Tanigawa, Y. *J. Org. Chem.* **1989**, *54*, (14), 3292-3303.

36. Nyffeler, P. T.; Liang, C. H.; Koeller, K. M.; Wong, C. H. *J. Am. Chem. Soc.* **2002**, 124, (36), 10773-10778.
37. Taylor, E. C.; Macor, J. E.; Pont, J. L. *Tetrahedron* **1987**, 43, (21), 5145-5158.
38. Taylor, E. C.; Pont, J. L. *Tetrahedron Lett.* **1987**, 28, (4), 379-382.
39. Tietze, L. F.; Bratz, M.; Pretor, M. *Chem. Ber.* **1989**, 122, (10), 1955-1961.
40. Vaultier, M.; Knouzi, N.; Carrie, R. *Tetrahedron Lett.* **1983**, 24, (8), 763-764.
41. Nilsson, B. L.; Kiessling, L. L.; Raines, R. T. *Org. Lett.* **2000**, 2, (13), 1939-1941.
42. Bezuglov, V. V.; Zinchenko, G. N.; Nikitina, L. A.; Buznikov, G. A. *Russ. J. Bioorg. Chem.* **2001**, 27, (3), 200-203.

